Transcriptional regulation by the oncoprotein STAT5: role of acetylation and deacetylation processes

DISSERTATION ZUR ERLANGUNG DES DOKTORGRADES
DER NATURWISSENSCHAFTEN (DR. RER. NAT.)
DER FAKULTÄT FÜR BIOLOGIE UND VORKLINISCHE MEDIZIN
DER UNIVERSITÄT REGENSBURG

vorgelegt von

Sophia Charlotte Pinz, geb. Schabel

aus

Vaihingen an der Enz

im Jahr 2017

Das Promotionsgesuch wurde eingereicht am:
01. März 2017

Die Arbeit wurde angeleitet von:
PD Dr. Anne Rascle

Unterschrift:

Sophia Pinz

Für Annika

Acknowledgment

An erster Stelle danke ich PD Dr. Anne Rascle für die intensive Betreuung während meiner Promotion und für die vielen Publikationen, die sie möglich machte.

Meinen Mentoren Prof. Dr. Axel Imhof und Prof. Dr. Joachim Griesenbeck danke ich für die wissenschaftlichen Diskussionen. Joachim Griesenbeck danke ich zudem für seine Expertise und rund-um-die-Uhr Unterstützung bei Gelfiltrationsanalysen.

Ich danke Prof. Dr. Daniela Männel und dem ganzen Institut für Immunologie für die Unterstützung während meiner Promotion und für die Nutzung der Labore.

Mein Dank gilt der ganzen "STAT5 Signaling Research Group" für die Zusammenarbeit. Besonders wertvoll war die exzellente technische Unterstützung von Lissy und Susanne. Samy, danke für die Experimente die du zu dieser Arbeit beigetragen hast. Bedanken möchte ich mich auch bei Dominik, Philipp, Krystina und Christina, die im Rahmen von Bachelorarbeit oder Praktikum an dieser Arbeit mitwirkten.

Für den Abschluss meiner Promotion wurde mir ein einjähriges Stipendium durch das "Bayrische Programm zur Realisierung der Chancengleichheit für Frauen in Forschung und Lehre" zuteil.

Martina, danke für dein allzeit offenes Ohr und für deine Ratschläge zu meiner Doktorarbeit.

Mein größter Dank gilt meinem Mann Thomas und meiner Tochter Annika. Ohne euch wäre diese Arbeit nicht zum Abschluss gekommen. Auch meinen Eltern und Schwestern danke ich für ihren unerschöpflichen Rückhalt und für ihre vielen motivierenden und aufmunternden Worte. Großer Dank gilt auch meiner Schwiegermutter für die vielen Nachmittage die sie mit Annika verbrachte und mir so Zeit zum Schreiben schenkte.

Contents

CHAPTER 1

Summary

Activated signal transducer and activator of transcription STAT5 induces the expression of genes essential for cell differentiation, proliferation and inhibition of apoptosis. Previous work from our group demonstrated that the deacetylase inhibitor trichostatin A (TSA) attenuates transcriptional activation of STAT5 target genes at a step following STAT5 binding to its DNA binding sites by abrogating the recruitment of TBP and RNA polymerase II. The goal of this thesis was to better understand the mechanism of transcriptional regulation by STAT5 via the characterization of the mechanism underlying its inhibition by TSA. Specific aims were the identification of (i) the deacetylase (so-called HDAC) involved and of (ii) the acetylated substrate. The identification of the HDAC was performed using class-selective HDAC inhibitors and siRNA-mediated knock-down of HDAC expression. We found that, similarly to TSA, the deacetylase inhibitors valproic acid (VPA) and apicidin - but not MGCD0103 and MS-275 - inhibited expression of STAT5 target genes. However, siRNA-mediated knock-down experiments did not allow to identify the specific HDAC(s) involved in STAT5 target gene expression. To investigate whether STAT5 might be the acetylated substrate targeted by HDACs, selected lysine residues within STAT5 potentially targeted for acetylation were mutated and their effect on STAT5-mediated transcription was investigated. None of the mutations affected STAT5 transcriptional activity, arguing against STAT5 being the acetylated substrate targeted by the sought HDAC. Interestingly however, inhibition of STAT5-mediated transcription by TSA, VPA and apicidin correlated with an increase in global histone H3 and H4 acetylation. It also correlated with a redistribution of the acetylated-histone-binding protein BRD2, a member of the bromodomain and extra-terminal (BET) protein family

described for its role in the recruitment of the transcriptional machinery and transcriptional activation. Notably, chromatin precipitation experiments revealed that BRD2 is associated with the actively-transcribed STAT5 target gene *Cis* in a STAT5-dependent manner, and that BRD2 binding to *Cis* is lost upon TSA treatment. In agreement with a role of BRD2 in STAT5-mediated transcription, the BET inhibitor (+)-JQ1 inhibited STAT5-mediated transcription of the *Cis* gene. Together, our data support a model in which the HDAC inhibitors TSA, VPA and apicidin target histone acetylation, resulting in a global increase in chromatin acetylation. This change in chromatin acetylation would result in the redistribution of BRD2 to hyperacetylated chromatin and a departure of BRD2 from STAT5 target genes. BRD2 loss at STAT5 target genes would in turn prevent the proper recruitment and maintenance of the transcriptional machinery, resulting in transcriptional inhibition. In summary, this thesis identified BRD2 as an important co-factor of STAT5-mediated transcription and demonstrated that deacetylase inhibitors inhibit STAT5-mediated transcription by interfering with BRD2 function. This study thus identified BRD2 as a potential target for the development of novel therapies against STAT5-associated cancers.

CHAPTER 2

Introduction

2.1 Transcription and chromatin

2.1.1 Eukaryotic transcription

In eukaryotes, transcriptional activation of a protein-coding gene is the result of a promoter-specific combinatorial interplay between site-specific transcription factors and the cofactors they recruit (Hill & Treisman, 1995; Métivier et al., 2003; Reményi et al., 2004; Venters & Pugh, 2009). Transcription factors bind to specific DNA recognition sequences, which are usually located within promoters adjacent to the regulated gene or within distal enhancers. Enhancers are brought in close proximity to the regulated gene through long-range chromatin looping (Whalen et al., 2016). DNA-bound transcription factors recruit co-activators or co-repressors, multiprotein complexes, and components of the basal transcription machinery to assist the assembly of the pre-initiation complex and eventually enable initiation of transcription by RNA polymerase II (Pfitzner et al., 1998; Nakajima et al., 2001; Métivier et al., 2003). Many of the interaction partners of transcription factors are chromatin remodeling or modifying complexes, demonstrating the importance of chromatin composition and physical accessibility of DNA for transcription processes (Pfitzner et al., 1998; Xu et al., 2007; Venters & Pugh, 2009; Tang et al., 2013).

2.1.2 Transcription factors

Transcription factors are key mediators of transcription initiation. Thus, the regulation of transcription factor availability and activity is a central control parameter of gene expression. Transcription factor availability can be regulated, for example, at the level of their production, degradation or subcellular localization (Baeuerle & Baltimore, 1988; Wang et al., 1999; Rodriguez et al., 2000). Transcription factor activity is frequently modulated by post-translational modifications like phosphorylation, acetylation, methylation, ubiquitylation or SUMOylation (Shuai et al., 1993; Rodriguez et al., 2000; Rogers et al., 2003; Chuikov et al., 2004; Yuan, 2005; Venne et al., 2014). Phosphorylation is the post-translational modification best known to activate or inhibit transcription factors, but it is evident that lysine acetylation has also tremendous impact on transcription factor activity. Acetylation of transcription factors like p53, E2F1, nuclear factor-κB (NF-κB), and signal transducers and activators of transcription (STATs) can modulate their activity at key steps such as protein stability, cellular localization, affinity for DNA or protein-protein interactions (Martínez-Balbás et al., 2000; Li et al., 2002; Kiernan et al., 2003; Krämer et al., 2006; Tang et al., 2007; Spange et al., 2009).

2.1.3 Chromatin

In the eukaryotic nucleus, chromosomal DNA and several associated proteins form a structure called chromatin. The basic unit of chromatin is the nucleosome consisting of a histone protein octamer core around which the DNA is wrapped in nearly two turns. The histone octamer itself consists of two histone H2A / histone H2B heterodimers and two histone H3 / histone H4 heterodimers (Luger et al., 1997). Successive nucleosomes and the linker DNA between them produce a beads-on-a-string-like conformation (Olins & Olins, 1974). Several additional layers of compaction follow until the highly condensed heterochromatin is formed. By contrast, euchromatin is less compacted and the DNA is more accessible. It is therefore not surprising that most of the transcribed genes are found in euchromatin (Grewal & Moazed, 2003; DesJarlais & Tummino, 2016).

Besides its stabilizing and compacting function, chromatin is a level of regulation for fundamental cellular processes like DNA replication, DNA repair and transcription. DNA which is tightly wrapped around the histone octamer core is less accessible for binding of regulatory proteins, transcription factors or other DNA binding proteins (Lorch et al., 1987; Côté et al., 1994; Tse et al., 1998; Lorch & Kornberg, 2015; DesJarlais & Tummino, 2016). For instance, nucleosome depletion increases transcription *in vivo* (Han & Grunstein, 1988), and nucleosomes occluding certain elements within the promoter can inhibit *in vitro* transcription initiation by RNA polymerase II (Lorch et al., 1987).

Despite having preferential positioning sequences (Kaplan et al., 2009), nucleosomes are dynamic in that they can be shifted along the DNA by ATP-dependent chromatin remodeling complexes such as SWI/SNF (Hirschhorn et al., 1992; Côté et al., 1994; Längst & Becker, 2004; Venters & Pugh, 2009) or can be dis- and reassembled through histone chaperones such as FACT (facilitates chromatin transcription complex) (Belotserkovskaya et al., 2003) and BRD2 (bromodomain-containing protein 2) (LeRoy et al., 2008). In a genome-wide analysis it has recently been demonstrated that nucleosome repositioning is a general mechanism of the regulation of transcription (Nocetti & Whitehouse, 2016). In addition to remodeling, chromatin can be covalently modified, especially at the accessible histone N-termini, to create binding sites for specific chromatin binding proteins. In doing so, chromatin remodelers together with chromatin modifiers establish a chromatin structure restrictive or permissive for transcription to enable the cell to proceed through the cell cycle and adapt to external or developmental stimuli (DesJarlais & Tummino, 2016; Nocetti & Whitehouse, 2016).

2.1.4 Chromatin acetylation

Chromatin acetylation is established by a tightly controlled balance between histone acetyltransferases (HATs, e.g. p300/CBP) and histone deacetylases (HDACs). Acetylation of histones takes place at their accessible amino-termini, which protrude from the nucleosomal core. The main acetylation sites of histone H3 are lysine residues K9, K14, K18 and K23 while histone H4 acetylation sites are K5, K8, K12 and K16 (Thorne et al., 1990).

The established pattern of histone acetylation together with histone methylation, ubiquitylation and other post-translational modifications generates a histone modification pattern (Jenuwein & Allis, 2001; Agalioti et al., 2002; Guccione et al., 2006; Tang et al., 2013), which can be recognized and bound by certain "reader" proteins, most of which have transcriptional, chromatin maintenance or scaffolding functions (Jacobson et al., 2000; Jacobs & Khorasanizadeh, 2002; Kasten et al., 2004; Denis et al., 2006; Zeng et al., 2008).

Bromodomains, for example, recognize acetylated lysine residues of proteins and thus direct different bromodomain-containing proteins to acetylated chromatin (Jacobson et al., 2000). The double bromodomain-containing protein BRD2, member of the bromodomain and extra terminal (BET) family of proteins, favors binding to acetylated H4K12 and is as such a specific chromatin "reader" protein (Kanno et al., 2004).

In general, histone acetylation has been correlated with transcriptional activity (Allfrey et al., 1964; Allegra et al., 1987; Hebbes et al., 1988; Schübeler et al., 2004; Roh et al., 2005). It has been postulated that lysine acetylation of histones, reducing the

positive charge of the histone tail, decondenses the chromatin structure and thus facilitates access of regulatory proteins to chromatin (Luger et al., 1997; Tse et al., 1998; Shogren-Knaak et al., 2006). However, upon histone deacetylase inhibitor treatment, inducing global histone hyperacetylation, the expression of only a small subset of genes is changed, and in most cases about half of the affected genes are downregulated (Glaser et al., 2003; Peart et al., 2005; Daly & Shirazi-Beechey, 2006; Rada-Iglesias et al., 2007; Halsall et al., 2015). When looking at the promoter context, it is evident that both, acetylation as well as deacetylation processes are associated with transcriptional activity (Agalioti et al., 2000; Deckert & Struhl, 2001; Rascle et al., 2003; Kurdistani et al., 2004; Aoyagi & Archer, 2007; Lin et al., 2014; Greer et al., 2015).

2.1.5 Bromodomain and extra-terminal (BET) proteins

One protein family of acetyl-histone binding proteins is the bromodomain and extra-terminal (BET) protein family. The mammalian BET family consists of bromodomain-containing protein 2 (BRD2), BRD3, BRD4 and BRDT. Their two N-terminal bromodomains bind to ε-amino-acetylated lysine residues of histones (Dey et al., 2003; Pivot-Pajot et al., 2003; Kanno et al., 2004; LeRoy et al., 2008; Morinière et al., 2009). In addition, they have a conserved extra-terminal domain, which mediates protein-protein interactions (Belkina & Denis, 2012). BET proteins are transcriptional regulators. They interact with chromatin modifying and remodeling complexes, transcriptional cofactors or components of the transcription machinery (Crowley et al., 2002; Denis et al., 2006; Peng et al., 2007; LeRoy et al., 2008; Rahman et al., 2011; Wang et al., 2012; Hnilicová et al., 2013; Greer et al., 2015).

BET proteins are very similar, especially BRD2 and BRD4 whose bromo- and extra-terminal domains are about 80% identical by sequence (Belkina & Denis, 2012). This structural similarity might contribute to a certain degree of functional redundancy between members of the BET family, for example during inflammation responses (Belkina et al., 2013). By contrast, their developmental functions are rather specific, since other family members cannot rescue embryonic lethal $BRD2^{null}$ or $BRD4^{null}$ knockout mice (Houzelstein et al., 2002; Gyuris et al., 2009; Shang et al., 2009).

2.2 Histone deacetylases (HDACs)

2.2.1 HDAC function

Histone deacetylases (HDACs) remove covalently attached acetyl groups from ε-amino-acetylated lysine residues of proteins. Besides acetylated histones, they have hundreds

of cytosolic as well as nuclear non-histone substrates, many of which are transcription factors (Choudhary et al., 2009; Spange et al., 2009). Although HDACs are part of several co-repressor complexes (Kelly & Cowley, 2013) and their opposing HATs are generally seen as co-activators (Holmqvist & Mannervik, 2013), HDACs as well as HATs are both associated with transcriptional repression and activation (Nusinzon & Horvath, 2003; Zupkovitz et al., 2006; Aoyagi & Archer, 2007; Wang et al., 2009; Holmqvist & Mannervik, 2013; Lin et al., 2014). Owing to the many proteins and genes regulated by acetylation, HDACs are essential regulators of important cellular processes such as cell-cycle progression and apoptosis (Dangond et al., 1998; Lagger et al., 2002; Zhu et al., 2004; Huang et al., 2005; Ropero & Esteller, 2007; Ji et al., 2014; Dasgupta et al., 2016). Furthermore, HDACs affect homeostasis and differentiation of various cell types, for instance in cardiovascular, immune, and nervous system, in kidney and in epidermis (Bai et al., 2005; Chen et al., 2011; Robertson et al., 2012; Nural-Guvener et al., 2014; Sun et al., 2014; Mathias et al., 2015; Hull et al., 2016).

Mammalian deacetylases can be grouped into 4 different HDAC classes based on primary structure and phylogenetic analysis (Gregoretti et al., 2004). HDAC class 1 contains HDAC1, 2, 3, and 8, which are ubiquitously expressed in most tissues and localize predominantly to the nucleus. Class II HDACs are subdivided into subclass IIA, containing HDAC4, 5, 7, and 9, and into subclass IIB, containing HDAC6 and 10. Class II HDACs show a higher degree of cell type-specific expression and typically shuttle between nucleus and cytoplasm. HDAC11 is the most recently discovered HDAC and the sole member of class IV HDACs. HDAC's class III contains the sirtuins (SIRT1-7) which are unrelated to the eleven classical HDACs (class I, II and IV) in terms of sequence and catalytic mechanism (Frye, 2000; Tanner et al., 2000; Ropero & Esteller, 2007).

Class IIA HDACs (HDAC4, 5, 7, 9) have only minor enzymatic deacetylase activity towards acetylated histone tails (Fischle et al., 2001, 2002; Lahm et al., 2007; Lobera et al., 2013; Di Giorgio et al., 2015), and HDAC6 is localized predominantly in the cytoplasm (Verdel et al., 2000), where α-tubulin is one of its main substrates (Liu et al., 2015). Therefore the major HDACs responsible for histone deacetylation are the mainly nuclear class I HDACs. HDAC1 and HDAC2 proteins are 80% identical in sequence (Dovey et al., 2013) and catalytic members of the same multiprotein chromatin modifying complexes. Those complexes are NuRD (nucleosome remodeling and deacetylation), CoRest (co-repressor for element-1- silencing transcription factor) and Sin3 (Kelly & Cowley, 2013). Biochemically, HDAC1 and HDAC2 make up most of the cellular HDAC activity. Their co-knockdown in T cells leads to almost 60% reduction of total nuclear histone deacetylase activity (Dovey et al., 2013). HDAC3 deacetylates histones as catalytic core of SMRT/NCoR (silencing mediator of retinoid and thyroid hormone receptors/nuclear

receptor co-repressor) (You et al., 2013), while HDAC8 also deacetylates histones, but seems to be active without incorporation into a protein complex (Wolfson et al., 2013).

2.2.2 Deacetylase inhibitors

Classical HDACs (class I, II and IV) have a similar catalytic core and contain a catalytic divalent metal ion like Zn^{2+} in their active center (Arrowsmith et al., 2012; Nechay et al., 2016). Deacetylase inhibitors occupy the acetyl-lysine channel of the active site and can be classified based on the metal ion binding group into hydroxamic acids (e.g. trichostatin A (TSA), suberoylanilide hydroxamic acid (SAHA)), benzamides (e.g. MS-275, MGCD0103), carboxylic acids (e.g. valproic acid and butyrate), and cyclic peptides (e.g. apicidin). Due to their different catalytic mechanism, which depends on NAD^+ as cofactor, sirtuins are not inhibited by the same inhibitors as the classical deacetylases (Tanner et al., 2000; Mai et al., 2005; Arrowsmith et al., 2012).

Several deacetylase inhibitors are currently undergoing clinical trials and four deacetylase inhibitors (SAHA, Romidepsin, Belinostat and Panbinostat) have been approved by the United States Food and Drug Administration for the treatment of certain hematologic cancers (Grant et al., 2007; Laubach et al., 2015; Lee et al., 2015; Foss et al., 2016; Yoon & Eom, 2016). Deacetylase inhibitors affect cancer at several different levels (Bolden et al., 2006). They induce cell death of cancer cells through various pathways (Ruefli et al., 2001; Ungerstedt et al., 2005; Gaymes et al., 2006), and lead to cell cycle arrest and senescence (Peart et al., 2005; Xu et al., 2005; Romanov et al., 2010). In addition, deacetylase inhibitors impair tumor angiogenesis as well as cancer cell migration and invasion (Kim et al., 2001; Jeon & Lee, 2010; Han et al., 2014; Hakami et al., 2016). In contrast to cancer cells, normal cells are relatively weakly affected by deacetylase inhibitor-mediated cell death, which contributes to the big interest in deacetylase inhibitors for therapeutic intervention in malignant neoplastic diseases (Burgess et al., 2004; Ungerstedt et al., 2005; Bolden et al., 2006; Gaymes et al., 2006).

2.3 The JAK/STAT signaling pathway

Signaling pathways allow cells to communicate and to react to external stimuli. Signals are transmitted via membrane bound receptor into the cell and further into the nucleus where the gene expression profile is changed in response to the respective signal. Of special importance and conserved from slime molds and insects to mammals is the JAK/STAT signaling pathway (Perrimon & Mahowald, 1986; Hou et al., 1996; Yan et al., 1996; Darnell, 1997; Kawata et al., 1997; Luo & Dearolf, 2001).

In mammals, the family of Janus kinases (JAK) is constituted by four nonreceptor tyrosine kinases (JAK1, JAK2, JAK3 and Tyk2). They associate with the cytosolic domain of class I and class II cytokine receptors, which themselves lack a catalytic kinase domain. The cytokine receptor undergoes conformational changes upon ligand binding, which brings the associated JAKs in close proximity and thus enables JAK activation by trans-autophosphorylation. Subsequently, JAKs phosphorylate tyrosine residues in the cytoplasmic domain of the receptor, creating docking sites for signal transducers and activators of transcription (STAT) (Hou et al., 1994; Lin et al., 1995).

There are seven known STATs in mammalian cells: STAT1, STAT2, STAT3, STAT4, STAT5A, STAT5B and STAT6. In the unstimulated cell, they reside as latent transcription factors in the cytoplasm. Following binding to the phosphorylated receptor, STATs themselves are phosphorylated by the JAK kinases at a highly conserved tyrosine residue in the C-terminal domain. This phosphorylation activates STAT proteins. It provides the prerequisite for STAT homo- or heterodimerization, nuclear translocation, DNA binding and induction of target genes (Grimley et al., 1999; Haan et al., 2006; Schindler & Plumlee, 2008). STAT heterodimers have been described between STAT1 and STAT2, STAT1 and STAT3, as well as between STAT5A and STAT5B (Ghislain et al., 2001; Ginter et al., 2012; Boehm et al., 2014).

2.3.1 Activation of STAT5 by interleukin-3

STAT5, originally named mammary gland-specific nuclear factor (MGF) (Schmitt-Ney et al., 1992) is an essential mediator of many different cytokines, growth factors or hormones like interleukin(IL)-2, IL-3, IL-5, granulocyte-macrophage colony-stimulating factor (GM-CSF), growth hormone, erythropoietin and prolactin. Proliferation and survival of the murine pro-B cell line Ba/F3, the model system of this work, depends on interleukin-3 (IL-3) and the subsequent activation of STAT5 (Rodriguez-Tarduchy et al., 1990; Mui et al., 1995; Nelson et al., 2004).

The IL-3 receptor consists of the IL-3-specific receptor α-chain and the common β-chain (shared by IL-3, IL-5 and GM-CSF). As class I cytokine receptor, the IL-3 receptor does not have intrinsic tyrosine kinase activity, which is instead provided by the associated cytoplasmic tyrosine kinase JAK2. JAK2 is the predominant β-chain-activating kinase and the most common JAK kinase involved in the activation of STAT5 by class I cytokines (Grimley et al., 1999; Martinez-Moczygemba & Huston, 2003).

Besides activating the STAT pathway, signaling through the common β-chain receptor also activates the mitogen-activated protein kinase (MAPK) and phosphatidylinositol 3-kinase/AKT signaling pathways (Dijkers et al., 1999). Downstream of the MAPK pathway, IL-3-inducible genes such as *c-Fos* and *JunB* are activated (Hodge et al., 1998;

Rascle et al., 2003).

2.3.2 Structure of STAT5

Like all STAT proteins, STAT5 has a modular structure of seven conserved protein domains (Fig. 4.9): N-terminal domain, coiled-coil domain, DNA binding domain, linker-domain, Src-homology-2 domain (SH-2), phosphotyrosine tail segment and transactivation domain (Grimley et al., 1999). Structural and functional information of STATs is derived mainly from crystallographic data on STAT1, STAT3 and STAT4 (Becker et al., 1998; Chen et al., 1998; Vinkemeier et al., 1998) as well as mutagenic and biochemical studies (Moriggl et al., 1996).

The N-terminal domain is an independently folded structure, which is involved in nuclear export (Shin & Reich, 2013) and STAT tetramerization. Tetramerization is mediated through N-terminal interactions between STAT dimers and thus promotes cooperativity upon binding to tandem response elements, for instance during the STAT5-dependent regulation of *Cis* or the IL-2 receptor α gene (Xu et al., 1996; Matsumoto et al., 1997; Verdier et al., 1998; Vinkemeier et al., 1998; John et al., 1999; Soldaini et al., 2000; Lin et al., 2012).

The SH-2 domain, a phosphotyrosine binding domain, is the most conserved domain among the members of the STAT family. It is essential for STAT recruitment to the phosphorylated receptor and for subsequent formation of the transcriptionally active STAT dimer. STAT dimerization occurs through reciprocal interactions between the SH-2 domain of one monomer and the phosphotyrosine of the other monomer (Grimley et al., 1999).

The short phosphotyrosine tail segment between SH-2 and transactivation domain contains the conserved tyrosine (Y694 of STAT5A and Y699 of STAT5B) whose phosphorylation is required for STAT dimerization (Grimley et al., 1999).

The transactivation domain, located at the C-terminus, is the most divergent domain between the members of the STAT family in general and between STAT5A and B in particular (Grimley et al., 1999; Lim & Cao, 2006). It is required and sufficient for induction of gene expression. C-terminally truncated STAT5 isoforms are dominant-negative transcriptional regulators (Moriggl et al., 1996; Meyer et al., 1998; Epling-Burnette et al., 2002), and GAL-4 fusion proteins containing only the C-terminal transactivation domain of STAT5A can activate reporter genes in GAL-4 luciferase reporter assays (Moriggl et al., 1996).

2.3.3 Function of STAT5A and STAT5B

Duplication of the STAT progenitor gene, giving rise to the homologous *Stat5a* and *Stat5b* genes, seems to be the most recent event in the evolution of STATs (Barillas-Mury et al., 1999). Human STAT5A and B proteins share a sequence similarity of 95% (Grimley et al., 1999).

STAT5A and B are important regulators of cell proliferation, differentiation and apoptosis (Grimley et al., 1999; Nosaka et al., 1999) and are relevant for liver metabolism (Udy et al., 1997), mammary gland development (Liu et al., 1997), immunoregulation (Snow et al., 2003) and hematopoiesis (Moriggl et al., 1999; Shelburne et al., 2003; Li et al., 2007). STAT5A and B have many overlapping, but also independent functions (Schindler & Plumlee, 2008). The most striking difference is the predominant role of STAT5A for prolactin signaling during mammary gland development and lactation (Liu et al., 1997; Metser et al., 2015), while STAT5B plays a key role in the development of T cells and growth hormone-dependent regulation of body growth (Udy et al., 1997; Chia et al., 2006; Nadeau et al., 2011; Villarino et al., 2016). In addition, it becomes increasingly appreciated that STAT5A and B exert distinct roles during carcinogenesis (Leong et al., 2002; Ren et al., 2002; Kazansky et al., 2003; Tang et al., 2010).

2.3.4 Transcriptional regulation by STAT5

Functional DNA recognition sites for STAT5 are usually located within the promoter of regulated genes like *Cis*, *Osm* and *Spi2.1*, but can also be found within introns or distal enhancers, as the case for *Id-1* and *c-Myc* (Basham et al., 2008; Pinz et al., 2016). Consistently, genome-wide analysis of STAT5 distribution using ChIP-sequencing showed a clustering of STAT5 binding around transcription start sites, and STAT5 binding was also detected at distal loci (Nelson et al., 2004; Villarino et al., 2016).

STAT5A and STAT5B recognize the same consensus DNA binding sequence (TTCNNNGAA) (Soldaini et al., 2000; Ehret et al., 2001), but subtle DNA sequence variations can favor one STAT5 over the other (Frasor et al., 2001). In addition to their different specificity regarding the DNA binding sequence, the STAT5A and STAT5B homo- and heterodimers also have different specificity regarding the presence of dimeric versus tetrameric STAT5 binding sites (Boucheron et al., 1998; Verdier et al., 1998; Soldaini et al., 2000). Accordingly, our group and others (Nelson et al., 2004; Basham et al., 2008; Kanai et al., 2014) demonstrated that STAT5A and STAT5B differentially contribute to the regulation of different STAT5 target genes. While some genes show redundant regulation by STAT5A and STAT5B, other genes require the presence of both STAT5 paralogs or show a preference for STAT5A or STAT5B (Nelson et al., 2004; Basham et al.,

2008; Kanai et al., 2014). Cell type-specific protein levels of STAT5A and STAT5B shift the balance between the different STAT5 dimers and thus influence STAT5 target gene expression (Metser et al., 2015; Villarino et al., 2016). The carboxy-terminal transactivation domain of STAT5 is the most divergent domain between STAT5A and STAT5B and might contribute to differences in gene regulation (Grimley et al., 1999), possibly through different interactions with regulatory proteins. However, no paralog-specific cofactor has been described so far.

During regulation of transcription, STAT5 proteins interact or cooperate with other transcription factors (Mukhopadhyay et al., 2001; Wyszomierski & Rosen, 2001; Magné et al., 2003), nuclear receptors (Engblom et al., 2007), transcriptional co-activators or -repressors (Pfitzner et al., 1998; Nakajima et al., 2001) as well as chromatin modifiers and remodelers (Xu et al., 2007; Mandal et al., 2011). For instance, during the well-studied induction of the STAT5 target gene β-casein during mammary epithelial differentiation, STAT5 cooperates with the transcription factor c-EBPβ and interacts with the nuclear glucocorticoid receptor (GR), the chromatin remodeling complex SWI/SNF, as well as the coactivators p300/CBP and NCoA-1 (Pfitzner et al., 1998; Wyszomierski & Rosen, 2001; Litterst et al., 2003; Xu et al., 2007). Consistent with the current model of transcriptional regulation (Venters & Pugh, 2009), STAT5 is a core element of promoter-specific multifunctional protein complexes which induce gene expression (Villarino et al., 2015).

It has been shown that a deacetylase activity is required for transcriptional activation by STAT5 (Rascle et al., 2003; Sebastián et al., 2008). Within a treatment of up to 2 h, the deacetylase inhibitor trichostatin A (TSA) reduced expression of all normally induced STAT5 target genes in IL-3-stimulated Ba/F3 cells, while only few non-target genes were inhibited (Rascle et al., 2003). Deacetylase inhibitor treatment leaves STAT5 phosphorylation, nuclear translocation and DNA binding unaffected. Instead, it inhibits STAT5 target gene expression by impairing the recruitment of the transcription machinery to the transcription start site of STAT5 target genes. Interestingly, further experiments indicated that the HDAC inhibitor TSA does not increase histone H3 and H4 acetylation levels around the promoter of the STAT5 target gene *Cis* and *Osm* (Rascle & Lees, 2003; Rascle et al., 2003), nor does it affect chromatin remodeling at the *Cis* promoter (Rascle et al., 2003). These findings suggested that the observed inhibition of STAT5 target gene expression by deacetylase inhibitors is not mediated through chromatin and hyperacetylated histones, but rather through an acetylated non-histone protein.

Despite a predominant role in transcriptional activation, STAT5 can also repress transcription. Alternative splicing or proteolytic cleavage can lead to loss of the C-terminal transactivation domain of STAT5, producing dominant negative STAT5 isoforms (Moriggl

et al., 1996; Meyer et al., 1998; Epling-Burnette et al., 2002). Furthermore, in pro-B cells, STAT5 tetramers recruit the histone methyltransferase EZH2 to guide H3K27me3 modifications to the *Igk* locus (encoding the immunoglobulin κ-chain complex) and thus repress transcription of this locus (Mandal et al., 2011). Based on genome-wide ChIP-sequencing data, it was further proposed that for many genes recruitment of STAT5 to tetrameric binding sites correlates with H3K27 trimethylated histones and gene repression (Mandal et al., 2011). By contrast, another report demonstrated that in T cells STAT5 tetramers preferentially mediate transcriptional activation (Lin et al., 2012). Thus, the functional role of STAT5 tetramers has not yet been clarified. Interaction of STAT5 with the nuclear receptor co-repressor SMRT has been reported, but the function of SMRT seems to be signal attenuation and downregulation of STAT5 activity, rather than active transcriptional gene repression (Nakajima et al., 2001).

2.3.5 Regulation of STAT5 activity

Tight control of STAT5 activity is essential to ensure an appropriate signal intensity and duration. In a normal cell, rapid STAT5 phosphorylation, nuclear accumulation and induction of target gene expression is followed by gradual signal decay involving constitutively expressed regulators such as phosphatases and PIAS, as well as the inducible members of the suppressors of cytokine signaling (SOCS) protein family. STAT5 signaling is furthermore attenuated by degradation of nuclear STAT5 via ubiquitin-proteasome pathway (Chen et al., 2006) and by receptor down-regulation (Martinez-Moczygemba et al., 2007).

Phosphatases from three different families have been implicated in negatively regulating the JAK/STAT pathway. First, there are the mainly cytoplasmic Src homology phosphatases SHP-1 and SHP-2, which can directly dephosphorylate STAT5 or act on the tyrosine phosphorylated JAK and receptor (Yi et al., 1993; Klingmüller et al., 1995; Paling & Welham, 2002; Chen et al., 2004). Second, phosphotyrosine phosphatase 1B (PTP1B), T cell protein tyrosine phosphatase (TC-PTP) and the nuclear splice variant TCP45 dephosphorylate and thus inactivate JAK kinases (Myers et al., 2001; Simoncic et al., 2002; Johnson et al., 2010) or STATs (ten Hoeve et al., 2002; Krämer et al., 2009). Third, the transmembrane phosphotyrosine phosphatase CD45 dephosphorylates and inactivates JAKs (Irie-Sasaki et al., 2001).

Protein inhibitor of activated STAT 3 (PIAS3) interacts with STAT5 and represses its transcriptional activity probably through interference with STAT5 DNA binding ability (Rycyzyn & Clevenger, 2002).

Among the eight SOCS family members, cytokine-induced SH2-domain-containing protein (CIS), SOCS1, SOCS2 and SOCS3 were shown to be direct STAT5 target genes

and negative feedback regulators involved in the attenuation of STAT5 signaling (Matsumoto et al., 1997; Tam et al., 2001; Vidal et al., 2007; Basham et al., 2008; Bachmann et al., 2011; Vitali et al., 2015). They compete with STAT5 for binding sites at the receptor, or inhibit the kinase activity of JAKs (Endo et al., 1997; Matsumoto et al., 1997; Ram & Waxman, 1999; Sasaki et al., 1999).

2.3.6 Post-translational modifications of STAT proteins

Phosphorylation of a highly conserved tyrosine residue within the phosphotyrosine tail segment is required for the formation of transcriptionally active STAT dimers (Grimley et al., 1999). In addition, serine phosphorylation within the transactivation domain has been shown to influence the activity of several STAT proteins (Decker & Kovarik, 2000). Serine phosphorylation of STAT5 has been demonstrated, but its biological significance remains to be clarified (Yamashita et al., 1998; Beuvink et al., 2000; Xue et al., 2002; Berger et al., 2013).

SUMOylation has been demonstrated to negatively regulate the activity of STAT1 and STAT5 (Ungureanu et al., 2005; Grönholm et al., 2012; Van Nguyen et al., 2012). The proposed SUMOylated lysine K696 of STAT5A (K701 of STAT5B) is also a target for acetylation (Ma et al., 2010; Van Nguyen et al., 2012).

2.3.6.1 STAT acetylation

The last decade has established acetylation as an important post-translational modification for the regulation of STAT proteins. STAT proteins were shown to be acetylated at one or multiple lysine residues in different domains (Wieczorek et al., 2012). The functional characterization of acetylation sites is usually undertaken by site-directed mutagenesis of candidate lysine residues. Mutation to arginine prevents acetylation through its mesomerically stabilized guanidino group. At the same time arginine retains a positive charge like the unmodified lysine residue. Mutation to the neutral amino acid glutamine mimics lysine acetylation, especially the loss of the positive charge. Furthermore, glutamine and acetylated lysine both contain an amide group in their side-chain (Li et al., 2002; Wang & Hayes, 2008; Krämer et al., 2009; Krämer & Heinzel, 2010). There are numerous examples where mutations to arginine or glutamine were successfully used to mimick deacetylated or acetylated lysine residues (Li et al., 2002; Wang & Hayes, 2008; Krämer et al., 2009). For instance, a STAT1 mutant carrying lysine to arginine mutations at lysine residues K410 and K413 behaves similarly as the unmodified wild-type STAT1 protein, while a STAT1 mutant carrying lysine to glutamine mutations at the same residues behaves similarly as the acetylated wildtype protein (Krämer et al., 2006,

2009).

Acetylation can affect different steps of the activation of STATs like STAT protein interactions, phosphorylation, dimerization, or transcriptional activity (Wieczorek et al., 2012). An additional level of regulation is added by the interplay of STAT acetylation with other STAT post-translational modifications like phosphorylation or SUMOylation (Krämer et al., 2009; Van Nguyen et al., 2012). The functional consequence of STAT acetylation is specific for each STAT family member (Ray et al., 2005; Yuan, 2005; Tang et al., 2007; Krämer et al., 2009; Nie et al., 2009; Ma et al., 2010; Ginter et al., 2012; Van Nguyen et al., 2012; Wieczorek et al., 2012). Furthermore, several controversial reports exist regarding specific STAT acetylation sites and their functional role (Nusinzon & Horvath, 2003; Klampfer et al., 2004; Ray et al., 2005; Yuan, 2005; Catania et al., 2006; Krämer et al., 2009; Nie et al., 2009; Gupta et al., 2012; Wieczorek et al., 2012; Kosan et al., 2013). This is probably a consequence of the complexity of STAT acetylation, which might be influenced by experimental conditions such as the activating cytokine (Ginter et al., 2012), the investigated cell-type (Nakajima et al., 2001; Rascle et al., 2003; Kosan et al., 2013) or treatment duration with deacetylase inhibitors (Nusinzon & Horvath, 2003; Klampfer et al., 2004; Sakamoto et al., 2004; Ginter et al., 2012).

Acetylation of STAT1 and STAT2

Acetylation of STAT1 within its DNA binding domain at K410 and K413 counteracts STAT1 phosphorylation and transcriptional activity. Acetylation supports the interaction of STAT1 with the T cell tyrosine phosphatase (TCP45) which correlates with STAT1 dephosphorylation and thus inactivation (Krämer et al., 2009; Ginter et al., 2012). While the finding of these studies that deacetylase inhibition of STAT1 acetylation impairs STAT1 phosphorylation is consistent with data from Klampfer et al. (2004), others use shorter deacetylase inhibitor treatments and report that deacetylase inhibition does not affect STAT1 phosphorylation (Nusinzon & Horvath, 2003; Chang et al., 2004; Sakamoto et al., 2004). Nevertheless, all cited reports are consistent in that deacetylase inhibitor treatment blocks interferon-induced transcriptional activity of STAT1.

Several acetylation sites of STAT2 were identified by mass spectrometry upon overexpression of STAT2 and the HATs CBP or p300 (Tang et al., 2007). Furthermore, it was shown that acetylation at K390 of STAT2 modulates the interaction between STAT2 and STAT1 and is required for the formation of transcriptionally active interferon stimulated gene factor 3 complex (ISGF3 consisting of STAT1, STAT2 and IRF9) upon interferon-α signaling (Tang et al., 2007).

Acetylation of STAT3

STAT3 was shown to be acetylated at K685 but not at nearby lysine residues, and this acetylation positively affects its transcriptional activity (Wang et al., 2005; Yuan, 2005). Mutation of K685 to arginine, leading to acetylation-deficient STAT3, does not affect STAT3 phosphorylation, but impairs its dimerization, DNA binding, and consequently its transcriptional activity (Yuan, 2005). By contrast, Nie et al. (2009) found by mass spectrometry that K679, K707 and K709 of STAT3 can also be acetylated. Mutation of all those lysine residues together with K685 to arginine reduced STAT3 phosphorylation much more than single or double mutations, suggesting that acetylation of all four lysine residues is functionally required for STAT3 phosphorylation and activity (Nie et al., 2009). In parallel it was found that K49 and K87 are acetylated, but that mutation of K49 and K87 to arginine does not affect STAT3 phosphorylation (Nie et al., 2009). Others investigated K49 and K87 in more details and found that besides slightly diminishing STAT3 phosphorylation, mutation of these lysines does not affect STAT3 dimerization or DNA binding, but abrogates the IL-6-induced transcriptional activity of STAT3 at its target gene $hAGT$ (Ray et al., 2005). Ray and coworkers suggested that acetylation is required for stable interaction of STAT3 with p300 and subsequent recruitment of RNA polymerase II and transcription induction (Ray et al., 2005; Hou et al., 2008).

All of the above mentioned studies on STAT3 are consistent in that deacetylase inhibitors and thus increased acetylation positively affect STAT3 activity. By contrast, Catania et al. (2006) found that deacetylase inhibitors interfere with PDGF-induced transcriptional activity of STAT3, while phosphorylation, nuclear translocation and DNA binding remained intact, and Gupta et al. (2012) found that in diffuse large B cell lymphoma deacetylase inhibitors lead to increased K685 acetylation and attenuate STAT3 tyrosine phosphorylation and transcriptional activity. Altogether the reports are controversial regarding which STAT3 lysine residue is acetylated and regarding the consequence of STAT3 acetylation on its transcriptional activity.

Acetylation of STAT5

STAT5B acetylation at K359, K694 and K701 (corresponding to K359, K689 and K696 of STAT5A) was demonstrated by Ma et al. (2010) through mass spectrometry and acetylation-site-specific antibodies. Mutation of K359, K694, and to a lesser extent K701 to arginine reduced prolactin-induced STAT5 activity in a luciferase reporter assay. Mutation of K694 or K701 (both localized within the phosphotyrosine tail segment near the SH-2 domain) was further demonstrated to impair dimerization of STAT5B, thus giving a possible explanation for the diminished STAT5 downstream activity (Ma et al., 2010).

By contrast, mutation of K359, which is located within the DNA binding domain, had a minimal positive effect on STAT5 dimerization but nevertheless abrogated the ability of STAT5 to induce a luciferase reporter gene. STAT5A acetylation at K696 and the negative effect of K696 arginine mutation on STAT5A transcriptional activity was independently demonstrated elsewhere in a luciferase reporter assay in growth hormone-stimulated mouse embryonic fibroblasts (Van Nguyen et al., 2012). K696 acetylation of STAT5A after deacetylase inhibitor treatment was additionally confirmed in a global quantitative mass spectrometric approach (Choudhary et al., 2009).

While Ma et al. (2010) and Van Nguyen et al. (2012) concluded that acetylation has a positive effect on STAT5 activity, Sebastián et al. (2008) and our group (Rascle et al., 2003) found in GM-CSF-dependent macrophages and in the IL-3-dependent pro-B cell line Ba/F3 respectively that deacetylase inhibitors block STAT5 transcriptional activity. Both groups consistently reported that deacetylase inhibitor treatment inhibits expression of STAT5 target genes by preventing the recruitment of RNA polymerase II. Upstream STAT5 activating events, however, remain unaffected, including STAT5 phosphorylation, nuclear translocation and binding to DNA target sites. Similar findings have been reported for STAT1, STAT2 and STAT3 after deacetylase inhibitor treatment (Nusinzon & Horvath, 2003; Sakamoto et al., 2004; Catania et al., 2006).

2.3.7 STAT5 in cancer

Aberrant continuous activity of STAT5 can be found in many hematologic malignancies and in solid tumor cancers like breast cancer, prostate cancer, squamous cell carcinoma of the head and neck, hepatocellular carcinoma and melanoma (Koppikar et al., 2008; Ferbeyre & Moriggl, 2011). Activating mutations within STAT5 have been described (Rajala et al., 2013; Kontro et al., 2014), however, it is much more common that STAT5 is activated downstream of constitutively active oncogenic tyrosine kinases like BCR-ABL or JAK2(V617F) (Gesbert & Griffin, 2000; Funakoshi-Tago et al., 2010; Hoelbl et al., 2010; Walz et al., 2012). In other cancers, STAT5 is activated by autocrine or paracrine cytokine loops (Li et al., 2004; Bernichtein et al., 2010). In addition, SOCS proteins, transcriptional negative feedback regulators of the JAK/STAT pathway, are often downregulated in cancers (Galm et al., 2003; Tokita et al., 2007; Zhang et al., 2015; Kang et al., 2016). Persistent STAT5 activation directly contributes to cancer initiation and progression (Hoelbl et al., 2010; Ferbeyre & Moriggl, 2011; Walz et al., 2012; Weber et al., 2015), most likely through the influence of STAT5 on key genes regulating cell proliferation and survival such as cyclin D1, *Bcl-x*, *c-Myc* and *Pim-1* (Mui et al., 1996; Matsumura et al., 1999; Nosaka et al., 1999; Gesbert & Griffin, 2000; Kontro et al., 2014; Pinz et al., 2016).

Several inhibitors of the STAT pathway are approved or currently under clinical trial, most of them targeting the upstream kinase (Savage & Antman, 2002; O'Shea et al., 2015). Additional inhibitors repressing STAT5 function at the transcriptional level have been described, including the natural compound sulforaphane, the bromodomain inhibitor (+)-JQ1, or deacetylase inhibitors (Rascle et al., 2003; Liu et al., 2014; Pinz et al., 2014b). The synthetic chalcones α-Br-TMC and α-CF_3-TMC inhibit IL-3-induced JAK2 and STAT5 phosphorylation (Pinz et al., 2014a; Jobst et al., 2016). Although there is progress in the development of compounds which inhibit STAT5 function by directly binding to STAT5, targeting transcription factors like STAT5 remains difficult (Weber et al., 2013; Elumalai et al., 2015; Liao et al., 2015). Transcription factors exert most of their functions through protein-protein and protein-DNA interactions and accordingly lack well-defined hydrophobic binding pockets which typically serve as target for conventional membrane-permeable small molecules (Arkin & Wells, 2004; Buchwald, 2010; Liao et al., 2015). The identification of better druggable cofactors thus contains major potential for the development of specific therapies against STAT5-associated diseases.

2.4 Objectives

Deacetylase inhibitors inhibit STAT5-mediated transcription by impairing the recruitment of the transcription machinery to STAT5 target genes, while STAT5 binding to DNA remains unaffected (Rascle et al., 2003). However, the factors involved and their role in the inhibition of STAT5-mediated transcription remain unknown. The goal of this thesis was to characterize the molecular mechanism of inhibition of STAT5-mediated transcription by deacetylase inhibitors. Specific aims were to identify and characterize (i) the HDAC(s) involved and (ii) its/their acetylated substrate(s).

To identify the deacetylase(s) involved in STAT5-mediated transcription, the effect of selective deacetylase inhibitors on expression of STAT5 target genes was analyzed. This should allow the identification of possible candidates among the 11 known HDAC family members. To further identify HDAC candidates, the effect of siRNA-mediated knockdown of HDAC expression on the regulation of STAT5 target genes was investigated.

The acetylated substrate targeted for deacetylation might be STAT5 itself, a STAT5-specific cofactor or histone proteins. To assess a possible implication of STAT5 acetylation, several potential acetylation sites within STAT5 were mutated and the transcriptional activity of the generated mutants was analyzed either using luciferase reporter assays or by RT-qPCR of endogenous STAT5 target genes. Persistent acetylation of STAT5 or of an unknown STAT5-specific cofactor upon deacetylase inhibitor treatment might disrupt protein interactions between STAT5 and components of the transcriptional ma-

chinery. To analyze whether deacetylase inhibitor treatment might disrupt STAT5- and RNA polymerase II-containing protein complexes and to obtain clues towards the possible involvement of an acetylated STAT5-specific cofactor, gel filtration chromatography was performed, comparing the composition of untreated and deacetylase-inhibitor-treated nuclear complexes. To investigate whether histones might be the acetylated substrate, the effect of deacetylase inhibitors on histone acetylation was assessed globally by western blot and locally at STAT5 target and control genes by chromatin immunoprecipitation.

Together, this study will contribute to a better understanding of the mechanism of STAT5-mediated transcription and of its inhibition by deacetylase inhibitors. Ultimately, it should provide the molecular basis for the development of novel therapies against STAT5-associated cancers.

CHAPTER 3

Material and methods

3.1 Material

3.1.1 Chemicals and reagents

Standard chemicals not mentioned in the following list were purchased from Sigma-Aldrich, Merck, or AppliChem.

Chemical/Reagent	Manufacturer
β-Mercaptoethanol (14,3 M)	Sigma-Aldrich
Acrylamid/Bisacrylamid Rotiphorese Gel 30	Roth
Agarose, LE	Biozym
Ammonium persulfate (APS)	Sigma-Aldrich
Ampicillin sodium salt	Sigma-Aldrich
Bovine serum albumin (BSA)	Sigma-Aldrich
Bromphenolblue	Merck
Coomassie Brilliant Blue R-250	AppliChem
Dimethyl sulfoxide (DMSO)	Sigma-Aldrich
Dithiothreitol (DTT)	Sigma-Aldrich
DMEM	Gibco, Life Sciences
DNA ladder, 100 bp and 1 kb ladder	New England Biolabs
Doxycycline	Sigma-Aldrich
Dry skimmed milk	Sucofin
Ethidum bromide	Promega
Fetal calf serum (FCS)	PAN Biotech and Life Technology
G418 disulfate salt	Sigma-Aldrich
Gene Pulser Electroporation buffer	Bio-Rad
Glycogen	Affimetrix
Hygromycin B	PAN Biotech
Insulin	Sigma-Aldrich
Kanamycin sulfate	Gibco, Life Technology
LB-agar (Luria/Miller)	Roth

Chemical/Reagent	Manufacturer
LB-medium (Luria/Miller)	Roth
Lipofectamine 2000	Invitrogen
N,N,N,N-Tetramethylethylenediamine (TEMED)	Sigma-Aldrich
Penicillin-Streptomycin solution (100x)	Invitrogen
Phenol/chlorophorm/isoamyl alcohol (25/24/1)	Roth
Phenylmethylsulfonylfluoride (PMSF)	Sigma-Aldrich
PicTIXX Pluster & LinerPen	C. Kreuel
Ponceau S	Sigma-Aldrich
Protein Marker VI (10-245) prestained	AppliChem
Protein-A sepharose beads	GE Healthcare
recombinant murine Interleukin-3 (rmIL-3)	ImmunoTools
Roti-Quant, 5x Bradford reagent	Roth
ROX passive reference dye, 50x	Bio-Rad
RPMI 1640	PAN Biotech
Salmon Sperm DNA	Invitrogen
Sodium fluoride	Sigma-Aldrich
Sodium orthovanadate	Sigma-Aldrich
Trypsin/EDTA	PAN Biotech
Tween-20	AppliChem
WST-1 cell proliferation reagent	Roche

3.1.2 Buffers

All buffers were prepared with ultrapure water purified with Milli-Q-Synthesis Water Purification System (Millipore).

Table 3.1: Buffers

Buffer	Composition
150 mM NaCl wash buffer	20 mM Tris pH 8.0, 150 mM NaCl, 5 mM EDTA, 0.2% w/v SDS, 1% w/v Triton X-100, 10 μg/mL aprotinin, 10 μg/mL leupeptin, 0.5 mM PMSF, 10 mM NaF
500 mM NaCl wash buffer	20 mM Tris pH 8.0, 500 mM NaCl, 5 mM EDTA, 0.2% w/v SDS, 1% w/v Triton X-100, 10 μg/mL aprotinin, 10 μg/mL leupeptin, 0.5 mM PMSF, 10 mM NaF
Brij lysis buffer	10 mM Tris/HCl pH 7.5, 150 mM NaCl, 2 mM EDTA pH 8.0, 0.875% v/v Brij 97, 0.125% v/v NP40, 10 μg/mL aprotinin, 10 μg/mL leupeptin, 0.5 mM PMSF, 10 mM NaF, 1 mM Na_3VO_4
buffer A	10 mM Hepes pH 7.6, 15 mM KCl, 2 mM $MgCl_2$, 0.1 mM EDTA, 10 μg/mL aprotinin, 10 μg/mL leupeptin, 0.5 mM PMSF, 10 mM NaF, 1 mM Na_3VO_4
buffer B	nuclei prep buffer A, 0.1-0.2% NP40
buffer C	50 mM Hepes pH 7.9, 400 mM KCl, 0.1 mM EDTA, 10% glycerol, 10 μg/mL aprotinin, 10 μg/mL leupeptin, 0.5 mM PMSF, 10 mM NaF, 1 mM Na_3VO_4

Buffer	**Composition**
buffer CBB	100 mM Tris pH 9.4, 100 mM DTT, 10 μg/mL aprotinin, 10 μg/mL leupeptin, 0.5 mM PMSF, 10 mM NaF
buffer MA	10 mM Hepes pH 6.5, 10 mM EDTA, 0.25% Triton X-100, 10 μg/mL aprotinin, 10 μg/mL leupeptin, 0.5 mM PMSF, 10 mM NaF
buffer MB	10 mM Hepes pH 6.5, 1 mM EDTA, 200 mM NaCl, 10 μg/mL aprotinin, 10 μg/mL leupeptin, 0.5 mM PMSF, 10 mM NaF
Coomassie Blue staining solution	0.25% w/v Coomassie Brilliant Blue R-250, 45% v/v methanol, 10% v/v acetic acid
DMEM-based medium	DMEM supplemented with 10% v/v heat inactivated fetal calf serum, 1x penicillin/streptomycin and 2 mM glutamine
DNA loading dye, 10x	50 mM Tris/HCl pH 7.6, 60% glycerol, bromphenol blue, xylene cyanol
FT buffer	600 mM NaCl, 20 mM Tris/HCl pH 8.0, 20% v/v glycerol, 10 μg/mL aprotinin, 10 μg/mL leupeptin, 0.5 mM PMSF
GF buffer	25 mM Hepes pH 7.2, 0.1 M KCl, 0.1 mM EDTA, 5% v/v glycerol, 1 mM DTT, 100 μg/mL insulin, 2 mM benzamidine-HCl, 1 mM PMSF
HDG 150	20 mM Hepes pH 7.6, 150 mM KCl, 10% v/v glycerol, 0.5 mM DTT, 10 μg/mL aprotinin, 10 μg/mL leupeptin, 0.5 mM PMSF, 10 mM NaF
IP buffer	1/3 Triton dilution buffer, 2/3 SDS buffer
Lämmli loading dye, 4x	250 mM Tris/HCl pH 6.8, 40% v/v glycerol, 5% w/v SDS, 0.005% w/v bromphenol blue, 10% v/v β-mercaptoethanol
Lämmli SDS running buffer, 5x	125 mM Tris, 960 mM glycine, 0.5% w/v SDS
LB agar plates	LB-agar (Luria/Miller) from Roth: 10 g/L tryptone, 5 g/L yeast extract, 10 g/L NaCl, 15 g/L agar
LB medium	LB-medium (Luria/Miller) from Roth: 10 g/L tryptone, 5 g/L yeast extract, 10 g/L NaCl
LiCl wash buffer	10 mM Tris pH 8.0, 250 mM LiCl, 1 mM EDTA, 0.5% v/v NP-40, 0.5% w/v Deoxycholic acid (sodium salt), 10 μg/mL aprotinin, 10 μg/mL leupeptin, 0.5 mM PMSF, 10 mM NaF
MNase Reconstitution buffer	5 mM Tris pH 6.8, 50 mM NaCl, 50% v/v glycerol
P1	50 mM Tris/HCl pH 8.0, 10 mM EDTA
P2	200 mM NaOH, 1% w/v SDS
P3	3 mM potassiumacetate, pH 5.5
PBS, 10x	1.37 M NaCl, 27 mM KCl, 100 mM Na_2HPO_4, 18 mM KH_2PO_4, adjust to pH 7.4
PBST	1x PBS, 0.02% v/v Tween 20
RPMI-based medium	RPMI 1640 supplemented with 10% v/v heat inactivated fetal calf serum, 1x penicillin/streptomycin and 2 mM glutamine

Buffer	**Composition**
SDS buffer	50 mM Tris pH 8.0, 100 mM NaCl, 5 mM EDTA, 0.5% w/v SDS, 10 μg/mL aprotinin, 10 μg/mL leupeptin, 0.5 mM PMSF, 10 mM NaF
SDS-PAGE separation gel, 10%	same as 8% with the following exceptions: 3.3 mL Acrylamid/Bisacrylamid (30%, 49:1), 2.9 mL H_2O
SDS-PAGE separation gel, 15%	same as 8% with the following exceptions: 5 mL Acrylamid/Bisacrylamid (30%, 49:1), 0.6 ml H_2O
SDS-PAGE separation gel, 8%	2.7 mL Acrylamid/Bisacrylamid (30%, 49:1), 2.9 mL H_2O, 3.75 mL 1 M Tris-HCl pH 8.8, 574 μL 85% glycerol, 100 μL 10% w/v SDS, 50 μL 10% w/v APS, 10 μL TEMED)
SDS-PAGE stacking gel	1.3 mL Acrylamid/Bisacrylamid (30%, 49:1), 7.3 mL H_2O, 1.25 mL 1 M Tris-HCl pH 6.8, 100 μL 10% w/v SDS, 50 μL 10% w/v APS, 10 μL TEMED
TAE, 50x	2 M Tris, 50 mM EDTA, 1 M acetic acid
TBS, 10x	500 mM Tris, 1.5 M NaCl, adjust to pH 7.5 with HCl
TBST	1x TBS, 0.02% v/v Tween 20
TE	20 mM Tris pH 8.0, 1 mM EDTA
TFBI + glycerol	1xTFBI, 15% v/v glycerol
TFBI, 10x	300 mM potassium acetate, 1 M RbCl, 100 mM $CaCl_2$ x 2 H_2O, 500 mM $MnCl_2$ x 4 H_2O
TFBII + glycerol	1xTFBII, 15% v/v glycerol
TFBII, 5x	50 mM MOPS, 50 mM RbCl, 370mM $CaCl_2$
Towbin/SDS transfer buffer	25 mM Tris, 0.02% w/v SDS, 192 mM glycine, 20% v/v methanol
Triton dilution buffer	100 mM Tris pH 8.0, 100 mM NaCl, 5 mM EDTA, 5% w/v Triton X-100, 10 μg/mL aprotinin, 10 μg/mL leupeptin, 0.5 mM PMSF, 10 mM NaF

3.1.3 Deacetylase inhibitors and other small molecule compounds for cell treatment

Table 3.2: Deacetylase inhibitors and other small molecule compounds

Compound	Supplier	Stock C.[1]	Vehicle[2]
(+)-JQ1	BIOMOL GmbH (BPS Bioscience #27401)	5 mM	DMSO
α-Br-TMC[3]	provided by Sabine Amslinger (Al-Rifai et al., 2013)	100 mM	DMSO
Apicidin	Enzo Life Sciences (BML-GR340)	10 mM	DMSO
MGCD0103	Absource Diagnostics GmbH (Selleck S1122)	50 mM	DMSO
MS-275	Enzo Life Sciences (ALX-270-378)	25 mM	DMSO
Salermide	Cayman Chemicals (No. 13178)	500 mM	DMSO
trans-Resveratrol	Cayman Chemicals (No. 70675)	500 mM	DMSO
Trichostatin A (TSA)	Sigma-Aldrich (T8552)	1 mM	DMSO
Valproic Acid (VPA)	Enzo Life Sciences (ALX-550-304)	300 mM	H_2O

[1] The compounds were diluted at the indicated stock concentration (Stock C.) in the vehicle DMSO, or in the case of VPA in H_2O. Final compound concentration is indicated in the figure legends.
[2] Vehicle concentration was adjusted to 0.02% DMSO in all TSA experiments. All other vehicle concentrations are indicated in the figure legends.
[3] α-Bromo-2',3,4,4'-Tetramethoxychalcone

3.1.4 Nucleic acids

3.1.4.1 Nucleotides

Desoxynucleotides from Fermentas were used in thermo-cycling- or PCR-based DNA synthesis for cloning purposes. Desoxynucleotides for quantitative PCR reactions were obtained from Qiagen.

3.1.4.2 DNA-oligonucleotides

All DNA-oligonucleotides were purchased from Metabion and reconstituted in ultrapure water at a concentration of 100 μM. Oligonucleotides for cloning and sequencing were designed with the NetPrimer software provided by Premier Biosoft (www.premierbiosoft.com/netprimer/).

Primers for site-directed mutagenesis were designed with the QuikChange Primer Design Program (Agilent) available at www.genomics.agilent.com/primerDesignProgram.jsp. In case the program did not find optimal primers, they were designed manually according to the manual of the QuikChange II Site-Directed Mutagenesis Kit from Agilent. Quantitative real-time PCR primers for gene expression analysis and ChIP experiments were designed by Dr. Anne Rascle using Primer Express software (Applied Biosystems).

Table 3.3: Mouse gene expression primers for quantitative RT-PCR
Refer to 3.2.1.4

Gene	ID	Expression primer[1], sequence 5'-3'	
36b4	O5	forward	GCGTCCTGGCATTGTCTGT
	O6	reverse	GCCGCAAATGCAGATGG
c-Fos	O15	forward	CGAAGGGAACGGAATAAGATGG
	O16	reverse	AGACCTCCAGTCAAATCCAGGG
c-Myc	O11	forward	AACAGGAACTATGACCTCG
	O12	reverse	AGCAGCTCGAATTTCTTC
Cis	O9	forward	CTGGACTCTAACTGCTTGTC
	O10	reverse	TAGGCAGCACCGAGTCAC
Hdac1	O50	forward	AACAGAGGATGAGAAAGAGAAAGATC
	O51	reverse	TCAGGCCAACTTGACCTCTTC
Hdac2	O52	forward	AAGAAGACAAGAAGGAGACAGAGG
	O53	reverse	TCAAGGGTTGCTGAGTTGTTC
Hdac3	O54	forward	TCCCGGCAGACCTCCTGACG
	O55	reverse	TTTCCTTGTCGTTGTCATGGTCGC
Hdac4	O178	forward	CACTCCTGCGTCCTGCCTT
	O179	reverse	CGCCTGCTGTCCCTTTGTAC
Hdac5	O150	forward	ACGCCTCCCTCCTACAAATTG
	O151	reverse	GGAAAGTCATCACGGCTGTCA
Hdac6	O58	forward	GGCCAAGATTCTTCTACTAGACAGCG
	O59	reverse	CTAGATTGGGGCTGGAGTGGG
Hdac7	O60	forward	GCCCTGCCCTCCAGCCAGAC
	O61	reverse	GGTGTTGCAGGGTCAGCAGCG
Hdac8	O62	forward	CTGCGACTCCCTTGTGAAGG
	O63	reverse	GCAGGGCATAGGCTTCGAT
Hdac9	O129	forward	AGTTCACCAAACAATGGCCC
	O130	reverse	TGAAGCCTCATTTTCGGTCAC
Hdac10	O156	forward	GCCTGTGTTTGTCAGCTTGTG
	O157	reverse	GGGCTATATATTCCGGGCTGT
Hdac11	O158	forward	GGTGACCTCGGGTGGGTAC
	O159	reverse	GAGACGCAGGGAAACTCAGG
JunB	O46	forward	CAGCTACTTTTCGGGTCAGGG
	O47	reverse	GGCTAGCTTCAGAGATGCGC
Osm	O13	forward	AGATACCTGAGCCCACACAGACAG
	O14	reverse	ATCGTCCCATTCCCTGAAGACC
S9	O1	forward	GCAAGATGAAGCTGGATTAC
	O2	reverse	GGGATGTTCACCACCTG
Spi2.1	O48	forward	GGCAGTGCCCTGTTTATTGAA
	O49	reverse	GCTGGAAATCTGCTGTGAAGG
Spp1	O64	forward	CACTTTCACTCCAATCGTCCC
	O65	reverse	AAGCCAAGCTATCACCTCGG

[1] The amplicon length is 51 - 254 bp.

Table 3.4: ChIP primers used to quantify mouse genomic DNA from ChIP
Refer to 3.2.7

Amplic.[1]	Gene	Position[2]	ID	ChIP primer[3], sequence 5'-3'	
A	*Cis*	-831/-755, distal promoter	O84 O85	for rev	AGGGCTGTCTGGGAGCTGA TCTCTGAGTGGACCGACAGTTG
B	*Cis*	-259/-199, STAT5 binding site	O86 O87	for rev	CAACTCTAGGAGCTCCCGCC AACACCTTTGACAGATTTCCAAGAAC
C	*Cis*	-188/-104, STAT5 binding site	O88 O89	for rev	GTCCAAAGCACTAGACGCCTG TTCCCGGAAGCCTCATCTT
D	*Cis*	-18/+55, TSS	O90 O91	for rev	GTTCGCACCACAGCCTTTCAGTCC GTCCAGGGGTGCGAAGGTCAGG
E	*Cis*	+261/+322, ORF	O263 O264	for rev	GGACTTCGAGTGGTGTGCCTA GGCTCCGTTTCCCTATCCA
F	*Cis*	+502/+553, ORF	O241 O242	for rev	CATTCCTCCGTCCCAGGTC ACCTCAGGCTGGCTTCCTAAG
G	*Cis*	+1061/+1112, ORF	O245 O246	for rev	AATTTTCGGACTCTTCGGCA CACCCAAGAAAGGAAGGCAG
H	*Cis*	+2236/+2308, ORF	O249 O250	for rev	GAGGACACTGCCTTCCCTCA AAGCTTCTACCCACTCCGGC
I	*Cis*	+3963/+4029, ORF	O92 O93	for rev	TACCCCTTCCAACTCTGACTGAGC TTCCCTCCAGGATGTGACTGTG
J	*Osm*	-184/-122, STAT5 binding site	O138 O139	for rev	CATCATCCTTGGGCGTGGGGC CGCTCCTCCTCCCGTTTTCTTCG
K	*Osm*	+25/+87, TSS	O140 O141	for rev	GCTGCCAGCCTGCAGGACAC GTACTCTGGCCCGTGCCTCTCAG
L	*c-Fos*	-259/-200, prox. promoter	O144 O145	for rev	GACCATCTCCGAAATCCTACACGC CACATTTGGGATCTTAGGGGGTCTC
M	*c-Fos*	-70/-1, TSS	O146 O147	for rev	GGAAGTCCATCCATTCACAGCG CAGTCGCGGTTGGAGTAGTAGGC
N	*p21*	-120/-61, prox. promoter	O293 O294	for rev	GAGGGCGGGCCAGCGAGTC CTCAGAGGCAGGACCAACCCACTC
O	*p21*	+75/+136, TSS	O295 O296	for rev	ATCCAGACATTCAGAGGTGAGAGC CATTGCTACGGGGAAGAACTATTG

[1] Amplicon name as depicted in Figure 4.17.
[2] The position of the amplified region is indicated relative to the TSS.
[3] The amplicon length is 52 - 85 bp.

Table 3.5: Mutagenesis primers
Refer to 3.2.1.15

ID	Mutations	Position	Mutagenesis primer, sequence 5'-3'		RS[1]
O26	K675Q	STAT5A TAD	for	TTATCTACGTGTTCCCCGATCGA-CCCCAGGACGAGGTCTTTGC	PvuI
O27	K675Q	STAT5A TAD	rev	GCAAAGACCTCGTCCTGGGGTC-GATCGGGGAACACGTAGATAA	

ID	Mutations	Position	Mutagenesis Primer, Sequence 5'-3'		RS[1]
O28	K675R	STAT5A TAD	for	CTTATCTACGTGTTCCCCGATCGA-CCCCGGGACGAGGTCTTTGCCA	PvuI
O29			rev	CGTATCCGTCAACTGCTCGCGCA-AGTACTGGAGTGTAATACTTGGC	
O30	K681Q	STAT5A TAD	for	AGGACGAGGTCTTTGCCCAGTAC-TACACTCCTGTACTTGC	ScaI
O31			rev	GCAAGTACAGGAGTGTAGTACTG-GGCAAAGACCTCGTCCT	
O32	K681R	STAT5A TAD	for	ACGAGGTCTTTGCCCGGTATTAC-ACTCCAGTACTTGCGAAAG	ScaI
O33			rev	CTTTCGCAAGTACTGGAGTGTAA-TACCGGGCAAAGACCTCGT	
O34	K689Q	STAT5A TAD	for	CCAAGTATTACACTCCAGTACTT-GCGCAAGCAGTTGACGGATA	ScaI
O35			rev	TATCCGTCAACTGCTTGCGCAA-GTACTGGAGTGTAATACTTGG	
O36	K689R	STAT5A TAD	for	GCCAAGTATTACACTCCAGTACT-TGCGCGAGCAGTTGACGGATACG	ScaI
O37			rev	CGTATCCGTCAACTGCTCGCGCA-AGTACTGGAGTGTAATACTTGGC	
O38	K696Q	STAT5A TAD	for	CGAAAGCAGTTGACGGATACGTA-CAGCCACAGATCAAGC	SnaBI
O39			rev	GCTTGATCTGTGGCTGTACGTAT-CCGTCAACTGCTTTCG	
O40	K696R	STAT5A TAD	for	GCGAAAGCAGTTGACGGATACGT-ACGGCCACAGATCAAGCAAGT	SnaBI
O41			rev	ACTTGCTTGATCTGTGGCCGTAC-GTATCCGTCAACTGCTTTCGC	
O42	K700Q	STAT5A TAD	for	TGAAGCCACAGATCCAGCAAGTG-GTACCTGAGTTCGTCAA	KpnI
O43			rev	TTGACGAACTCAGGTACCACTTG-CTGGATCTGTGGCTTCA	
O44	K700R	STAT5A TAD	for	CGTGAAGCCACAGATCCGGCAAG-TGGTACCTGAGTTCGTCAATG	KpnI
O45			rev	CATTGACGAACTCAGGTACCACT-TGCCGGATCTGTGGCTTCACG	
O110	Y694F	STAT5A TAD	for	CCTGTACTTGCGAAAGCAGTCGA-CGGATTCGTGAAGCCAC	SalI
O111			rev	GTGGCTTCACGAATCCGTCGACT-GCTTTCGCAAGTACAGG	
O229	K675Q, K681Q	STAT5A TAD	for	CAGACCGACCCCAGGACGAGG-TCTTTGCCCAATATTACACTC	SspI
O230			rev	GAGTGTAATATTGGGCAAAGACC-TCGTCCTGGGGTCGGTCTG	
O231	K675R, K681R	STAT5A TAD	for	CAGACCGACCCCGGGACGAGGT-CTTTGCCAGGTATTACAC	SmaI/ XmaI
O232			rev	GTGTAATACCTGGCAAAGACCTC-GTCCCGGGGTCGGTCTG	

ID	Mutations	Position	Mutagenesis Primer, Sequence 5'-3'		RS[1]
O233	K696Q, K700Q	STAT5A TAD	for	GACGGATACGTACAGCCACAGATCCAGCAAGTGGTCC	SnaBI
O234			rev	GGACCACTTGCTGGATCTGTGGCTGTACGTATCCGTC	
O235	K696R, K700R	STAT5A TAD	for	GACGGATACGTAAGGCCACAGATCAGGCAAGTGGTCC	SnaBI
O236			rev	GGACCACTTGCCTGATCTGTGGCCTTACGTATCCGTC	
O273	K84Q	STAT5A N-term	for	ATGGGTTTTTGCTGCAGATCAAGCTTGGGCACTATGCCAC	HindIII
O274			rev	GTGGCATAGTGCCCAAGCTTGATCTGCAGCAAAAACCCAT	
O275	K84R	STAT5A N-term	for	GGGAAGATGGGTTTTTGCTGAGGATCAAGCTTGGGCACTATGC	HindIII
O276			rev	GCATAGTGCCCAAGCTTGATCCTCAGCAAAAACCCATCTTCCC	
O277	K359Q	STAT5A DBD	for	CCACCGTGCGCCTACTAGTGGGGGGACAGCTGAATG	SpeI
O278			rev	CATTCAGCTGTCCCCCCACTAGTAGGCGCACGGTGG	
O279	K359R	STAT5A DBD	for	CACCGTGCGCCTACTAGTGGGGGGAAGGCTGAATGTG	SpeI
O280			rev	CACATTCAGCCTTCCCCCCACTAGTAGGCGCACGGTG	
O281	K384Q	STAT5A DBD	for	GTCCCTGCTCCAGAATGAGAACACGCGTAATGAGTGCAGC	MluI
O282			rev	GCTGCACTCATTACGCGTGTTCTCATTCTGGAGCAGGGAC	
O283	K384R	STAT5A DBD	for	GTCCCTGCTCAGGAATGAGAACACGCGTAATGAGTGCAGC	MluI
O284			rev	GCTGCACTCATTACGCGTGTTCTCATTCCTGAGCAGGGAC	

[1] Restriction site created within the primer for screening.

Table 3.6: PCR Primers for cloning
Refer to 3.2.1.10

ID	Position	Cloning primer, sequence 5'-3'		RS[1]
O22	STAT5A CDS incl. AA666	for	GCGAATTCTTATCTACGTGTTCCC	EcoRI
O23	STAT5A CDS incl. stop codon	rev	CAAGTAAGCTTCAGGACAGGGAG	HindIII
O24	STAT5A CDS incl. AA666	for	GGCGAATTCTTATATATGTGTTTCC	EcoRI
O25	STAT5A CDS incl. stop codon	rev	CCGATAAGCTTCATGACTGTGC	HindIII

[1] Restriction site created within the primer for restriction digest and subsequent ligation of the PCR-amplicon with a vector backbone.

Table 3.7: Sequencing primers

ID	Sequencing primer[1], sequence 5'-3'		Position[2]
O17	for	CGACATCATCATCGGAAGAGAGTAG	pFA-CMV, 5' of MCS
O18	rev	ATGAGCCTTGGGACTGTGAATC	pFA-CMV, 3' of MCS
O19	for	GAACTGCTCCTCAGTGGATGTTG	pME18S, 5' of MCS
O20	rev	TATGTTTCAGGTTCAGGGGGAG	pME18S, 3' of MCS
O21	for	CGGAAGCAGCAGACCATCATC	STAT5A/B CDS

[1] In addition to the listed sequencing primers, primers provided by the sequencing service GeneArt (Thermo Fischer Scientific, Regensburg) were used: T7-Promotor, SP6, N-CMV-30 and BGHrev. MCS, multiple cloning site; CDS, coding sequence.
[2] The sequencing primer recognizes the indicated parental plasmid and all plasmids derived thereof.

3.1.4.3 Plasmids

All plasmids used in this study were verified by sequencing (GeneArt Sequencing Service, Regensburg). The plasmid pFA-mSTAT5A 666-793 (P20) expressing the fusion protein GAL4-STAT5A666 was generated by PCR cloning (3.2.1.10) as follows: The insert comprising amino acids 666-793(Stop) of mouse STAT5A was amplified by PCR (3.2.1.10) using the template pME18S-mSTAT5A (P02) and the primers O22 and O23 (shown in Table 3.6). The vector backbone was pFA-CMV (P04), which expresses the yeast GAL4 DNA binding domain (amino acids 1-147). The insert as well as the vector backbone were digested with the restriction enzymes EcoRI and HindIII (3.2.1.13), and subsequently ligated (3.2.1.14) to generate the plasmid. pFA-mSTAT5B 666-786 (P21) was generated likewise using the template pME18S-mSTAT5B (P03) as well as the primers O24 and O25.

Single or multiple lysine-to-glutamine or lysine-to-arginine mutations in GAL4-STAT5A666 (generating plasmids P22-P31) and in STAT5A-1∗6 (generating plasmids P120-P135 and P152-P157) were made by site-directed mutagenesis (3.2.1.15) using plasmid template and primers indicated in Table 3.8. As a positive control for an inactivating mutation, the tyrosine residue Y694 of STAT5A-1∗6 was mutated to phenylalanine, generating pcDNA3-mSTAT5A-1∗6-Y694F- FLAG (P151).

Table 3.8: Plasmids

ID	Plasmid	Generation/Details	Function	Reference
P02	pME18S-mSTAT5A		subcloning	S. Watanabe
P03	pME18S-mSTAT5B		subcloning	S. Watanabe
P04	pFA-CMV		empty vector control	Stratagene

ID	Plasmid	Generation/Details	Function	Reference
P05	pFA-mSTAT5A 709-793	Watanabe et al. (2001)	expression vector for GAL4-STAT5A709	S. Watanabe/ Tohru Itoh
P20	pFA-mSTAT5A 666-793	PCR amplicon from P02 with primers O22/O23 inserted into P04, see above	expression vector for GAL4-STAT5A666	S. Pinz
P21	pFA-mSTAT5B 666-786	PCR amplicon from P03 with primers O24/O25 inserted into P04, see above	expression vector	S. Pinz
P22	pFA-mSTAT5A 666-793 K675Q	made from P20 by SDM[1] with primers O26/O27	expression vector	S. Pinz
P23	pFA-mSTAT5A 666-793 K675R	made from P20 by SDM[1] with primers O28/O29	expression vector	S. Pinz
P24	pFA-mSTAT5A 666-793 K681Q	made from P20 by SDM[1] with primers O30/O31	expression vector	S. Pinz
P25	pFA-mSTAT5A 666-793 K681R	made from P20 by SDM[1] with primers O32/O33	expression vector	S. Pinz
P26	pFA-mSTAT5A 666-793 K689Q	made from P20 by SDM[1] with primers O34/O35	expression vector	S. Pinz
P27	pFA-mSTAT5A 666-793 K689R	made from P20 by SDM[1] with primers O36/O37	expression vector	S. Pinz
P28	pFA-mSTAT5A 666-793 K696Q	made from P20 by SDM[1] with primers O38/O39	expression vector	S. Pinz
P29	pFA-mSTAT5A 666-793 K696R	made from P20 by SDM[1] with primers O40/O41	expression vector	S. Pinz
P30	pFA-mSTAT5A 666-793 K700Q	made from P20 by SDM[1] with primers O42/O43	expression vector	S. Pinz
P31	pFA-mSTAT5A 666-793 K700R	made from P20 by SDM[1] with primers O44/O45	expression vector	S. Pinz
P33	pcDNA3		empty vector control	Invitrogen
P37	pMX.neo.mStat5Awt-FLAG		subcloning	T. Kitamura
P40	pMX.neo.mStat5A-1∗6-FLAG		subcloning	T. Kitamura
P49	phRL-CMV		*Renilla* luciferase reporter	Promega
P50	pRL-null		*Renilla* luciferase reporter	Promega

ID	Plasmid	Generation/Details	Function	Reference
P54	pcDNA3-mSTAT5Awt-FLAG	subcloned from P37 into P33 by EcoRI/NotI digest	expression vector	S. Unser
P55	pcDNA3-mSTAT5A-1∗6-FLAG	subcloned from P40 into P33 by EcoRI/NotI digest	expression vector	S. Unser/ L. Besl
P66	pGL4.35	contains 9 x GAL4 UAS and the *Firefly* luciferase luc2P gene	*Firefly* luciferase reporter	Promega
P103	pGVB-CisA-Luc	contains wt mouse *Cis* promoter fragment (-608/+67), Matsumoto et al. (1997)	*Firefly* luciferase reporter	A. Yoshimura
P106	pGVB-CisD-Luc	contains mouse *Cis* promoter fragment (-608/+67) with mutated STAT5 bs, Matsumoto et al. (1997)	*Firefly* luciferase reporter	A. Yoshimura
P111	pGVB-β-casein-Luc	contains rat β-casein promoter fragment (-105/+1), Chida et al. (1998)	*Firefly* luciferase reporter	A. Yoshimura
P120	pcDNA3-mSTAT5A-1∗6-K696Q-FLAG	made from P55 by SDM[1] with primers O38/O39	expression vector	S. Pinz/ L. Besl
P121	pcDNA3-mSTAT5A-1∗6-K696R-FLAG	made from P55 by SDM[1] with primers O40/O41	expression vector	S. Pinz/ L. Besl
P122	pcDNA3-mSTAT5A-1∗6-K700Q-FLAG	made from P55 by SDM[1] with primers O42/O43	expression vector	S. Pinz/ L. Besl
P123	pcDNA3-mSTAT5A-1∗6-K700R-FLAG	made from P55 by SDM[1] with primers O44/O45	expression vector	S. Pinz/ L. Besl
P124	pcDNA3-mSTAT5A-1∗6-K681Q-FLAG	made from P55 by SDM[1] with primers O30/O31	expression vector	S. Pinz/ L. Besl
P125	pcDNA3-mSTAT5A-1∗6-K681R-FLAG	made from P55 by SDM[1] with primers O32/O33	expression vector	S. Pinz/ L. Besl
P126	pcDNA3-mSTAT5A-1∗6-K689Q-FLAG	made from P55 by SDM[1] with primers O34/O35	expression vector	S. Pinz
P127	pcDNA3-mSTAT5A-1∗6-K689R-FLAG	made from P55 by SDM[1] with primers O36/O37	expression vector	S. Pinz/ L. Besl
P128	pcDNA3-mSTAT5A-1∗6-K675Q-FLAG	made from P55 by SDM[1] with primers O26/O27	expression vector	S. Pinz
P129	pcDNA3-mSTAT5A-1∗6-K675R-FLAG	made from P55 by SDM[1] with primers O28/O29	expression vector	S. Pinz/ L. Besl
P130	pcDNA3-mSTAT5A-1∗6-K696/700Q-FLAG	made from P55 by SDM[1] with primers O233/O234	expression vector	S. Pinz

ID	Plasmid	Generation/Details	Function	Reference
P131	pcDNA3-mSTAT5A-1∗6-K696/700R-FLAG	made from P55 by SDM[1] with primers O235/O236	expression vector	S. Pinz
P132	pcDNA3-mSTAT5A-1∗6-K689/696/700Q-FLAG	made from P126 by SDM[1] with primers O233/O234	expression vector	S. Pinz
P133	pcDNA3-mSTAT5A-1∗6-K689/696/700R-FLAG	made from P127 by SDM[1] with primers O235/O236	expression vector	S. Pinz
P134	pcDNA3-mSTAT5A-1∗6-K675/681/689/696/700Q-FLAG	made from P132 by SDM[1] with primers O229/O230	expression vector	S. Pinz
P135	pcDNA3-mSTAT5A-1∗6-K675/681/689/696/700R-FLAG	made from P133 by SDM[1] with primers O231/O232	expression vector	S. Pinz
P151	pcDNA3-mSTAT5A-1∗6-Y694F-FLAG	made from P55 by SDM[1] with primers O110/110	expression vector	S. Pinz
P152	pcDNA3-mSTAT5A-1∗6-K84Q-FLAG	made from P55 by SDM[1] with primers O273/O274	expression vector	S. Pinz
P153	pcDNA3-mSTAT5A-1∗6-K84R-FLAG	made from P55 by SDM[1] with primers O275/O276	expression vector	S. Pinz
P154	pcDNA3-mSTAT5A-1∗6-K359Q-FLAG	made from P55 by SDM[1] with primers O277/278	expression vector	S. Pinz
P155	pcDNA3-mSTAT5A-1∗6-K359R-FLAG	made from P55 by SDM[1] with primers O279/280	expression vector	S. Pinz
P156	pcDNA3-mSTAT5A-1∗6-K384Q-FLAG	made from P55 by SDM[1] with primers O281/282	expression vector	S. Pinz
P157	pcDNA3-mSTAT5A-1∗6-K384R-FLAG	made from P55 by SDM[1] with primers O283/284	expression vector	S. Pinz

[1] Site-directed mutagenesis, described in 3.2.1.15. Mutagenesis primers are listed in Table 3.5.

3.1.4.4 RNA-oligonucleotides

Control and mouse HDAC-specific siRNAs were double-stranded RNAs with dTdT overhangs on the 3' end of both strands. The siRNAs were obtained from Sigma Aldrich (MISSION siRNA), except for HD2.1 and ScI, which were from Dharmacon. The lyophilized siRNA was reconstituted in nuclease free H_2O to a concentration of 100 μM.

Table 3.9: siRNAs for transfections
Refer to 3.2.3.8.

Gene	ID	Antisense sequence 5'-3'
Hdac1	HD1.3	GCAGCGUCUCUUUGAGAAC[dT][dT]
Hdac2	HD2.1	GCAUCAGGGUUCUGCUAUG[dT][dT]
Hdac3	HD3.1	GUAUCCUGGAGCUGCUUAA[dT][dT]
Hdac5	HD5.1	CCUAGUCUCCGCUGGGUUU[dT][dT]
Hdac5	HD5.2	GUGACACGGUGUGGAAUGA[dT][dT]
Scramble I control	ScI	CAGUCGCGUUUGCGACUGG[dT][dT]

3.1.5 Enzymes

Table 3.10: Enzymes

Enzyme	Manufacturer
DNaseI	Roche
DpnI	New England Biolabs
HotStar Taq Polymerase	Qiagen
MNase	Sigma-Aldrich
Phusion High-Fidelity DNA Polymerase	Thermo Scientific
Proteinase K	Sigma-Aldrich
Restriction enzymes	New England Biolabs
RNaseA	Sigma-Aldrich
T4 DNA Ligase	New England Biolabs
Trypsin/EDTA	PAN Biotech

3.1.6 Antibodies

Table 3.11: Primary antibodies for western blot or ChIP
Refer to 3.2.5.6 or 3.2.7.

Antibody target	ID	Species	Company, order number	WB dilution[1]
acetylated histone H3	AB31	rabbit	Millipore, #06-599	1:5000
acetylated histone H4	AB32	rabbit	Millipore, #06-866	1:2000
α-tubulin	AB07	mouse	Santa Cruz, sc-32293	1:200
BRD2	AB61	rabbit	Bethyl, A302-583A	1:2000
FLAG	AB12	mouse	Sigma-Aldrich, F-1804	1:500
GAL4	AB11	mouse	Santa Cruz, sc-510	1:200
histone H3	AB40	rabbit	Abcam, ab1791	1:10000
HDAC1	AB08	mouse	Millipore, #05-100	1:1000
HDAC2	AB30	rabbit	Zymed/Invitrogen, 51-5100	1:1000
HDAC3	AB27	rabbit	Cell Signaling, #2632	1:500
HDAC5	AB39	rabbit	Abcam, ab1439	1:500
HDAC11	AB42	rabbit	Abgent, AP1111b	1:200
RNA Pol II (N-20)	AB34	rabbit	Santa Cruz, sc-899	1:1000
pSTAT5	AB06	rabbit	Cell Signaling, #9351	1:1000
STAT5 (C-17)	AB02	rabbit	Santa Cruz, sc-835	1:1000
STAT5A (L-20)	AB01	rabbit	Santa Cruz, sc-1081	1:1000
STAT5B (G-2)	AB45	mouse	Santa Cruz, sc-1656	1:200
IgG from rabbit serum	AB33	rabbit	Sigma-Aldrich, I-5006	

[1] Antibody dilution used for western blot (WB) (refer to 3.2.5.6).

Table 3.12: Secondary antibodies for western blot
Refer to 3.2.5.6

Secondary antibody	Enzyme[1]	Company, order number	WB dilution[2]
anti-mouse IgG	HRP	Sigma-Aldrich, A-8924	1: 10 000
anti-rabbit IgG	HRP	Sigma-Aldrich, A-0545	1: 20 000

[1] All secondary antibodies were coupled to horseradish peroxidase (HRP).
[2] Antibody dilution used for western blot (WB) (refer to 3.2.5.6).

3.1.7 Instruments

Only basic instruments are listed. All other method-specific instruments are mentioned in the respective method part.

Instrument	Manufacturer
-20°C freezer	Liebherr
-80°C freezer, Forma 900 Series	Thermo Scientific
4°C fridge	Liebherr
Cell cryo-tank, 810 ETERNE with TEC 2000 monitor	Chart MVE
Centrifuges 5417R, 5810R	Eppendorf
CO_2 Incubator, BBD 6220	Heraeus
Heating Block Thermostat, Bio TDB-100	Biosan
Heating oven	Binder GmbH
Hybridization oven	GFL 7601
Ice Flaker, AF8	Scotsman, Hubbard Systems
Liquid N2 tank, EURO-CYL 230/4	Chart MVE
Magnetic Stirrer	Heidolph
MaxQ 4000 Benchtop Orbital Shaker for *E. coli*	Thermo Scientific
Microwave	Panasonic
Milli-Q-Synthesis Water Purification System	Millipore
Mini-Centrifuge Sprout	Kisker
NanoPhotometer P300	Implen
pH meter, inoLab	WTW
Pipet-Lite P2, P20, P200, P1000	Rainin
Pipet-X Lightweight controler	Rainin
Power supply, PowerPac 300	Bio-Rad
Power supply, PowerPac Basic	Bio-Rad
Power supply, PowerPac HC	Bio-Rad
Precision scale, CP224S	Sartorius AG
Scale, EMB 220-1	KERN
Sterile bench, Hera Safe	Thermo Scientific
Thermocycler, MyCycler	Bio-Rad
ThermoMixer 5436	Eppendorf
Vortex Genie2	Scientific Industries

3.1.8 Consumables

Standard plastic consumables not mentioned in the following list were from Sarstedt.

Consumable	Manufacturer
0.1 mL PCR-Tubes and Caps for RotorGene Q	Kisker

Consumable	Manufacturer
384-well plate for quantitative PCR	Applied Biosystems, Peqlab
96-well microplate, black	Berthold Technologies
Cannula	BD
Cell culture flasks, T25, T75, T125	Sarstedt
Cell culture plates, 6-well, 24-well, 96-well, P10	Falcon, Fisher Scientific
Collodion Bags	Sartorius
Cryo vials	Sarstedt
Cuvettes for electroporation, 1 mm or 4 mm gap	VWR
Cuvettes, polystyrene 10 x 4 mm, 10 mm optical pathway	Sarstedt
Immobilon-P PVDF Membrane, 0.45 μm	Millipore
Optical adhesive cover for 384-well plate	Applied Biosystems, Bio-Rad
Pipette tips, LTS	Rainin
Syringe	BD
Whatman blotting paper	A. Hartenstein

3.2 Methods

3.2.1 DNA and RNA analysis and methods

3.2.1.1 RNA preparation

0.04 x 10^6 cells were washed in 1 mL PBS and centrifuged at 2000 rcf for 1 min at 4°C. 100 μL iScript RT-qPCR Sample Preparation Reagent (170-8899, Bio-Rad) was added to the cell pellet and the sample was vortexed for 30 sec at medium speed. The lysate was cleared by centrifugation at 15000 rcf for 2 min at 4°C. Usually it was immediately proceeded with cDNA synthesis (3.2.1.2). The remaining stabilized RNA-containing lysate was snap-frozen in liquid nitrogen and stored at -80°C.

Where indicated, total RNA was purified with MN NucleoSpin RNA II kit as recommended by the manufacturer.

3.2.1.2 cDNA synthesis

cDNA was synthesized from 1 μL RNA preparation (from 3.2.1.1) according to Bio-Rad's recommendations for the iScript cDNA Synthesis Kit (170-8891, Bio-Rad). In brief, 1 μL RNA-template was added to 14 μL nuclease free H_2O and then mixed with 4 μL 5x iScript reaction mix and 1 μL reverse transcriptase. The sample was placed in a thermocycler with the following program: 5 min at 25°C, 30 min at 42°C, 5 min at 85°C, hold at 16°C. The cDNA samples were stored at -20°C.

3.2.1.3 Quantitative real-time polymerase chain reaction (qPCR)

Quantitative real-time PCR (qPCR) was performed on a RotorGene Q (Qiagen), except for a few initial experiments on a 7900HT Real-Time PCR System (Applied Biosystems). The obtained data were very similar on both systems.

For analysis on the RotorGene Q, qPCR reactions were performed in 20 μL final volume in 0.1 mL tubes. A reaction contained 0.02 U/μL HotStarTaq Polymerase (Qiagen), 0.25 μL of a 1:500000 SYBR-Green I-dilution in DMSO (starting from a 10000x SYBR Green I stock solution from Roche), 1x PCR buffer (Qiagen), 1 mM additional $MgCl_2$ (already 1.5 mM $MgCl_2$ from 1x PCR buffer), 0.2 mM dNTPs (each), 0.4 μM forward and reverse primer as well as 0.3 - 0.6 μL cDNA (3.2.1.2) or 2.5 - 5 μL genomic ChIP DNA (3.2.7).

For analysis on the 7900HT Real-Time PCR System, qPCR reactions were performed in 10 μL final volume in 384-well plates. The reaction mix had the same composition as for RotorGene Q, except that 1x ROX passive reference dye was added and 0.3 μL cDNA were used per analysis.

PCR and signal acquisition were performed with the following parameters: An initial step of 15 min at 95°C was followed by a 2-step cycling program (15 s at 95°C, 60 s at 60°C), which was repeated 40 times. Eventually a program was added to determine the melt curve of the generated amplicons.

Amplification curves and threshold cycles (C_t) were calculated with the basic Quantitation Analysis Tool of the Rotor-Gene Q Series Software 2.0.3 or the equivalent software of the 7900HT Real-Time PCR System.

3.2.1.4 Gene expression analysis by quantitative reverse transcription PCR (quantitative RT-PCR)

RNA was prepared with iScript RT-qPCR sample preparation reagent (Bio-Rad) as described in 3.2.1.1, followed by reverse transcription cDNA synthesis as described in 3.2.1.2. The cDNA was used as template for quantitative PCR (3.2.1.3) using expression primers listed in Table 3.3. The obtained threshold cycle (C_t) for the gene of interest was normalized to the C_t of the reference gene mouse ribosomal protein S9 using the ΔC_t method with the following formula: expression target gene/reference gene=$2^{-\Delta C_t}$, where $\Delta C_t = C_{t(\text{target gene})} - C_{t(\text{reference gene})}$. To improve the clarity of the graphs, the obtained values were multiplied by 10000. qPCR was performed in duplicate or triplicate, and data shown are mean +/- standard deviation from one representative of at least two independent experiments.

3.2.1.5 Phenol extraction

After addition of one volume phenol/chloroform/isoamyl alcohol (25/24/1, pH 8.0) to an aqueous DNA solution, the sample was vortexed for 10-30 s and then centrifuged at 20000 rcf for 60 s at RT. The upper, DNA-containing, aqueous phase was transferred to a new reaction tube and the DNA was subjected to ethanol precipitation (3.2.1.6).

3.2.1.6 Ethanol precipitation

0.06 μg/μL glycogen, 1/10$^{\text{th}}$ volume 3 M sodiumacetate pH 5.2, and 2.5 volumes ethanol (pre-cooled at -20°C) were added to an aqueous DNA solution. After vortexing and incubation at -20°C for 15 min, the DNA was precipitated by centrifugation at 20000 rcf for 10 min at 4°C. The DNA pellet was washed in 500 μL 70% v/v ethanol (pre-cooled at -20°C), air-dried, and dissolved in TE or ultrapure H_2O for further applications.

3.2.1.7 Isopropanol precipitation

DNA was precipitated from an aqueous solution by addition of 1 volume isopropanol, followed by vortexing and centrifugation at 20000 rcf for 10 min at RT. The DNA pellet was washed in 500 μL 70% v/v ethanol (pre-cooled at -20°C), air-dried, and dissolved in TE or ultrapure H_2O for further applications.

3.2.1.8 Plasmid preparation

Small scale plasmid preparations for screening purposes were prepared from 1.5 mL *E. coli* LB-culture (3.2.2.1) using buffers listed in Table 3.1. The bacteria were pelleted at 9000 rcf for 3 min at 4°C and resuspended in 250 μL buffer P1 supplemented with 10 μg/mL RNase1. 250 μL buffer P2 were added, and the sample was mixed by gently inverting the tube. After incubation for 4-5 min at RT, addition of 250 μL buffer P3, and gentle inversion of the tube, the samples were incubated for 15 min on ice and debris was removed by centrifugation (20000 rcf, 10 min, RT). The supernatant was subjected to isopropanol precipitation (3.2.1.7), and the DNA pellet was dissolved in 50 μL ultrapure H_2O. 2-5 μL of the plasmid preparation were analyzed by agarose gel electrophoresis (3.2.1.11).

Expression plasmid DNA was prepared according to the high yield protocol of the Qiagen Plasmid Pure Midi Kit. All required buffers and consumables were included in the kit. In brief, *E. coli* from 35 mL LB-culture (3.2.2.1) were lysed using 4 mL each of kit buffer P1, P2 and P3. After clearing the lysate through a filter-cartridge, 2 mL binding buffer BB were added, and the DNA was purified on a Qiagen Plasmid Plus spin column. The DNA was eluted from the column with 200 μL buffer EB. The DNA concentration of

the plasmid preparation was measured by UV spectroscopy (3.2.1.9). The total amount of eluted DNA usually varied between 100 and 400 μg.

3.2.1.9 DNA quantification by UV spectroscopy

The DNA concentration of aqueous DNA solutions was determined by UV spectroscopy on a NanoPhotometer P300 (Implen). After measuring the absorbance at 260 nm, the DNA concentration was calculated by the instrument according to the Lambert-Beer Law:

$A = \varepsilon * c * L \longrightarrow c = A / (\varepsilon * L)$

A: Absorbance (measured at 260 nm)
c: concentration
ε: extinction coefficient ($\varepsilon_{\text{DNA, 260 nm}} = 0.02$ mL/(μg*cm)
L: length of the light path through the sample

In addition, absorbance at 280 nm was measured to determine the purity of the sample. For pure DNA, the A_{260}/A_{280} ratio is 1.8.

3.2.1.10 PCR cloning

Polymerase chain reaction (PCR) was used to amplify DNA sequences for plasmid cloning. The used cloning primers (Tab. 3.6) contained 5' overhanging restriction sites for later restriction enzyme digest and ligation into the equally digested plasmid backbone. A 50 μL PCR reaction was set up, containing 1x Taq Buffer, 250 nM of each dNTP, 250 nM forward and reverse primer, 30 pg plasmid DNA template, and 1 μL Taq (prepared by AG Hehlgans from the Institute of Immunology). The PCR was performed in a thermocycler with the following parameters: An initial step of 4 min denaturation at 95°C was followed by 35 repeats of a cycling program (30 sec at 95°C, 30 sec at 52°C and 60 sec at 72°C). The program closed with a final elongation at 72°C for 10 min and a cooling-down to 16°C.

The PCR reaction was separated by agarose gel elecrophoresis and the DNA fragment of expected size was purified from the gel (3.2.1.12) for further digest (3.2.1.13) and ligation (3.2.1.14).

3.2.1.11 Agarose gel electrophoresis

Agarose was dissolved in 0.5x TAE at a concentration of 0.7 to 2.0% w/v in a microwave oven. 0.2 μg/mL ethidium bromide was added and the gel was casted in a horizontal gel chamber ((Wide) Mini-Sub Cell GT, Bio-Rad). DNA samples were adjusted to 1x DNA

loading dye, loaded onto the gel, and separated at 100-120 V in 0.5x TAE as running buffer. In addition to the samples, a DNA ladder (1 kb or 100 bp DNA ladder from NEB) was loaded onto the gel, which allowed to estimate the size and quantity of the DNA fragments if interest. The DNA was visualized in the GeneGenious Gel Imaging System (Syngene) through the fluorescent, DNA-intercalating ethidium bromide, which emits light at 605 nm after excitation with ultraviolet light.

3.2.1.12 Purification of DNA fragments from agarose gel

The DNA was separated according to size by agarose gel electrophoresis (3.2.1.11). The fragment of expected size was excised from the gel and purified with the column-based Wizard SV Gel and PCR Clean-Up System (Promega) according to the manufacturer's recommendations. Eventually, the DNA was eluted from the purification column using 50 μL ultrapure H_2O. The DNA concentration was determined by UV spectroscopy (3.2.1.9).

3.2.1.13 Restriction enzyme digest

All sequence specific restriction endonucleases were from NEB. 1-2 units restriction enzyme were used to digest 1 μg plasmid DNA. To limit enzyme inhibition by glycerol contained in the enzyme storage buffer, the volume of enzyme should not exceed 10% of the total reaction volume. For a test digest, 0.5 μg plasmid DNA were digested in 10 μL total volume within 1 h incubation. A preparative digest involved 20 μg DNA and 40 units restriction enzyme in 50 μL final volume, as well as 2 h incubation. Incubation temperature, buffer and BSA content of the reaction were adjusted for each enzyme as recommended by the manufacturer.

3.2.1.14 Ligation

Digested (3.2.1.13) and purified (3.2.1.12) vector-backbone and insert were ligated in a ratio of 1:1.5 - 1:6 (vector:insert), while the total DNA amount was adjusted to 50 ng. The final volume of the reaction was 15 μL including 1.5 μL 10x T4 DNA ligase buffer (NEB) and 1 μL T4 DNA ligase (NEB). The reaction was placed in an insulating box, which was closed at RT and kept O/N at 4°C.

3.2.1.15 Site-directed mutagenesis

Three steps were required to introduce mutations into a plasmid by site-directed mutagenesis.

First, the mutant DNA was synthesized by thermal cycling using a DNA polymerase and mutagenesis primers (for a list of all mutagenesis primers see Table 3.5). In addition to the point mutation leading to the desired amino acid exchange, each primer contained a silent mutation which created a restriction site for screening. A reaction of 50 μL volume contained 1x HF-Buffer (Thermo Fischer Scientific), 0.5 mM additional $MgCl_2$ (1.5 mM $MgCl_2$ provided by HF-buffer), 250 μM of each dNTP, 1 U Phusion High-Fidelity DNA Polymerase, 125 ng forward and reverse primer, and 10-50 ng plasmid DNA template. The reaction conditions were 1 min initial denaturation at 95°C, followed by 16 cycles of denaturation at 95°C for 30 s, primer annealing at 58°C for 1 min, and elongation at 68°C for 5-8 min (1 min elongation per kb plasmid template), finishing with a final hold at 16°C.

Second, 1 U methylation sensitive endonuclease DpnI was added, and the reaction was incubated for 1 hour at 37°C. DpnI cuts only parental methylated or hemimethylated DNA, while leaving newly synthesized, unmethylated DNA intact.

Third, 10 μL of the digested sample was used for transformation (3.2.2.4) of 100 μL chemically competent XL1-Blue *E. coli*. Plasmid DNA was prepared (3.2.1.8) and screened by digestion with the restriction endonuclease whose recognition site was created in the mutagenesis primer (Tab. 3.5). The correct coding sequence of the STAT5A-1∗6 mutants was verified with the forward primers T7P, O21 and the reverse primer SP6 by sequencing (GeneArt Sequencing Service, Thermo Fischer Scientific, Regensburg). In case of the GAL4-STAT5A666 mutants, the sequence was verified with O18 (for a list of sequencing primers see Table 3.7).

3.2.2 Manipulation of *Escherichia coli*

3.2.2.1 *Escherichia coli* (*E. coli*) cultures in LB medium

LB medium was inoculated with *E. coli* and incubated O/N at 37°C on a shaker. In case the culture was designated for plasmid isolation (3.2.1.8) or glycerol-stock (3.2.2.2), antibiotics had been added to the LB medium at a concentration of 200 μg/mL ampicillin or 25 μg/mL kanamycin.

3.2.2.2 *E. coli* glycerol-stock

1 mL *E. coli* LB-culture (3.2.2.1) was added to 500 μL 60% v/v glycerol to yield a final glycerol concentration of 20% v/v. The glycerol-stock was first cooled to -20°C and then stored at -80°C.

3.2.2.3 Chemically competent *E. coli*

100 mL LB medium were inoculated with 500 μL XL1-Blue *E. coli* culture (3.2.2.1) and incubated at 37°C on a shaker until an OD_{600} of 0.5 - 0.6 was reached. The flask was placed in an ice bath and stirred for 15 min, followed by centrifugation at 3200 rcf for 5 min at 4°C. After resuspending the pellet in 40 mL TFBI + glycerol (pre-cooled on ice) and 15 min incubation on ice, the bacteria were centrifuged as before. The pellet was resuspended in 4 mL TFBII + glycerol. Aliquots were snap frozen in liquid nitrogen and stored at -80°C.

3.2.2.4 Transformation of *E. coli*

100 μL chemically competent XL1-Blue *E. coli* (3.2.2.3) were mixed with 5 μL ligation reaction (3.2.1.14). 30 min incubation on ice were followed by a heat shock of 1.5 min at 42°C and immediate cooling on ice for 3-5 min. 500 μL LB medium were added, and the bacteria were allowed to recover for 1 h at 37°C. To concentrate the bacteria prior to plating, they were pelleted (8000 rcf, 30 sec, RT) and 400 μL supernatant was removed. The *E. coli* were resuspended in the remaining 200 μL volume and plated on an LB agar plate containing 200 μg/mL ampicillin or 25 μg/mL kanamycin, depending on the resistance gene encoded on the plasmid. The plates were incubated at 37°C O/N.

In case purified plasmid DNA was to be transformed instead of a ligation reaction, the same protocol applied, except for the following changes: A few ng of the plasmid DNA and 50 μL chemically competent XL1-Blue were used. For recovery, 250 μL LB-medium were added and 50 μL of the sample were plated, omitting the centrifugation step.

3.2.3 Eukaryotic cell culture

3.2.3.1 Cell maintenance

All eukaryotic cells were cultured in a humidified incubator at 37°C under 5% CO_2.

Cell lines based on the murine pro B-cell line Ba/F3 were grown in RPMI 1640 supplemented with 10% v/v heat inactivated FCS, 1x penicillin/streptomycin (100 U/mL penicillin, 100 μg/mL streptomycin) and 2 mM glutamine. This cell culture medium will be referred to as RPMI-based medium thereafter. RPMI-based medium for the parental non-tumorigenic, immortalized, IL-3-dependent cell line Ba/F3 contained additionally 2 ng/mL rmIL-3 (IL-3). The Ba/F3-1∗6 cell line (clone F7, described in Pinz et al., 2014a), expressing stably integrated, FLAG-tagged, constitutively active mouse STAT5A-1∗6, was grown in RPMI-based medium containing 0.6 mg/mL G418. Ba/F3-tet-on-1∗6 cells (clone D4.1, described in Pinz et al., 2015) express the rtTA- Advanced transactivator

and carry stably integrated FLAG-tagged mouse STAT5A-1∗6, whose expression can be induced conditionally upon addition of tetracycline. During maintenance, Ba/F3-tet-on-1∗6 cells were grown in RPMI-based medium supplemented with 2 ng/mL IL-3, 0.6 mg/mL G418, and 0.8 mg/mL hygromycin. For induction of STAT5A-1∗6, the cells were cultured in RPMI-based medium containing 1 μg/mL of the tetracycline doxycycline. The Ba/F3-G4-Luc2P cell line, carrying the stably integrated *Firefly* luciferase Luc2P gene together with its 9xUAS (upstream activating sequences), was generated by stably transfecting Ba/F3 cells by electroporation with the plasmid pGL4.35 (P66). Stable clones were selected in the presence of hygromycin B and screed for basal luciferase activity. Clone 2.A was chosen for this study. Ba/F3-G4-Luc2P cells were maintained in RPMI-based medium containing 2 ng/mL IL-3 and 0.6 mg/mL hygromycin B (This cell line was generated together with Susanne Brüggemann and Dr. Anne Rascle). All Ba/F3-derived suspension cells were split every 2-3 days and grown to a cell density of maximally 1 x 10^6 cells/mL.

Cos-7 cells were cultured in DMEM supplemented with 10% v/v heat inactivated FCS, 1x penicillin/streptomycin (100 U/mL penicillin, 100 μg/mL streptomycin), and 2 mM glutamine (referred to as DMEM-based medium thereafter). The adherently growing Cos-7 cells were trypsinized for passaging at 70-90% confluency (every 2-3 days). After 3-5 min incubation in Trypsin/EDTA at 37°C, the reaction was stopped by addition of two volumes DMEM-based medium. The cells were pelleted by centrifugation at 300 rcf for 5 min, resuspended in DMEM-based medium, and seeded in the appropriate cell culture flasks or plates.

3.2.3.2 Cryopreservation of mammalian cells

Cells were pelleted (suspension cells directly, adherent cells after trypsinization (3.2.3.1)) and suspended in FCS containing 10% v/v DMSO. 1 mL aliquots of the cells were frozen in cryo vials at -80°C. They were transferred to the liquid nitrogen tank for long term storage. For Ba/F3 cells, 5 x 10^6 cells were frozen per aliquot. In case of Cos-7 cells, seven 1 mL aliquots were prepared per 70-90% confluent T75 flask.

3.2.3.3 Thawing of mammalian cells

Cryopreserved cells (3.2.3.2) were thawed and immediately transferred to the appropriate cell culture medium (10 mL for suspension cells, 5 mL for adherent cells) in a T25 flask. The culture medium required for the different cell lines is described in 3.2.3.1, however, selection antibiotics were omitted. After 4-6 h recovery, suspension cells were spun down (300 rcf, 5 min). The DMSO-containing supernatant was aspirated, and the cells were

cultured in fresh culture medium with the appropriate selection antibiotics. In case of adherent Cos-7 cells, the supernatant was aspirated and substituted with fresh DMEM-based medium as soon as the cells had attached to the plate.

3.2.3.4 Cell resting and IL-3 stimulation

Ba/F3 or Ba/F3-tet-on-1∗6 cells were washed twice in RPMI 1640 (centrifugation at 300 rcf, 5 min) and subsequently cultured for 6-12 h in RPMI-based medium before cytokine stimulation with 2 ng/mL rmIL-3. The duration of stimulation depended on the downstream assay and is indicated in the figure legends.

3.2.3.5 WST1 cytotoxicity assay

The WST-1 cytotoxicity assay (Roche) was performed as recommended by the manufacturer. 0.75 x 10^5 rested Ba/F3 cells were pre-incubated for 30 min with the deacetylase inhibitor in 100 μL RPMI-based medium in a clear flat-bottom 96-well cell culture plate. 10 μL WST-1 reagent plus IL-3 (for 2 ng/mL final IL-3 concentration) were added, followed by another 90 min incubation. This protocol reflects the IL-3 stimulation setting used in other experiments, while allowing sufficient incubation for cleavage of the WST-1 reagent. The stronger the cytotoxic effect of the inhibitor, the less active are the mitochondrial dehydrogenases of the cells and the less WST-1 (a tetrazolium salt) is cleaved. The water-soluble cleavage product (formazan) leads to a strong increase in absorbance at 450 nm, which was measured with a multiplate reader (Mithras LB 940, Berthold Technologies). To account for background signals, absorbance at 620 nm was subtracted from the value obtained at 450 nm. Cytotoxicity was calculated relative to vehicle control (0% cytotoxicity) and treatment with 1% Triton X-100 (100% cytotoxicity) according to the following equation: $(A_{\text{sample}}\text{-}A_{\text{vehicle control}})/(A_{\text{Triton X-100}}\text{-}A_{\text{vehicle control}})\text{x}100$. WST-1 reactions were performed in duplicate (quadruplicate for vehicle controls) and data shown are mean +/- standard deviation from one representative of at least two independent experiments.

3.2.3.6 Plasmid transient transfection of Cos-7 cells by Lipofectamine 2000

On the day before transfection, 0.25 x 10^6 Cos-7 cells were seeded per well of a 6-well plate in 2.5 mL DMEM-based medium. Thus, the cells reached 70% confluency for transfection.

2 μL Lipofectamine 2000 (Invitrogen) were mixed gently with 248 μL DMEM and incubated for 5 min at RT. The Lipofectamine dilution was combined with 1-2 μg plasmid DNA diluted in 250 μL DMEM (500 μL final volume). The Lipofectamine-DNA-mix was incubated for 20 min at RT. The mix was then added to the Cos-7 cells, whose medium

had been changed to 1 mL DMEM. The cells were incubated for 4 h in the humidified cell culture incubator at 37°C and 5% CO_2. Eventually, 1 mL DMEM supplemented with 25% v/v heat inactivated FCS, 1x penicillin/streptomycin and 2 mM glutamine was added to each well to yield the usual FCS concentration of 10%. The cells were harvested 24 h after transfection.

3.2.3.7 Plasmid transient transfection of Ba/F3 cells by electroporation

Ba/F3 or Ba/F2-G4-Luc2P cells (grown to a cell density of 0.7-0.9 x 10^6 cells/mL) were pelleted at 300 rcf for 5 min and washed once in RPMI 1640. 4 x 10^6 cells were mixed with 8-10 μg plasmid DNA in 800 μL RPMI 1640 and incubated for 10 min at RT. The cells were transferred to a 4 mm gap electroporation cuvette, and a pulse of 320 V, 950 μF was delivered using the exponential decay program of the Gene Pulser Xcell with CE module (Bio-Rad). The pulsed samples were incubated for 5 min at RT and then transferred to RPMI - based medium containing IL-3 where indicated but no selection antibiotics. The incubation time until cell harvest depended on the downstream assay.

The only exception were transient transfections of Ba/F3 cells with the expression vectors for pFA-CMV (P04), GAL4-STAT5A666 (P20) and GAL4-STAT5A709 (P05) (Fig. 4.10B). They were performed as described for siRNA transfection (3.2.3.8), except that per transfection 2 μg DNA were used instead of siRNA. For luciferase assays, 3 transfections were performed per condition, and the cells were harvested 8 h after transfection. For analysis of protein levels, 2 transfections were performed per condition, and the cells were harvested 24 h after transfection.

3.2.3.8 siRNA transfection by electroporation

Ba/F3-1∗6 cells were transfected with siRNA (Tab. 3.9) twice in an interval of 24 h. 48-72 h after the first transfection, the cells were harvested to analyze gene expression and protein levels.

Ba/F3-1∗6 cells, grown to a cell density of 0.7-0.9 x 10^6 cells/mL, were pelleted at 300 rcf for 5 min and washed once in PBS. Per transfection, 1 x 10^6 cells were resuspended in 100 μL Gene Pulser Electroporation buffer (Bio-Rad) containing 0.5 μM (single knockdown) or 0.6 μM (multiple knockdown) siRNA. The sample was transferred to a 1 mm gap electroporation cuvette, and a pulse was delivered with the following parameters of the Gene Pulser Xcell with CE module (Bio-Rad): square wave program, 95 V, 5 ms, 2 pulses, 0.1 s interval. The sample was transferred to a 6-well plate containing 3 mL RPMI-based medium per well. After 24 h there were usually 1-1.2 x 10^6 cells per condition. The cells were washed and transfected again as described.

48-72 h after the first transfection, the cells were harvested. One aliquot of each sample was processed for gene expression analysis by quantitative RT-PCR (3.2.1.4). The remaining cells were lysed for subsequent analysis of protein levels by western blot (3.2.5.6).

3.2.4 Preparation of cell lysates

3.2.4.1 Whole-cell brij lysate

Cells were pelleted (2000 rcf, 1 min, 4°C) and washed once in PBS. 2 x 10^6 cells were suspended in 40-50 μL Brij lysis buffer and kept on ice for 30 min. The lysate was centrifuged at full speed (20000 rcf) for 10 min at 4°C, and the pellet was discarded. The protein concentration of the lysate was determined by Bradford protein assay (3.2.5.1).

3.2.4.2 Freeze-thaw lysate for analysis of histone acetylation

Cells were pelleted (2000 rcf, 1 min, 4°C), washed once in PBS, and then suspended in 50 μL FT-buffer per 1 x 10^6 cells. In case the cells had been treated with deacetylase inhibitors, the FT-buffer was supplemented with the same inhibitor concentrations. The samples were subjected to three freeze-thaw cycles in liquid nitrogen and at 37°C respectively. The $MgCl_2$ concentration was adjusted to 5 mM, and DNaseI was added to yield a concentration of 0.1 μg/μL. The samples were incubated for 45 min at 4°C on a rotating wheel, adjusted to 1x Lämmli loading dye, heated for 10 min at 95°C, and eventually centrifuged at maximum speed (20000 rcf) for 15 min at 10°C to remove cell debris. This lysis procedure extracts histones from chromatin so that they can be separated by 15% SDS-PAGE (3.2.5.2) and analyzed by western blot (3.2.5.6).

3.2.4.3 Nuclear and cytosolic lysate

1 x 10^7 cells were pelleted (350 rcf, 5 min, 4°C) and washed once in PBS. The cells were washed once in buffer A with centrifugation at 350 rcf for 30 s at 4°C. Then, they were resuspended gently in 200 μL buffer B until a homogenous suspension was obtained. Buffer B disrupts the plasma membrane while leaving the nuclear envelope intact. The nuclei were pelleted at 350 rcf, 30 s, 4°C, and the supernatant, representing the cytosolic fraction, was collected. After a wash in buffer A (350 rcf, 30 s, 4°C), the nuclei were lysed in 50 μL buffer C for 30 min on ice with occasional vortexing. Eventually, the nuclear lysate was cleared by centrifugation at maximum speed (20000 rcf) for 15 min at 4°C.

3.2.5 Protein analysis and methods

3.2.5.1 Protein quantification by Bradford protein assay

1 to 2 μL cell lysate (and the same volume of lysis buffer as a control) was mixed with 1 mL 1x Roti-Quant Bradford reagent in polystyrene cuvettes with 10 mm optical pathway and incubated for at least 6 min at RT. In parallel, a standard curve was generated by addition of 2 μg, 3 μg, 5 μg, 10 μg and 15 μg BSA to 1 mL 1x Bradford reagent each. Absorbance was measured at 595 nm with a UV/Vis spectrophotometer (NanoPhotometer P300, Implen). The protein content of the lysate was derived from the standard curve. The value of the lysis buffer control was subtracted to obtain the corrected protein concentration of the lysates.

3.2.5.2 SDS - polyacrylamide gel electrophoresis (SDS-PAGE)

A discontinuous polyacrylamide gel was casted between gel plates with 0.75 mm, 1 mm or 1.5 mm spacer (10- and 15-well: Mini-PROTEAN system from Bio-Rad, or 20-well system: PeqLab Biotechnologie GmbH). It consisted of the upper stacking-gel containing 4% acrylamide, and the lower separating-gel containing 8 - 15% polyacrylamide (see Table 3.1 for recipes). The protein lysate (3.2.4) was adjusted to 1x Lämmli loading dye and heated for 5 min at 95°C prior to loading on the polyacrylamide gel. In addition to the samples, 3 μL prestained Protein Marker VI (AppliChem) was loaded onto the gel as molecular weight protein marker. Application of voltage led to vertical separation of the proteins according to their approximate molecular weight. The gel was run in Lämmli SDS running buffer for 15 min at 80 V and for ∼1h at 180-200 V until the bromphenol blue running front reached the end of the gel.

3.2.5.3 Coomassie staining

Proteins separated by SDS-PAGE (3.2.5.2) can be stained by incubating the polyacrylamide gel in Coomassie Blue staining solution for 30 min, followed by destaining of the background through several changes of distilled H_2O. The gel was dried on Whatman paper in a gel dryer (Slab Dryer Model 483, Bio-Rad) for 1 h at 60°C under vacuum.

3.2.5.4 Semi-dry transfer of proteins

Semi-Dry transfer of proteins is a method to transfer the separated proteins from an SDS-PAGE gel (3.2.5.2) onto a membrane for further protein-specific analysis.

The gel was equilibrated in Towbin/SDS transfer buffer for 5-10 min, depending on the thickness of the gel. A PVDF membrane (Immobilon-P, 0.45 μm) was first soaked

in methanol, then in transfer buffer. Three transfer buffer-soaked Whatman papers were placed on the anode plate of the Trans-Blot SD Semi-Dry Transfer Cell (Bio-Rad), followed by the membrane, the gel, and again three soaked Whatman papers. The system was closed with the cathode plate, and 24 V were applied for 1 h.

3.2.5.5 Ponceau staining

To verify consistent protein transfer from an acrylamide gel onto a membrane (3.2.5.4), the membrane was stained by 2 min incubation with Ponceau S directly after the transfer. The stained membrane was washed in H_2O to remove the background stain and thus visualize the protein bands. A wash in 5% dry skimmed milk in PBST finally destained the membrane completely, so that the membrane could be used for western blot analysis (3.2.5.6).

3.2.5.6 Western blot

Proteins in cell lysates (3.2.4) were separated by SDS-PAGE (3.2.5.2) and transferred onto a PVDF membrane (3.2.5.4). The membrane was blocked in PBST + 5% w/v dry skimmed milk for 30 min at RT, or O/N at 4°C. It was incubated with the primary antibody diluted in PBST + 3% w/v dry skimmed milk for 1 h at RT, or O/N at 4°C. After two 5 min and two 10 min washes in PBST, the membrane was incubated with the secondary antibody diluted in PBST + 3% w/v dry skimmed milk for 1 h at RT. The membrane was washed again as before.

As exception, the phospho-STAT5 specific antibody (AB06) required the use of 3% w/v BSA in TBST (instead of dry skimmed milk in PBST) for blocking of the membrane and dilution of primary and secondary antibody. In that case the membrane washes took place in TBST.

While the primary antibody bound the protein of interest, the secondary, horseradish peroxidase-coupled antibody was directed against the IgG species of the respective primary antibody. A list of primary and secondary antibodies and their dilutions in western blot can be found in Table 3.11 and Table 3.12.

The membrane was rinsed in distilled H_2O prior to signal detection with the ECL reagents Amersham ECL Prime (GE Healthcare) or SuperSignal West Femto Maximum Sensitivity Substrate (Thermo Fisher Scientific) according to the manufacturer's recommendations. The membrane was incubated in the ECL reagent for 5 min. The prestained protein marker bands were retraced using the phosphorescent PicTIXX Pluster & LinerPen. Images were captured with an ImageQuant LAS 4000 mini imaging system (GE Healthcare).

3.2.5.7 Co-immunoprecipitation

For co-immunoprecipitation using non-crosslinked cells, 250 μg nuclear protein lysate (3.2.4.3) from Ba/F3-tet-on-1∗6 cells, which had been grown for 9 h in the presence of 1 μg/mL doxycycline and in the absence of IL-3, was adjusted to 625 μL with Brij buffer (∼1:10 dilution). The lysate was pre-cleared by rotating at 4°C for 1 h with 25 μL protein-A sepharose beads (50% slurry containing 500 μg/μL fatty acid free BSA and 200 μg/μL salmon sperm DNA). The beads were removed by centrifugation (500 rcf, 1 min, 4°C). 1.2 μg antibody was added to the pre-cleared lysate, followed by rotating at 4°C for 3 h without, and for 2 h with 25 μ L protein-A sepharose beads (50% slurry as above). The beads, containing the immunocomplexes, were pelleted (500 rcf, 1 min, 4°C), and the supernatant (SN fraction) was collected. The beads were washed 3 times in 900 μL Brij buffer and then boiled in 60 μL 2 x Lämmli loading dye (bead fraction). 50% of the bead fraction as well as 3% of supernatant and an equal amount of input (corresponding to 8 μg nuclear proteins) were separated by SDS-PAGE (3.2.5.2) and subsequently analyzed by western blot (3.2.5.6).

Co-immunoprecipitation using formaldehyde-crosslinked cells was performed following the ChIP (3.2.7) protocol with the following changes: Per immunoprecipitation nuclei from 7 x 10^6 formaldehyde-crosslinked Ba/F3-1∗6 cells, 2.4 μg anti-STAT5A, anti-BRD2 or rabbit IgG antibody, and 50 μL protein-A sepharose beads were used. 40% of the washed immunocomplex-containing beads were boiled in Lämmli loading dye and the immunoprecipitated proteins were analyzed by western blot. In parallel to the bead fractions, 3% supernatant and an equal amount of input were analyzed. 20% of the washed beads were processed by ChIP protocol to analyze co-precipitated DNA by qPCR.

3.2.5.8 Gel filtration chromatography

Gel filtration chromatography was performed to analyze size-differences of native STAT5-containing protein complexes in nuclear lysate from deacetylase inhibitor-treated or untreated cells. First, nuclear lysate was prepared from 5 x 10^7 TSA- or vehicle-treated Ba/F3-1∗6 cells as described in 3.2.4.3. The nuclear lysate was dialyzed in collodion bags against 250 mL GF buffer. For dialyzes of TSA-treated samples, the GF buffer was supplemented with 20 nM TSA. After 50 min dialyzes, the conductivity of the samples was similar as the conductivity of fresh GF buffer, indicating that dialysis was sufficient. The volume of the lysate was adjusted to 600 μL with GF buffer (20 nM TSA was added for TSA-treated samples) and cleared from cell debris by centrifugation (13000 rpm, 15 min, 4°C). 500 μL of the cleared lysate was loaded onto an ÄKTA FPLC system (GE Healthcare) with TSK Gel 4000SW column (Tosoh Bioscience). Protein separation was

performed at a flow rate of 0.5 mL/min in GF buffer (+ 20 nM TSA for TSA-treated samples). 30 x 500 μL elution fractions were collected and analyzed by western blot. Purified thyroglobulin (669 kDa) and BSA (66 kDa) were analyzed in a separate chromatography run and served as molecular weight protein markers. Gel filtration chromatography experiments were performed at the institute of Biochemistry III of the University of Regensburg with the support of Dr. Joachim Giesenbeck.

3.2.6 Dual-luciferase reporter assay

Cos-7 cells were transiently co-transfected with 125 ng GAL4-STAT5A expression vector (pFA-CMV based vectors, see Table 3.8), 1 μg pGL4.35 (*Firefly* luciferase reporter, P66) and 1.5 ng phRL-CMV (constitutive *Renilla* luciferase reporter, P49). pGL4.35 contains 9 repeats of the GAL4 UAS, which can be bound by the GAL4 moiety (yeast GAL4 DNA binding domain, amino acids 1-147) of the GAL4-STAT5A fusion proteins and thus drive expression of the *Firefly* luciferase reporter gene. phRL-CMV shows constitutive *Renilla* luciferase expression and serves as internal control reporter. Cos-7 transfection by Lipofectamine 2000 was performed as described in 3.2.3.6. 24 h after transfection, the cells were washed once in ice-cold PBS, before addition of 100 μL PLB, and lysis during a 5 min incubation on a shaker at RT.

Ba/F3 cells were transiently co-transfected by electroporation (3.2.3.7) with a plasmid mix consisting of 1 μg FLAG-tagged STAT5A expression vector (pcDNA3-based vectors, see Table 3.8), 8 μg *Firefly* luciferase reporter (pGVB-based vectors, P103, P106, P111) and 0.15 μg constitutive *Renilla* luciferase reporter (pRL-null, P50). pRL-null, like phRL-CMV, shows constitutive *Renilla* luciferase expression and thus serves as internal control reporter upon co-transfection with a STAT5-inducible pGVB-based *Firefly* luciferase reporter containing a *Cis* (P103 and P106) or β-casein (P111) promoter. For luciferase assays with GAL4-STAT5A fusion proteins, Ba/F3 cells were transiently co-transfected with 1.3 μg GAL4-STAT5A expression vector (pFA-based vectors, see Table 3.8), 0.5 μg pGL4.35 *Firefly* luciferase reporter (P66), and 0.2 μg pRL-null (P50, constitutive *Renilla* luciferase reporter). Ba/F3-G4-Luc2P cells were transiently transfected with 10 μg expression vector for GAL4-STAT5A fusion proteins (pFA-CMV based vectors, see Table 3.8) and 10 ng phRL-CMV. 8-24 h after transfection, as indicated in the figure legends, the Ba/F3 or Ba/F3-G4-Luc2P cells were harvested by centrifugation at 200 rcf for 5 min at 4°C. The cells were washed in 1 mL PBS, pelleted at 2000 rcf for 1 min at 4°C and resuspended in 35-75 μL passive lysis buffer (PLB, Promega Dual-Luciferase Reporter Assay) with or without 10 mM NaF and 1 mM Na_3VO_4. The cells were lysed by shaking for 10 min at RT in a thermo-mixer. The lysate was cleared by centrifugation at 20000 rcf for 3 min at 4°C.

Luciferase activity of the Ba/F3, Ba/F3-G4-Luc2P, or Cos-7 PLB-lysates was analyzed with the Dual-Luciferase Reporter Assay System (Promega) as recommended by the manufacturer. Protein concentration of the lysates was determined by Bradford protein assay (3.2.5.1). Equal protein amounts were plated in the wells of a black 96-well plate, and all volumes were adjusted to 20 μL with PLB. Each reaction was performed in duplicate. Using a double-injector luminometer (GloMax 96 Microplate Luminometer, Promega), 100 μL of LARII as well as Stop& Glo reagent were dispensed to the lysate, followed by 2 s measurement delay, and 10 s read time after each reagent addition.

After subtraction of the background luminescence measured with PLB buffer, *Firefly* luciferase RLUs were normalized to the *Renilla* luciferase internal control reporter. Eventually, data was represented as fold induction relative to the sample transfected with the corresponding empty vector (pcDNA3 or pFA-CMV). All samples were measured in duplicate and data shown are mean + standard deviation from one representative of at least two independent experiments.

3.2.7 Chromatin immunoprecipitation (ChIP)

For chromatin-crosslinking, 1% formaldehyde was added directly to the culture medium of 50 x 10^6 Ba/F3-1∗6 cells, followed by incubation for 10 min at RT. To stop the crosslinking, glycine was added to a final concentration of 125 mM. After 5 min incubation at RT, the cells were pelleted at 2000 rcf for 2 min at 4°C and washed twice in ice-cold PBS.

To enrich for nuclei of formaldehyde-crosslinked Ba/F3-1∗6 cells, a protocol was established based on a publication by Métivier et al. (2003). The crosslinked cells were resuspended by vortexing in 1 mL cell collection buffer (CBB). The samples were incubated for 15 min on ice, vortexed, incubated for 15 min at 30°C and again vortexed. After centrifugation at 2000 rcf for 1 min at 4°C, the supernatant was aspirated, while the nuclei pellet was washed first in 1 mL buffer MA and then in 1 mL buffer MB. In each buffer, the pellet was resuspended by vortexing (Fig. 3.1A).

A protocol from Okada & Fukagawa (2006), describing chromatin-fragmentation by MNase digest, was adapted for formaldehyde-crosslinked Ba/F3-1∗6 nuclei. First, the nuclei were sonicated in 1 mL HDG 150 buffer in the absence of SDS with a Branson Sonifier 250 (Branson) and 3 mm microtip in an ice-bath. 6 pulses of 20 sec duration/ 40 sec pause were delivered at 50% duty cycle and output setting 3, leading to a limited shearing of DNA to fragments of more than 10 kb length (Fig. 3.1B and data not shown). The $CaCl_2$ concentration was adjusted to 3 mM, and the chromatin was digested during a 1 h rotation at 4°C using 0.25 U micrococcal nuclease (MNase) per 1x 10^6 cells to obtain DNA fragments of about 500 bp length (Fig. 3.1B). The MNase (Sigma N-3755)

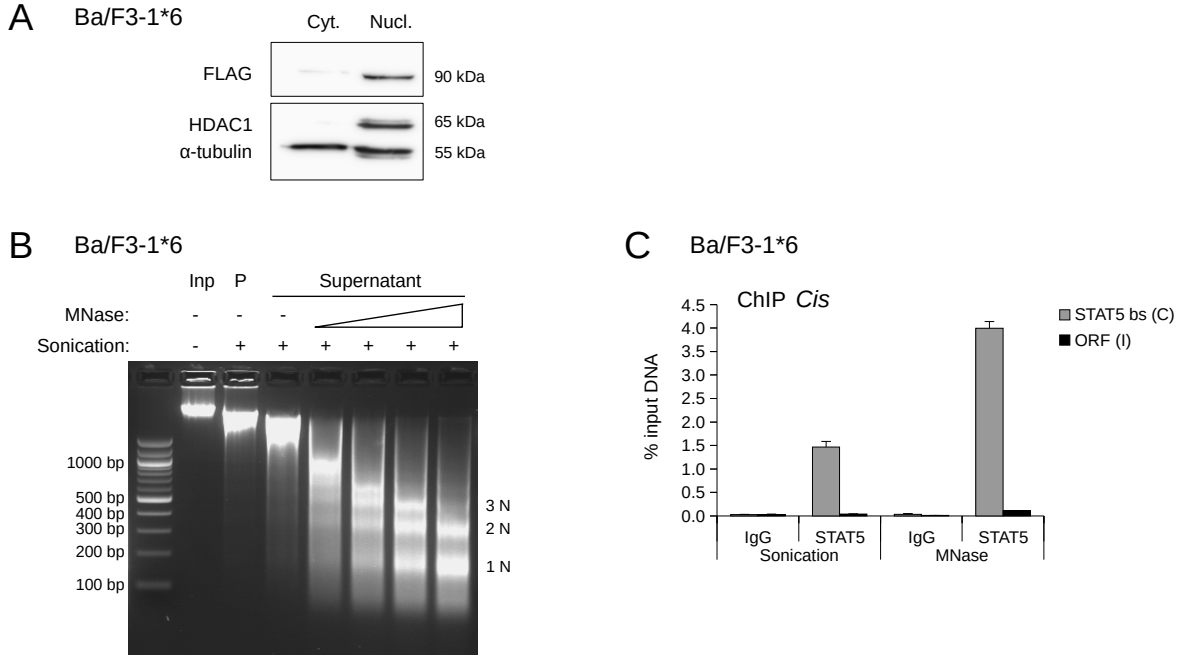

Figure 3.1: DNA fractionation by MNase digest instead of sonication strongly improves the detection of STAT5 binding to DNA by ChIP.
(**A**) Nuclei from formaldehyde-crosslinked Ba/F3-1∗6 cells were prepared as described in the ChIP protocol (Material and methods 3.2.7). An aliquot of nuclear (Nucl.) as well as cytosolic (Cyt., supernatant in CBB buffer) fraction was analyzed by western blot using antibodies directed against the nuclear marker HDAC1 and the cytosolic marker α-tubulin to verify cell fractionation efficiency. In addition, an antibody directed against the FLAG tag of STAT5A-1∗6 was used to monitor STAT5A-1∗6 expression and to confirm that this protein of interest is present in the analyzed nuclear fraction. (**B**) Optimization of MNase-based DNA digest for ChIP. Nuclei from formaldehyde-crosslinked Ba/F3-1∗6 cells were sonified in HDG 150 buffer and digested with increasing amounts of MNase, as described in the ChIP protocol (Material and methods 3.2.7). The MNase amount was 0.125, 0.25, 0.5 and 1 U MNase per 1 x 10^6 cells. Before the MNase digest, the samples had been spun at 20 000 rcf for 10 min at 4°C. The supernatant was subjected to MNase digest. MNase digested supernatant, the pellet (P) from the centrifugation step and non-sonified input (Inp) were treated with 0.1 μg/μL proteinase K in the presence of 0.06 μg/μL glycogen during a 3.5 h incubation at 55°C. The formaldehyde crosslink was reversed O/N at 65°C. DNA was isolated by phenol extraction (Material and methods 3.2.1.5) and subjected to ethanol precipitation (Material and methods 3.2.1.6). 1 μg/μL RNase A was added and RNA was digested for 60 min at 37°C. All samples were analyzed in parallel to a 100 bp DNA ladder (reference marker) by agarose gel electrophoresis as described in Material and methods 3.2.1.11. 0.25 U MNase per 1x 10^6 cells was the optimal condition for the ChIP protocol. 1N, mono-nucleosome; 2N di-nucleosome; 3N tri-nucleosome. (**C**) Nuclei from Ba/F3-1∗6 cells were isolated according to the optimized ChIP protocol, as described in Material and methods (3.2.7). DNA was either fragmented by MNase digest after sonication in HDG 150 buffer according to the ChIP protocol or DNA was fragmented by sonication. In the latter case, the sonication took place in SDS buffer (instead of HDG 150 buffer) using the sonication parameters described in the protocol, and the MNase digest was omitted. The DNA fragments were about 500 bp of size. STAT5 was immunoprecipitated using 3 μg STAT5 plus 3 μg STAT5A antibody. The rabbit-IgG control antibody served to determine the background signal. Co-precipitated DNA of the *Cis* locus was detected by qPCR using primers specific for the STAT5 binding site (bs) (amplicon C) or for the distal open reading frame (ORF) (amplicon I). The location of the respective amplicons C and I along *Cis* is depicted in Figure 4.17. (Figure modified after Pinz & Rascle (2017) fig. 1 and fig. 2.)

was reconstituted in MNase Reconstitution buffer and stored at -20°C. The calcium ion-dependent DNA digest was stopped through addition of EGTA to a final concentration of 5 mM. The cell concentration was adjusted to 0.01 x 10^6 cells/μL with IP buffer, and the samples were rotated for 20 min at 4°C. The lysate was cleared from debris by centrifugation at 3220 rcf for 10 min at 4°C.

For preclearing of the lysate, 500 μL protein-A sepharose beads (50% slurry containing 500 μg/μL fatty-acid-free BSA and 200 μg/μL salmon sperm DNA) were added per 50 x 10^6 cells, and the samples were rotated for 1 h at 4°C. The samples were spun at 500 rcf for 1 min at 4°C and the pelleted beads were discarded. For immunoprecipitation, precleared lysate from 3.5 x 10^6 cells was used and adjusted to 500 μL with IP buffer. 1.2 μg anti-STAT5A, 3 μg anti-BRD2 or 3 μg rabbit IgG antibody were added, and the samples were rotated for 3 h at 4°C. 25 μL protein-A sepharose beads (50% slurry, as above) were added, followed by another 2 h rotation at 4°C. The beads were pelleted at 500 rcf for 1 min at 4°C, and the supernatant was aspirated. The beads were washed in 900 μL of each of the following buffers: IP buffer, 150 mM NaCl wash buffer, 500 mM NaCl wash buffer, LiCl wash buffer and TE. In 500 mM NaCl wash buffer and LiCl wash buffer, the beads were rotated for 5 min at 4°C.

In parallel to the ChIP samples, 20 μL of the precleared lysate was processed as input sample from this step on. 120 μL 1%SDS, 0.1 M $NaHCO_3$ and 6 μL 5 M NaCl were added to the ChIP samples. 100 μL 1%SDS, 0.1 M $NaHCO_3$ and 6 μL 5 M NaCl were added to the input. All samples were incubated O/N at 65°C to reverse the crosslinking. The beads were pelleted at 500 rcf, for 1 min at 4°C. 30 μg RNase A was added to the supernatants, and they were incubated for 1-2 h at 37°C. 50 μg Proteinase K was added, followed by 1-2 h incubation at 55°C.

The DNA was purified with MN nucleospin PCR clean-up kit and MN NTB buffer (both from MACHEREY-NAGEL). 600 μL NTB buffer was added to each sample, which was then loaded onto the purification column. It was proceeded as recommended by the manufacturer. Elution was performed twice with 50 μL pre-warmed (70°C) buffer NE. 200 μL H_2O was added to each ChIP sample, while the input samples were diluted with 600 μL H_2O and 200 μL buffer NE.

Eventually, the samples were analyzed by quantitative PCR in duplicate or triplicate on a RotorGene Q (Qiagen) (3.2.1.3), using primers listed in Table 3.4. Co-immunoprecipitated DNA was calculated as percentage of total input DNA. Data from one representative experiment are shown as mean +/- standard deviation of the qPCR performed in duplicate or triplicate.

This optimized ChIP protocol, which combines nuclei isolation and MNase digest-based DNA fractionation, improved the detection of STAT5 binding to DNA, as mani-

fested in the increased amount of co-precipitated DNA (% input) and in the increased enrichment relative to IgG background (Fig. 3.1C). A detailed description of this optimized ChIP protocol has been recently published (Pinz & Rascle, 2017).

3.2.8 Sequence alignments

Human and mouse STAT3 (accession No. NP_644805.1 and AAL59017.1), STAT5A (accession No. NP_001275647.1 and AAF78237.2) and STAT5B (accession No. NP_036580.2 and AAF62911.2) multiple sequence alignment of the region covering K675-K700 of STAT5A was performed using the online tool Clustal Omega (version 1.2.1) with preset standard settings.

CHAPTER 4

Results

4.1 Characterization of the experimental system

4.1.1 Deacetylase inhibitors repress STAT5 target gene expression in Ba/F3 and Ba/F3-1∗6 cells

To study the mechanism of deacetylase inhibitor-induced repression of STAT5-mediated transcription, the IL-3-dependent mouse pro-B cell line Ba/F3 was used. Its proliferation and survival depends on interleukin-3 (IL-3) and the subsequent activation of STAT5 (Rodriguez-Tarduchy et al., 1990; Nelson et al., 2004). By removing IL-3 from the culture medium of Ba/F3 cells, the STAT5 pathway is turned off. Addition of IL-3 to those IL-3-withdrawn, rested cells activates the STAT5 pathway and induces the expression of STAT5 target genes. Treatment of Ba/F3 cells with deacetylase inhibitors such as trichostatin A (TSA) represses STAT5 target gene induction upon IL-3 stimulation (Rascle et al., 2003). Thus, this system is well suited to study the mechanism of deacetylase inhibitor-induced repression of STAT5-mediated transcription.

In addition to Ba/F3 cells, the IL-3-independent Ba/F3-1∗6 cell line was used, which stably expresses the well-described constitutively active mouse STAT5A-1∗6 mutant (Onishi et al., 1998). STAT5A-1∗6 carries two point mutations (H298R and S710F), which make its activation independent of cytokine signaling (Onishi et al., 1998). The advantage of this cell line is the IL-3-independent, constitutive expression of STAT5 target genes. By contrast, in the parental Ba/F3 cell line growing in the presence of IL-3, basal expression of STAT5 target genes is low (data not shown) and IL-3 withdrawal followed by IL-3

stimulation is needed to stimulate expression of STAT5 target genes. However, whether deacetylase inhibitors repress STAT5A-1∗6-mediated expression of STAT5 target genes has not been shown so far.

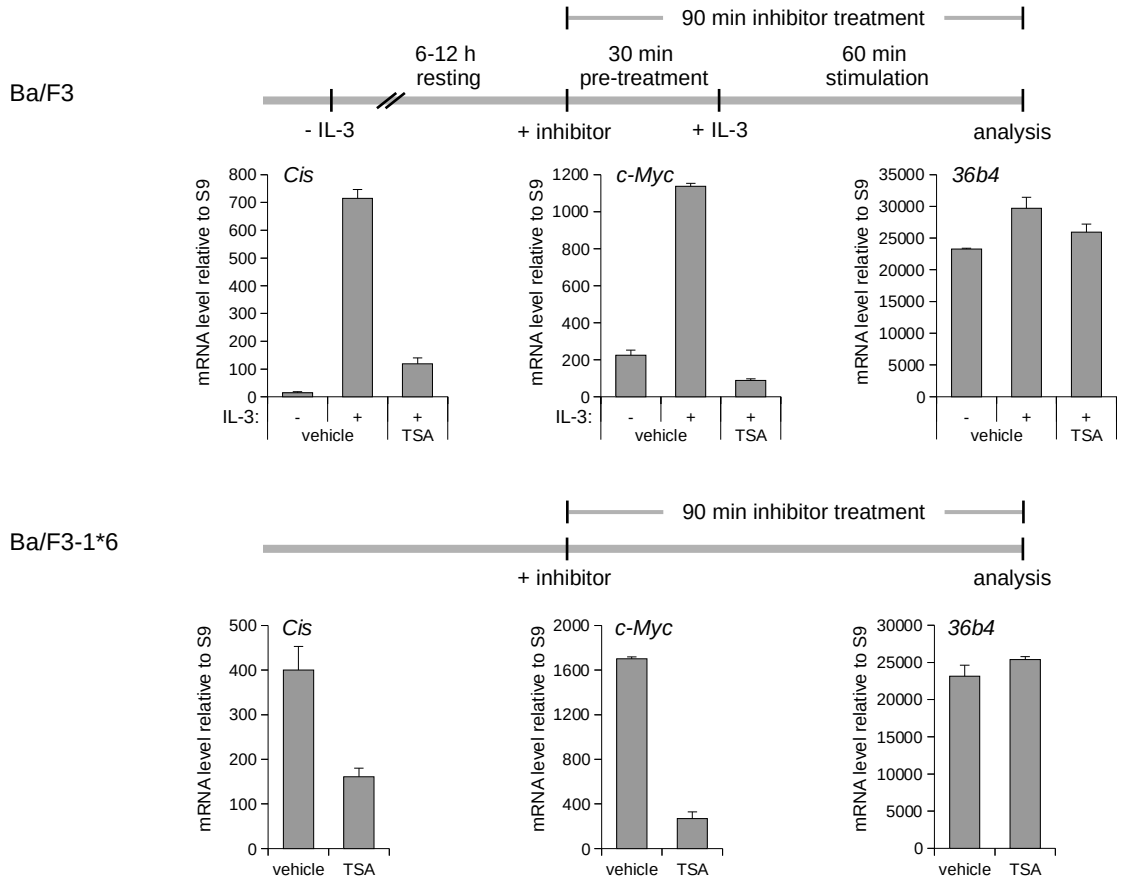

Figure 4.1: TSA inhibits the transcriptional activity of wild-type STAT5 and of constitutively active STAT5A-1∗6
Rested Ba/F3 cells were pre-treated for 30 min with 200 nM TSA and then stimulated for 60 min with IL-3 (in total 90 min TSA treatment). Ba/F3-1∗6 cells, expressing constitutively active STAT5A-1∗6, received 90 min treatment with 200 nM TSA. RNA and cDNA were prepared and analyzed by quantitative RT-PCR as described in Material and methods 3.2.1.4, using primers for the STAT5 target genes *Cis* and *c-Myc* as well as for the housekeeping gene *36b4*. Vehicle was 0.02% DMSO.

To confirm that STAT5A-1∗6-mediated transcription is sensitive to deacetylase inhibitors, Ba/F3-1∗6 cells were treated with the deacetylase inhibitor trichostatin A (TSA) or vehicle (dimethyl sulfoxide (DMSO)) for 90 min. Expression of the STAT5 target genes *Cis* and *c-Myc* (Matsumoto et al., 1997; Pinz et al., 2016) as well as the housekeeping gene *36b4* was analyzed at the RNA level by cell lysis and RNA stabilization followed by cDNA synthesis and quantitative PCR (quantitative RT-PCR) (Fig. 4.1). Gene expression of the housekeeping gene *36b4* served as a negative control (Rascle et al., 2003) throughout this study. Its expression should not change in response to experimental factors such as deacetylase inhibitors or IL-3 stimulation. Ba/F3 cells, and thus wild-type STAT5,

served as a positive control for TSA-sensitivity. Ba/F3 cells were first withdrawn from IL-3 to turn off the STAT5 pathway, then pre-treated with TSA or vehicle for 30 min, and finally stimulated with IL-3 for 60 min to activate STAT5. In Ba/F3-1∗6 cells, similarly as in Ba/F3 cells, expression of the STAT5 target genes *Cis* and *c-Myc* were downregulated upon TSA treatment, while, as expected, the housekeeping gene *36b4* remained unaffected (Fig. 4.1). This demonstrates, that STAT5A-1∗6-mediated transcription is similarly sensitive to TSA as transcription mediated by wild-type STAT5.

Our group demonstrated before that upon deacetylase inhibitor treatment DNA binding of wild-type STAT5 is not affected but that RNA polymerase II is lost from STAT5 target genes in Ba/F3 cells (Rascle et al., 2003; Rascle & Lees, 2003). We could now confirm that DNA binding of STAT5A-1∗6 was also unaffected by deacetylase inhibitor treatment and that RNA polymerase II was also lost from the STAT5 target gene *Cis* in Ba/F3-1∗6 cells (Fig. 4.19A and data not shown, Dr. Anne Rascle and Samy Unser, Pinz et al., 2015, fig. 1). Together, these data confirm that STAT5A-1∗6 and wild-type STAT5 behave similarly in response to TSA and that the Ba/F3 and the Ba/F3-1∗6 cell line are good model systems to investigate how deacetylase inhibitors repress STAT5-mediated transcription.

4.2 Identification of the HDAC involved in deacetylase inhibitor-mediated inhibition of STAT5-mediated transcription

Our group demonstrated before that STAT5-mediated transcription is inhibited by the deacetylase inhibitors trichostatin A (TSA), suberoylanilide hydroxamic acid (SAHA) and sodium butyrate (Rascle et al., 2003). These inhibitors are pan-inhibitors targeting all eleven classical HDACs, HDAC1-11, from classes I, IIA, IIB and IV (Witt et al., 2009), suggesting that one or several of those classical HDACs (referred to as HDAC(s) thereafter) are involved in STAT5-mediated transcription. The first goal of this study was to identify the HDAC among the eleven family members which is involved in STAT5-mediated transcription and responsible for the inhibitory effect of deacetylase inhibitors.

4.2.1 Selective deacetylase inhibitors differentially impair STAT5-mediated transcription

To identify HDAC candidates possibly involved in inhibition of STAT5-mediated transcription, several selective deacetylase inhibitors were tested for their ability to inhibit

induction of STAT5 target gene expression in IL-3-stimulated Ba/F3 cells. Inhibition of gene expression by deacetylase inhibitors can be observed best when the analyzed IL-3-dependent genes are well induced. Therefore, to determine the optimal IL-3 stimulation duration to analyze the effect of deacetylase inhibitor treatment in our cells, the gene induction profiles of STAT5 target and control genes was determined. STAT5 target genes with early, sustained (*Cis* and *c-Myc*), early, transient (*Osm*), and late, sustained (*Spi2.1*) IL-3 induction profile were chosen (Rascle et al., 2003; Basham et al., 2008). The IL-3-inducible, STAT5-independent control genes *JunB* and *c-Fos* are early, transient genes (Rascle et al., 2003), while the control gene *Spp1* (osteopontin) is a late IL-3-induced gene. *Spp1* expression begins to increase at about 2 h IL-3 stimulation in Ba/F3- derived Ba/F3-β cells (Rascle et al., 2003), and *Spp1* is expressed within 3 h IL-3 stimulation in primary IL-3-dependent mouse bone marrow cells (Lin et al., 2000). The housekeeping gene *36b4* served as a negative control, since its expression should not change in response to any experimental factors such as IL-3 (Rascle et al., 2003).

Rested Ba/F3 cells (withdrawn from IL-3 to turn off the STAT5 pathway) were stimulated with IL-3 for 0.5, 1 or 2 hours or left unstimulated and gene expression was analyzed by quantitative RT-PCR as described above. All genes behaved as expected (Rascle et al., 2003; Basham et al., 2008). The STAT5 target genes *Cis*, *c-Myc* and *Osm* were well induced and *Spi2.1* was significantly induced after 1 h IL-3 stimulation (Fig. 4.2A). After 1 h stimulation the IL-3-inducible, MAPK-regulated control genes *c-Fos* and *JunB* showed partial and maximal induction respectively (Fig. 4.2B). The IL-3-inducible but late responding gene *Spp1* and the housekeeping gene *36b4* did not change their expression levels in the course of this experiment (Fig. 4.2B and C). In summary, all IL-3-inducible STAT5 target genes and all IL-3-inducible control genes except for the late responding *Spp1* were well induced after 1 h IL-3 stimulation. Consequently, 1 h IL-3 stimulation was used for the following study investigating the effect of deacetylase inhibitors on the expression of these genes.

To narrow down the HDAC candidates possibly involved in inhibition of STAT5-mediated transcription, deacetylase inhibitors from different chemical classes and with different HDAC selectivity were chosen for the following experiments. The selective deacetylase inhibitor valproic acid (VPA) is a carboxylic acid (Gottlicher et al., 2001; Phiel et al., 2001), apicidin is a cyclic peptide (Darkin-Rattray et al., 1996; Han et al., 2000), and MS-275 (Saito et al., 1999; Suzuki et al., 1999) as well as MGCD0103 (Fournel et al., 2008) contain a benzamide group mediating deacetylase inhibition. All these inhibitors inhibit predominantly class I HDACs with different selectivity towards the members of this class. In addition, they inhibit some non-class I HDACs (Gurvich et al., 2004; Hess-Stumpp et al., 2007; Khan et al., 2008; Arts et al., 2009). Their different se-

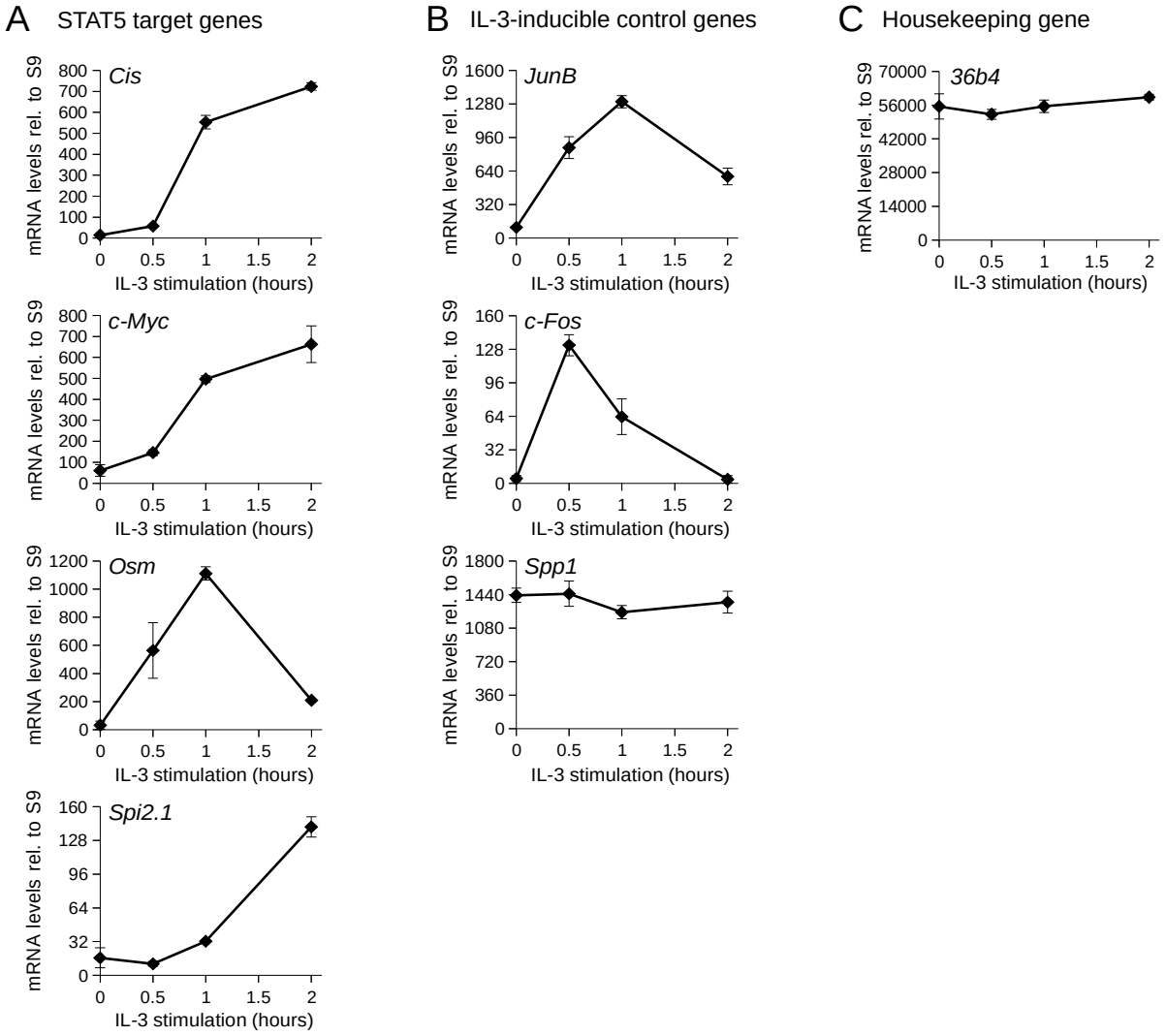

Figure 4.2: Expression profile of STAT5 target genes and control genes in Ba/F3 cells upon IL-3 stimulation

Ba/F3 cells were rested for 6 h before stimulation with IL-3. Cells were harvested at 0, 0.5, 1 and 2 hours IL-3 stimulation, and expression of STAT5 target genes and control genes was analyzed by quantitative RT-PCR. Primers were used, specific for the STAT5 target genes *Cis*, *c-Myc*, *Osm* and *Spi2.1*(**A**), for the IL-3-inducible control genes *JunB*, *c-Fos* and *Spp1* (late induced gene, expression starts to increase at about 2 h IL-3 stimulation in Ba/F3-derived cells (Rascle et al., 2003))(**B**), or for the housekeeping gene *36b4* (**C**). Since all genes were well expressed after 1 h IL-3 stimulation, this stimulation duration was chosen for the analysis of the inhibitory effect of deacetylase inhibitors on these genes.

lectivity will allow us, by combination of the data from all inhibitors, to more specifically identify the HDAC possibly involved in inhibition in STAT5-mediated transcription. The pan-inhibitor TSA (Yoshida et al., 1990; Khan et al., 2008), a hydroxamic acid, was used as a positive control, since our group showed before that it inhibits STAT5-mediated transcription (Rascle et al., 2003).

The inhibitory potency of a substance can be described by the half maximal inhibitory concentration (IC_{50}), which is the inhibitor concentration required to inhibit a biological process by 50% (Cheng & Prusoff, 1973). The reported IC_{50} of deacetylase inhibitors towards different HDACs have to be taken with caution as they were obtained *in vitro* for purified recombinant human HDACs (Gurvich et al., 2004; Khan et al., 2008; Arts et al., 2009), while this study was conducted in a murine cell line. Furthermore, IC_{50} values of deacetylase inhibitors vary a lot between some publications (Fournel et al., 2008; Khan et al., 2008; Estiu et al., 2010), probably a consequence of different experimental conditions during determination of HDAC activity such as HDAC protein source, type of substrate, as well as pre-incubation time with the inhibitor (Chou et al., 2008; Delcuve et al., 2012; Vaidya et al., 2012; Hull et al., 2016). Therefore, IC_{50} values reported by a single study (Khan et al., 2008) were used as a reference (Tab. 4.1A). To complement inhibitor/HDAC combinations not tested in the study by Khan et al. (2008), IC_{50} values from other publications were used where available (Gurvich et al., 2004; Hess-Stumpp et al., 2007; Arts et al., 2009) and marked with an asterisk in Table 4.1. Table 4.1 depicts the inhibitory potency of the chosen deacetylase inhibitors against HDAC1-11 relative to the respective most sensitive HDAC determined by Khan et al. (2008). The IC_{50} for HDACs in the group "strong inhibition" (black) is less than 5 times the IC_{50} of the most sensitive HDAC. For the group "weak inhibition" (dark gray) the IC_{50} is more than 5 times the IC_{50} of the most sensitive HDAC and the group "no inhibition" (light gray) contains HDACs for which the IC_{50} is more than 100 times the IC_{50} of the most sensitive HDAC. To narrow down the possible candidate HDACs involved in STAT5-mediated transcription, a concentration of 5 to 10 times the IC_{50} of the most sensitive HDAC was selected as a reference concentration for each inhibitor (Fig. 4.3, dashed bars).

To evaluate the effect of the selected deacetylase inhibitors on STAT5-mediated transcription, increasing concentrations of VPA, apicidin, MGCD0103 and MS-275 were added to rested Ba/F3 cells 30 min before IL-3 stimulation. The inhibitor concentrations were minimally 0.3 times and maximally 100 times the IC_{50} of the most sensitive HDAC. TSA treatment was used as a positive control. After 1 h IL-3 stimulation, expression of STAT5 target and control genes was evaluated at the RNA level by quantitative RT-PCR (Fig. 4.3). Similarly to the pan-inhibitor TSA (Fig. 4.3A and Rascle et al., 2003), the selective inhibitors VPA and apicidin specifically inhibited the STAT5 target

A

IC_{50}		Class I				Class IIA				Class IIB		Class IV	unit of IC_{50}
		HDAC1	HDAC2	HDAC3	HDAC8	HDAC4	HDAC5	HDAC7	HDAC9	HDAC6	HDAC10	HDAC11	
pan-inhibitor:	TSA	**2**	3	4	456	6	nd	5	6	3	12*	nd	nM
selective inhibitors:	VPA	**1.6**	3.1	3.1	7.4	1.5*	1.0*				*	nd	mM
	Apicidin		120	**43**	575		nd				nd	nd	nM
	MGCD0103	**34**	**34**	998					*		*	195*	nM
	MS-275	**181**	1155	2311			nd		505		*	nd	nM

B

		Class I				Class IIA				Class IIB		Class IV	Inhibition of STAT5
		HDAC1	HDAC2	HDAC3	HDAC8	HDAC4	HDAC5	HDAC7	HDAC9	HDAC6	HDAC10	HDAC11	
pan-inhibitor:	TSA	√	√	√		√	nd √	√	√	√	*	nd √	+
selective inhibitors:	VPA	√	√	√	√	* √	* √				*	nd √	+
	Apicidin		√	√			nd √				nd √	nd √	+
	MGCD0103			√	√	√	√	√	* √	√	* √	* √	-
	MS-275		√	√	√	√	nd √	√		√	* √	nd √	-

stong inhibition | weak inhibition | no inhibition | nd no data available

* data from other publications than Khan et al. (2008)

√ possible candidate for involvement in STAT5 transactivation

Table 4.1: HDAC inhibition profile of selective deacetylase inhibitors
The table was adapted according to Witt et al. (2009), using IC_{50} values from Khan et al. (2008) as a reference (**A**). For HDACs that were not tested by Khan et al. (2008), IC_{50} values from other publications (Gurvich et al., 2004; Hess-Stumpp et al., 2007; Arts et al., 2009) were used and marked with an asterisk. The reported IC_{50} values were determined *in vitro* using recombinant human HDACs. The IC_{50} of the most sensitive HDAC is underlined and displayed in bold (A). The inhibitory potency of deacetylase inhibitors relative to the most sensitive HDAC is depicted by gray scale. Strong inhibition: the IC_{50} is less than 5 times the IC_{50} of the most sensitive HDAC. Weak inhibition: the IC_{50} is more than 5 times the IC_{50} of the most sensitive HDAC. No inhibition: IC_{50} is more than 100 times the IC_{50} of the most sensitive HDAC. The last column in (**B**) indicates whether STAT5 target gene expression is inhibited (+), or not (-) by deacetylase inhibitors at a concentration of 5-10 times the IC_{50} of the most sensitive HDAC. For inhibitors repressing STAT5 target genes, all strongly inhibited HDACs were considered as potential candidates and indicated by a check mark in (**B**). For inhibitors which had no effect on STAT5-mediated transcription, all weakly and all not inhibited HDACs were considered as potential candidates and indicated by a check mark. HDACs for which there was no data available were considered apriori as potential candidates. Those HDACs which were candidates for inhibition of STAT5-mediated transcription by combining the results from all deacetylase inhibitor experiments are highlighted by columns framed in bold gray (B).

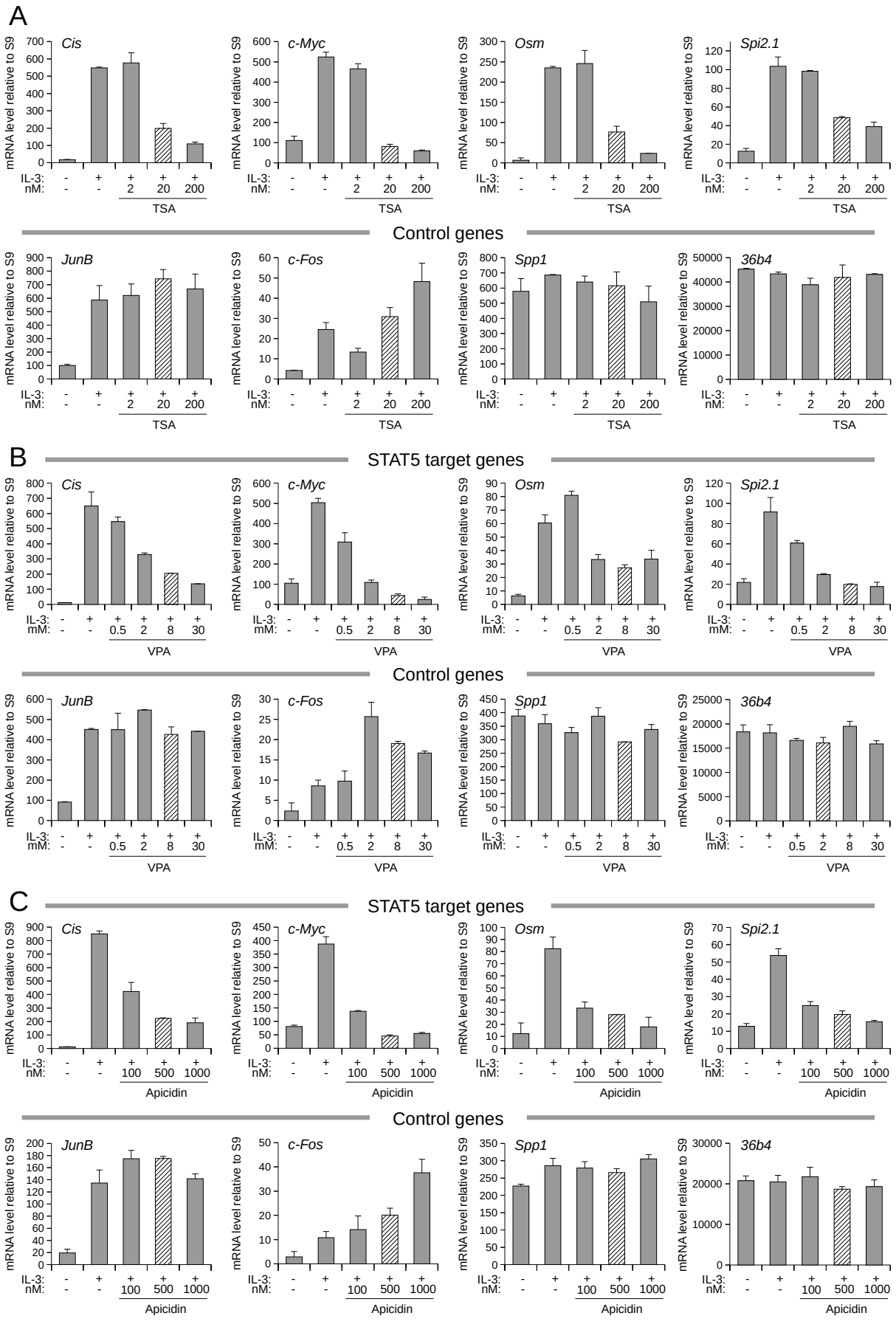
A
Cis
c-Myc
Osm
Spi2.1
mRNA level relative to S9
IL-3:
nM:
TSA
Control genes
JunB
c-Fos
Spp1
36b4
B
STAT5 target genes
VPA
C
Apicidin

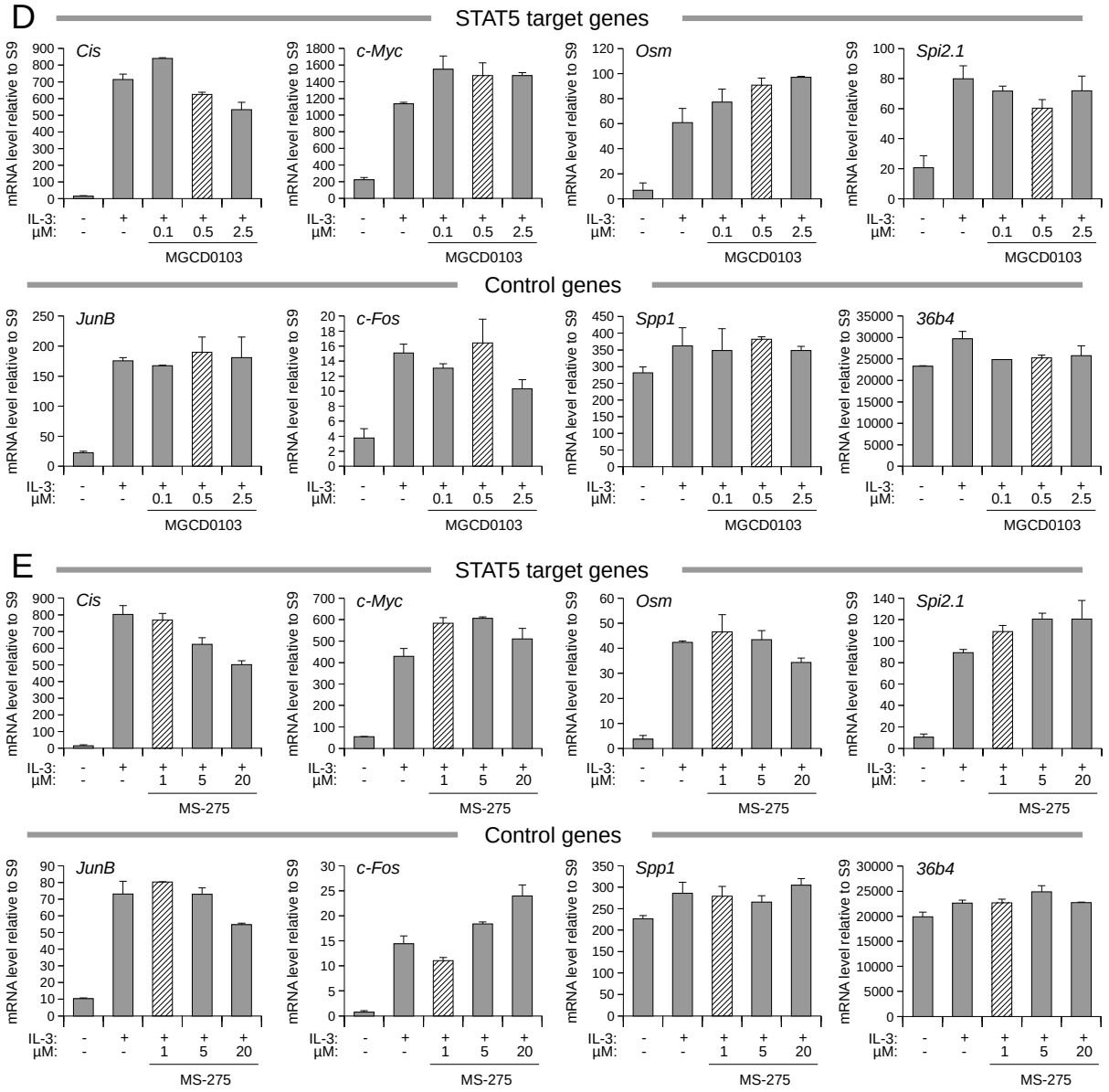

Figure 4.3: Selective deacetylase inhibitors affect expression of STAT5 target genes differentially

6 h-rested Ba/F3 cells were pre-treated for 15 min with the indicated concentrations of the pan-inhibitor TSA (**A**) or for 30 min with the indicated concentrations of the selective deacetylase inhibitors VPA (**B**), apicidin (**C**), MGCD0103 (**D**) and MS-275 (**E**). IL-3 was added to the pre-treated cells and the cells were stimulated for 60 min before analysis of gene expression by quantitative RT-PCR as described in Material and methods 3.2.1.4, using expression primers for the STAT5 target genes *Cis*, *c-Myc*, *Osm* and *Spi2.1* or for the control genes *JunB*, *c-Fos*, *SppI* and *36b4*. All samples in (A), (C) and (D) were adjusted to 0.02% DMSO. In (B), no DMSO was added since VPA was solved in H_2O. In (E) DMSO was adjusted to 0.02% for 0-5 μM MS-275 and to 0.08% DMSO for 20 μM MS-275. The dashed bar indicates an inhibitor concentration of 5-10x the IC_{50} of the most sensitive HDAC, as determined by Khan et al. (2008) in *in vitro* deacetylation assays, except for MGCD0103 where a concentration of 15x the *in vitro* IC_{50} of the most sensitive HDAC is marked.

genes *Cis*, *c-Myc*, *Osm* and *Spi2.1*, upregulated the control gene *c-Fos* and left *JunB*, *Spp1* and *36b4* unaffected (Fig. 4.3B and C). MS-275 and MGCD0103, by contrast, were no inhibitors of STAT5 target genes under these experimental conditions (Fig. 4.3D and E). They did not or only marginally affect expression of STAT5 target or control genes. The housekeeping gene *36b4* remained unaffected in all conditions (Fig. 4.3A-E), indicating that the observed inhibitory effect was not the result of unspecific transcriptional inhibition or the result of toxicity. If STAT5 transcriptional activity was inhibited at the reference concentration of 5 to 10 times the IC_{50} of the most sensitive HDAC (Fig. 4.3, dashed bars), which was the case for TSA, VPA, and apicidin, all HDACs of the category "strong inhibition" were considered as possible candidates and indicated by a check mark in Table 4.1B. For MGCD0103 and MS-275, which were ineffective at the reference concentration, HDACs of the category "strong inhibition" were excluded as possible candidates, and all HDACs of the categories "weak inhibition" or "no inhibition" remained possible candidates. In case no data were available for certain inhibitor/HDAC combinations, the respective HDACs were considered apriori as possible candidates. After combining the data from all inhibitors, HDAC3, HDAC5, and HDAC11 were the most likely candidates for involvement in inhibition of STAT5-mediated transcription (Table 4.1B, columns framed in bold gray).

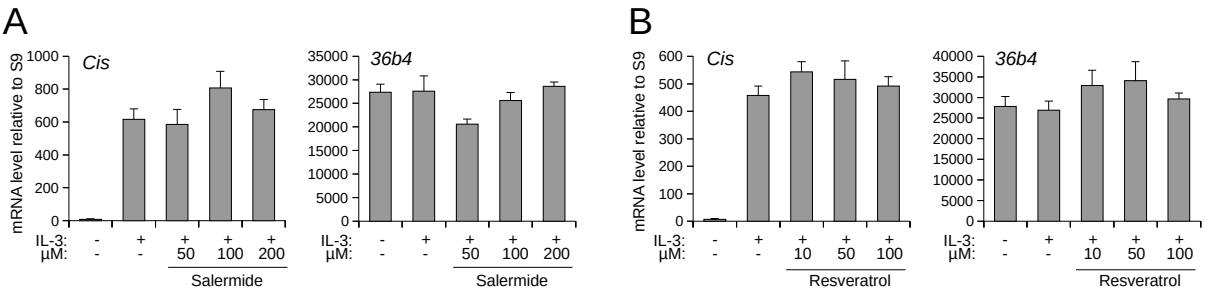

Figure 4.4: Sirtuin targeting drugs do not affect expression of the STAT5 target gene *Cis*
6 h rested Ba/F3 cells were pre-treated for 30 min with 50, 100 and 200 M of the sirtuin inhibitor salermide (**A**) or 10, 50 and 100 M of the sirtuin activator resveratrol (**B**).The pre-treated cells were further stimulated with IL-3 for 60 min before analysis of gene expression by quantitative RT-PCR using expression primers for the STAT5 target gene *Cis* or the housekeeping gene *36b4*, as described in Material and methods 3.2.1.4. The final DMSO concentration was adjusted to 0.04% in (A) and to 0.02% DMSO in (B).

Next to the classical HDACs (HDAC class I, II and IV) discussed so far, sirtuins constitute class III histone deacetylases. They use an NAD^+-dependent catalytic mechanism for deacetylation of target proteins and are therefore inhibited by other small molecules than the classical divalent metal ion-dependent HDACs (Mai et al., 2005; Nechay et al., 2016). For instance, the small molecule salermide is a sirtuin inhibitor (Lara et al., 2009), and resveratrol is a sirtuin activating drug (Howitz et al., 2003). To confirm that sirtuins are not involved in STAT5-mediated transcription, the effect of the sirtuin-targeting drugs

salermide and resveratrol on expression of the STAT5 target gene *Cis* was analyzed. The housekeeping gene *36b4* was analyzed as a negative control (Fig. 4.4). At concentrations at which they were described to be effective (Howitz et al., 2003; Kaeberlein et al., 2005; Lara et al., 2009), neither the sirtuin inhibitor salermide, nor the sirtuin activator resveratrol showed an effect on the expression of *Cis* or *36b4* (Fig. 4.4A and B). Thus, in this experimental setting a role of sirtuins in STAT5-mediated transcription can be excluded.

4.2.2 Inhibition of STAT5-mediated transcription by deacetylase inhibitors in Ba/F3 cells is not due to cytotoxicity

Although deacetylase inhibitors did not affect expression of the housekeeping gene *36b4* and showed differential effects on gene expression of the other analyzed genes, it cannot be excluded that these effects on gene expression are due, at least in part, to cell toxicity. To confirm that the inhibitory effect of the deacetylase inhibitors on STAT5 target gene expression was not a consequence of cytotoxicity, WST-1 cytotoxicity assays were performed. The WST-1 assay is based on cellular mitochondrial dehydogenases, whose activity correlates with the metabolic activity of the cell, and which cleave the WST-1 tetrazolium salt to a reaction product with strong absorption of light at a wavelength of 450 nm. Cytotoxic compounds reduce the activity of mitochondrial dehydrogenases and thus lead to less WST-1 cleavage and absorbance at 450 nm. The percentage of cytotoxicity was calculated relative to vehicle control (0% cytotoxicity) and to a positive control (1% Triton-X-100 treatment, 100% cytotoxicity).

Rested Ba/F3 cells were pre-treated with increasing concentrations of deacetylase inhibitors. The highest inhibitor concentration was either equivalent to (TSA, VPA, apicidin) or 5 times higher (MGCD0103 and MS-275) than in the gene expression studies (Fig. 4.3). 4-100 μM α-bromo-2',3,4,4'-tetramethoxychalcone (α-Br-TMC) was included in the assay as a reference cytotoxic compound at 100 μM (Pinz et al., 2014a). After 30 min inhibitor treatment, WST-1 reagent together with IL-3 was added for 90 min and absorbance was measured. This setting was chosen to reflect the experimental design of the gene expression analysis after inhibitor treatment (Fig. 4.1 and Fig. 4.3).

Upon treatment with the positive control, 100 μM α-Br-TMC, 78% cytotoxicity was detected, which confirms the validity of the assay. Treatment with deacetylase inhibitors, even at the highest concentrations, resulted in no to low (<20%) cytotoxicity (Fig. 4.5). Therefore, the observed inhibitory effect of TSA, VPA and apicidin on STAT5 target gene expression was not due to cytotoxicity.

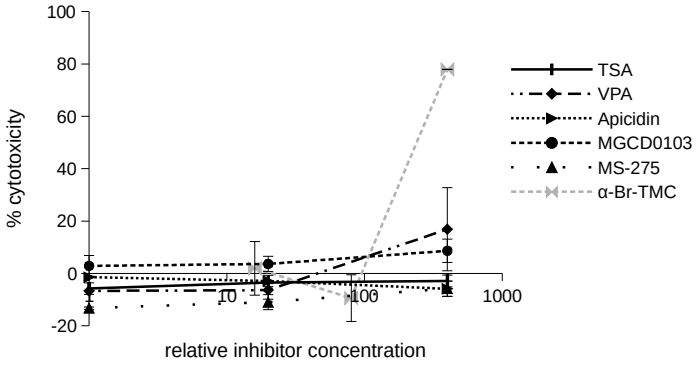

Figure 4.5: The deacetylase inhibitors are not or only marginally cytotoxic in Ba/F3 cells 6 h rested Ba/F3 cells were pre-treated with deacetylase inhibitors or control compounds for 30 min and then treated with IL-3 and WST-1 reagent for 90 min. Inhibitor concentrations were as follows: 0.5, 10 and 200 nM TSA, 0.075, 1.5 and 30 mM VPA, 2.5, 50 and 1000 nM apicidin, 0.025, 0.5 and 10 μM MGCD0103, 0.25, 5 and 100 μM MS-275, or 4, 20 and 100 μM α-bromo-2',3,4,4'-tetramethoxychalcone (α-Br-TMC). α-Br-TMC served as reference cytotoxic compound (Pinz et al., 2014a). The absorbance was measured and the percentage of cytotoxicity was calculated relative to vehicle control (0% cytotoxicity) and 1% Triton-X-100 treatment (100% cytotoxicity), as described in Material and methods 3.2.3.5. Vehicle was adjusted to 0.02% DMSO for all samples, except for MS-275 samples and respective vehicle control (0.4% DMSO) as well as α-Br-TMC samples and respective vehicle control (0.1% DMSO).

4.2.3 Most HDAC family members are expressed in Ba/F3 cells

The involvement of specific HDACs in STAT5-mediated transcription would be further supported by their expression in Ba/F3 cells. To verify whether the HDACs, in particular the candidates HDAC3, HDAC5, and HDAC11, are expressed in Ba/F3 cells, the mRNA levels of HDAC1-11 were determined by quantitative RT-PCR. To account for the possibility that HDAC expression in Ba/F3 cells might be IL-3-dependent, HDAC expression was analyzed in unstimulated or IL-3-stimulated Ba/F3 cells. The conventional protocol for gene expression analysis, which uses stabilized RNA-containing lysates as template for cDNA synthesis, led to undetectable *Hdac9* and *Hdac11* mRNA levels (data not shown were generated by Dr. Anne Rascle). To increase the sensitivity of the assay, cDNAs were synthesized from purified total RNA. In agreement with the literature (Dovey et al., 2013; Kelly & Cowley, 2013), *Hdac1* and *Hdac2* showed the highest mRNA levels of all HDACs in Ba/F3 cells (Fig. 4.6A). *Hdac3-8* and *Hdac10* mRNAs were readily detectable, while *Hdac9* and *Hdac11* mRNA levels were at the limit of detection. *Hdac9* and *Hdac11* mRNA levels were only slightly higher than the respective primer-specific signal detected in the negative control (Fig. 4.6B). The negative control had been prepared in parallel to the cDNA reactions. It contained the same amount of RNA preparation (including possible DNA contaminations), but lacked the enzyme reverse transcriptase so that no cDNA was synthesized. No apparent effect of IL-3 on HDAC expression was observed (Fig. 4.6A). Thus the candidates HDAC3 and HDAC5 are expressed in Ba/F3 cells at

the RNA level, which supports their possible involvement in STAT5-mediated transcription. By contrast, the absence of readily detectable HDAC11 mRNA argues against the involvement of HDAC11 in STAT5-mediated transcription in Ba/F3 cells.

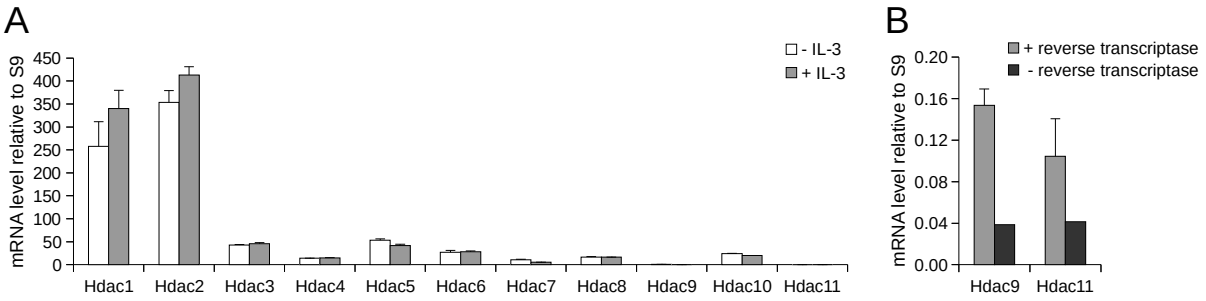

Figure 4.6: HDAC gene expression in Ba/F3 cells
(**A**) HDAC expression was analyzed in Ba/F3 cells that had been rested and then stimulated for 2 h with IL-3 or left unstimulated. For higher sensitivity of the assay, RNAs were purified with MN NucleoSpin RNA II kit. cDNA synthesis and quantitative RT-PCR were performed as before, using primers for *Hdac1* - *Hdac11*. (**B**) The y-axis was adjusted to show *Hdac9* and *Hdac11* expression of the IL-3-stimulated cells from (A) (+ reverse transcriptase). In addition, background signals are shown from a cDNA reaction prepared without reverse transcriptase (- reverse transcriptase). (Data shown in this figure were generated by Dr. Anne Rascle.)

Since mRNA levels do not always directly correlate with protein levels and since eventually the amount of protein in the cell is relevant, the protein abundance of the candidate HDAC proteins was analyzed in Ba/F3 or Ba/F3-1∗6 cell lysates by western blot. HDAC3 protein levels were readily detectable in Ba/F3-1∗6 cells by western blot using an HDAC3-specific antibody (Fig. 4.7B and Fig. 4.8B). In line with the very low mRNA level of *Hdac11*, the HDAC11 protein could not be detected in Ba/F3 cell lysates, although the available antibody detected HDAC11-FLAG that had been overexpressed in Cos-7 cells (data not shown were generated together with Dr. Anne Rascle). Due to its low RNA and protein levels in Ba/F3 cells, HDAC11 was unlikely to be involved in STAT5-mediated transcription. The HDAC5 protein was also not detectable in Ba/F3 cell lysates by western blot, probably due to a combination of low HDAC5 protein abundance and a suboptimal antibody that gave rise to background signals (data not shown were generated together with Dominik Buob, Bachelor Thesis 2013). Nevertheless, HDAC5 was still included for further analysis since its RNA level could be quantified. Thus, the data collected so far suggest that HDAC3 and HDAC5 are the most likely candidates involved in STAT5-mediated transcription and in inhibition of STAT5-mediated transcription by deacetylase inhibitors.

4.2.4 Knockdown of HDAC gene expression does not affect STAT5-mediated transcription

Since inhibition of enzymatic HDAC activity represses STAT5-mediated transcription, depletion of the involved HDAC probably also represses STAT5-mediated transcription. Therefore, to confirm the involvement of one or both of the remaining putative candidate HDACs, HDAC3 and HDAC5, in STAT5-mediated transcription, these HDACs were depleted by siRNA-mediated knockdown, and the effect on expression of STAT5 target genes was analyzed.

Ba/F3 cells are difficult to transfect with siRNA or plasmid DNA. Among several tested transfection methods and reagents like X-treme Gene 9 (Roche), or polyethyleneamine (PEI) (data not shown), only electroporation allowed to successfully transfect Ba/F3 cells and was therefore used as transfection method throughout this study for all Ba/F3-derived cell lines. Electroporation conditions which achieve a higher transfection efficiency typically lead to a higher cell death rate (data not shown). To prevent additional cell loss and stress for the cells by IL-3 withdrawal/IL-3 stimulation, which would be required for analysis of STAT5 target gene expression in Ba/F3 cells, Ba/F3-1∗6 cells were used for siRNA transfection experiments. As described above, Ba/F3-1∗6 cells are well suited to investigate STAT5-mediated transcription (Fig. 4.1). Furthermore STAT5A-1∗6-mediated transcription is sensitive to TSA (Fig. 4.1) and should therefore be sensitive as well to a knockdown of the HDAC responsible for inhibition of STAT5-mediated transcription by deacetylase inhibitors.

As a control for the knockdown, HDAC2-specific siRNA was used for two reasons: (i) HDAC2 served as a positive control for efficient knockdown since an efficient HDAC2-specific siRNA was available and since HDAC2 protein levels are readily detectable by western blot using an HDAC2-specific antibody. (ii) HDAC2 knockdown served as a negative control at the level of STAT5 target gene expression, since HDAC2 was none of the candidates and therefore should not affect STAT5 target gene expression. In addition, as a non-specific control siRNA, a scramble siRNA (ScI) was used (Rascle & Lees, 2003). Thus Ba/F3-1∗6 cells were transfected with non-specific scramble siRNA (ScI) or siRNA directed against HDAC2, HDAC3 and HDAC5. HDAC knockdown efficiency was analyzed at the RNA level by quantitative RT-PCR and at the protein level by western blot. Furthermore, the effect of HDAC knockdown on the expression of the STAT5 target genes *Cis* and *c-Myc*, as well as the housekeeping gene *36b4* was analyzed. siRNA-mediated knockdown of HDAC2 and HDAC3 was successful at the RNA level (80% and 73% knockdown respectively) and at the protein level (Fig. 4.7A and B). The HDAC5 mRNA level was reduced by 38% and its protein level could not be verified, as described

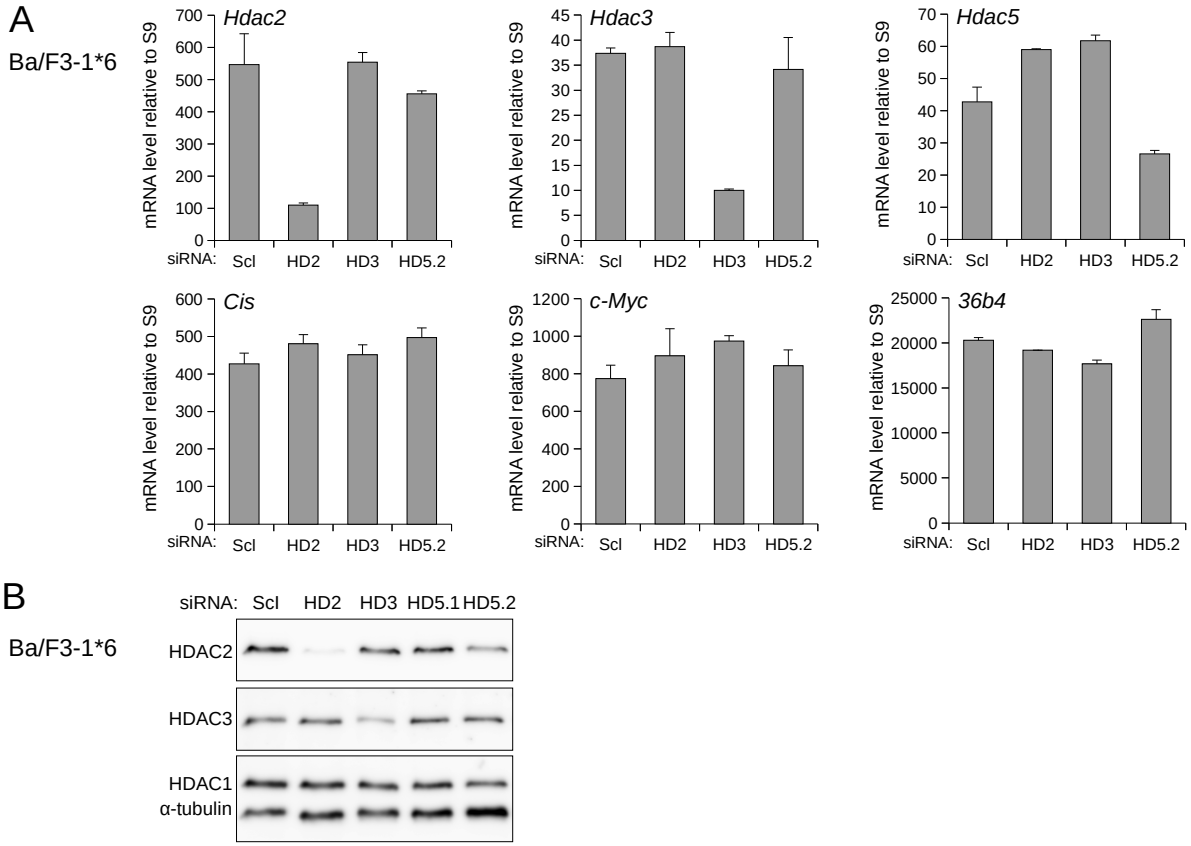

Figure 4.7: HDAC knockdown does not affect STAT5A-1∗6-mediated transcription
Ba/F3-1∗6 cells were transfected twice in an interval of 24 h with 0.5 μM siRNA specific for HDAC2 (HD2), HDAC3 (HD3), and HDAC5 (HD5.1 and HD5.2) as described in Material and methods 3.2.3.8. Scramble siRNA (ScI) served as a non-specific control. Cells were harvested 72 h after the first transfection. (**A**) Gene expression analysis by quantitative RT-PCR was performed using primers specific for *Hdac2, 3*, and *5*, for the STAT5 target genes (*Cis* and *c-Myc*), or for the control gene *36b4*. (**B**) To verify the HDAC knockdown efficiency at the protein level, whole-cell Brij lysates were prepared and analyzed by western blot using antibodies directed against HDAC1, HDAC2, HDAC3 and against the loading control α-tubulin. Because of the high conservation between HDACs, HDAC1 protein levels were also analyzed to verify the specificity of the knockdown. (Data shown in this figure were generated together with Dominik Buob, Bachelor Thesis 2013)

above (Results 4.2.3). Expression of the housekeeping gene *36b4* remained unaffected in all conditions. As expected, HDAC2 knockdown did not affect expression of the STAT5 target genes *Cis* or *c-Myc* (Fig. 4.7A), but unexpectedly, knockdown of the candidates HDAC3 or HDAC5 also did not reduce expression of these genes. Thus, the involvement of HDAC3 or HDAC5 in STAT5-mediated transcription could not be confirmed by these data.

Therefore, a possible functional redundancy of HDAC3 and HDAC5 was considered and was next investigated by their co-knockdown. As a positive control for a cellular response upon HDAC knockdown served a co-knockdown of HDAC1, HDAC2, and HDAC3. HDAC1 and HDAC2 play key roles in the deacetylation of chromatin (Dovey

et al., 2013; Kelly & Cowley, 2013) and are the most highly expressed HDACs in Ba/F3 cells (Fig. 4.6). HDAC3 also deacetylates histones (You et al., 2013). Simultaneously reducing the protein levels of HDAC1, HDAC2 and HDAC3, should lead to increased global histone acetylation, which can be detected by western blot using antibodies specific for acetylated histone H3 and H4.

For siRNA transfection, Ba/F3-1∗6 cells were used as before. They were transfected with an siRNA mix targeting HDAC3 and HDAC5, with an siRNA mix targeting HDAC1, HDAC2 and HDAC3 or with the non-specific siRNA ScI (Fig. 4.8A and B). Knockdown efficiency was analyzed at the RNA level by quantitative RT-PCR and at the protein level by western blot. Furthermore, the effect of HDAC knockdown on STAT5 target gene expression and on global histone acetylation was analyzed. Unfortunately, in the attempted triple knockdown, HDAC1 mRNA as well as protein levels remained unchanged, although HDAC1 individual siRNA transfection successfully reduced its RNA as well as protein levels (data not shown). The absence of effect on HDAC1 in the attempted triple knockdown might be due to a reduced efficiency of HDAC-specific siRNA, an elevated stability of HDAC1 mRNA and protein, or the lower amount of HDAC1-specific siRNA in the triple compared to a single knockdown. HDAC2 and HDAC3 mRNA levels were reduced by 75% and 85% respectively (Fig. 4.8A) and their protein levels were also reduced (Fig. 4.8B). This control knockdown showed slightly increased histone H3 and histone H4 acetylation (Fig. 4.8B), suggesting that the knockdown conditions were strong enough for a global cellular response. Nevertheless, even with a strong HDAC3 and partial HDAC5 co-knockdown (86% and 48% knockdown at the RNA level respectively), expression of the STAT5 target gene *Cis* was not reduced (Fig. 4.8A). Thus, neither individual nor co-knockdown experiments could confirm the involvement of HDAC3 or HDAC5 or both in STAT5-mediated transcription.

Since the analysis with selective inhibitors might have missed possible candidates, Ba/F3-1∗6 cells were transfected with siRNA directed against the remaining HDACs, namely HDAC4, HDAC6-10 and HDAC11 (data not shown were generated together with Dr. Anne Rascle and Dominik Buob, Bachelor Thesis 2013, Pinz et al., 2015, fig. S4). Again, no effect on expression of STAT5 target genes was observed.

Altogether, neither siRNA-mediated knockdown of all individual HDACs nor co-knockdown of several HDACs inhibited STAT5 target gene expression. This absence of effect on STAT5 target gene expression might be caused on the one hand by insufficient knockdown efficiency of each HDAC, which is supported by the weak effect of HDAC co-knockdown on histone acetylation (Fig. 4.8B), and on the other hand by a possible functional redundancy of several HDACs in the regulation of STAT5-mediated transcription.

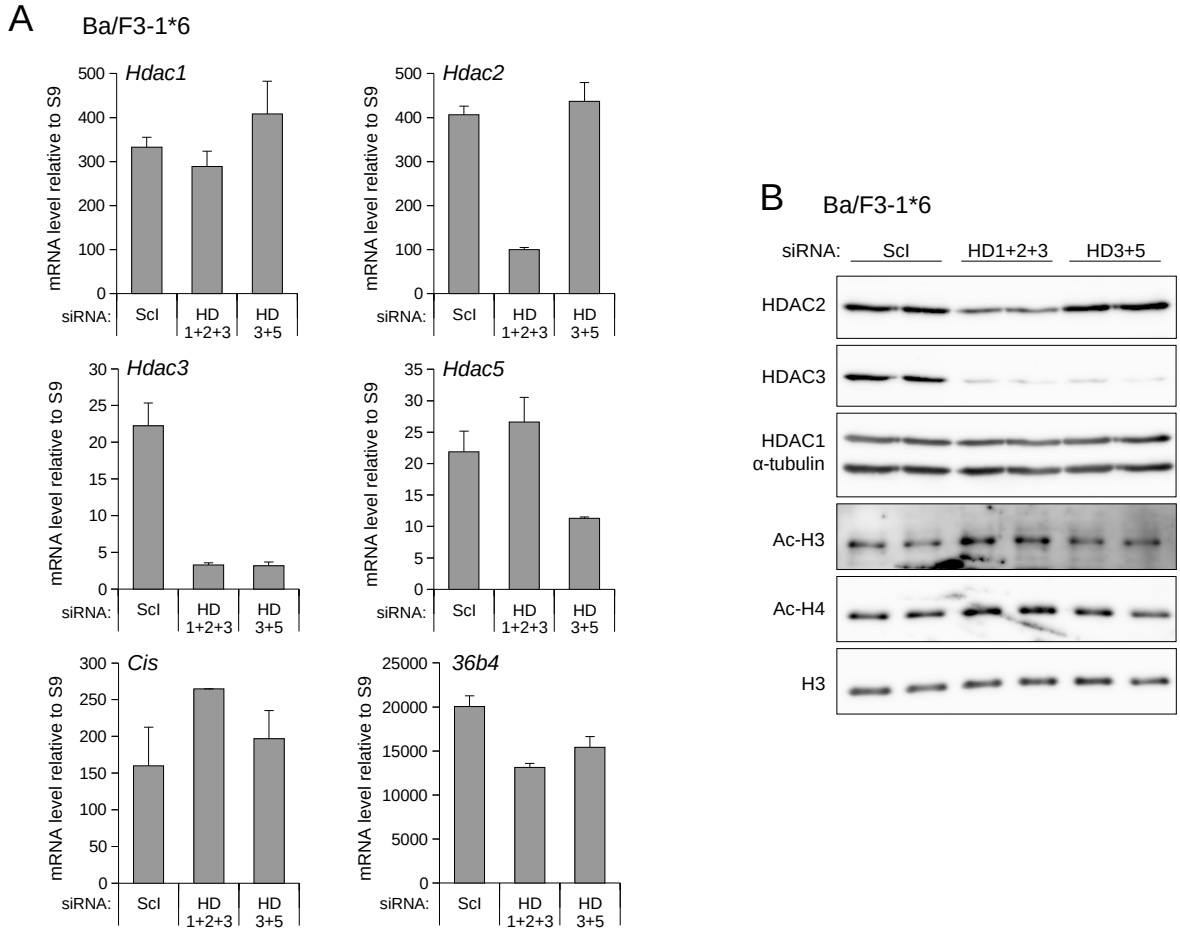

Figure 4.8: Co-knockdown of multiple HDACs does not affect STAT5A-1∗6-mediated transcription

Ba/F3-1∗6 cells were transfected with siRNA twice in an interval of 24 h and were harvested 48 h after the first transfection. For the co-knockdown of HDAC1, HDAC2, and HDAC3 (HD1+2+3) and for the co-knockdown of HDAC3 and HDAC5 (HD3+5) the following concentrations of HDAC (HD)-specific siRNA were used: 0.25 μM HDAC1 siRNA, 0.1 μM HDAC2 siRNA, 0.25 μM HDAC3 siRNA, and 0.35 μM HDAC5 siRNA (HD5.2). 0.6 μM scramble (ScI) siRNA served as a non-specific control. (**A**) Gene expression was analyzed by quantitative RT-PCR using primers specific for *Hdac1*, *Hdac2*, *Hdac3*, *Hdac5*, *Cis*, and *36b4*. (**B**) Whole-cell protein lysates were prepared by freeze/thaw protocol (Material and methods 3.2.4.2) and analyzed by western blot to determine the HDAC knockdown efficiency at the protein level and the effect of HDAC knockdown on histone acetylation. For western blot, antibodies directed against HDAC1, HDAC2, HDAC3, α-tubulin, acetylated histone H3 (Ac-H3), acetylated histone H4 (Ac-H4), and against total histone H3 (H3) were used. α-tubulin and total histone H3 served as loading controls.

In summary, the screen with selective deacetylase inhibitors suggested the participation of HDAC3, HDAC5 or HDAC11 in STAT5-mediated transcription. However, siRNA-mediated HDAC knockdown could not confirm the involvement of one specific HDAC, but rather supports a model of functional redundancy of several HDACs in the regulation of STAT5-mediated transcription. A model of functional redundancy is further supported by the finding that overexpression of individual HDACs through transfection of HDAC expression plasmids did not affect STAT5 target gene expression (data not shown were generated together with Philipp Fischer, internship 2013) and by the fact that selective deacetylase inhibitors which repress STAT5 target genes (TSA, VPA and apicidin) each target several HDACs simultaneously (Fig. 4.3 and Tab. 4.1).

4.3 Identification of the acetylated substrate involved in deacetylase inhibitor-mediated inhibition of STAT5-mediated transcription

In addition to HDACs, their acetylated substrate is very likely also involved in inhibition of STAT5-mediated transcription by deacetylase inhibitors. To identify the acetylated substrate, we investigated if it might be acetylated STAT5, an unknown acetylated STAT5-specific cofactor or acetylated histones.

4.3.1 Establishment of a GAL4-STAT5A luciferase reporter assay

STATs, in particular STAT5 and STAT3, are regulated by acetylation (Choudhary et al., 2009; Ma et al., 2010; Van Nguyen et al., 2012; Wieczorek et al., 2012). Therefore, STAT5 might be the acetylated substrate involved in inhibition of STAT5-mediated transcription by deacetylase inhibitors. In case this assumption is true and increased STAT5 acetylation upon deacetylase inhibitor treatment inhibits STAT5-mediated transcription, STAT5 acetylation would probably inhibit STAT5-mediated transcription per se. To investigate if acetylation of STAT5 at specific lysines might inhibit STAT5-mediated transcription, we analyzed whether mutation of specific lysine residues within STAT5 to glutamine, mimicking the acetylated lysine, or to arginine, mimicking the unmodified lysine, affects STAT5 transcriptional activity. A lysine-to-glutamine mutation of a residue whose acetylation inhibits STAT5-mediated transcription is expected to inhibit STAT5-mediated transcription, while mutation of such lysine residue to arginine is expected to leave STAT5-mediated transcription either unaffected or lead to increased activity.

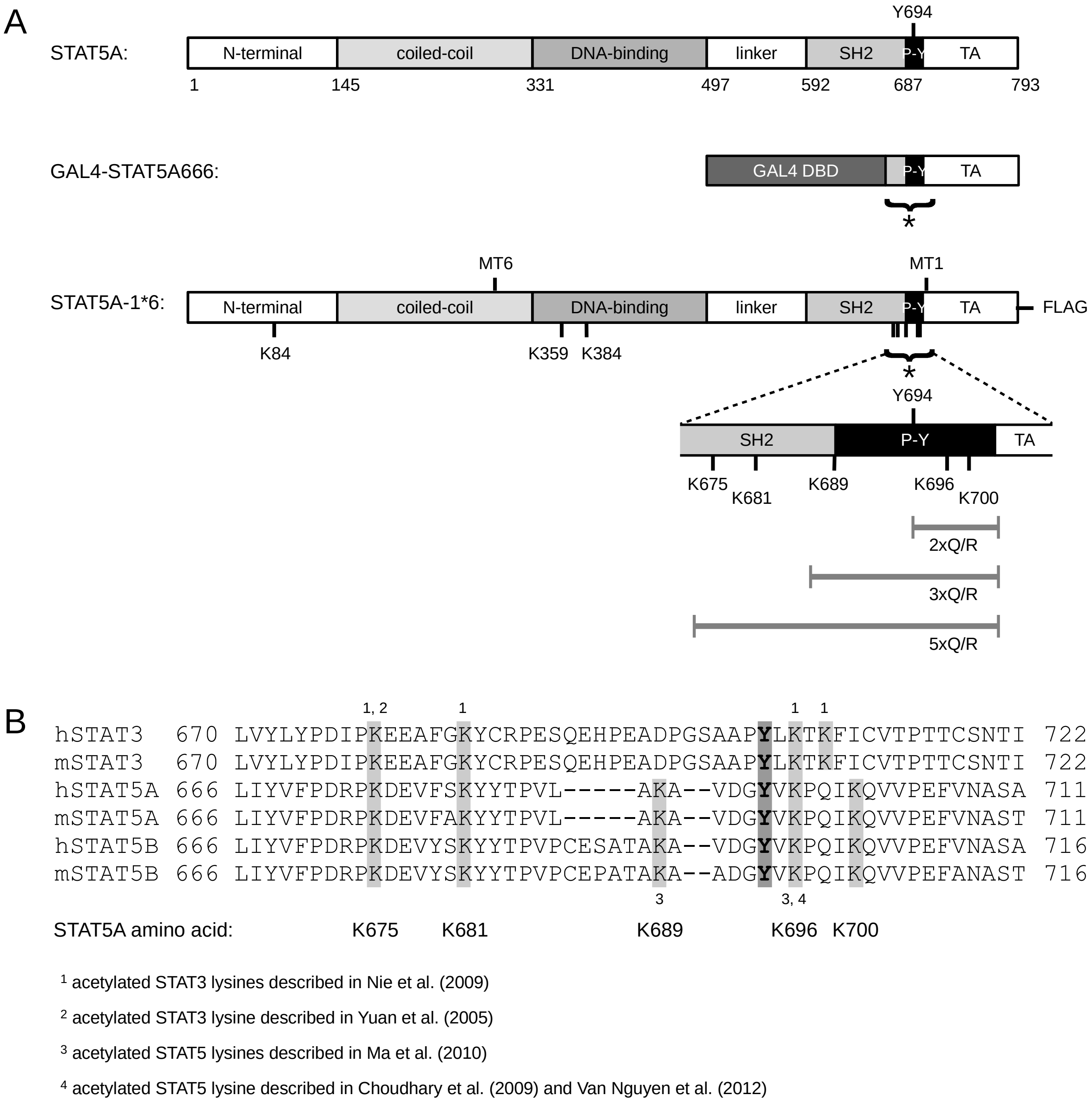

Figure 4.9: Location of mutated lysine residues within STAT5A-1∗6 and GAL4-STAT5A666 (**A**) Schematic representation of mouse STAT5A, STAT5A-1∗6, and GAL4-STAT5A666. The depicted domain structure is inherent to all STAT proteins. Mouse STAT5A-1∗6 was expressed from a pcDNA3 expression vector in frame with a C-terminal FLAG tag. The C-terminus of mouse STAT5A, comprising amino acids 666-793, was cloned in fusion with the *Saccharomyces cerevisiae* GAL4 DNA binding domain of the pFA-CMV expression vector to generate the GAL4-STAT5A666 fusion protein. Indicated are the conserved phosphotyrosine Y694 as well as the two point-mutations MT1 (S710F) and MT6 (H298R) conferring constitutive activity to STAT5A-1∗6. Lysines K84, K359, K384, K675, K681, K689, K696, and K700 were mutated by site-directed mutagenesis to either glutamine or arginine in the context of STAT5A-1∗6 or GAL4-STAT5A666. In addition, the lysine residues that are mutated within the double (2xQ/R), triple (3xQ/R), and quintuple mutants (5xQ/R) to glutamine or arginine are indicated. All structures are drawn to scale. (**B**) The alignment of human and mouse STAT3, STAT5A and STAT5B was generated as described in Material and methods 3.2.8. Conserved lysine residues are indicated in gray, the phosphorylated tyrosine in bold. P-Y, phosphotyrosine tail segment; TA, transactivation domain; GAL4 DBD, GAL4 DNA binding domain.

Five lysine residues located within the C-terminal SH2 and the transactivation domain of STAT5 (K675, K681, K689, K696 and K700 of STAT5A) are well conserved among mouse and human STAT5A and B and to a certain extent between STAT5 and its paralog STAT3 (Fig. 4.9B). Acetylation of these lysines was reported either for STAT5 (Choudhary et al., 2009; Ma et al., 2010) or for the corresponding lysine in STAT3 (Wang et al., 2005; Yuan, 2005; Nie et al., 2009) (Fig. 4.9B). Furthermore, K689 and K696 of STAT5A, or the corresponding lysine in STAT5B, were demonstrated to be critical for the regulation of STAT5 (Ma et al., 2010; Van Nguyen et al., 2012). The lysines corresponding to K675, K681, K696 and K700 of STAT5A were demonstrated to be critical for the regulation of STAT3 (Wang et al., 2005; Yuan, 2005; Nie et al., 2009). Together, this makes K675, K681, K689, K696 and K700 the most likely lysine residues whose acetylation might regulate STAT5-mediated transcription.

STAT acetylation affects different initial activation steps within the pathway like STAT phosphorylation, dimerization or nuclear translocation (Yuan, 2005; Krämer et al., 2009; Nie et al., 2009; Ma et al., 2010; Gupta et al., 2012). Lysine mutations which disrupt important acetylation sites might thus interfere with STAT5 activity at an earlier activation step and abrogate further downstream processes such as DNA binding and transcriptional activation. Therefore, to investigate specifically the effect of lysine mutations on DNA-bound STAT5 at the transcriptional level, an experimental system was designed, using a GAL4-STAT5 reporter assay, which circumvents the need for initial STAT5 activation steps. The GAL4 DNA binding domain of the GAL4 transcriptional activator of *Saccharomyces cerevisiae* (amino acids 1-147) binds specifically to GAL4 DNA binding sites, so-called GAL4 upstream activator sequences (UAS), but fails to activate transcription (Ma & Ptashne, 1987; Kakidani & Ptashne, 1988; Ma et al., 1988). It can thus be used as part of a fusion protein to confer DNA binding activity to another protein domain such as the STAT5 transactivation domain, to characterize its ability to activate transcription of a reporter gene (Ma & Ptashne, 1987; Sadowski et al., 1988; Moriggl et al., 1996). For the experiments shown here, a *Firefly* luciferase reporter construct was used, which contains nine repeats of the GAL4 UAS. Transcriptionally active GAL4 fusion proteins thus induce the production of the *Firefly* luciferase enzyme, which can be readily quantified by means of the bioluminescent reaction which it catalyzes.

Therefore, an expression vector was generated for the expression of a fusion protein between the GAL4 DNA binding domain and the mouse STAT5A C-terminus from amino acid 666 to amino acid 793 (Stop), comprising the lysines of interest. The resulting GAL4-STAT5A666 protein contains part of the STAT5 SH2-domain, its phosphotyrosine tail segment, and its complete transactivation domain (Fig. 4.9A). The lysines corresponding to K675, K681, K689, K696 and K700 of STAT5A were mutated within

GAL4-STAT5A666 by site-directed mutagenesis to glutamine and to arginine.

The generated expression plasmids encoding either the GAL4-STAT5A666 fusion protein, or its lysine mutants, or the corresponding empty vector (negative control) were transiently co-transfected together with the GAL4 UAS luciferase reporter into Cos-7 cells. As an internal control for transfection efficiency, an expression plasmid harboring a constitutively expressed *Renilla* luciferase gene was additionally co-transfected for all luciferase assays in this study. Since *Renilla* luciferase uses a different substrate than *Firefly* luciferase, both enzymatic activities can be measured in the same lysate by Dual-Luciferase Reporter Assay (Promega). The measured *Firefly* luciferase activity can then be normalized to the respective *Renilla* luciferase activity. In addition to measuring luciferase activity of the transfected cells, expression of the fusion proteins was verified by western blot. As shown by western blot using GAL4- and STAT5-specific antibodies, GAL4-STAT5A666 and its mutants showed similar but low protein levels (Fig. 4.10A). Accordingly, GAL4-STAT5A666 induced the reporter gene by only 1.9-fold relative to empty vector control. All GAL4-STAT5A666 lysine mutants activated the luciferase reporter by 1.5- to 2.3-fold (Fig. 4.10A) and thus with a similar efficiency as parental GAL4-STAT5A666, arguing against a functional role of these lysine residues in STAT5-mediated transcription. However, the low protein levels, the weak induction of the luciferase reporter and the non-physiological experimental system, using Cos-7 cells which normally do not operate the STAT5 signaling pathway, might be responsible for this result. Therefore, no definite conclusion could be drawn from these experiments.

Therefore, to use a more physiological experimental system, Ba/F3 cells were used for the luciferase reporter assays, since the STAT5 pathway is activated in these IL-3-dependent cells (Rodriguez-Tarduchy et al., 1990; Nelson et al., 2004) and all cofactors involved in STAT5-mediated transcription should be available. Ba/F3 cells were transiently co-transfected by electroporation with the GAL4 UAS luciferase reporter and the expression plasmid encoding the GAL4-STAT5A666 fusion protein or the empty control vector. As a positive control, the GAL4-STAT5A709 construct, comprising STAT5A amino acids 709-793(Stop) (Watanabe et al., 2001), was used. Similar GAL4-STAT5A fusion constructs had been successfully used to characterize the STAT5 transactivation domain (Moriggl et al., 1996; Watanabe et al., 2001). The positive control GAL4-STAT5A709 was well expressed and induced the luciferase reporter almost 8-fold (Fig. 4.10B). The GAL4-STAT5A666 fusion protein induced the luciferase reporter 3-fold (Fig. 4.10B), which was higher than in Cos-7 cells, but unfortunately, the protein level of GAL4-STAT5A666 fusion proteins was below detection level in western blot (Fig. 4.10B and data not shown). Therefore, it was impossible to properly evaluate the transcriptional activity of the lysine mutants (data not shown). Another caveat of the GAL4-luciferase

assay in Ba/F3 cells were the low *Firefly* relative light units (RLU) measured (up to 800 RLU for GAL4-STAT5A666 in Ba/F3 cells compared to 700,000 RLU in the previous Cos-7 assay). The low luciferase activity made the assay susceptible to inter-experiment variation.

With the aim to solve those problems, and in regard of the low transfection efficiency of plasmid DNA into Ba/F3 cells (data not shown), the Ba/F3-G4-Luc2P cell line was generated (together with Dr. Anne Rascle), carrying the stably integrated 9x GAL4 UAS *Firefly* luciferase reporter. Individual clones were tested for basal luciferase activity and for inducibility of luciferase activity upon transfection of the positive control GAL4-STAT5A709. Clone 2.A was chosen for further experiments since it was one of the best inducible clones (up to 8.5-fold induction with GAL4-STAT5A709, Fig. 4.10C and D). Furthermore, Clone 2.A showed a basal luciferase activity of about 20,000 RLU, compared to about 50 RLU of another clone (clone 3.D) (data not shown were obtained from 95 μg total protein of non-transfected cells during 10 sec measurement time in a luminometer), so that the obtained RLUs in the luciferase assay were in a well detectable range.

Ba/F3-G4-Luc2P cells were transfected with GAL4-STAT5A666, the 696Q/R and 700Q/R lysine mutants, the positive control GAL4-STAT5A709 or the empty control vector. The GAL4-STAT5A666 protein was detectable at the protein level by western blot using STAT5- or GAL4-specific antibodies, but its protein level was still low (Fig. 4.10C). The protein level of GAL4-STAT5A666 was lower than that of GAL4-STAT5A709, as revealed by GAL4-specific antibody. In contrast to GAL4-STAT5A709, which induced the reporter 4- to 8.5-fold relative to empty vector control (Fig. 4.10C and D), GAL4-STAT5A666 and its mutants failed to activate the reporter (1.2- to 1.6-fold induction, Fig. 4.10C and D). Thus, no conclusion regarding the effect of lysine mutations on STAT5-mediated transcription could be drawn.

In summary, we tried but failed to establish a luciferase assay in Ba/F3-derived cells using the GAL4-STAT5A666 fusion protein. In Cos-7 cells, lysine-mutated GAL4-STAT5A666 fusion proteins induced the luciferase reporter similarly strong as parental GAL4-STAT5A666, which argues against an involvement of those lysine residues in STAT5-mediated transcription. Furthermore, the absence of inhibition of STAT5-mediated transcription by glutamine mutants, mimicking the acetylated lysine, argues against an inhibition of STAT5-mediated transcription by lysine acetylation. However, low protein abundance of GAL4-STAT5A666 concomitant with weak induction of the luciferase reporter might be responsible for the observed result. Therefore, no definite conclusion could be drawn from these experiments and an alternative approach was started.

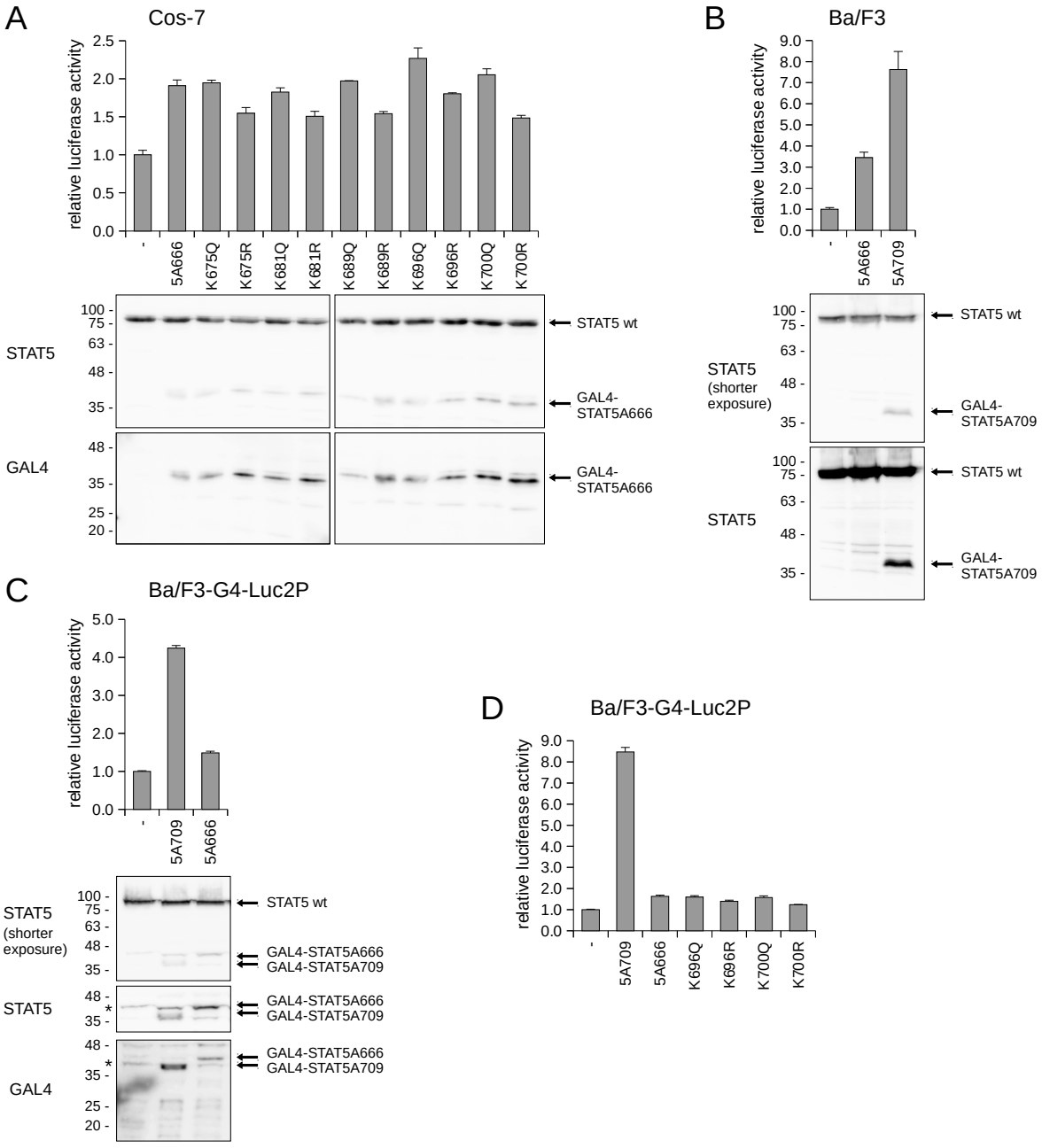

Figure 4.10: Mutation of lysine residues does not impair GAL4-STAT5A666 transcriptional activity in luciferase assays

(**A**) Cos-7 cells were transiently co-transfected with the GAL4 UAS *Firefly* luciferase reporter pGL4.35 and with the empty control vector pFA-CMV (-), or a pFA-CMV-based expression plasmid for either GAL4-STAT5A666 (5A666) or for a GAL4-STAT5A666 lysine mutant (K675Q, K675R, K681Q, K681R, K689Q, K689R, K696Q, K696R, K700Q, K700R). The cells were analyzed for luciferase activity as described in Material and methods 3.2.6. Western blot was performed from the same PLB lysate to confirm expression of the GAL4-STAT5A666 fusion proteins. *(Continued on next page)*

Figure 4.10: *(Continued)* **(B)** Ba/F3 cells were transiently co-transfected with the GAL4 UAS *Firefly* luciferase reporter pGL4.35 and with the empty control vector pFA-CMV (-) or the expression plasmid for either GAL4-STAT5A666 (5A666) or the positive control GAL4-STAT5A709 (5A709). The cells were harvested 8 hours after transfection for luciferase assay and 24 h after transfection for analysis of protein expression from Brij whole-cell lysate by western blot. (**C**), (**D**) Ba/F3 cells with stably integrated GAL4 UAS *Firefly* luciferase reporter (pGL4.35), so-called Ba/F3-G4-Luc2P cells, were transiently transfected with the empty control vector pFA-CMV (-) or with an expression plasmid for either GAL4-STAT5A709 (5A709), GAL4-STAT5A666 (5A666), or for one of the STAT5A666 mutants as indicated. Luciferase assay was performed 18 h after transfection. For the western blot in (C), transfected cells were lysed in Brij whole-cell lysis buffer. In (A)-(D), *Firefly* luciferase activity was normalized to co-transfected constitutively expressed *Renilla* luciferase and presented as fold induction relative to empty vector control. For the western blots shown in (A)-(C), antibodies directed against STAT5 and the GAL4 DNA binding domain were used. The STAT5-specific antibody is directed against a C-terminal epitope of STAT5 and thus recognizes endogenous wild-type STAT5 (STAT5 wt) as well as GAL4-STAT5A666 and GAL4-STAT5A709. The STAT5 signal, especially the shorter exposures in (B) and (C), served as a loading control. The expected size of the fusion proteins is about 30 kDa, however, in western blot the protein signals appeared above the 35 kDa marker. Of note, the GAL4 DNA binding domain (17 kDa, appear in western blot around the 20 kDa marker, Jobst et al., 2016, fig. 2) expressed from empty control vector was not detectable in (A) and (C) by western blot using a GAL4-specific antibody. The asterisks in (C) mark unspecific signals overlapping the signal for GAL4-STAT5 fusion proteins. These signals probably appeared because the blot was developed with the highly sensitive ECL reagent SuperSignal West Femto Maximum Sensitivity Substrate (Thermo Fisher Scientific).

4.3.2 Mutation of specific lysines of STAT5A-1∗6 does not affect STAT5A-1∗6 transcriptional activity in luciferase assays

As alternative approach, the well-described constitutively active STAT5A-1∗6 was used instead of GAL4-STAT5A666 to analyze the effect of lysine mutations on STAT5 transcriptional activity. STAT5A-1∗6, like GAL4-STAT5 fusion proteins, does not need an external activation stimulus to mediate transcription. Furthermore, STAT5A-1∗6 and wild-type STAT5 are similarly sensitive to TSA (Fig. 4.1), and should therefore be similarly sensitive to mutation of potentially acetylated lysine residues. Thus, STAT5A-1∗6 is a suitable model to investigate whether mutation of potentially acetylated lysines affects STAT5-mediated transcription. In order to investigate a possible functional redundancy between the investigated lysine residues, double (2xQ/R), triple (3xQ/R) and quintuple (5xQ/R) lysine mutations were created within full-length STAT5A-1∗6 (Fig. 4.9A), in addition to the single lysine mutations described above. The 2xQ and 2xR mutants carry mutations at K696 and K700, the 3xQ and 3xR mutants carry mutations at K689, K696, and K700, and the 5xQ and 5xR mutants carry mutations at all 5 investigated lysine residues (K675, K681, K689, K696, and K700) to glutamine (Q) or arginine (R), as depicted in Figure 4.9A. STAT5A-1∗6 and all of its mutants were expressed from a pcDNA3 vector backbone and carry a C-terminal FLAG tag, which can be used to distinguish these proteins from endogenous STAT5 by western blot using a FLAG-specific antibody. The activity of the lysine mutants was evaluated in luciferase reporter assays

using reporter constructs bearing the STAT5-responsive β-casein (Chida et al., 1998) or *Cis* (Matsumoto et al., 1997) promoter.

Therefore, STAT5A-1∗6 or its mutants were transiently co-transfected together with the rat β-casein-driven luciferase reporter (called β-casein luciferase reporter thereafter) (Chida et al., 1998) into Ba/F3 cells. To allow optimal recovery of the transfected cells from electroporation, they were cultured in the presence of IL-3, so that endogenous STAT5 was at its basal activity in these cells. Western blot analysis using a FLAG-specific antibody showed that STAT5A-1∗6 and its mutants were well expressed at the protein level. The only exception were STAT5A-1∗6 proteins containing mutations at K675 (K675Q/R and 5xQ/R mutants). These proteins were poorly detectable by western blot, likely due to protein instability (Fig. 4.11A and B). Therefore, their activity in luciferase assay could not be evaluated. STAT5A-1∗6 activated the β-casein luciferase reporter 7- to 11-fold above endogenous STAT5 (empty vector control) (Fig. 4.11A and B). All well expressed lysine mutants induced the reporter as efficiently as parental STAT5A-1∗6 (0.8- to 1.4-fold relative to STAT5A-1∗6, Fig. 4.11A and B), suggesting that none of these lysine residues (K681, K689, K696, and K700) are essential for STAT5-mediated transcription. Furthermore, since none of the glutamine mutations, mimicking the acetylated lysine, inhibited STAT5-mediated transcription, acetylation of those lysines is unlikely to affect STAT5-mediated transcription.

In contrast to the β-casein gene, which is mainly relevant during lactation in the mammary gland (Groner & Gouilleux, 1995; Chida et al., 1998), the STAT5 target gene *Cis* is induced in response to IL-3 and well characterized in the pro-B cell line Ba/F3 (Matsumoto et al., 1997; Rascle et al., 2003; Basham et al., 2008). Therefore, next, a mouse *Cis* promoter-driven luciferase reporter (called *Cis* luciferase reporter thereafter) was used. To avoid induction of the reporter by endogenous STAT5, transfected cells were first recovered in the presence of IL-3 and then cultured for the last 12 h under IL-3-free conditions. Furthermore, these conditions, in which endogenous STAT5 is inactive, should prevent that a possible inactivity of STAT5A-1∗6 lysine mutants is concealed by the formation of hypothetically functional heterodimers consisting of inactive STAT5A-1∗6 lysine mutants and transcriptionally active phosphorylated endogenous STAT5. In addition, as a control to better characterize the experimental system, cells transfected with wild-type STAT5 and STAT5A-1∗6 were cultured in the presence of IL-3 throughout the experiment. Like STAT5A-1∗6, wild-type STAT5 was also expressed with a C-terminal FLAG tag from a pcDNA3 vector backbone. As expected in the absence of IL-3, transfected wild-type STAT5A did not induce expression of the *Cis* luciferase reporter (Fig. 4.12A, B, and C). In the presence of IL-3, endogenous STAT5 failed to activate the reporter (empty vector control, +IL-3) and transfected wild-type STAT5

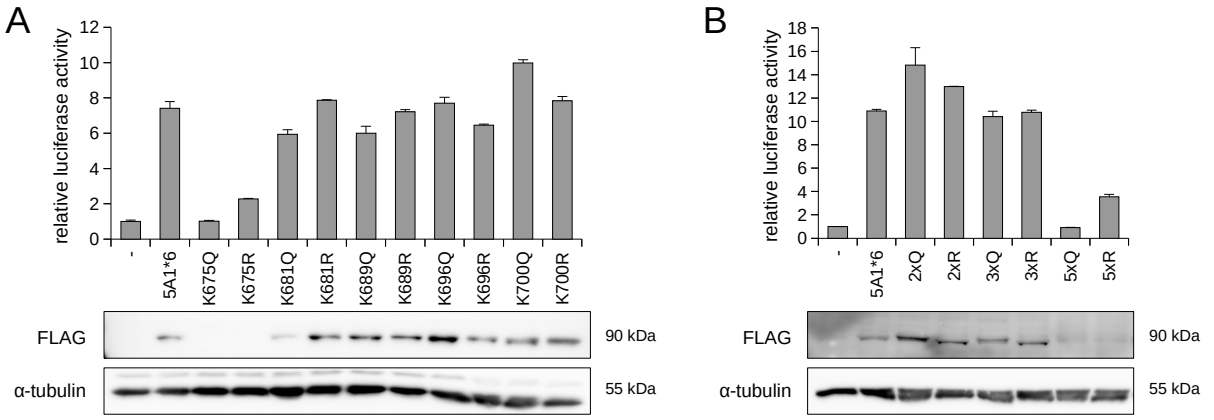

Figure 4.11: In β-casein promoter-driven luciferase assays, lysine mutations do not impair the transcriptional activity of STAT5A-1∗6
Ba/F3 cells were transiently co-transfected with the *Firefly* luciferase reporter pGVB-β-casein, and with the empty control vector pcDNA3 (-) or the pcDNA3-based expression plasmid of either mSTAT5A-1∗6-FLAG (5A1∗6) or of one of its mutants (K675Q, K675R, K681Q, K681R, K689Q, K689R, K696Q, K696R, K700Q, K700R, 2xQ, 2xR, 3xQ, 3xR, 5xQ, 5xR). The cells were cultured in the presence of IL-3 and harvested 18 h (A) or 19 h (B) after transfection. (**A**) Part of the cells were lysed in PLB and analysis of luciferase activity was performed as described in Material and methods 3.2.6. *Firefly* luciferase activity was normalized to co-transfected constitutively expressed *Renilla* luciferase and presented as fold induction relative to empty vector control. The remaining cells were subjected to Brij lysis (Material and methods 3.2.4.1) and western blot analysis. An antibody specific for the FLAG tag was used for western blot, to confirm protein expression of STAT5A-1∗6 or its lysine mutants. An antibody directed against α-tubulin served as a loading control. (**B**) The experiment was performed as described in (A), except that all transfected cells were lysed in PLB buffer and western blot was performed from this PLB-lysate.

induced the reporter only 4-fold (Fig. 4.12A). By contrast, STAT5A-1∗6 transfection resulted in a strong activation of the *Cis* luciferase reporter of 14- to 28-fold in the absence of IL-3 (Fig. 4.12A, B, and C). The presence of IL-3 did not have an additional affect on STAT5A-1∗6-dependent activation of the luciferase reporter (Fig. 4.12A), further demonstrating the transactivation potential of STAT5A-1∗6 independently of external stimuli. As a positive control for an inactivating STAT5A-1∗6 mutation, the conserved tyrosine Y694, which is essential for STAT5 phosphorylation and activation (Onishi et al., 1998), was mutated to phenylalanine (Fig. 4.12C, Y694F mutant). Western blot using a FLAG-specific antibody revealed low protein abundance of STAT5A-1∗6-Y694F (Fig. 4.12C). However, additional experiments confirmed a lack of transcriptional activity of STAT5A-1∗6-Y694F while being well expressed (Fig. 4.13A), demonstrating that STAT5A-1∗6 can be inactivated. Disruption of all STAT5 binding sites within the *Cis* promoter (Matsumoto et al., 1997) abolished induction of the luciferase reporter (Fig. 4.12A, mut *Cis* promoter), confirming the specific induction of the *Cis* luciferase reporter by STAT5. Consequently, this reporter assay, constituted by components from one organism - mouse STAT5A-1∗6, a mouse *Cis*-promoter driven luciferase reporter, and mouse Ba/F3 cells cultured in the absence of IL-3 - is an optimal experimental system to investigate the effect of lysine mutations on STAT5 transcriptional activity.

This reporter assay was now used to assess the influence of the triple mutants 3xQ and 3xR (containing mutations at K689, K696, and K700) on STAT5A-1∗6 transcriptional activity. The 5xQ/R mutants were not tested due to their weak protein levels shown previously (Fig. 4.11B). Interestingly, the transfected 3xQ and 3xR mutants induced the luciferase reporter with similar efficiency as STAT5A-1∗6 (about 1.1-1.6-fold above STAT5A-1∗6, Fig. 4.12B), demonstrating that the triple mutations have no effect on the transcriptional activity of STAT5A-1∗6. Therefore, the corresponding single mutants were not tested. The absence of effect of the triple mutations on STAT5A-1∗6 transcriptional activity confirms that K689, K696 and K700 are indeed not essential for STAT5-mediated transcription, and provides evidence against a functional redundancy of these adjacent lysine residues. Furthermore, since the glutamine mutations, mimicking acetylated lysine residues, did not inhibit STAT5-mediated transcription, an inhibition of STAT5-mediated transcription by acetylation is unlikely.

Besides the investigated lysine residues, which are all located next to the transactivation domain, there are additional putative acetylation sites in STAT5 at K84, located within the N-terminal, and K359 and K384, located within the DNA binding domain (Fig. 4.9A) (Ma et al., 2010; Wieczorek et al., 2012). Acetylation of K359 has been demonstrated by mass spectrometry and an acetylation-site-specific antibody (Ma et al., 2010). Mutation of K359 to arginine abrogated the ability of STAT5B to induce a luciferase reporter in the prostate cancer cell line PC3 (Ma et al., 2010). Acetylation of K384 was found by two independent high throughput mass spectrometric approaches documented by PhosphoSitePlus (www.phosphosite.org), an online resource for the study of post-translational modifications (Wieczorek et al., 2012; Hornbeck et al., 2015), but the functional relevance of K384 or its acetylation for STAT5 activity has not been investigated. According to Wieczorek et al. (2012), acetylation of K84 was also described by PhosphoSitePlus. Furthermore, a nearby lysine residue within STAT3 (K87), has been shown to be acetylated and essential for STAT3-mediated transcription (Ray et al., 2005; Nie et al., 2009). No further STAT5 acetylation sites are reported by PhosphoSitePlus (www.phosphosite.org, February 2017) (Hornbeck et al., 2015). To determine the relevance of K84, K359, and K384 for STAT5-mediated transcription, these lysine residues were mutated within STAT5A-1∗6 to glutamine and arginine and the resultant mutants were tested for their transcriptional activity in the *Cis* luciferase reporter assay. However, similarly as the other mutants before, these new lysine mutants induced the luciferase reporter with similar efficiency as STAT5A-1∗6 (0.9- to 1.3-fold induction relative to STAT5A-1∗6, Fig. 4.12C), demonstrating that K84, K359, and K384 are also functionally dispensable for STAT5-mediated transcription and that acetylation of these residues is unlikely to affect STAT5-mediated transcription.

In summary, eight lysine residues within STAT5, which have been previously proposed to be involved in the regulation of STAT5 or whose corresponding lysines have been proposed to be essential for the regulation of STAT3, were investigated. Mutating these lysine residues did not affect STAT5-mediated transcription in luciferase reporter assays, suggesting that acetylation of these lysine residues, which was mimicked by the mutation to glutamine, does not inhibit STAT5-mediated transcription. Thus, inhibition of STAT5-mediated transcription by deacetylase inhibitors is probably not mediated by an increase in acetylation of STAT5, and STAT5 is probably not the acetylated factor involved in inhibition of STAT5-mediated transcription by deacetylase inhibitors.

4.3.3 Mutation of specific lysine residues does not affect STAT5A-1∗6-mediated activation of endogenous STAT5 target genes

The observation that the investigated lysine residues were not required for STAT5A-1∗6 activity in luciferase assays doesn't exclude the possibility that these lysines and their de-/acetylation affect the activation of endogenous STAT5 target genes in their natural enhancer, promoter and chromatin context. To address this point, the transactivation potential of the STAT5A-1∗6 lysine mutants on endogenous genes was assessed in Ba/F3 cells.

Ba/F3 cells were transfected with the expression plasmids for the STAT5A-1∗6 lysine mutants and subsequently maintained in IL-3-free medium to ensure that endogenous STAT5 is kept in its unphosphorylated, inactive state. To assess the transcriptional activity of the STAT5A-1∗6 lysine mutants, mRNA levels of the STAT5 target gene *Cis* were measured by quantitative RT-PCR. Furthermore, the protein levels of the STAT5A-1∗6 mutants and their activation by tyrosine-phosphorylation were analyzed by western blot (Fig. 4.13A and B).

All generated single and multiple STAT5A-1∗6 lysine mutants were tested in this assay. A construct encoding wild-type STAT5A, which is inactive in the absence of IL-3, was transfected as a negative control. Western blot confirmed that endogenous STAT5 (empty vector control) as well as exogenous wild-type STAT5 were unphosphorylated, as expected in the absence of IL-3. Accordingly, wild-type STAT5 only marginally induced *Cis* expression. By contrast, phosphorylated and thus active STAT5A-1∗6 strongly induced *Cis* expression (Fig. 4.13A and B). The positive control for a STAT5A-1∗6 inactivating mutation, Y694F, was well expressed, but did not induce expression of the target gene *Cis*, as expected (Fig. 4.13A).

These data confirm the results of the luciferase assays, that none of the investigated ly-

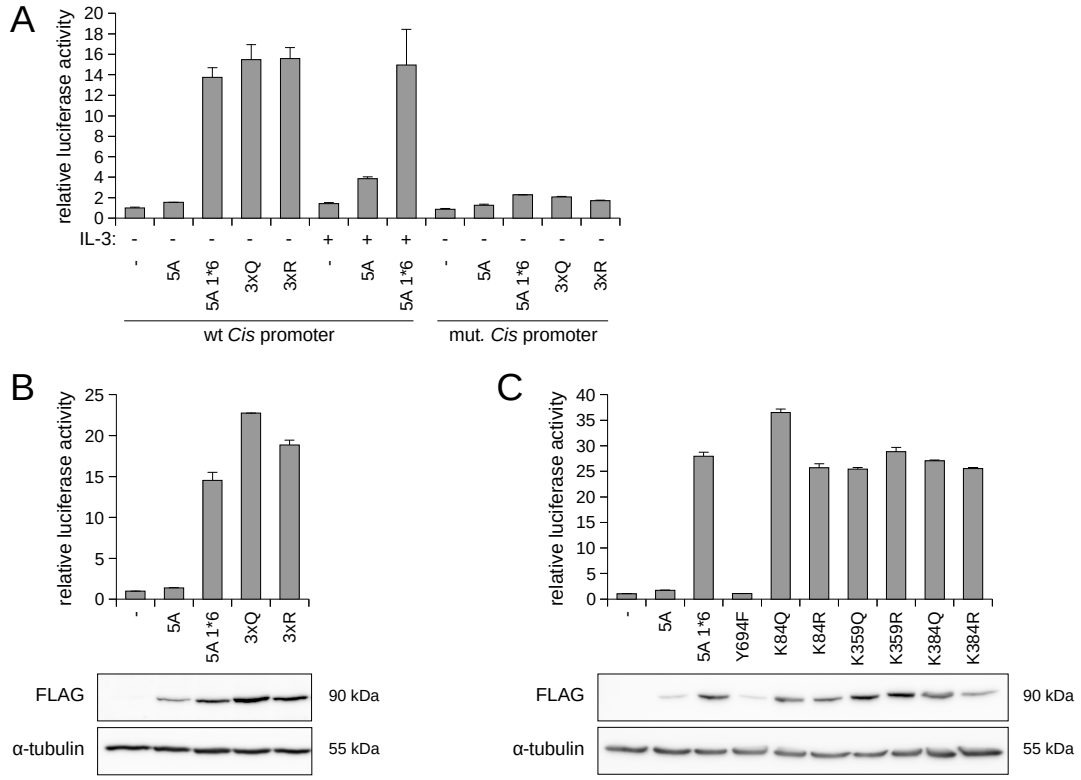

Figure 4.12: In *Cis* promoter-driven luciferase assays, none of the mutated lysine residues is required for STAT5A-1∗6 transcriptional activity
(**A**) Ba/F3 cells were transiently co-transfected with the *Firefly* luciferase reporter construct pGVB-CisA (wt *Cis* promoter) or pGVB-CisD (mut. *Cis* promoter, containing mutated STAT5 binding sites), and with either the empty vector pcDNA3 (-) or the expression vector for wild-type mSTAT5A-FLAG (5A), or for mSTAT5A-1∗6-FLAG (5A1∗6), or for a mSTAT5A-1∗6-FLAG mutant (3xQ, 3xR) containing mutations at K689, K696 and K700. After 12 h recovery in the presence of IL-3, the cells were cultured for a further 12 h in the absence or presence of IL-3, as indicated. *Firefly* luciferase activity was normalized to co-transfected constitutively expressed *Renilla* luciferase and presented as fold induction relative to the pcDNA/pGVB-CisA/-IL-3 sample. (**B**), (**C**) Ba/F3 cells were transiently co-transfected with the *Firefly* luciferase reporter pGVB-CisA, containing the wild-type *Cis* promoter, and with either the empty vector pcDNA3 (-) or the expression vector for wild-type mSTAT5A-FLAG (5A), or for mSTAT5A-1∗6-FLAG (5A1∗6), or for a mSTAT5A-1∗6-FLAG mutant (3xQ, 3xR, K84Q, K84R, K359Q, 359R, K384Q, K384R, Y694F). After 12 h recovery in the presence of IL-3, the cells were rested for 12 h in IL-3-free medium. Cell lysis and analysis for luciferase activity were performed as described in Material and methods 3.2.6. *Firefly* luciferase activity was normalized to co-transfected constitutively expressed *Renilla* luciferase and presented as fold induction relative to empty vector control. Using a FLAG tag-specific antibody, western blot was performed from the same lysate to confirm protein expression from the different STAT5 expression vectors. An antibody directed against α-tubulin was used as a loading control.

sine mutations affect STAT5A-1∗6-mediated transcription. This indicates that increased STAT5 acetylation (mimicked by the lysine to glutamine mutation), at least at the investigated lysine residues, probably does not inhibit STAT5-mediated transcription, and this indicates that, in contrast to our assumption, STAT5 is probably not the acetylated factor responsible for inhibition of STAT5-mediated transcription by deacetylase inhibitors. Consequently, the observed inhibition of STAT5-mediated transcription by deacetylase inhibitors is probably transmitted independently of a change in STAT5 acetylation. Of note, although K675 mutants in the context of STAT5A-1∗6 were not detectable at the protein level, GAL4-STAT5A666 proteins containing a mutation at K675 exhibited similar protein levels as the other GAL4-STAT5A666-based proteins and also induced the luciferase reporter similarly strong (Fig. 4.10A). Although the GAL4-STAT5A666 luciferase reporter system is less physiological than the assay based on induction of endogenous target genes by STAT5A-1∗6, this indicates that K675 does probably also not affect STAT5-mediated transcription and that acetylation of this residue is probably also not involved in inhibition of STAT5-mediated transcription by deacetylase inhibitors.

Eventually, the absence of effect of lysine mutations on STAT-mediated transcription demonstrate that other post-translational modifications of the investigated lysines, such as SUMOylation or methylation are also unlikely to regulate STAT5-mediated transcription in Ba/F3 cells.

The conclusion that deacetylase inhibitors act very likely independently of STAT5 acetylation at the investigated lysine residues implies that they also act independently of these STAT5 lysine residues themselves. Consequently, deacetylase inhibitors should inhibit STAT5-mediated transcription irrespective of the absence or presence of STAT5 lysine mutations. To confirm this proposition, the sensitivity of STAT5A-1∗6 lysine mutants towards the deacetylase inhibitor TSA was analyzed.

Using the same experimental setting as before, Ba/F3 cells transiently transfected with expression plasmids for STAT5A-1∗6, STAT5A-1∗6-3xQ or -3xR (containing mutations at K689, K696 and K700) and cultured in the absence of IL-3 were treated with the deacetylase inhibitor TSA or vehicle for 90 min. Protein levels of the transfected mutants, their phosphorylation status and expression of STAT5 target genes was analyzed. As expected (Fig. 4.1), TSA treatment inhibited STAT5A-1∗6-induced expression of the STAT5 target genes *Cis* and *c-Myc* (Fig. 4.13C). Importantly, TSA treatment also inhibited expression of *Cis* and *c-Myc* induced by the 3xQ and 3xR mutants (Fig. 4.13C). The control gene *36b4* was not affected by TSA treatment or by transfection of STAT5A-1∗6 and its mutants. The protein levels of the mutants, as determined by western blot using a FLAG-specific antibody, were unaffected by TSA treatment (Fig. 4.13D), demonstrating that the observed inhibition of STAT5 target genes upon TSA treatment was not a con-

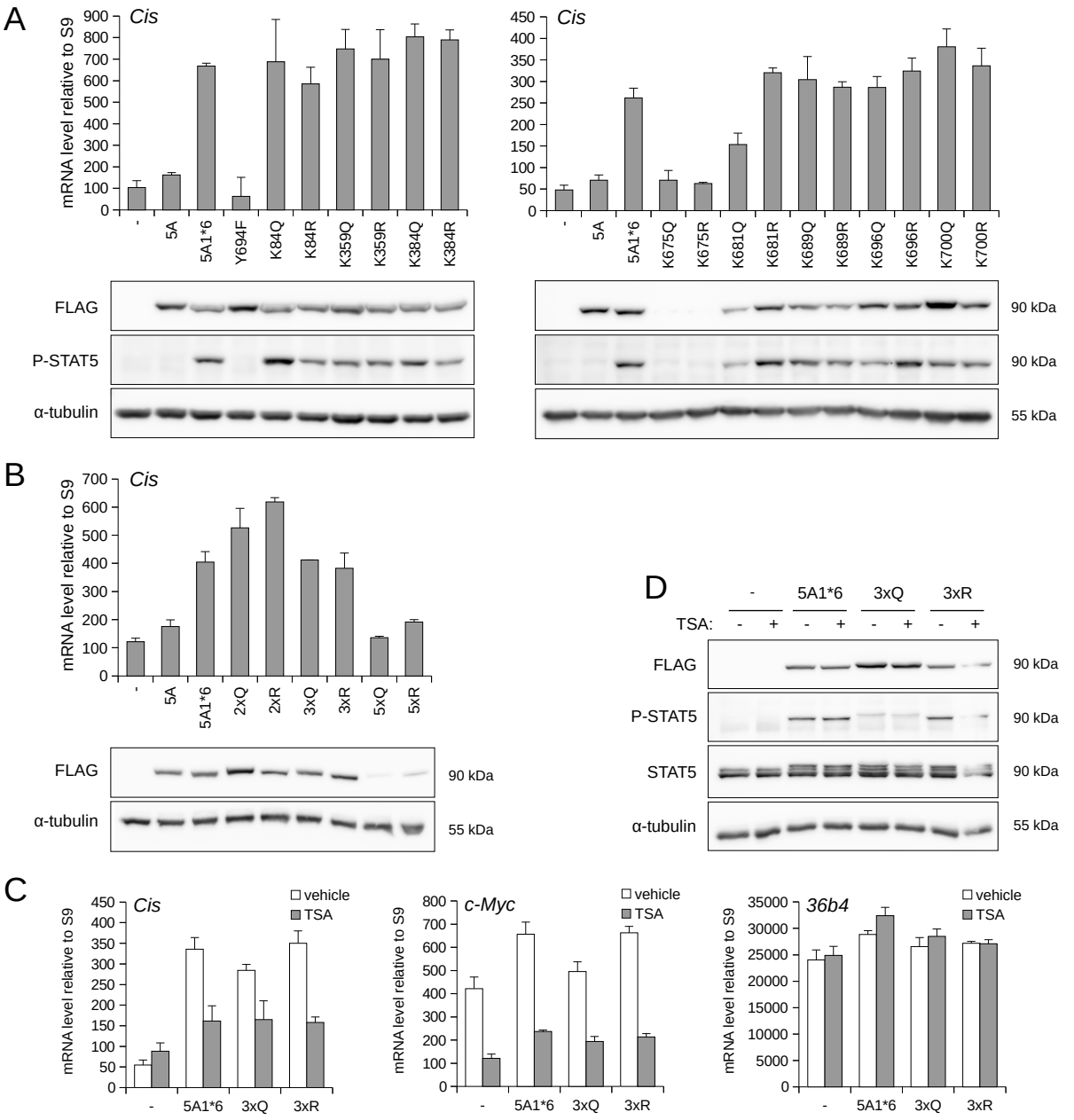

Figure 4.13: All STAT5A-1∗6 lysine mutants induce endogenous STAT5 target genes and retain TSA sensitivity.
(**A**), (**B**), Ba/F3 cells were transiently transfected, as described in Material and methods 3.2.3.7, with 8 μg of either the empty vector pcDNA3 (-), or the pcDNA3-based expression vector for mSTAT5A-FLAG (5A), for mSTAT5A-1∗6-FLAG (5A1∗6), or for one of the mutants of mSTAT5A-1∗6-FLAG (2xQ, 2xR, 3xQ, 3xR, 5xQ, 5xR, K84Q, K84R, K359Q, 359R, K384Q, K384R, K675Q, K675R, K681Q, K681R, K689Q, K689R, K696Q, K696R, K700Q, K700R, Y694F). Transfected cells were cultured for 10 h in the absence of IL-3, to prevent activation of endogenous STAT5. Gene expression was analyzed by quantitative RT-PCR, using expression primers for the STAT5 target gene *Cis*, as described in Material and methods 3.2.1.4. Brij whole-cell protein lysate was prepared to analyze expression of the exogenous proteins by western blot using antibodies against their C-terminal FLAG tag. The phospho-STAT5-specific antibody served to assess the activation status of the mutants and the α-tubulin-specific antibody served as a loading control. (**C**) The experiment was performed as in (A) and (B), except that cells were treated with 200 nM TSA or vehicle (0.02% DMSO) 90 min before the harvest. In addition to expression of *Cis*, expression of *c-Myc* and *36b4* is shown. (**D**) Western blot of the samples from (C). An antibody against total STAT5 was used in addition to the antibodies used in (A).

sequence of altered protein levels. The phosphorylation levels of STAT5A-1∗6 and of the mutants were unaffected by TSA treatment, as expected given the lack of effect of TSA on phosphorylation of wild-type STAT5 (Rascle et al., 2003). Of note, the 3xQ lysine mutants repeatedly showed low phosphorylation signals in western blot using a phospho-STAT5-specific antibody (Fig. 4.13D and data not shown) despite transcriptional activity of those proteins in luciferase assay (Fig. 4.12A and B) and in endogenous gene expression assays (Fig. 4.13B). Noteworthy, another phospho-STAT5-specific antibody (Cell Signaling, #4322) did not detect STAT5A-1∗6 mutants containing a K696Q/R mutation (data not shown). The lysine mutations of the affected mutants, at K689, K696, and K700, are close to the Y694 phosphorylation site and are therefore likely to interfere with epitope recognition by phospho-STAT5-specific antibodies. These results demonstrate that, as expected, STAT5A-1∗6-3xQ/R lysine mutants remained sensitive to TSA. These experiments thus confirm that inhibition of STAT5A-1∗6-mediated transcription by deacetylase inhibitors is mediated independently of the investigated lysine residues and thus probably independently of STAT5 acetylation at those residues. Thus, STAT5 is probably not the acetylated substrate involved in inhibition of STAT5-mediated transcription by deacetylase inhibitors.

4.3.4 Wild-type latent endogenous STAT5 does not contribute to STAT5A-1*6-mediated transcription

Analysis of the transcriptional activity of the STAT5A-1∗6 lysine mutants took place in IL-3-lacking culture conditions in which latent endogenous STAT5 is unphosphorylated, inactive (Fig. 4.13A and B), and located in the cytosol. Furthermore, even in the presence of IL-3, endogenous STAT5 does not significantly contribute to the induction of a *Cis* promoter-driven luciferase reporter (Fig. 4.12A, wt *Cis* promoter, empty vector control, -/+IL-3). However, we cannot exclude that the observed transcriptional activation ascribed to the STAT5A-1∗6 lysine mutants was induced by the co-translocation of endogenous wild-type STAT5 to the nucleus, possibly through the formation of heterodimers.

To confirm that constitutively active STAT5A-1∗6 does not induce the co-translocation of latent endogenous STAT5 to the nucleus, the Ba/F3-tet-on-1∗6 cell line was used, which permits the doxycycline-induced conditional expression of STAT5A-1∗6. Before and after induction of STAT5A-1∗6 expression in the absence of IL-3, cytosolic and nuclear lysates were prepared and analyzed by western blot for the presence of endogenous STAT5B in the nuclear fraction. Ba/F3-tet-on-1∗6 cells cultured in the presence of IL-3 throughout the experiment were used as a positive

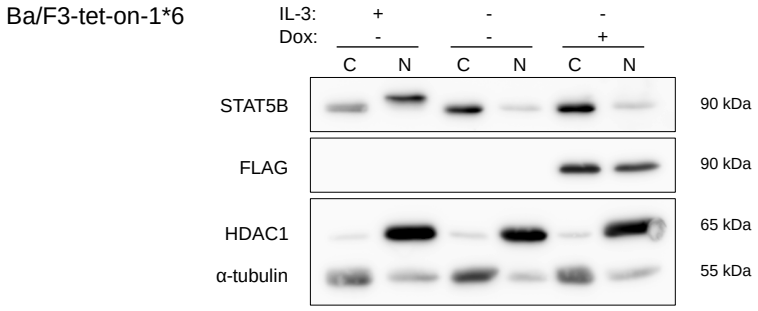

Figure 4.14: STAT5A-1∗6 induction does not lead to an enrichment of latent endogenous STAT5B in the nucleus of rested cells
Ba/F3-tet-on-1∗6 cells, conditionally expressing mSTAT5A-1∗6-FLAG upon doxycycline (Dox) treatment, were grown in the presence or absence of Dox for 23 h. Upon starting the experiment, all cells were cultured in the presence of IL-3. To turn off endogenous STAT5 in samples indicated as -IL-3, the cells were washed in RPMI 1640 after 12 h and then kept for the last 11 h in IL-3-lacking medium, containing doxycycline or not as before. Control Ba/F3-tet-on-1∗6 cells, indicated as +IL-3, were kept in IL-3-containing medium without doxycycline throughout the experiment. Cytosolic (C) and nuclear (N) lysates were prepared as described in Material and methods 3.2.4.3. Equal protein amounts of cytosolic and nuclear lysate were analyzed by western blot using antibodies specific for STAT5B (recognizing endogenous STAT5B), FLAG (recognizing STAT5A-1∗6), HDAC1 and α-tubulin. HDAC1 served as nuclear marker and as a loading control, α-tubulin as cytosolic marker and as a loading control. The upward mobility shifted STAT5B band in IL-3-treated nuclear lysate represents tyrosine-phosphorylated STAT5B. (Data shown in this figure were generated by Dr. Anne Rascle and Christina Seisenberger.)

control for nuclear endogenous STAT5B. As shown using an antibody directed against the C-terminal FLAG tag of STAT5A-1∗6, doxycycline treatment led to a strong signal of cytoplasmic as well as nuclear STAT5A-1∗6 (Fig. 4.14). In the presence of IL-3, STAT5B was found in the nucleus of Ba/F3-tet-on-1∗6 cells, as expected. This nuclear STAT5B signal disappeared upon IL-3 withdrawal and, importantly, did not increase upon STAT5A-1∗6 expression (Fig. 4.14). These data confirm that constitutively active STAT5A-1∗6 does not induce the co-translocation of latent endogenous STAT5 to the nucleus. In addition, no interaction between STAT5A-1∗6 and latent endogenous STAT5B was detected in co-immunoprecipitation assays (data not shown were generated together with Krystina Beer, internship 2013), indicating that no heterodimers or tetramers between these proteins were formed. This supports the observed absence of co-translocation. It is therefore unlikely that the observed transcriptional activation ascribed to the STAT5A-1∗6 lysine mutants was induced by the co-translocation of endogenous wild-type STAT5 to the nucleus. Therefore, these data do not contradict the absence of effect of the lysine mutations on STAT5A-1∗6 transcriptional activity. Altogether our data argue against the involvement of STAT5 acetylation, at least at the investigated lysine residues, in inhibition of STAT5-mediated transcription by deacetylase inhibitors.

4.3.5 TSA does not disrupt soluble nuclear STAT5-containing protein complexes

Our group demonstrated before (Rascle et al., 2003) that deacetylase inhibitors induce a loss of components of the transcriptional machinery, RNA polymerase II and TBP, from STAT5 target genes, suggesting that deacetylase inhibition might inhibit STAT5-mediated transcription by disruption of protein interactions between STAT5 and essential components of the transcriptional machinery. This disruption of protein interactions might be mediated by increased acetylation of STAT5 itself, or of an unknown STAT5-specific cofactor. Along these lines, acetylation has been shown to disrupt protein interactions of several transcriptional regulators and as a consequence to enhance or to inhibit transcription (Waltzer & Bienz, 1998; Chen et al., 1999; Munshi et al., 2001; Vo et al., 2001; Purbey et al., 2009). For example, acetylation leads to transcriptional inhibition through disruption of the association of coactivator complexes with transcription factors like T-cell factor (TCF) (Waltzer & Bienz, 1998) and estrogen receptor (Chen et al., 1999), or through destabilization of the interferon-beta enhanceosome (Munshi et al., 1998, 2001).

Thus, our model predicts that deacetylase inhibition disrupts protein interactions between STAT5 and the transcriptional machinery by an increase in acetylation of STAT5 or of a specific STAT5-associated cofactor and that consequently RNA polymerase II and possibly the unknown acetylated cofactor are lost from STAT5-containing complexes. To address whether deacetylase inhibition disrupts nuclear STAT5- and RNA polymerase II-containing protein complexes, and to possibly obtain clues towards the loss of an unknown STAT5-specific cofactor from STAT5-containing complexes, gel filtration chromatography was performed using 60 min TSA- or vehicle-treated Ba/F3-1∗6 cells. Since transcriptionally relevant STAT5-containing complexes are expected in the nucleus, gel filtration was performed using nuclear lysates. The quality of the nuclear lysates was verified by western blot (Fig. 4.15A), using HDAC1 as a nuclear marker and α-tubulin as a cytosolic marker as before. The nuclear lysates were applied onto a size exclusion-column to separate proteins and protein complexes by size. Different elution fractions were collected and analyzed by western blot using antibodies directed against the FLAG tag of STAT5A-1∗6 or against total STAT5 or against RNA polymerase II. In the absence of IL-3, endogenous STAT5 was not co-translocated to the nucleus together with STAT5A-1∗6 (Fig. 4.14), so that only STAT5A-1∗6 should be present in the analyzed nuclear fraction and consequently the total STAT5 signal should be equivalent to the FLAG signal. Thus the two antibodies were used to confirm each other. A mixture of purified thyroglobulin and BSA (bovine serum albumin) served as approximate molecular weight

standards for the gel filtration. Thyroglobulin, with a molecular weight of 669 kDa, eluted from the column in fraction 13, while BSA, with a molecular weight of 66 kDa, eluted in fractions 23 and 24 (not shown). The strongest STAT5 signal of TSA-treated or untreated cells was found by western blot in fraction 20 (Fig. 4.15B), likely corresponding to the 180 kDa STAT5 dimer. Importantly, no difference was apparent between the STAT5A-1∗6 elution profile from TSA- and vehicle-treated cells. Furthermore, the RNA polymerase II elution profile was also not changed upon TSA treatment. This suggests that soluble nuclear STAT5-containing protein complexes were not disrupted upon TSA treatment. Therefore, our data do not support a model in which an increase in acetylation of STAT5 or of a STAT5-specific cofactor upon deacetylase inhibition disrupts protein interactions between STAT5 and the transcriptional machinery. Furthermore, these data do not support the involvement of an acetylated STAT5-specific cofactor in inhibition of STAT5-mediated transcription by deacetylase inhibitors.

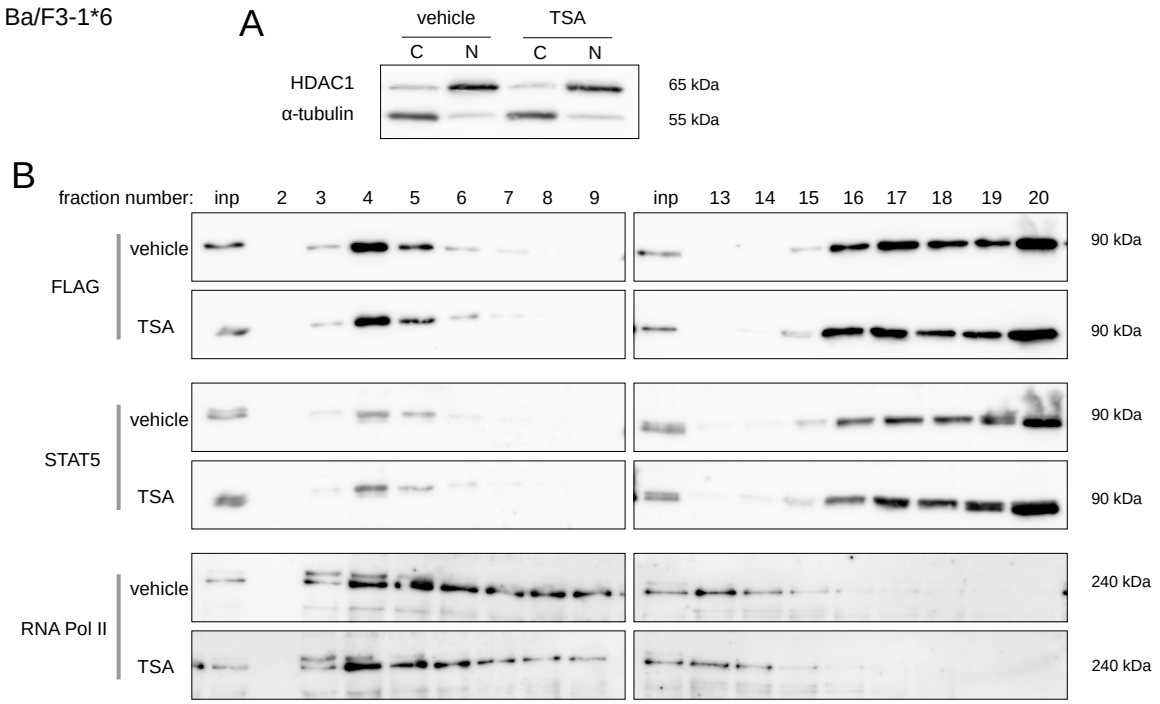

Figure 4.15: TSA treatment does not affect the composition of soluble nuclear STAT5-containing protein complexes
(**A**) Nuclear (N) and cytosolic (C) lysates from 60 min 200 nM TSA- or vehicle (0.02% DMSO)-treated Ba/F3-1∗6 cells were analyzed by western blot. To assess the quality of the nuclear lysate, antibodies against HDAC1 were used as a nuclear marker and against α-tubulin as a cytosolic marker. (**B**) Nuclear lysate from (A) was fractionated by gel filtration chromatography on a TSK Gel 4000SW column, as described in Material and methods 3.2.5.8. An equal volume of each elution fraction (and twice as much input (inp)) was subjected to SDS-PAGE and analyzed by western blot using antibodies directed against the FLAG tag of STAT5A-1∗6, against total STAT5 and against RNA polymerase II (RNA Pol II). No STAT5 signal was detected in fractions 10-12, which were therefore not shown. The molecular weight marker thyroglobulin (669 kDa) eluted from the column in fraction 13, while the marker BSA (66 kDa) eluted in fractions 23 and 24 (not shown).

Of note, the nuclear fraction which was analyzed by gel filtration chromatography contained mostly soluble nuclear proteins and was largely devoid of insoluble chromatin and its associated proteins. We can therefore from those results not exclude that deacetylase inhibitors might disrupt STAT5-containing protein complexes associated with chromatin. Furthermore, we cannot exclude that a STAT5-specific cofactor associated with chromatin might be involved in inhibition of STAT5-mediated transcription by deacetylase inhibitors. Thus, the finding that neither acetylation of STAT5 nor soluble nuclear protein complex disruption seem to account for the inhibition of STAT5-mediated transcription by deacetylase inhibitors, strengthened the possibility that the inhibition might take place at the chromatin level.

4.3.6 Inhibition of STAT5-mediated transcription by deacetylase inhibitors correlates with rapid induction of global chromatin hyperacetylation

For reasons stated above, the focus was changed to acetylated histones as possible acetylated substrate involved in inhibition of STAT5-mediated transcription by deacetylase inhibitors. Several arguments, in agreement with the data collected so far, support a possible involvement of acetylated histones: Acetylated histones are well characterized substrates of HDACs, histone acetylation is affected by several partially redundant HDACs (Jurkin et al., 2011; Dovey et al., 2013; Kelly & Cowley, 2013; Wolfson et al., 2013; You et al., 2013), histone acetylation is affected by deacetylase inhibitors (Yoshida et al., 1990; Richon et al., 2000; Rada-Iglesias et al., 2007; Wang et al., 2009), and changes in histone acetylation are known to affect transcription (Allfrey et al., 1964; Allegra et al., 1987; Tse et al., 1998; Agalioti et al., 2000; Richon et al., 2000; Deckert & Struhl, 2001; Aoyagi & Archer, 2007; Lin et al., 2014). Initially, acetylated histones were not considered the most likely factor involved in STAT5-mediated transcription, since previous work of our group argued against an involvement of histone acetylation (Rascle & Lees, 2003). Chromatin immunoprecipitation (ChIP) experiments presented in that work showed that, while TSA induced histone hyperacetylation at the control gene *c-Fos* in IL-3-stimulated or unstimulated cells, TSA did not significantly change histone H3 and H4 acetylation at the STAT5 target gene *Cis* (Rascle & Lees (2003), fig. 3C and D). This led us to the conclusion that deacetylase inhibitors inhibit STAT5-mediated transcription independently of local changes of histone acetylation at STAT5 target genes (Rascle & Lees, 2003). However, in that study histone H3 and H4 acetylation levels were not normalized to total nucleosome occupancy, since no validated ChIP grade H3 antibody as a marker for nucleosome occupancy was available at that time. Thus, a local effect of TSA on

histone acetylation and on histone occupancy might have been missed. Therefore, a possible involvement of acetylated histones in inhibition of STAT5-meditated transcription was reassessed.

In case an increase in histone acetylation upon deacetylase inhibitor treatment is involved, this increased acetylation should occur within the same time frame as inhibition of STAT5-mediated transcription. Inhibition of STAT5-mediated transcription is already evident after 5 min TSA treatment at the level of dissociation of RNA polymerase II from STAT5 target genes and at 20 min at the level of reduced *Cis* mRNA levels (Rascle et al., 2003). Consequently, a rapid increase in global histone acetylation is expected upon treatment with TSA, VPA and apicidin, which inhibited STAT5-mediated transcription, but not upon treatment with MGCD0103 and MS-275, which had no effect on STAT5-mediated transcription (Fig. 4.3). The effect of deacetylase inhibitors on global histone H3 and H4 acetylation levels was analyzed by western blot. Ba/F3 cells were treated for 0-60 min with selective deacetylase inhibitors using concentrations at which these were effective (200 nM TSA, 3 mM VPA, 500 nM apicidin) or ineffective (1 μM MGCD0103, 5 μM MS-275) in inhibiting STAT5-mediated transcription. Whole-cell lysates were prepared and analyzed by western blot using antibodies directed against acetylated histone H3 and H4, as well as against total histone H3 as a loading control. Within up to 60 min treatment with MGCD0103 or MS-275, which did not inhibit STAT5-mediated transcription (Fig. 4.3D and E), no change in histone acetylation was detectable (Fig. 4.16). By contrast, TSA, VPA, and apicidin, which did inhibit STAT5 target gene induction (Fig. 4.3A, B, and C), quickly induced an increase in global histone H3 and H4 acetylation in a time-dependent manner (Fig. 4.16). Changes in histone acetylation were already evident after 15 min treatment (Fig. 4.16), which is in accordance with the rapid inhibition of STAT5-mediated transcription by deacetylase inhibitors (Rascle et al., 2003). Thus, the concomitance of deacetylase inhibitor-mediated repression of STAT5-mediated transcription and of increased histone H3 and H4 acetylation supports the possible involvement of histone acetylation in inhibition of STAT5-mediated transcription by deacetylase inhibitors.

Noteworthy, in the literature, an increase in histone acetylation was reported after 4-24 h treatment with the benzamide deacetylase inhibitors MGCD0103 or MS-275, at similar inhibitor concentrations as in the this study (Hu et al., 2003; Fournel et al., 2008; Khan et al., 2008; Arts et al., 2009; Duque-Afonso et al., 2011). Thus, the absence of effect of MGCD0103 and MS-275 on histone acetylation presented here might be a consequence of the short treatment duration of up to 1.5 h. Accordingly, 10 h treatment with MS-275 increased histone acetylation and inhibited expression of the STAT5 target gene *Cis* in Ba/F3 cells (data not shown, Dr. Anne Rascle, Pinz et al., 2015, fig. S5).

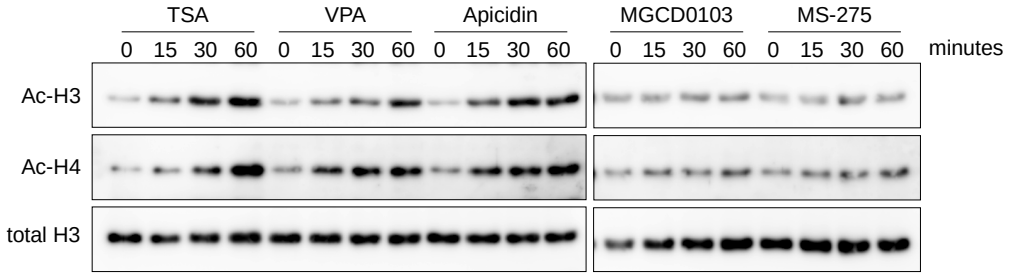

Figure 4.16: The deacetylase inhibitors TSA, VPA and apicidin, which inhibit STAT5 transactivation, rapidly induce global histone hyperacetylation
Ba/F3 cells were treated with the deacetylase inhibitors TSA (200 nM), VPA (3 mM), apicidin (500 nM), MGCD0103 (1 μM) or MS-275 (5 μM) for 0-60 min, as indicated. For histone analysis, freeze-thaw lysates were prepared as described in Material and methods 3.2.4.2, followed by western blot with antibodies directed against acetylated histone H3 (Ac-H3), against acetylated histone H4 (Ac-H4), or against total histone H3 (H3). Total histone H3 served as a loading control. (Data shown in this figure were generated by Dr. Anne Rascle.)

4.3.7 TSA treatment induces changes in histone occupancy and acetylation at multiple genes and differentially affects recruitment of RNA polymerase II

Histone acetylation modulates chromatin structure and nucleosome stability (Wirén et al., 2005; Shogren-Knaak et al., 2006; Di Cerbo et al., 2014; Felisbino et al., 2014; Frank et al., 2016), and deacetylase inactivation can lead to nucleosome loss in yeast (Wirén et al., 2005; Chen et al., 2012). Therefore, the strong increase in histone acetylation occurring upon deacetylase inhibitor treatment might affect chromatin organization in Ba/F3 cells. Furthermore, histone acetylation as well as chromatin structure and nucleosome occupancy affect transcription (Allfrey et al., 1964; Allegra et al., 1987; Lorch et al., 1987; Han & Grunstein, 1988; Tse et al., 1998; Wyrick et al., 1999; Agalioti et al., 2000; Richon et al., 2000; Aoyagi & Archer, 2007; Rada-Iglesias et al., 2007; Lin et al., 2014). There do not seem to be universal changes in chromatin organization upon deacetylase inhibitor treatment that determine increased or decreased transcription of the modified gene (Ellis et al., 2008; Halsall et al., 2015). However, at the level of specific genes, local changes in chromatin organization might be involved in altered transcriptional activity. Therefore, local changes in chromatin organization at STAT5 target genes upon deacetylase inhibitor treatment might be involved in inhibition of STAT5-mediated transcription. This involvement would be further supported if those changes occurred at all STAT5 target genes and if those changes correlated with RNA polymerase II recruitment.

Thus, to identify on the one hand deacetylase-inhibitor induced changes in chromatin organization in general and on the other hand local changes in chromatin organization at STAT5 target genes in particular, chromatin immunoprecipitation (ChIP) experiments

were performed. Nucleosome occupancy, histone H3 and H4 acetylation, and RNA polymerase II recruitment were analyzed at the STAT5 target genes *Cis* and *Osm* as well as at the control genes *c-Fos* and *p21*. The two STAT5-independent control genes *c-Fos* and *p21* are both IL-3-inducible, but in contrast to STAT5 target genes which are inhibited, they are upregulated by deacetylase inhibitors (Xiao et al., 1999; Richon et al., 2000; Rascle et al., 2003; Rascle & Lees, 2003; Sachweh et al., 2013). Besides chromatin alterations caused by TSA, chromatin alterations might also be caused by STAT5 and by abrogated transcription. To identify chromatin changes caused by TSA, unstimulated Ba/F3 cells were used. In that condition, STAT5 target genes are not actively transcribed, so that chromatin changes detected upon TSA treatment of unstimulated cells are caused only by TSA treatment, and not by STAT5 or abrogated transcription. The TSA-induced chromatin organization can then be compared to chromatin organization at the STAT5-bound actively transcribed gene in the presence of IL-3 and to chromatin organization of the STAT5-bound inhibited gene (abrogated transcription) in the presence of IL-3 and TSA.

First, TSA-induced changes of histone H3 occupancy, as a marker for nucleosome occupancy, and RNA polymerase II recruitment were analyzed by ChIP at STAT5 target and control genes. Rested Ba/F3 cells were treated with TSA or vehicle for 60 min, of which the last 30 min were in the absence or presence of IL-3. To characterize time-dependent changes of chromatin alterations caused by TSA in the absence of STAT5-binding or abrogated transcription, 5, 15 and 30 min TSA-treated, unstimulated Ba/F3 cells were analyzed in the assay as well. Cells were crosslinked with formaldehyde, chromatin was sheared by sonication to fragments of about 500 bp DNA length, and immunoprecipitation was performed using antibodies directed against total histone H3 and against RNA polymerase II. DNA co-precipitated with histones was analyzed by quantitative PCR using primers covering the proximal promoters of STAT5 target or control genes. At STAT5 target genes, the investigated locus encompasses STAT5 binding sites. The proximal promoter was chosen for analysis, since changes in chromatin organization at that locus are most likely to affect (STAT5-dependent) assembly of the transcriptional machinery. DNA co-precipitated with RNA polymerase II was analyzed using primers covering regions around the transcription start site (TSS) of the investigated genes (Fig. 4.18). ChIP revealed that histone H3 occupancy at the promoter was higher in unstimulated than in IL-3-stimulated cells at all four investigated genes. Interestingly, in unstimulated cells, TSA induced a time-dependent loss of histone H3 at all four promoters. In IL-3 stimulated cells, histone occupancy at the promoter of STAT5 target genes remained at a similar level irrespective whether TSA was absent or present. Thus, histone occupancy at inhibited STAT5 target genes upon TSA treatment was similar to histone occupancy

at transcriptionally active genes. As expected from the IL-3-dependent induction of the analyzed genes (Fig. 4.2 and Fig. 4.3) and in accordance with previous reports (Richon et al., 2000; Rascle et al., 2003; Rascle & Lees, 2003), RNA polymerase II association with all four genes was low in the absence of IL-3 and high upon IL-3 stimulation (Fig. 4.18). Furthermore, in agreement with previous reports (Rascle et al., 2003; Rascle & Lees, 2003), TSA abrogated recruitment of RNA polymerase II to target genes upon IL-3 stimulation, while it did not affect recruitment of RNA polymerase II to control genes. Interestingly, at all four genes, TSA treatment led to an increase in RNA polymerase II association in the absence of IL-3, possibly a consequence of increased DNA accessibility upon histone loss. However, RNA polymerase II association in TSA-treated, unstimulated cells compared to vehicle-treated stimulated cells remained about 3-fold lower at STAT5 target genes, while it reached a similar level at control genes (Fig. 4.18 and data not shown, Dr. Anne Rascle and Samy Unser, Pinz et al., 2015, fig. 8). This suggests that RNA polymerase II is recruited to STAT5 target and control genes by distinct mechanisms.

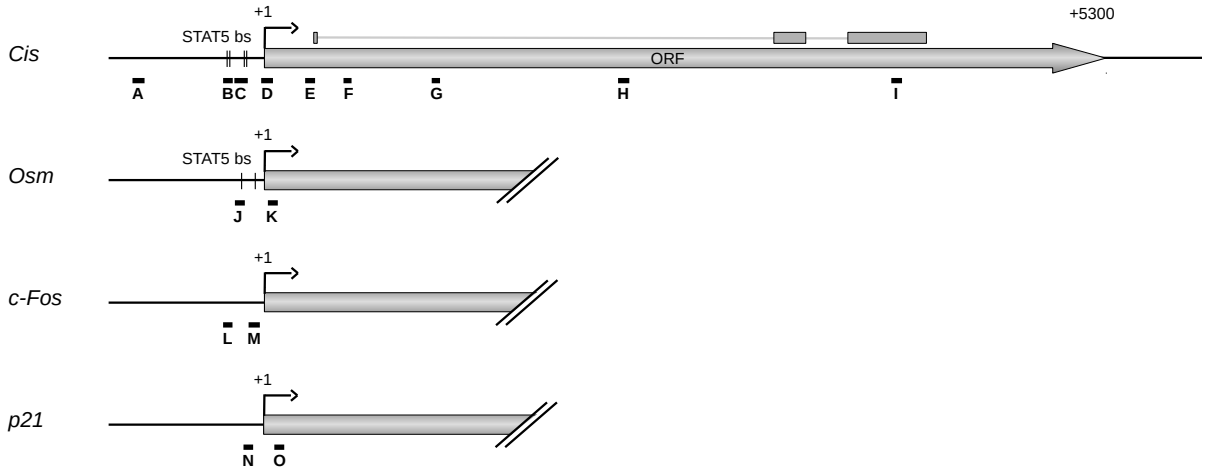

Figure 4.17: Schematic representation of the location of ChIP amplicons
Schematic representation of the *Cis* gene locus as well as the promoter regions of *Osm*, *c-Fos* and *p21*. Distances along the DNA are drawn to scale. *Cis* exons (grex boxes) are depicted above its open reading frame (ORF). In the proximal promoter of *Cis* there are four STAT5 binding sites (bs) arranged in two clusters, and there are two STAT5 binding sites in the promoter of *Osm*. Below the genes, the ChIP amplicons are depicted and labeled with capital letters A-O.

In summary, local histone occupancy at STAT5 target genes did not correlate with RNA polymerase II recruitment, and furthermore, histone occupancy of repressed STAT5 target genes was similar as histone occupancy of the active genes, an occupancy that normally allows recruitment of the transcriptional machinery. Together this suggests that local nucleosome occupancy is unlikely to be involved in the specific loss of RNA polymerase II from STAT5 target genes upon deacetylase inhibitor treatment. When looking at the general effect of deacetylase inhibitors, the striking loss of histone H3 occupancy

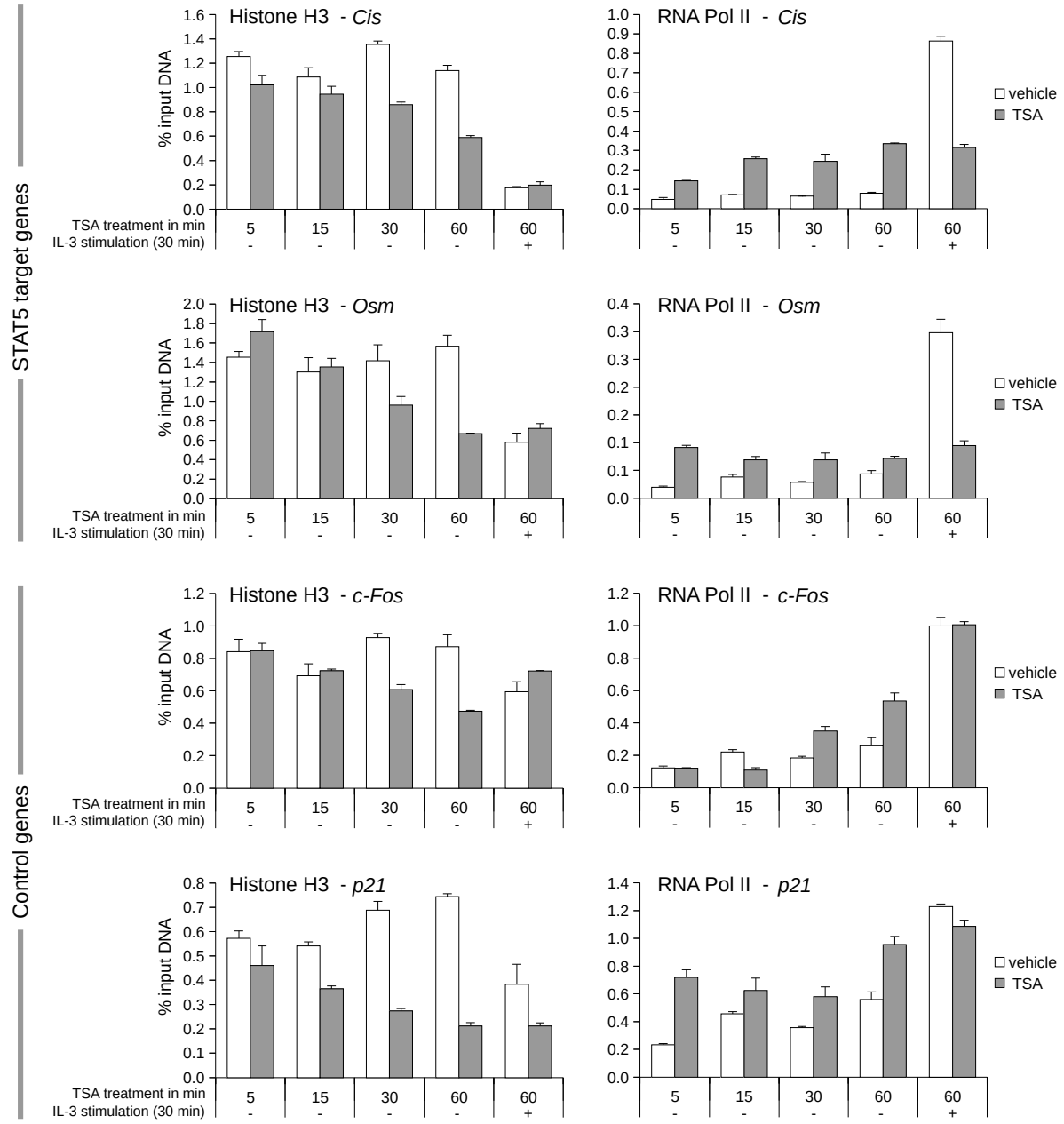

Figure 4.18: TSA induces a rapid loss of histone H3 occupancy at all investigated genes, while differentially affecting recruitment of RNA polymerase II to STAT5-dependent versus -independent genes

Ba/F3 cells were withdrawn from IL-3 for 10 h and then treated with vehicle (0.02% DMSO), or 200 nM TSA for 5, 15, 30 or 60 min. In addition, part of the 60 min vehicle or TSA treated cells were stimulated with IL-3 for the last 30 min. Cells were formaldehyde-crosslinked and subjected to ChIP according to the conventional protocol as previously described (Rascle et al., 2003; Pinz et al., 2014a, 2015), using antibodies specific for histone H3 or RNA polymerase II. DNA co-precipitated with histone H3 was analyzed by qPCR using primers specific for the proximal promoter of the STAT5-dependent genes *Cis* (amplicon C) and *Osm* (amplicon J) or the IL-3-inducible STAT5-independent genes *c-Fos* (amplicon L) and *p21* (amplicon N). In the case of STAT5-dependent genes, the analyzed locus covered STAT5 binding sites (bs). DNA co-precipitated with RNA polymerase II was analyzed using primers specific for the TSS of the same genes (amplicons D, K, M, O). The location of the respective amplicons C-O are depicted in Figure 4.17. (Data shown in this figure were generated together with Dr. Anne Rascle and Samy Unser.)

upon deacetylase inhibitor treatment at all investigated genes, concomitant to global histone hyperacetylation, suggests that chromatin is reorganized, resulting in similar changes in chromatin organization at multiple genes. By contrast, the consequences of deacetylase inhibitor treatment for the recruitment of RNA polymerase II to these genes were different. Together this indicates that RNA polymerase II is recruited by a different mechanism to STAT5 target genes than to control genes. Furthermore, this might indicate that a chromatin-associated, STAT5-specific factor might be involved in the recruitment of RNA polymerase II to STAT5 target genes and that this factor might be lost upon deacetylase inhibitor-induced, global chromatin reorganization.

To better characterize deacetylase inhibitor-induced changes in histone H3 occupancy, histone H3 occupancy was analyzed along *Cis*, from basepair -800 to + 4000 relative to the TSS (data not shown, Dr. Anne Rascle and Samy Unser, Pinz et al., 2015, fig. 7). ChIP experiments revealed that the same changes of histone H3 occupancy occurred along the whole gene as at the promoter: The TSA-induced loss of histone H3 in unstimulated cells occurred uniformly along the gene, and resulted, in stimulated and unstimulated cells, in a histone H3 occupancy along the whole gene which was similar as histone H3 occupancy of the transcriptionally active gene. Since this nucleosome occupancy normally allows RNA polymerase II recruitment, the absence of RNA polymerase II after TSA treatment has to be explained by different factors than by local changes of histone occupancy along STAT5 target genes.

To further characterize the effect of deacetylase inhibitor treatment on chromatin organization at different genes, and to investigate whether local changes in histone acetylation might be involved in the loss of RNA polymerase II from STAT5 target genes, acetylation of histone H3 and H4 was analyzed along *Cis* (data not shown, Dr. Anne Rascle and Samy Unser, Pinz et al., 2015, fig. 7). To account for changes in nucleosome occupancy, histone H3 and H4 acetylation signals were normalized to total histone H3 signals. ChIP experiments showed that in untreated cells histone acetylation increased along the *Cis* gene upon IL-3 stimulation. In unstimulated cells, TSA treatment evenly increased histone H3 and H4 acetylation along the *Cis* gene, in accordance with the global histone hyperacetylation induced by deacetylase inhibitors. This TSA-induced acetylation pattern only slightly changed upon IL-3 stimulation and thus was similar for unstimulated and IL-3-stimulated cells. Importantly, in IL-3-stimulated cells, the TSA-induced acetylation pattern of the repressed gene differed from the acetylation pattern of the active gene in the absence of TSA. These acetylation differences might be a cause of RNA polymerase II loss or a consequence of RNA polymerase II loss or most likely a combination thereof. Thus, these differences indicate that TSA-induced changes in chromatin organization might possibly be involved in the impaired recruitment of RNA

polymerase II to STAT5 target genes.

Analysis of histone acetylation within the promoter of the control genes *c-Fos* and *p21* (data not shown, Dr. Anne Rascle and Samy Unser, Pinz et al., 2015, fig. 8) revealed similar changes as observed at STAT5 target genes: TSA induced an increase in histone acetylation in unstimulated cells and this acetylation pattern was only slightly changed upon IL-3-stimulation of TSA-treated cells, however, the acetylation pattern upon TSA treatment differed from the acetylation pattern of IL-3-induced genes in the absence of TSA. Thus, similar changes in histone acetylation upon TSA treatment occurred at all investigated genes.

Together these data demonstrate that deacetylase inhibitor treatment - probably via global increase in histone acetylation - induces similar changes in chromatin organization, namely loss of histone H3 and altered histone H3 and H4 acetylation levels, at all genes investigated. Since, furthermore, deacetylase inhibitor treatment had different consequences for the transcription of specific genes, our data suggest that chromatin-associated, gene-specific cofactors might be responsible for transcriptional up- or down-regulation following deacetylase inhibitor treatment and that these cofactors are possibly sensitive to histone acetylation. At STAT5 target genes in particular, local changes in chromatin organization suggest that the function of such proposed chromatin-associated cofactor is probably not affected by local deacetylase inhibitor-induced histone loss, but might be affected by local or global changes in histone acetylation.

4.4 BRD2 association with the STAT5 target gene *Cis* is lost upon TSA treatment

A chromatin-associated factor that is implicated in the regulation of STAT5, sensitive to histone acetylation and that interacts with the transcriptional machinery, is bromodomain-containing protein 2 (BRD2). BRD2, a member of the bromodomain and extra-terminal (BET) protein family, is involved in the regulation of STAT5 activity in dendritic cells and in leukemia cell lines (Liu et al., 2014; Toniolo et al., 2015) and interacts with acetylated histones (Kanno et al., 2004; LeRoy et al., 2008) and with the transcription machinery components TBP and RNA polymerase II (Crowley et al., 2002; Peng et al., 2007; LeRoy et al., 2008). BET proteins such as BRD2 can be inhibited by the BET-specific inhibitor (+)-JQ1 (referred to as JQ1 thereafter), which binds competitively to the acetyl-lysine recognition motif of BET bromodomains and thus interferes with binding of BET family members to acetylated histones (Filippakopoulos et al., 2010). JQ1 interferes with induction of STAT5 target genes in leukemia cells lines (Liu et al.,

2014), and we could show that JQ1 inhibits IL-3-induced expression of the STAT5 target genes *Cis*, *Osm*, and *c-Myc* in a dose-dependent manner in Ba/F3 cells (data not shown, Dr. Anne Rascle, Pinz et al., 2015, fig. 9). This supports a possible involvement of BET proteins such as BRD2 in the regulation of STAT5-mediated transcription in Ba/F3 cells.

4.4.1 BRD2 binds to *Cis* and is lost upon TSA or JQ1 treatment

In case BRD2 is required for STAT5-mediated transcription, it probably associates with actively transcribed STAT5 target genes. Therefore, a possible association of BRD2 with the STAT5 target gene *Cis* was analyzed in Ba/F3 cells by ChIP using primers covering the *Cis* gene from basepair -800 to + 4000 relative to the transcription start site (TSS) (data not shown, Dr. Anne Rascle and Samy Unser, Pinz et al., 2015, fig. 11A). Ba/F3 cells were left unstimulated or stimulated with IL-3 for 30 min to activate STAT5. Upon IL-3 stimulation, a specific recruitment of BRD2 to the transcription start site (TSS) of *Cis* was detected, demonstrating that BRD2 is associated with actively transcribed *Cis* and suggesting that its recruitment might be STAT5-dependent.

Of note, although the BRD2 signal at the TSS was well above the background signal obtained using an unspecific rabbit IgG antibody, the co-precipitated DNA was only 0.05% enriched relative to input DNA (data not shown, Dr. Anne Rascle and Samy Unser, Pinz et al., 2015, fig. 11A). Therefore, to increase the sensitivity of the assay, the ChIP protocol was optimized to increase the amount of specifically co-precipitated DNA (refer to Material and methods 3.2.7 and Pinz & Rascle, 2017). In short, the most relevant differences to the conventional protocol were, first, the enrichment of nuclei from formaldehyde-crosslinked cells, instead of using whole cells, and second, the fractionation of chromatin by MNase to obtain DNA fragments of about 500 bp length (Fig. 3.1), instead of using sonication for DNA fractionation. Immunoprecipitation and analysis of co-precipitated DNA were performed similarly as in the conventional protocol (Fig. 3.1 and Pinz & Rascle, 2017). This optimized protocol is described in details in Material and methods 3.2.7 and Pinz & Rascle (2017) and was used for all further ChIP experiments in this study.

The question remained whether and how deacetylase inhibitors might affect BRD2 function and by that inhibit STAT5-mediated transcription. In case BRD2 is required for STAT5-mediated transcription, STAT5-mediated transcription is probably inhibited by loss of BRD2 from STAT5 target genes. This proposition is supported by the inhibition of STAT5-mediated transcription by the BET-specific inhibitor JQ1, which interferes with binding of BET proteins such as BRD2 to acetylated histones and like that induces a loss

of BET proteins from chromatin in general (Filippakopoulos et al., 2010) and possibly of BRD2 from STAT5 target genes in particular. Thus, JQ1 probably inhibits STAT5-mediated transcription by inducing a loss of BRD2 from STAT5 target genes. This suggests that TSA might similarly inhibit STAT5-mediated transcription by inducing a loss of BRD2 from STAT5 target genes.

In case JQ1 inhibits STAT5-mediated transcription by loss of BRD2 and not by affecting upstream steps of the STAT5 pathway, DNA binding of STAT5 should remain unaffected by JQ1 treatment. Therefore, to validate the above model, we confirmed that JQ1 treatment does not affect STAT5 DNA binding. STAT5 binding to its binding sites at the promoter of its target genes *Cis* and *Osm* was analyzed in Ba/F3-1∗6 cells treated for 60 min with 1 μM JQ1, 200 nM TSA or vehicle (DMSO) by ChIP using antibodies directed against STAT5A-1∗6. TSA treatment served as a negative control since it does not affect DNA binding of wild-type STAT5 (Rascle et al., 2003; Pinz et al., 2014a) and is unlikely to affect DNA binding of STAT5A-1∗6 in Ba/F3-1∗6 cells. In untreated cells at actively transcribed STAT5 target genes, constitutively active STAT5A-1∗6 was bound to its binding sites at the promoter of its target genes *Cis* and *Osm* (Fig. 4.19A), as expected. No association of STAT5A-1∗6 was detected with the proximal promoter of the IL-3 inducible control gene *c-Fos* or with a downstream control locus within the open reading frame (ORF) of *Cis* (Fig. 4.19A). Importantly, STAT5A-1∗6 binding to its binding sites at the target genes *Cis* or *Osm* (Fig. 4.19A) was neither affected by TSA nor by JQ1. This confirms that JQ1 does not inhibit STAT5-mediated transcription by impairing DNA binding of STAT5 or by impairing one of the upstream STAT5 activation steps which would also result in less DNA-bound STAT5. These results are in agreement with Liu et al. (2014), which demonstrated that JQ1 does not not affect STAT5 binding to *Cis* in leukemic cell lines. Thus, our data support the model that JQ1 inhibits STAT5-mediated transcription via loss of BRD2 from STAT5 target genes.

To further validate above model, the effect of TSA and JQ1 on association of BRD2 with STAT5 target genes was investigated. Therefore, Ba/F3-1∗6 cells were treated for 60 min with 200 nM TSA, 1 μM JQ1, or vehicle (DMSO), and were then subjected to the optimized ChIP protocol using antibodies directed against BRD2. DNA co-precipitated with BRD2 was analyzed using primers covering the *Cis* gene from basepair -800 to + 4000 relative to the TSS, as before. Similarly as in IL-3-stimulated Ba/F3 cells, in Ba/F3-1∗6 cells, BRD2 was associated with the transcription start site and the 5' region of the open reading frame (Fig. 4.19B). JQ1 strongly reduced BRD2 binding along *Cis*, as expected from its inhibitory activity towards BET bromodomains. Strikingly, TSA treatment similarly reduced BRD2 binding, albeit to a lesser extent than JQ1 treatment. By contrast, at the control genes *c-Fos* and *p21*, BRD2 binding to the transcription start

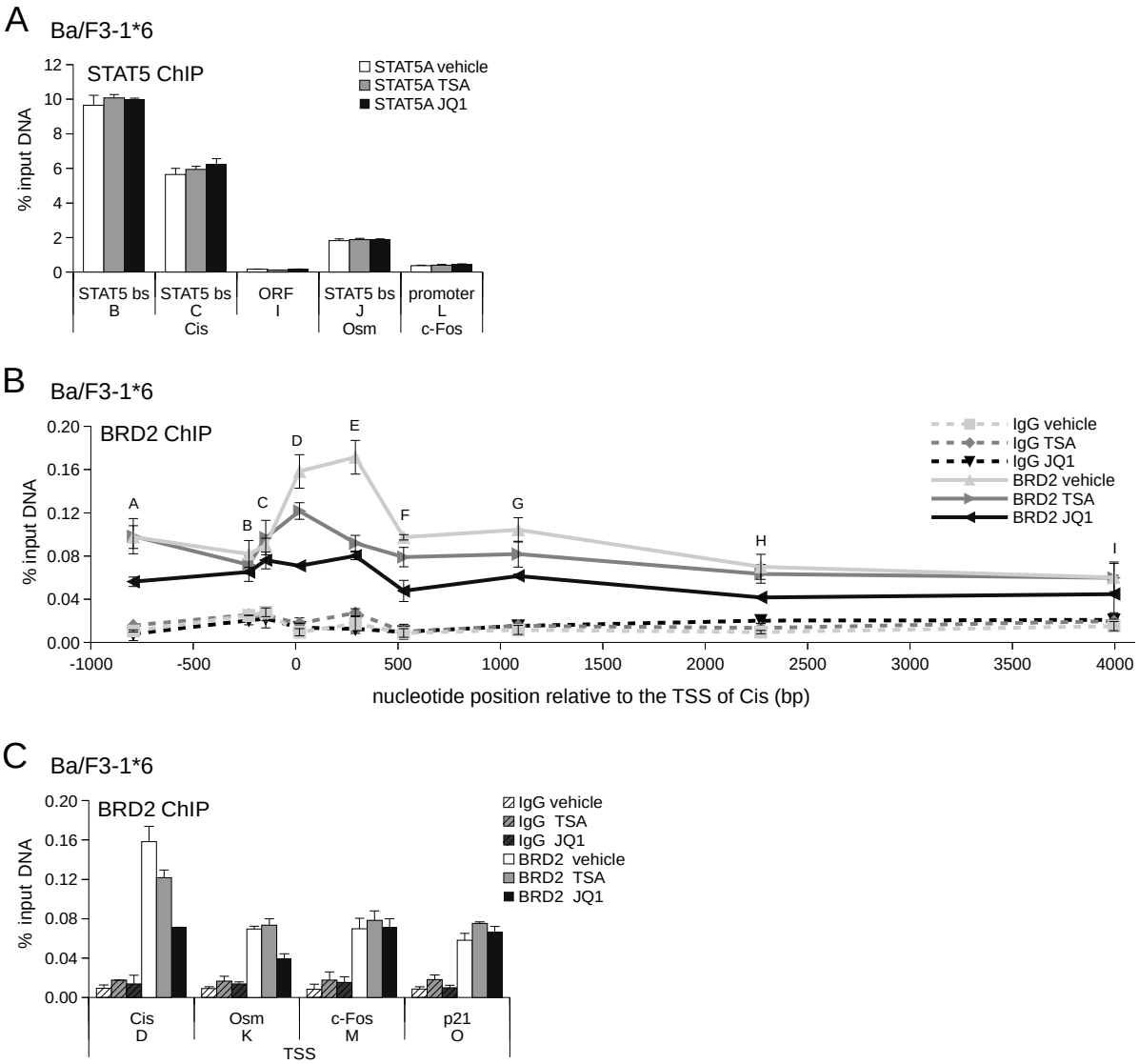

Figure 4.19: BRD2 associates with TSS and ORF of the STAT5 target gene *Cis* and is lost upon TSA and JQ1 treatment

Ba/F3-1∗6 cells were treated with vehicle (0.02% DMSO), TSA (200 nM) or the BET inhibitor JQ1 (1 μM) for 60 min before they were formaldehyde-crosslinked and subjected to ChIP. The ChIP assay was performed as described in Material and methods 3.2.7, using antibodies specific for STAT5A, recognizing STAT5A-1∗6 (**A**), or using antibodies specific for BRD2 (**B**), (**C**). In addition, a rabbit-IgG control antibody was used to determine the background signal. Co-precipitated DNA was analyzed by qPCR with primers specific for the STAT5 binding site (bs), for the transcription start site (TSS), and for the open reading frame (ORF) of the indicated STAT5 target or control genes. The respective amplicons A-O are depicted in Figure 4.17. (Data shown in this figure were generated together with Dr. Anne Rascle.)

site was low and remained unaffected by TSA or JQ1 treatment (Fig. 4.19C). Of note, equally low BRD2 binding was detected at the transcription start site of the STAT5 target gene *Osm*, and although BRD2 binding was slightly reduced upon JQ1 treatment, it remained unaffected upon TSA treatment.

These data demonstrate that inhibition of STAT5-mediated transcription by TSA and JQ1 correlates with loss of BRD2 from the STAT5 target gene *Cis*. This suggests, that STAT5-mediated transcription of *Cis* might be inhibited by loss of BRD2 from the gene. Furthermore, this indicates that BRD2 regulates *Cis* and possibly other STAT5 target genes under normal conditions, and that TSA, and JQ1, might inhibit STAT5-mediated transcription by loss of BRD2 and possibly of other BET proteins from STAT5 target genes.

4.4.2 BRD2 is depleted from the soluble nuclear fraction upon TSA treatment, and is possibly relocated to hyperacetylated chromatin

To investigate how deacetylase inhibitors might induce a loss of BRD2 from STAT5 target genes, we analyzed whether TSA affects the subcellular localization of BRD2 in Ba/F3 cells. Given the hyperacetylation induced by deacetylase inhibitors (Fig. 4.16) and given the preferential binding of BRD2 to acetylated histones (Kanno et al., 2004; LeRoy et al., 2008), BRD2 is expected to be recruited to the chromatin fraction upon TSA treatment. TSA-treated or untreated Ba/F3 cells were successively lysed to obtain cytosolic, soluble nuclear (representing the nucleosol) and insoluble nuclear fractions (containing mainly chromatin-associated proteins). These fractions were analyzed by western blot (data not shown, Dr. Anne Rascle, Pinz et al., 2015, fig. 10C). BRD2 was exclusively found in the nucleus within the soluble and insoluble nuclear fractions. Strikingly, 60 min treatment with the deacetylase inhibitors TSA, VPA and apicidin at concentrations at which they inhibited STAT5 target genes and induced an increase in histone H3 and H4 acetylation, led to a rapid depletion of BRD2 from the soluble nuclear fraction. Treatment with MGCD0103 and MS-275 under conditions in which they did not inhibit STAT5-mediated transcription, did not deplete BRD2 from the soluble nuclear fraction. Interestingly, BRD2 depletion by TSA, VPA and apicidin was accompanied by a specific depletion of TBP from the soluble nuclear fraction. Unexpectedly, no notable increase in BRD2 protein abundance was detected in the insoluble nuclear fraction and also not in the cytosol. Since the proteasome inhibitor MG132 did not prevent the depletion of BRD2 upon TSA treatment (data not shown, Dr. Anne Rascle, Pinz et al., 2015, fig. 10A), proteasomal degradation of BRD2 could be excluded as explanation for BRD2 depletion

from the soluble nuclear fraction. Since TSA did not affect the mRNA level of *Brd2* (data not shown, Dr. Anne Rascle, Pinz et al., 2015, fig. 10B), inhibition of *Brd2* gene expression by TSA can also be excluded as explanation for BRD2 protein depletion. Thus, the unexpected absence of enrichment of BRD2 in the insoluble nuclear fraction could be due to the incomplete extraction method, which left behind a pellet that could not be subjected to SDS-PAGE and western blot analysis. These data strongly suggest that upon deacetylase inhibitor treatment, BRD2 is not degraded but rather delocalized, possibly together with TBP and other interacting proteins, away from the soluble nuclear fraction, probably towards hyperacetylated chromatin.

4.4.3 No direct interaction between STAT5 and BRD2 was observed in solution

To investigate the mechanism of BRD2 recruitment to STAT5 target genes, it was analyzed whether STAT5 and BRD2 interact directly. Co-immunoprecipitation experiments from formaldehyde-crosslinked Ba/F3-1∗6 cells were conducted according to the optimized ChIP protocol (Material and methods 3.2.7), using antibodies directed against STAT5A and BRD2. Beside analysis of (co-)precipitated proteins by western blot, co-precipitated *Cis* DNA was analyzed by quantitative PCR as a control to confirm efficiency and specificity of the co-immunoprecipitation. In western blot, no co-immunoprecipitation between STAT5A and BRD2 was detected after either STAT5A or BRD2 pull-down (Fig. 4.20A). However, while STAT5 was efficiently immunoprecipitated by its antibody, no BRD2 was detectable in western blot after BRD2 immunoprecipitation, despite a similar DNA co-precipitation efficiency and specificity of BRD2 (and STAT5A) as observed before (Fig. 4.19A and B, and Fig. 4.20B). The low BRD2 pull-down detected in western blot might contribute to the overall low DNA enrichment after BRD2 immunoprecipitation (up to 0.16% input DNA) as compared to STAT5A immunoprecipitation (up to 10% input DNA) (Fig. 4.19A and B, and Fig. 4.20B). The low BRD2 pull-down is probably the result of experimental conditions such as buffer composition and/or epitope masking in the formaldehyde-crosslinked cells, which might be suboptimal for the BRD2 antibody. The weak immunoprecipitation efficiency of BRD2 made it difficult to observe a possible co-immunoprecipitation of STAT5. Therefore, immunoprecipitation of BRD2 was repeated, this time from nuclear lysate of non-crosslinked STAT5A-1∗6-expressing cells. Now BRD2 was efficiently immunoprecipitated by its antibody, however, no STAT5 co-immunoprecipitation was detected (Fig. 4.20C). Thus, no direct interaction between soluble STAT5A-1∗6 and BRD2 could be observed. Therefore, BRD2 seems to be

recruited to STAT5 target genes by a different mechanism than by direct interaction with soluble STAT5.

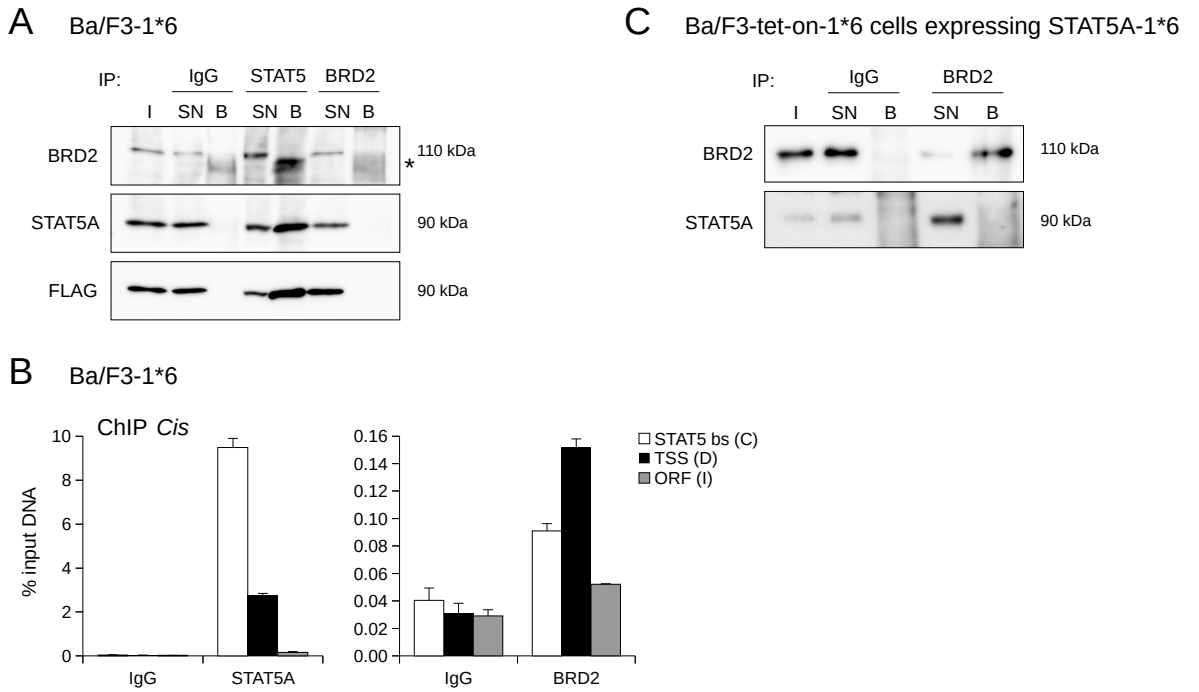

Figure 4.20: No direct interaction between BRD2 and constitutively active STAT5A-1∗6 was observed in solution
(**A**), (**B**) STAT5A or BRD2 were immunoprecipitated following the ChIP protocol, as described in Material and methods 3.2.5.7. The rabbit-IgG control antibody served to determine the background signal. Immunoprecipitated proteins were analyzed by western blot using antibodies directed against BRD2, STAT5A, or FLAG (recognizing STAT5A-1∗6) (A). The asterisk marks an unspecific signal associated with the bead fractions. Co-precipitated DNA of the *Cis* locus was analyzed by qPCR using primers specific for STAT5 binding sites (bs) (amplicon C), for the TSS (amplicon D), or for the distal ORF (amplicon I) (B). The location of the respective amplicons C, D and I along *Cis* is depicted in Figure 4.17. (**C**) BRD2 was immunoprecipitated from non-crosslinked Ba/F3-tet-on-1∗6 cells treated for 9 h with doxycycline to induce expression of STAT5A-1∗6. Immunoprecipitation was performed in mild buffer conditions, as described in Material and methods 3.2.5.7. The immunoprecipitation with rabbit-IgG control antibody served to determine the background signal. The precipitated proteins were analyzed by western blot using antibodies directed against BRD2 and STAT5A. I, input; SN, supernatant; B, bead fraction.

CHAPTER 5

Discussion

STAT5-mediated transcription is inhibited by deacetylase inhibitors. Characterization of the underlying inhibitory mechanism should contribute to a better understanding of the mechanism of transcriptional regulation by STAT5. This thesis aimed to investigate the mechanism of inhibition of STAT5-mediated transcription by deacetylase inhibitors. We focused on the identification of the deacetylase involved and of its acetylated substrate. We provide evidence that inhibition of (a) yet-unknown HDAC(s) target(s) histone proteins, resulting in chromatin hyperacetylation, in turn altering the function of the acetylated-chromatin-associated factor and STAT5-cofactor BRD2, as discussed below.

5.1 Inhibition of STAT5-mediated transcription by deacetylase inhibitors involves histone but not STAT5 acetylation

In previous studies we showed that deacetylase inhibitors had only marginal effects on local histone acetylation at STAT5 target genes (Rascle et al., 2003; Rascle & Lees, 2003), so that we considered that STAT5, instead of histones, might be the acetylated substrate of the deacetylase involved in inhibition of STAT5-mediated transcription. We found that lysine-to-glutamine or lysine-to-arginine mutations of selected STAT5 lysine residues (K84, K359, K384, K675, K681, K689, K696 and K700) potentially targeted for acetylation did not affect STAT5-mediated transcription. This suggests that STAT5 acetylation does not affect STAT5-mediated transcription and consequently that STAT5

is probably not the acetylated substrate involved in inhibition of STAT5-mediated transcription. On the other hand, the performed lysine-to-glutamine mutations might not mimic acetylated STAT5 lysines close enough to exert their potential inhibitory function. While the mutation to glutamine, similarly as acetylation, neutralizes the positive charge of the lysine residue, glutamine has a shorter side chain than the acetylated lysine and might therefore not be able to assume structural functions of the acetylated lysine residue. Thus, although the analyzed lysine-to-glutamine mutations did not affect STAT5-mediated transcription (Fig. 4.10, Fig. 4.11, Fig. 4.12, and Fig. 4.13), we cannot exclude that increased acetylation of these lysine residues might possibly modulate STAT5-mediated transcription. Furthermore, the absence of effect of lysine-to-arginine mutations, preserving the positive charge of the unmodified lysine, does also not contradict a potential inhibitory role of lysine acetylation in inhibition of STAT5-mediated transcription by deacetylase inhibitors. In case STAT5 is normally deacetylated when bound to DNA, a lysine-to-arginine mutation, preventing a potential inhibitory acetylation, would not induce a derepression of STAT5 and hence no increase in STAT5-mediated transcription. However, importantly, the lysine mutants remained sensitive to TSA, at least those mutants containing mutations at K689, K696 and K700 which were analyzed in the TSA-sensitivity assay (Fig. 4.13C and D). Thus, we can exclude that the inhibitory effect of TSA on STAT5-mediated transcription is mediated by an increase in acetylation of STAT5 at the investigated lysine residues. There are further lysine residues in the STAT5 sequence and their influence on STAT5 transcriptional activity cannot be excluded, but all lysine residues within STAT5 which were either reported to be acetylated or whose conserved lysine residue in STAT3 was reported to be acetylated were investigated. Therefore the presented data suggest that TSA does not inhibit STAT5-mediated transcription by targeting STAT5 via these lysine residues. Thus, acetylated STAT5 is unlikely to be the acetylated substrate involved in inhibition of STAT5-mediated transcription by deacetylase inhibitors.

Other groups found that lysine mutations regulate STAT5 activity (Ma et al., 2010; Van Nguyen et al., 2012), which is in apparent contradiction to the absence of effect of lysine-to-arginine or lysine-to-glutamine mutations presented here (Fig. 4.11, Fig. 4.12, and Fig. 4.13). However, given the stabilized phosphorylation and possibly enhanced dimerization of STAT5A-1∗6 (Onishi et al., 1998), our data do not exclude the possibility that the mutated lysine residues might be required for a STAT5 activation step, irrelevant to STAT5A-1∗6, preceding DNA binding and transcription activation. Our data therefore do not contradict the report by Ma et al. (2010), in which loss of transcriptional activity upon K694R mutation within STAT5B (corresponding to K689 of STAT5A) is likely a result of abolished STAT5 dimerization. The lack of luciferase re-

porter gene induction by the lysine mutant in that study is thus likely a consequence of missing nuclear transcriptionally-competent dimers and not a consequence of impaired STAT5-mediated transcription. The same explanation of impaired dimerization might also account for the reduced luciferase reporter induction of a STAT5A K696R mutant in growth hormone-stimulated mouse embryonic fibroblast (MEF) cells (Van Nguyen et al., 2012).

The effect of lysine mutations on STAT5-mediated transcription was investigated in the context of constitutively active full-length STAT5A-1∗6 (Fig. 4.11, Fig. 4.12, and Fig. 4.13). Therefore our data remain to be confirmed in the context of wild-type STAT5. However, the mutations that render STAT5A-1∗6 constitutively active are likely to affect only upstream STAT5 activation steps, namely stabilization of tyrosine phosphorylation and possibly dimerization (Onishi et al., 1998). The proposition that STAT5A-1∗6 constitutive activity is conveyed through stabilization of its tyrosine phosphorylation (Onishi et al., 1998) is supported by the abolished STAT5A-1∗6-mediated transcription upon mutation of the essential phosphorylation site, tyrosine Y694 (Fig. 4.12 and Fig. 4.13). Although initial activation steps of STAT5A-1∗6 might function differently than activation of wild-type STAT5, both proteins probably use the same transactivation mechanism. This is supported by the similar inhibition of STAT5A-1∗6-mediated and wild-type STAT5-mediated transcription by TSA, in terms of persistent STAT5 DNA binding but abrogated recruitment of RNA polymerase II (Fig. 4.1, Fig. 4.18, Fig. 4.19A, and Rascle et al., 2003). Therefore, it is highly likely that the results obtained using STAT5A-1∗6 lysine mutants can be transferred to wild-type STAT5-mediated transcription. To definitely confirm our findings on wild-type STAT5 in Ba/F3 cells, an inducible STAT5 knock-down cell line could be used together with the transient transfection of wild-type or mutant STAT5 expression constructs (rescue experiment). However, lysine residues which are essential for initial STAT5 activation steps, such as dimerization, cannot be analyzed for their influence on STAT5-mediated transcription using this system.

Interestingly, inhibition of STAT5-mediated transcription correlated with a rapid increase in global histone acetylation, which was induced by the deacetylase inhibitors TSA, VPA and apicidin, but not by MGCD0103 and MS-275 (Fig. 4.3 and Fig. 4.16). This suggests, that global histone hyperacetylation might be involved in inhibition of STAT5-mediated transcription. The absence of induction of rapid histone hyperacetylation by the benzamide deacetylase inhibitors MGCD0103 and MS-275 in our study is probably a consequence of their time-dependent mode of action. A mechanism has been proposed for benzamides bound to HDAC2 (Bressi et al., 2010), in which an internal hydrogen bond within the transiently-bound compound is gradually disrupted over time to convert to the tightly-bound form providing increased deacetylase inhibition. This is in agreement with

the treatment duration of 4 to 24 h after which MGCD0103 and MS-275 were shown to induce histone hyperacetylation (Hu et al., 2003; Fournel et al., 2008; Khan et al., 2008; Arts et al., 2009; Duque-Afonso et al., 2011). Thus, the treatment of 15 min to 1.5 h in the present work might have been too short for the benzamides MGCD0103 and MS-275 to exhibit their inhibitory function. Accordingly, we found that 10 h treatment with MS-275 induced histone hyperacetylation in Ba/F3 cells. Together with induction of histone hyperacetylation, MS-275 inhibited expression of the STAT5 target gene *Cis* (Dr. Anne Rascle, Pinz et al., 2015, fig. S5), supporting the involvement of histone hyperacetylation in inhibition of STAT5-mediated transcription.

The concurrence of increased histone acetylation and inhibition of STAT5-mediated transcription indicates that local changes in chromatin organization at STAT5 target genes might possibly be involved in STAT5-mediated transcription. However, the local loss of histone occupancy observed after TSA treatment in unstimulated Ba/F3 cells, in the absence of STAT5 DNA binding and in the absence of transcription, led to a histone occupancy which was similar to that of the actively transcribed gene (Fig. 4.18), making it unlikely that the histone occupancy established upon TSA treatment inhibits recruitment of the transcription machinery. It might still be possible that nucleosomes were shifted, obscuring a DNA position directly or indirectly required for recruitment of the transcription machinery. However, a previous study of our group (Rascle et al., 2003) demonstrated that the DNA accessibility at the proximal promoter around STAT5 binding sites up to the transcription start site of the STAT5 target gene *Cis* did not change upon deacetylase inhibitor treatment, demonstrating that TSA does not affect nucleosome positioning at that locus. Thus, local changes in nucleosome occupancy or positioning are unlikely to be responsible for the inhibition of STAT5-mediated transcription by deacetylase inhibitors.

Local changes in histone acetylation at STAT5 target genes were reassessed, since in our initial study no chromatin immunoprecipitation (ChIP)-grade H3 antibody suitable for normalization of histone acetylation to histone occupancy was available (Rascle & Lees, 2003). The now observed local changes in histone acetylation at STAT5 target genes and upregulated control genes upon deacetylase inhibitor treatment did not correlate with transcriptional activity (Results 4.3.7 and Dr. Anne Rascle and Samy Unser, Pinz et al., 2015, fig. 8) in agreement with other reports (Ellis et al., 2009; Halsall et al., 2015). However, since similar local changes in histone H3 and H4 acetylation upon deacetylase inhibitor treatment were observed at both STAT5 target genes investigated, we cannot rule out that these local changes, in addition to global histone hyperacetylation, might contribute to inhibition of STAT5-mediated transcription.

Sirtuins, class III HDACs, which are inhibited by different small molecule inhibitors

than the classical HDACs mentioned so far, also deacetylate histones (Vaquero et al., 2004, 2007; Hsu et al., 2016) which raises the possibility that sirtuin inhibitors might also inhibit STAT5-mediated transcription via increase in global histone acetylation. By contrast, we found that the sirtuin inhibitor salermide did not inhibit STAT5-mediated transcription (Fig. 4.4), suggesting that the global level of histone acetylation was probably not increased in those experiments. So far, global histone H3 and H4 acetylation after salermide treatment has only been analyzed after 24 h treatment in a human pancreatic cell line (Yar Saglam et al., 2016), and a 2- to 3-fold increase in histone acetylation was found (while MS-275 induced an up to 4-fold increase in histone acetylation in that study) (Yar Saglam et al., 2016). Although we used similar salermide concentrations as Yar Saglam et al. (2016), the shorter treatment of up to 1.5 h in our study might not have been long enough to induce global histone hyperacetylation and thereby inhibit STAT5-mediated transcription. However, sirtuin inhibition that induces a global increase in histone acetylation, as shown for instance by Kim et al. (2015), would be a valuable tool to confirm whether histone hyperacetylation is sufficient to inhibit STAT5-mediated transcription, or whether additional effects specific for classical HDACs are involved.

5.2 Inhibition of STAT5-mediated transcription by deacetylase inhibitors probably involves redundant class I HDAC activity

The finding that the effect of deacetylase inhibitors on STAT5-mediated transcription is probably induced through histone hyperacetylation, suggests that the effect of deacetylase inhibitors is probably mediated by class I HDACs, HDAC1, HDAC2, HDAC3, and HDAC8, since these are the major HDACs responsible for the deacetylation of histones (Verdel et al., 2000; Fischle et al., 2001, 2002; Lahm et al., 2007; Dovey et al., 2013; Kelly & Cowley, 2013; Lobera et al., 2013; Wolfson et al., 2013; You et al., 2013; Di Giorgio et al., 2015; Liu et al., 2015).

Surprisingly, of the four class I HDACs only HDAC3, together with HDAC5 and HDAC11, was among the candidates for involvement in STAT5-mediated transcription according to our screen with several selective deacetylase inhibitors (Tab. 4.1). This result might be (i) due to the difficulty to determine accurate *in vivo* IC_{50} values of the inhibitors for the individual HDACs (Chou et al., 2008; Delcuve et al., 2012; Vaidya et al., 2012; Hull et al., 2016) or (ii) due to the late mode of action of MS-275 and MGCD0103 discussed above (Hu et al., 2003; Fournel et al., 2008; Khan et al., 2008; Arts et al., 2009; Bressi et al., 2010; Duque-Afonso et al., 2011), which was not taken into account

during the analysis, so that their targeted HDACs were misleadingly excluded as possible candidates in the inhibitor screen. However, since the selective deacetylase inhibitors VPA and apicidin, which induced histone hyperacetylation and inhibited STAT5-mediated transcription, are class I deacetylase inhibitors, and since after a longer incubation time the class I inhibitor MS-275 also inhibited STAT5-mediated transcription (Dr. Anne Rascle, Pinz et al., 2015, fig. S5), the data obtained with these selective deacetylase inhibitors support the proposed involvement of class I deacetylases in inhibition of STAT5-mediated transcription.

SiRNA-mediated knock-down of individual HDACs or of combinations thereof failed to identify the HDACs responsible for inhibition of STAT5-mediated transcription (Fig. 4.7, Fig. 4.8, and Pinz et al., 2015, fig. S4). Unexpectedly, even co-transfection of siRNAs targeting the class I HDACs HDAC1, HDAC2 and HDAC3 failed to induce a strong histone hyperacetylation and to inhibit STAT5-mediated transcription (Fig. 4.8). This is probably a consequence of the incomplete knockdown of the individual HDACs in that experiment. Together with the functional redundancy of these class I HDACs regarding histone deacetylation (Montgomery et al., 2007; Jurkin et al., 2011; Dovey et al., 2013) and together with the high expression level of HDAC1 and HDAC2 in Ba/F3 cells (Fig. 4.6), the remaining deacetylase activity was probably able to maintain low-acetylated chromatin.

Alternatively, the different effects of treatment with deacetylase inhibitors and depletion of HDACs by siRNA-mediated knockdown might reflect the phenomenon that enzymatic HDAC inhibition and physical depletion of HDACs sometimes induce different cellular effects (Mottus et al., 2000; Dejligbjerg et al., 2008; Krämer, 2009; Chen et al., 2012; Shah et al., 2013). Such different effects might be due to an HDAC-independent mode of action of deacetylase inhibitors (Shah et al., 2013), or due to deacetylase activity-independent, probably structural functions of HDACs in multiprotein complexes (Mottus et al., 2000; Krämer, 2009; Chen et al., 2012). However, since physical elimination of HDACs had no effect on STAT5-mediated transcription, our data do not support a predominantly structural role of HDACs during inhibition of STAT5-mediated transcription. Isoform-specific deacetylase inhibitors or more efficient HDAC knock-down strategies such as lentiviral delivery of siRNA expression cassettes might help to confirm the involvement of one or several HDACs and their exact function during inhibition of STAT5-mediated transcription by deacetylase inhibitors.

5.3 Deacetylase inhibitors inhibit STAT5-mediated transcription by affecting bromodomain and extraterminal domain (BET) protein function

The involvement of histone acetylation in inhibition of STAT5-mediated transcription suggests that chromatin-associated factors which are sensitive to histone acetylation might be involved in inhibition of STAT5-mediated transcription. The acetyl-histone binding protein BRD2, a member of the BET protein family, has been shown before to regulate STAT5-mediated transcription in human leukemia cell lines (Liu et al., 2014). Using chromatin immunoprecipitation (ChIP), we could now demonstrate for the first time that BRD2 is directly associated with the STAT5 target gene *Cis* in a STAT5-dependent manner, further supporting the involvement of BRD2 in STAT5-mediated transcription. In addition, our data provided evidence that the BET inhibitor (+)-JQ1 (JQ1) inhibits STAT5-mediated transcription not only in leukemic cells (Liu et al., 2014), but also in the non-tumorigenic pro-B cell line Ba/F3 (Dr. Anne Rascle, Pinz et al., 2015, fig. 9). Therefore, our data strongly support BRD2 and possibly other BET proteins as cofactors of STAT5-mediated transcription.

The BET inhibitor JQ1 seems to inhibit STAT5 not only at the level of STAT5-mediated transcription (this work and Liu et al., 2014), but longer treatment with JQ1 (3-25 h) was shown to reduce the activating tyrosine phosphorylation of STAT5 in monocyte-derived dendritic cells (MO-DCs) and in several leukemia and lymphoma cell lines (Ott et al., 2012; Liu et al., 2014; Toniolo et al., 2015). However, in agreement with the absence of JAK kinase inhibitor activity of JQ1 (Liu et al., 2014) and in agreement with the delayed onset of reduced STAT5 phosphorylation, this phenomenon seems to be a secondary effect of JQ1 treatment. Reduced STAT5 phosphorylation in JQ1 treated cells can be explained at least in part by suppressed transcription of components of cytokine receptors responsible for STAT5 activation, for instance of the interleukin-7 receptor in B cell acute lymphocytic leukemia (B-ALL) cell lines (Ott et al., 2012) or of the GM-CSF receptor in MO-DCs (Toniolo et al., 2015). Interestingly, the affected GM-CSF receptor α chain gene is a STAT5 target gene (Toniolo et al., 2015), indicating that inhibition of STAT5-mediated transcription by JQ1 might be involved in inhibition of expression of this receptor subunit. Further support for JQ1-mediated inhibition of STAT5-mediated transcription is given by the absence of reduction of STAT5 phosphorylation in several leukemic cell lines (HEL, K562 and ALL-SIL cell lines) (Liu et al., 2014). In these cell lines JQ1 inhibited STAT5 target gene expression, confirming that inhibition of STAT5-mediated transcription by JQ1 occurred independently of impaired

STAT5 phosphorylation (Liu et al., 2014). While it remains to be confirmed whether JQ1 affects the interleukin-3-dependent activating phosphorylation of wild-type STAT5 in Ba/F3 cells, our group observed an immediate inhibition of STAT5 target gene expression (within 1.5 h JQ1 treatment, Dr. Anne Rascle, Pinz et al., 2015, fig. 9), which is unlikely to be the consequence of a delayed reduction of STAT5 phosphorylation. Furthermore, we could show using ChIP that JQ1 does not affect binding of constitutively active STAT5A-1∗6 to its target genes in Ba/F3-1∗6 cells (Fig. 4.19A). This indicates that upstream steps of STAT5A-1∗6 activation were not impaired by JQ1 treatment. Altogether, and in agreement with the literature (Liu et al., 2014), our data support the proposition that the immediate inhibition of STAT5 by JQ1 occurs at the level of STAT5-mediated transcription, which supports BET proteins as cofactors of STAT5-mediated transcription.

Importantly, we found that TSA treatment resulted in the loss of BRD2 from the STAT5 target gene *Cis* (Fig. 4.19B). Similarly, JQ1 treatment also resulted in the loss of BRD2 from the *Cis* gene (Fig. 4.19B), as expected from the mode of action of JQ1, which competitively binds to BET bromodomains and thus interferes with binding of BET proteins to acetylated histones and to chromatin (Filippakopoulos et al., 2010). Since STAT5-mediated transcription is inhibited by both compounds, this strongly suggests that STAT5-mediated transcription can be inhibited by loss of BRD2 from its target genes. This proposition is further supported by the demonstration that depletion of the BRD2 protein level also inhibits STAT5-mediated transcription (Liu et al., 2014). Together, these observations support a model in which deacetylase inhibitors repress STAT5-mediated transcription by inducing a loss of BRD2 from STAT5 target genes.

The loss of BRD2 from the *Cis* gene upon deacetylase inhibitor treatment coincided with a nuclear redistribution of BRD2 (Results 4.4.2 and Dr. Anne Rascle, Pinz et al., 2015, fig. 10) and with a global increase in histone acetylation (Fig. 4.16). The multiple newly acetylated histones created upon deacetylase inhibitor treatment probably compete for binding of the acetyl-histone binding protein BRD2 (Kanno et al., 2004; LeRoy et al., 2008), which might lead to the observed redistribution of BRD2 and to BRD2 loss from the sites it normally binds to such as the STAT5 target gene *Cis*. Although we could demonstrate that BRD2 is depleted from the nucleosol as histone acetylation increases, the expected enrichment of BRD2 in the insoluble chromatin fraction could not be observed (Results 4.4.2 and Dr. Anne Rascle, Pinz et al., 2015, fig. 10C). This might be explained by our failure to achieve complete protein extraction from the insoluble chromatin fraction, so that part of the chromatin-associated proteins might not have been included in the analysis. We could demonstrate that deacetylase inhibitor treatment affects neither BRD2 mRNA abundance nor BRD2 proteasomal degradation.

These findings are in agreement with a recent proteomics study (Mackmull et al., 2015) demonstrating that although many bromodomain-containing proteins are downregulated upon 12-48 h deacetylase inhibitor treatment, protein abundance of BRD2 was rather increased. Furthermore, fluorescence intensity after photobleaching (FLIP) experiments (Dey et al., 2003) demonstrated that the mobility of BRD2 decreases upon deacetylase inhibitor treatment, indicating that a higher fraction of BRD2 is stably associated with chromatin. Thus, in agreement with the literature, our data strongly suggest that the loss of BRD2 from STAT5 target genes and its depletion from the nucleosol are no consequence of BRD2 degradation, but rather a consequence of BRD2 redistribution to hyperacetylated chromatin. Importantly, further evidence for BET protein relocation after deacetylase inhibitor treatment is given by the redistribution of BRD4 in a human breast cancer cell line (Greer et al., 2015). Similarly to what we propose for BRD2, Greer et al. (2015) demonstrated in a genome-wide approach that BRD4 binding is shifted towards newly acetylated sites in gene bodies and intergenic regions and away from the highly acetylated promoters and enhancers it normally binds to. A similar ChIP-sequencing approach could be performed to demonstrate the genomic distribution of BRD2 before and after deacetylase inhibitor treatment to confirm the proposed redistribution of BRD2 to hyperacetylated chromatin.

One of the many transcriptional regulators shown to interact with BRD2 is HDAC11 (Denis et al., 2006). Thus, it cannot be excluded that inhibition of HDACs might contribute to the redistribution of BRD2 by directly disrupting or destabilizing BRD2-containing protein complexes. This is in accordance with other reports demonstrating that deacetylase inhibitors can act through protein complex disruption (Brush et al., 2004; Matsuoka et al., 2007; Krämer, 2009). Since acetylation increases upon IL-3 stimulation at transcriptionally active STAT5 target genes (Results 4.3.7 and Dr. Anne Rascle and Samy Unser, Pinz et al., 2015, fig. 7 and fig. 8 and Pinz et al., 2014b, fig. 7), the substrate of such HDAC within a BRD2 complex would likely be a non-histone protein. Or the HDAC in such complex could have a rather structural function, in agreement with the indication that catalytically inactive HDAC2 proteins can partially assume functions of the wild-type protein (Montgomery et al., 2007; Zimmermann et al., 2007; Guan et al., 2009; Krämer, 2009). Once the HDAC(s) responsible for inhibition of STAT5-mediated transcription are identified, the influence of specific HDAC(s) on BRD2 function at STAT5 target genes can be further elucidated by using HDAC knock-down, catalytically inactive HDAC mutants or possibly HDAC isoform-specific inhibitors.

The recruitment of BRD2 to *Cis* seems to be STAT5-dependent, but a mechanism similar to the transcription factor E2F-1, whose binding to BRD4 is dependent on lysine acetylation of E2F-1 (Ghari et al., 2016), can be excluded since no potential STAT5 acety-

lation site affecting its transcriptional activity was identified, and since a direct interaction between BRD2 and STAT5 could not be observed in co-immunoprecipitation assays (Fig. 4.20). Further indication against a stable complex between BRD2 and STAT5, in addition to the absence of co-immunoprecipitation of these proteins, is given first by the absence of alterations of soluble nuclear STAT5 complexes upon TSA treatment in gel filtration experiments (Fig. 4.15), second by the absence of STAT5 redistribution together with BRD2 upon deacetylase inhibitor treatment (Results 4.4.2 and Dr. Anne Rascle, Pinz et al., 2015, fig. 10C) and third by the fact that BRD2 loss from *Cis* by JQ1 or TSA treatment did not affect STAT5 DNA binding (Fig. 4.19A and Liu et al., 2014). Nevertheless, since BRD2 and other BET proteins are part of multiprotein transcriptional complexes (Jiang et al., 1998; Denis et al., 2006; Rahman et al., 2011), and since BRD2 seems to be involved in STAT5-mediated transcription, BRD2 is likely part of a STAT5-containing transcriptional complex. Denis et al. (2000, 2006) reported that the stability of BRD2-containing complexes is ATP-dependent, while no ATP was added to the buffers in our co-immunoprecipitation or gel filtration experiments. This suggests that the formation of a STAT5 and BRD2-containing complex, and thereby the recruitment of BRD2 to STAT5 target genes, might be ATP-dependent. On the other hand, our data are also in agreement with a model in which BRD2 recruitment or stabilization is mediated via chromatin. Considering the preferential binding of BRD2 to acetylated histones (Kanno et al., 2004; LeRoy et al., 2008), its recruitment to STAT5 target genes could possibly be induced by an increase in local histone acetylation. This proposition is supported by increased histone H3 and histone H4 acetylation at STAT5 target genes upon IL-3 stimulation of Ba/F3 cells concomitant to BRD2 recruitment to the transcription start site (TSS) of *Cis* (Results 4.3.7 and Dr. Anne Rascle and Samy Unser, Pinz et al., 2015, fig. 7, fig. 8, and fig. 11A and Pinz et al., 2014b, fig. 7). Furthermore, blocking BRD2 bromodomains with the small molecule JQ1 leads to BRD2 loss from STAT5 target gene *Cis* (Fig. 4.19B), indicating that BRD2-acetyl-histone interactions are important for the association of BRD2 with STAT5 target genes. Together this suggests that the STAT5-dependent recruitment of BRD2 to STAT5 target genes is ATP-dependent, or takes place at the chromatin level via histone acetylation, or both. To further elucidate the mechanism of BRD2 recruitment to STAT5 target genes, STAT5-BRD2 co-immunoprecipitation experiments in the presence of ATP might be carried out. Furthermore, STAT5-containing transcriptional complexes could be analyzed by ChIP coupled with mass spectrometry (ChIP-MS) to analyze whether BET proteins are present in these complexes and to identify factors possibly bridging STAT5 to BRD2 or other BET proteins. To show whether increased acetylation at STAT5 target genes is required for BRD2 recruitment, HAT inhibitors could be used to possibly prevent the

increase in histone acetylation at STAT5 target genes upon IL-3 stimulation.

BRD2 interacts with transcriptional co-activators, transcription factors, components of the transcriptional machinery, especially TATA-binding protein (TBP) and RNA polymerase II, associates with high-acetylated chromatin of transcribed genes and was proposed to act as a scaffold (Crowley et al., 2002; Kanno et al., 2004; Denis et al., 2006; Peng et al., 2007; LeRoy et al., 2008). Furthermore, we found that, together with BRD2 depletion from the nucleosol upon deacetylase inhibitor treatment, TBP is also depleted from the nucleosol (Results 4.4.2 and Dr. Anne Rascle, Pinz et al., 2015, fig. 10C). Thus, the redistribution of BRD2 together with its interacting proteins upon deacetylase inhibitor treatment is likely to interfere with the proper recruitment of the transcription machinery to the genes normally regulated by BRD2, such as the STAT5 target gene *Cis*. This proposition is supported by the loss of key components of the transcription complex, RNA polymerase II and TBP, from STAT5 target genes upon inhibition of STAT5-mediated transcription by deacetylase inhibitor treatment in Ba/F3-1∗6 and IL-3-stimulated Ba/F3 cells (Fig. 4.18 and Rascle et al., 2003). In case interactions of BRD2 with the transcription machinery are indeed required for STAT5-mediated transcription, the overexpression of a BRD2 deletion mutant lacking 26 amino acids required for the interaction of BRD2 with TBP (Peng et al., 2007) would be expected to impair STAT5-mediated transcription. Altogether, BRD2 is probably the deacetylase inhibitor-sensitive factor proposed earlier to be involved in the recruitment of the transcription machinery to STAT5 target genes (Rascle et al., 2003; Rascle & Lees, 2003), and its loss probably inhibits STAT5-mediated transcription by interfering with the recruitment of the transcription machinery. Despite inhibition of the STAT5 target gene *Osm* by the BET inhibitor JQ1, BRD2 association with the *Osm* gene was lower than with the *Cis* gene and not affected by TSA treatment (Fig. 4.19C). Thus, the *Osm* gene might possibly be regulated by another BET family member. Similarly, while BRD2 was associated with the enhancer of the STAT5 target gene *c-Myc* in Ba/F3-1∗6 cells, no BRD2 was detected at the enhancer upon IL-3 stimulation in Ba/F3 cells (data not shown, Dr. Anne Rascle, Pinz et al., 2016, fig. 4). This raises the possibility that several BET family members are involved in the regulation of STAT5 target genes. BET proteins share high sequence homology (Belkina & Denis, 2012) and have a certain degree of functional redundancy (LeRoy et al., 2008; Belkina et al., 2013). On the other hand, the different isoforms seem to have specific developmental functions, which cannot be assumed by other family members (Houzelstein et al., 2002; Gyuris et al., 2009; Shang et al., 2009). Furthermore, BET proteins seem to influence transcription by various mechanisms: BRD2 loss from the STAT5 target gene *Cis* correlated with loss of the transcriptional machinery, while impairment with BRD4 function does not seem to affect recruitment of the transcrip-

tional machinery, but rather inhibits transcription elongation (Greer et al., 2015). It is thus obvious that more effort is required to elucidate specificity versus functional redundancy of BET proteins and their role in the regulation of transcription of different STAT5 target genes. Knockdown of individual BET proteins followed by cDNA microarray analysis would show which STAT5 target genes are regulated by individual BET proteins. ChIP-sequencing of BET proteins would confirm whether the identified BET proteins are associated with different STAT5 target genes.

5.4 Model of regulation of STAT5-mediated transcription by BET proteins and of its inhibition by deacetylase inhibitors

In summary, this work provides evidence that BET proteins such as BRD2 are important cofactors of STAT5-mediated transcription. We propose that a local increase in histone acetylation upon STAT5 DNA binding contributes to the recruitment of BET proteins and that BET proteins assist in the recruitment of the transcription machinery to STAT5 target genes. Furthermore, the data presented here suggest that deacetylase inhibitors inhibit STAT5-mediated transcription independently of STAT5 acetylation, but instead via induction of global histone hyperacetylation and concomitant redistribution of the acetyl-histone-binding protein BRD2, and likely other BET family members, to hyperacetylated chromatin. This competition for binding to acetyl-histones would result in the dissociation of BRD2 from STAT5 target genes (Fig. 5.1). Our group previously demonstrated that deacetylase inhibitor treatment does not affect STAT5 binding to DNA, but impairs assembly of the transcription machinery at STAT5 target genes. Therefore, the loss of BRD2- and likely of other BET family members - probably interferes with the proper assembly of the transcription machinery at STAT5 target genes (Fig. 5.1C) and might be responsible for the inhibition of STAT5-mediated transcription following deacetylase inhibitor treatment. Eventually, the sought HDACs involved in inhibition of STAT5-mediated transcription by deacetylase inhibitors remain to be identified but our data suggest that they belong to class I HDACs.

This proposed model is in agreement with genome-wide ChIP-sequencing experiments which have been published in the meantime (Greer et al., 2015; Halsall et al., 2015). Those experiments revealed that the transcription start sites of genes which are up- or down-regulated by deacetylase inhibitors were packed in highly acetylated chromatin before inhibitor treatment, in agreement with our model of highly acetylated STAT5 target genes proposed previously (Rascle & Lees, 2003) and in the present study. Furthermore,

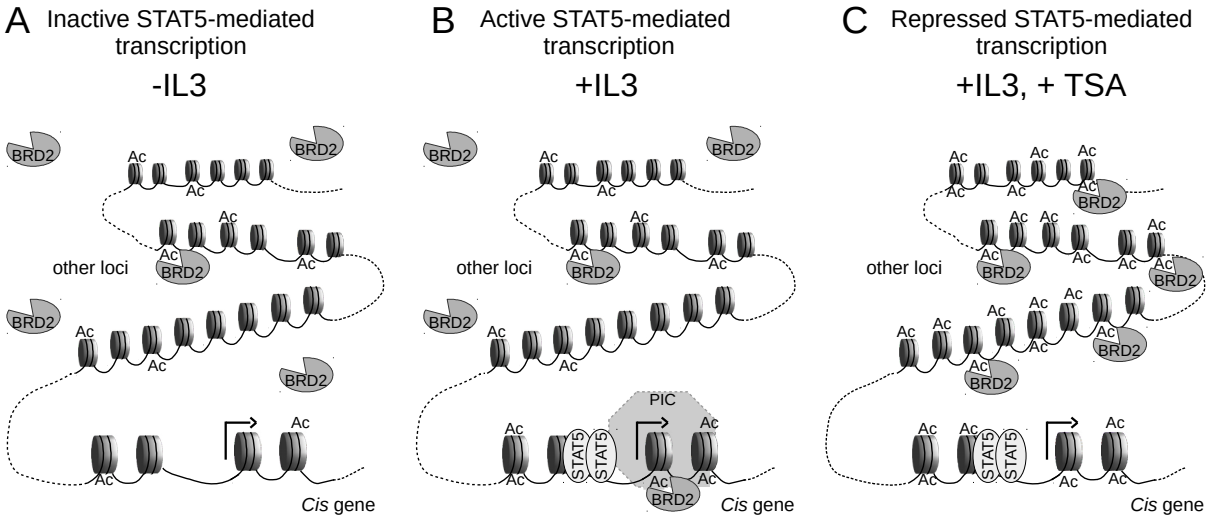

Figure 5.1: Model of regulation of STAT5-mediated transcription by BET proteins and of its inhibition by deacetylase inhibitors
BRD2 is normally associated with chromatin and present in the nucleosol (**A**), (**B**). Following IL-3 stimulation and activation of STAT5, an increase in histone acetylation (Ac) around the transcription start site (TSS) of the *Cis* gene probably contributes to the recruitment of BRD2 to the *Cis* gene (**B**). BRD2 in turn probably assists in the recruitment and stabilization of the transcription machinery (pre-initiation complex (PIC)) (**B**) and is therefore required for the induction of *Cis* gene expression. The deacetylase inhibitors trichostatin A (TSA), VPA, and apicidin induce global chromatin hyperacetylation (**C**). The multiple newly acetylated histones compete for binding of BRD2 and are therefore probably responsible for BRD2 depletion from the nucleosol and from the genes it normally regulates (**C**). Previous data demonstrated that deacetylase inhibitor treatment does not affect STAT5 binding to DNA but prevents the recruitment of the transcription machinery to STAT5 target genes. Together this suggests that loss of BRD2 from the *Cis* gene interferes with the recruitment of the transcription machinery (PIC) (**C**) and is thus responsible for the inhibition of *Cis* gene expression. Our data suggest that besides BRD2, other chromatin associated factors, such as other BET proteins, might be involved in STAT5-mediated transcription and in its inhibition by deacetylase inhibitors. The HDACs involved in this model have not yet been identified, but due to the implication of histone hyperacetylation, those HDACs are probably class I HDACs. Ac, acetylation.

Greer et al. (2015) showed that the highly acetylated genes downregulated by deacetylase inhibitors were associated with the BET protein BRD4 before inhibitor treatment. Upon inhibitor treatment, BRD4 was redistributed towards newly acetylated sites in gene bodies and intergenic regions and away from the highly acetylated promoters and enhancers it normally binds to. This mechanism is similar to the association of BRD2 with the deacetylase inhibitor-sensitive STAT5 target gene *Cis* and to the demonstrated BRD2 redistribution upon deacetylase inhibitor treatment presented in this thesis. Halsall et al. (2015) suggested that the high acetylation of certain genes is an inherent cellular adaptive feature to up- or down-regulate these genes in response to increased global chromatin acetylation in order to slow cell growth and to allow the cell to adjust to and counteract hyperacetylation. It is tempting to propose that BET proteins are part of this cellular adaptive mechanism and play a role in gene downregulation upon chromatin

hyperacetylation. Inhibition of STAT5-mediated transcription by deacetylase inhibitors via interference with BET protein function might be one phenomenon of this general cellular adaptive mechanism to hyperacetylation. Inhibition of proliferation-promoting STAT5 target genes (Mui et al., 1996; Matsumura et al., 1999; Nosaka et al., 1999; Rascle et al., 2003; Basham et al., 2008) together with other genes implicated in cell growth (Halsall et al., 2015) might serve to prevent cells with aberrant chromatin acetylation from growing and proliferating.

To confirm our model of regulation of STAT5-mediated transcription by BET proteins and deacetylase inhibitors, and to confirm the involvement of the different BET proteins in the general cellular response to hyperacetylation, genome wide analysis of the distribution of the different BET family members upon deacetylase inhibitor treatment should be performed. Those experiments would confirm whether all BET proteins are predominantly associated with genes that are downregulated by deacetylase inhibitors and whether the different BET proteins show similar genomic redistributions upon deacetylase inhibitor treatment. Those experiments would also reveal which BET family members are associated with different STAT5 target genes. Investigating the mechanism and specificity of BET protein recruitment to STAT5 target genes would help to further characterize the mechanism of STAT5-mediated transcription and its regulation by BET proteins.

In conclusion, the novel aspects of the regulation of the oncoprotein STAT5 presented in this study have wide implication in the clinical field, especially since the other main players, BET proteins and HDACs, are also implicated in oncogenesis. BET proteins and HDACs are thus presented here as attractive targets for the development of novel therapies against STAT5-associated cancers.

Publications

Part of the data shown and discussed in this work has been published:

Jobst, B., Weigl, J., Michl, C., Vivarelli, F., Pinz, S., Amslinger, S., & Rascle, A. (2016). Inhibition of interleukin-3- and interferon-α-induced JAK/STAT signaling by the synthetic α-X-2′,3,4,4′-tetramethoxychalcones α-Br-TMC and α-CF3-TMC. *Biological Chemistry, 397*(11), 1187-1204.

Pinz, S., & Rascle, A. (2017). Assessing HDAC Function in the Regulation of Signal Transducer and Activator of Transcription 5 (STAT5) Activity Using Chromatin Immunoprecipitation (ChIP). *Methods in Molecular Biology (Clifton, N.J.), 1510*, 257-276.

Pinz, S., Unser, S., & Rascle, A. (2016). Signal transducer and activator of transcription STAT5 is recruited to c-Myc super-enhancer. *BMC molecular biology, 17*(1), 10.

Pinz, S., Unser, S., Buob, D., Fischer, P., Jobst, B., & Rascle, A. (2015). Deacetylase inhibitors repress STAT5-mediated transcription by interfering with bromodomain and extra-terminal (BET) protein function. *Nucleic Acids Research, 43(7)*, 3524-3545.

Pinz, S., Unser, S., Brueggemann, S., Besl, E., Al-Rifai, N., Petkes, H., Amslinger, S., & Rascle, A. (2014a). The Synthetic α-Bromo-2′,3,4,4′-Tetramethoxychalcone (α-Br-TMC) Inhibits the JAK/STAT Signaling Pathway. *PloS one, 9*(3), e90275.

Pinz, S., Unser, S., & Rascle, A. (2014b). The Natural Chemopreventive Agent Sulforaphane Inhibits STAT5 Activity. *PloS one, 9*(6), e99391.

List of Figures

List of Tables

Abbreviations

α-Br-TMC	α-Bromo-2',3,4,4'-Tetramethoxychalcone
α-CF_3-TMC	α-CF_3-2',3,4,4'-Tetramethoxychalcone
E. coli	*Escherichia coli*
Taq	*Thermus aquaticus*
Ac-H3	acetylated histone H3
Ac-H4	acetylated histone H4
APS	ammonium persulfate
ATP	adenosine triphosphate
BET	bromodomain and extra-terminal protein
bp	base pair(s)
BRD	bromodomain-containing protein
bs	binding site
BSA	bovine serum albumin
C-terminal	carboxy-terminal
CBP	CREB binding protein
cDNA	complementary DNA
CDS	coding sequence
ChIP	chromatin immunoprecipitation
Da	dalton
DBD	DNA binding domain
DMSO	dimethyl sulfoxide
DNA	desoxynucleic acid
DTT	DL-Dithiothreitol
ECL	enhanced chemiluminescence
EDTA	ethylenediaminetetraacetic acid
EGTA	Ethylene glycol-bis(2-aminoethylether)-N,N,N',N'-tetraacetic acid
FCS	fetal calf serum
Fig.	figure
for	forward primer
GM-CSF	granulocyte-macrophage colony-stimulating factor (GM-CSF
h	hour(s)

H3	histone H3
HAT	histone acetyltransferase
HD	HDAC
HDAC	histone deacetylase
HDACi	histone deacetylase inhibitor
HRP	horseradish peroxidase
IC_{50}	half inhibitory concentration
ID	internal identifier for primers, plasmids, siRNA and antibodies
IgG	Immunoglobulin G
IL-3	interleukin-3
IP	immunoprecipitation
JAK	Janus kinase
JQ1	(+)- JQ1, inhibitor of BET proteins
kb	kilo base pair(s)
kDa	kilodalton
LB	lysogeny broth
MAPK	mitogen-activated protein kinase
MCS	multiple cloning site
min	minute(s)
MNase	micrococcal nuclease
mRNA	messenger RNA
MW	molecular weight
N-terminal	amino-terminal
NAD^+	nicotinamide adenine dinucleotide
O/N	over night
OD	optical density
ORF	open reading frame
PAGE	poly acryl amide electrophoresis
PBS	phosphate buffered saline
PCR	polymerase chain reaction
pH	negative decadic logarithm of [H+]
PLB	passive lysis buffer (for luciferase assay)
PMSF	phenylmethylsulfonyl fluoride
qPCR	quantitative real-time PCR
rcf	relative centrifugal force
rev	reverse primer
RLU	relative light unit(s)
rmIL-3	recombinant murine interleukin-3
RNA	ribonucleic acid
RNA Pol II	RNA polymerase II
RS	restriction site
RT	room temperature
RT-PCR	reverse transcription PCR
RT-qPCR	quantitative reverse transcription PCR
SAHA	suberoylanilide hydroxamic acid
SDM	site-directed mutagenesis

SDS	sodium dodecyl sulfate
SDS-PAGE	SDS polyacrylamide gel electrophoresis
SH-2 domain	Src-homology-2 domain
siRNA	small interfering RNA
SMRT	silencing mediator for retinoic acid receptor and thyroid hormone receptor
SOCS	suppressors of cytokine signaling
STAT	signal transducer and activator of transcription
STAT5 bs	STAT5 binding site
STAT5A-1∗6	constitutively active STAT5A mutant
Tab.	Table
TAD	transactivation domain
TAE	tris acetate buffer
TBP	TATA-box binding protein
TBS	tris buffered saline
TEMED	N,N,N,N-Tetramethylethylenediamine
Tris	tris(hydroxymethyl)aminomethane
TSA	trichostatin A
TSS	transcription start site
U	units
UAS	upstream activator sequence
UV	ultraviolet
v/v	volume per volume
VPA	valproic acid
w/v	weight per volume
WB	western blot
wt	wild-type

References

Agalioti, T., Chen, G., & Thanos, D. (2002). Deciphering the transcriptional histone acetylation code for a human gene. *Cell*, *111*(3), 381–392.

Agalioti, T., Lomvardas, S., Parekh, B., Yie, J., Maniatis, T., & Thanos, D. (2000). Ordered recruitment of chromatin modifying and general transcription factors to the IFN-beta promoter. *Cell*, *103*(4), 667–678.

Al-Rifai, N., Rücker, H., & Amslinger, S. (2013). Opening or closing the lock? When reactivity is the key to biological activity. *Chemistry (Weinheim an Der Bergstrasse, Germany)*, *19*(45), 15384–15395.

Allegra, P., Sterner, R., Clayton, D. F., & Allfrey, V. G. (1987). Affinity chromatographic purification of nucleosomes containing transcriptionally active DNA sequences. *Journal of Molecular Biology*, *196*(2), 379–388.

Allfrey, V. G., Faulkner, R., & Mirsky, A. E. (1964). ACETYLATION AND METHYLATION OF HISTONES AND THEIR POSSIBLE ROLE IN THE REGULATION OF RNA SYNTHESIS. *Proceedings of the National Academy of Sciences of the United States of America*, *51*, 786–794.

Aoyagi, S., & Archer, T. K. (2007). Dynamic histone acetylation/deacetylation with progesterone receptor-mediated transcription. *Molecular Endocrinology (Baltimore, Md.)*, *21*(4), 843–856.

Arkin, M. R., & Wells, J. A. (2004). Small-molecule inhibitors of protein-protein interactions: progressing towards the dream. *Nature Reviews. Drug Discovery*, *3*(4), 301–317.

Arrowsmith, C. H., Bountra, C., Fish, P. V., Lee, K., & Schapira, M. (2012). Epigenetic protein families: a new frontier for drug discovery. *Nature Reviews. Drug Discovery*, *11*(5), 384–400.

Arts, J., King, P., Mariën, A., Floren, W., Beliën, A., Janssen, L., Pilatte, I., Roux, B., Decrane, L., Gilissen, R., Hickson, I., Vreys, V., Cox, E., Bol, K., Talloen, W., Goris,

I., Andries, L., Du Jardin, M., Janicot, M., Page, M., van Emelen, K., & Angibaud, P. (2009). JNJ-26481585, a novel "second-generation" oral histone deacetylase inhibitor, shows broad-spectrum preclinical antitumoral activity. *Clinical Cancer Research: An Official Journal of the American Association for Cancer Research*, *15*(22), 6841–6851.

Bachmann, J., Raue, A., Schilling, M., Böhm, M. E., Kreutz, C., Kaschek, D., Busch, H., Gretz, N., Lehmann, W. D., Timmer, J., & Klingmüller, U. (2011). Division of labor by dual feedback regulators controls JAK2/STAT5 signaling over broad ligand range. *Molecular Systems Biology*, *7*, 516.

Baeuerle, P. A., & Baltimore, D. (1988). I kappa B: a specific inhibitor of the NF-kappa B transcription factor. *Science (New York, N.Y.)*, *242*(4878), 540–546.

Bai, S., Ghoshal, K., Datta, J., Majumder, S., Yoon, S. O., & Jacob, S. T. (2005). DNA methyltransferase 3b regulates nerve growth factor-induced differentiation of PC12 cells by recruiting histone deacetylase 2. *Molecular and Cellular Biology*, *25*(2), 751–766.

Barillas-Mury, C., Han, Y. S., Seeley, D., & Kafatos, F. C. (1999). Anopheles gambiae Ag-STAT, a new insect member of the STAT family, is activated in response to bacterial infection. *The EMBO journal*, *18*(4), 959–967.

Basham, B., Sathe, M., Grein, J., McClanahan, T., D'Andrea, A., Lees, E., & Rascle, A. (2008). In vivo identification of novel STAT5 target genes. *Nucleic acids research*, *36*(11), 3802–3818.

Becker, S., Groner, B., & Müller, C. W. (1998). Three-dimensional structure of the Stat3beta homodimer bound to DNA. *Nature*, *394*(6689), 145–151.

Belkina, A. C., & Denis, G. V. (2012). BET domain co-regulators in obesity, inflammation and cancer. *Nature Reviews. Cancer*, *12*(7), 465–477.

Belkina, A. C., Nikolajczyk, B. S., & Denis, G. V. (2013). BET protein function is required for inflammation: Brd2 genetic disruption and BET inhibitor JQ1 impair mouse macrophage inflammatory responses. *Journal of Immunology (Baltimore, Md.: 1950)*, *190*(7), 3670–3678.

Belotserkovskaya, R., Oh, S., Bondarenko, V. A., Orphanides, G., Studitsky, V. M., & Reinberg, D. (2003). FACT facilitates transcription-dependent nucleosome alteration. *Science (New York, N.Y.)*, *301*(5636), 1090–1093.

Berger, A., Hoelbl-Kovacic, A., Bourgeais, J., Hoefling, L., Warsch, W., Grundschober, E., Uras, I. Z., Menzl, I., Putz, E. M., Hoermann, G., Schuster, C., Fajmann, S., Leitner, E., Kubicek, S., Moriggl, R., Gouilleux, F., & Sexl, V. (2013). PAK-dependent STAT5 serine phosphorylation is required for BCR-ABL-induced leukemogenesis. *Leukemia*.

Bernichtein, S., Touraine, P., & Goffin, V. (2010). New concepts in prolactin biology. *The Journal of Endocrinology*, *206*(1), 1–11.

Beuvink, I., Hess, D., Flotow, H., Hofsteenge, J., Groner, B., & Hynes, N. E. (2000). Stat5a serine phosphorylation. Serine 779 is constitutively phosphorylated in the mammary gland, and serine 725 phosphorylation influences prolactin-stimulated in vitro DNA binding activity. *The Journal of Biological Chemistry*, *275*(14), 10247–10255.

Boehm, M. E., Adlung, L., Schilling, M., Roth, S., Klingmüller, U., & Lehmann, W. D. (2014). Identification of Isoform-Specific Dynamics in Phosphorylation-Dependent STAT5 Dimerization by Quantitative Mass Spectrometry and Mathematical Modeling. *Journal of Proteome Research*.

Bolden, J. E., Peart, M. J., & Johnstone, R. W. (2006). Anticancer activities of histone deacetylase inhibitors. *Nature Reviews. Drug Discovery*, *5*(9), 769–784.

Boucheron, C., Dumon, S., Santos, S. C., Moriggl, R., Hennighausen, L., Gisselbrecht, S., & Gouilleux, F. (1998). A single amino acid in the DNA binding regions of STAT5a and STAT5b confers distinct DNA binding specificities. *The Journal of Biological Chemistry*, *273*(51), 33936–33941.

Bressi, J. C., Jennings, A. J., Skene, R., Wu, Y., Melkus, R., De Jong, R., O'Connell, S., Grimshaw, C. E., Navre, M., & Gangloff, A. R. (2010). Exploration of the HDAC2 foot pocket: Synthesis and SAR of substituted N-(2-aminophenyl)benzamides. *Bioorganic & Medicinal Chemistry Letters*, *20*(10), 3142–3145.

Brush, M. H., Guardiola, A., Connor, J. H., Yao, T.-P., & Shenolikar, S. (2004). Deactylase inhibitors disrupt cellular complexes containing protein phosphatases and deacetylases. *The Journal of Biological Chemistry*, *279*(9), 7685–7691.

Buchwald, P. (2010). Small-molecule protein-protein interaction inhibitors: therapeutic potential in light of molecular size, chemical space, and ligand binding efficiency considerations. *IUBMB life*, *62*(10), 724–731.

Burgess, A., Ruefli, A., Beamish, H., Warrener, R., Saunders, N., Johnstone, R., & Gabrielli, B. (2004). Histone deacetylase inhibitors specifically kill nonproliferating tumour cells. *Oncogene*, *23*(40), 6693–6701.

Catania, A., Iavarone, C., Carlomagno, S. M., & Chiariello, M. (2006). Selective transcription and cellular proliferation induced by PDGF require histone deacetylase activity. *Biochemical and biophysical research communications*, *343*(2), 544–554.

Chang, H.-M., Paulson, M., Holko, M., Rice, C. M., Williams, B. R. G., Marié, I., & Levy, D. E. (2004). Induction of interferon-stimulated gene expression and antiviral responses require protein deacetylase activity. *Proceedings of the National Academy of Sciences of the United States of America*, *101*(26), 9578–9583.

Chen, H., Lin, R. J., Xie, W., Wilpitz, D., & Evans, R. M. (1999). Regulation of hormone-induced histone hyperacetylation and gene activation via acetylation of an acetylase. *Cell*, *98*(5), 675–686.

Chen, J., Yu, W.-M., Bunting, K. D., & Qu, C.-K. (2004). A negative role of SHP-2 tyrosine phosphatase in growth factor-dependent hematopoietic cell survival. *Oncogene*, *23*(20), 3659–3669.

Chen, S., Bellew, C., Yao, X., Stefkova, J., Dipp, S., Saifudeen, Z., Bachvarov, D., & El-Dahr, S. S. (2011). Histone deacetylase (HDAC) activity is critical for embryonic kidney gene expression, growth, and differentiation. *The Journal of Biological Chemistry*, *286*(37), 32775–32789.

Chen, X., Vinkemeier, U., Zhao, Y., Jeruzalmi, D., Darnell, J. E., & Kuriyan, J. (1998). Crystal structure of a tyrosine phosphorylated STAT-1 dimer bound to DNA. *Cell*, *93*(5), 827–839.

Chen, X.-F., Kuryan, B., Kitada, T., Tran, N., Li, J.-Y., Kurdistani, S., Grunstein, M., Li, B., & Carey, M. (2012). The Rpd3 core complex is a chromatin stabilization module. *Current biology: CB*, *22*(1), 56–63.

Chen, Y., Dai, X., Haas, A. L., Wen, R., & Wang, D. (2006). Proteasome-dependent down-regulation of activated Stat5a in the nucleus. *Blood*, *108*(2), 566–574.

Cheng, Y., & Prusoff, W. H. (1973). Relationship between the inhibition constant (K1) and the concentration of inhibitor which causes 50 per cent inhibition (I50) of an enzymatic reaction. *Biochemical Pharmacology*, *22*(23), 3099–3108.

Chia, D. J., Subbian, E., Buck, T. M., Hwa, V., Rosenfeld, R. G., Skach, W. R., Shinde, U., & Rotwein, P. (2006). Aberrant folding of a mutant Stat5b causes growth hormone insensitivity and proteasomal dysfunction. *The Journal of Biological Chemistry*, *281*(10), 6552–6558.

Chida, D., Wakao, H., Yoshimura, A., & Miyajima, A. (1998). Transcriptional regulation of the beta-casein gene by cytokines: cross-talk between STAT5 and other signaling molecules. *Molecular Endocrinology (Baltimore, Md.)*, *12*(11), 1792–1806.

Chou, C. J., Herman, D., & Gottesfeld, J. M. (2008). Pimelic diphenylamide 106 is a slow, tight-binding inhibitor of class I histone deacetylases. *The Journal of Biological Chemistry*, *283*(51), 35402–35409.

Choudhary, C., Kumar, C., Gnad, F., Nielsen, M. L., Rehman, M., Walther, T. C., Olsen, J. V., & Mann, M. (2009). Lysine acetylation targets protein complexes and co-regulates major cellular functions. *Science (New York, N.Y.)*, *325*(5942), 834–840.

Chuikov, S., Kurash, J. K., Wilson, J. R., Xiao, B., Justin, N., Ivanov, G. S., McKinney, K., Tempst, P., Prives, C., Gamblin, S. J., Barlev, N. A., & Reinberg, D. (2004). Regulation of p53 activity through lysine methylation. *Nature*, *432*(7015), 353–360.

Côté, J., Quinn, J., Workman, J. L., & Peterson, C. L. (1994). Stimulation of GAL4 derivative binding to nucleosomal DNA by the yeast SWI/SNF complex. *Science (New York, N.Y.)*, *265*(5168), 53–60.

Crowley, T. E., Kaine, E. M., Yoshida, M., Nandi, A., & Wolgemuth, D. J. (2002). Reproductive cycle regulation of nuclear import, euchromatic localization, and association with components of Pol II mediator of a mammalian double-bromodomain protein. *Molecular Endocrinology (Baltimore, Md.)*, *16*(8), 1727–1737.

Daly, K., & Shirazi-Beechey, S. P. (2006). Microarray analysis of butyrate regulated genes in colonic epithelial cells. *DNA and cell biology*, *25*(1), 49–62.

Dangond, F., Hafler, D. A., Tong, J. K., Randall, J., Kojima, R., Utku, N., & Gullans, S. R. (1998). Differential display cloning of a novel human histone deacetylase (HDAC3) cDNA from PHA-activated immune cells. *Biochemical and Biophysical Research Communications*, *242*(3), 648–652.

Darkin-Rattray, S. J., Gurnett, A. M., Myers, R. W., Dulski, P. M., Crumley, T. M., Allocco, J. J., Cannova, C., Meinke, P. T., Colletti, S. L., Bednarek, M. A., Singh, S. B., Goetz, M. A., Dombrowski, A. W., Polishook, J. D., & Schmatz, D. M. (1996). Apicidin: a novel antiprotozoal agent that inhibits parasite histone deacetylase. *Proceedings of the National Academy of Sciences of the United States of America*, *93*(23), 13143–13147.

Darnell, J. E. (1997). Phosphotyrosine signaling and the single cell:metazoan boundary. *Proceedings of the National Academy of Sciences of the United States of America*, *94*(22), 11767–11769.

Dasgupta, T., Antony, J., Braithwaite, A. W., & Horsfield, J. A. (2016). HDAC8 Inhibition Blocks SMC3 Deacetylation and Delays Cell Cycle Progression Without Affecting Cohesin-Dependent Transcription in MCF7 Cancer Cells. *The Journal of Biological Chemistry*.

Decker, T., & Kovarik, P. (2000). Serine phosphorylation of STATs. *Oncogene*, *19*(21), 2628–2637.

Deckert, J., & Struhl, K. (2001). Histone acetylation at promoters is differentially affected by specific activators and repressors. *Molecular and Cellular Biology*, *21*(8), 2726–2735.

Dejligbjerg, M., Grauslund, M., Litman, T., Collins, L., Qian, X., Jeffers, M., Lichenstein, H., Jensen, P. B., & Sehested, M. (2008). Differential effects of class I isoform histone deacetylase depletion and enzymatic inhibition by belinostat or valproic acid in HeLa cells. *Molecular Cancer*, *7*, 70.

Delcuve, G. P., Khan, D. H., & Davie, J. R. (2012). Roles of histone deacetylases in epigenetic regulation: emerging paradigms from studies with inhibitors. *Clinical Epigenetics*, *4*(1), 5.

Denis, G. V., McComb, M. E., Faller, D. V., Sinha, A., Romesser, P. B., & Costello, C. E. (2006). Identification of transcription complexes that contain the double bromodomain protein Brd2 and chromatin remodeling machines. *Journal of Proteome Research*, *5*(3), 502–511.

Denis, G. V., Vaziri, C., Guo, N., & Faller, D. V. (2000). RING3 kinase transactivates promoters of cell cycle regulatory genes through E2f. *Cell Growth & Differentiation: The Molecular Biology Journal of the American Association for Cancer Research*, *11*(8), 417–424.

DesJarlais, R., & Tummino, P. J. (2016). Role of Histone-Modifying Enzymes and Their Complexes in Regulation of Chromatin Biology. *Biochemistry*.

Dey, A., Chitsaz, F., Abbasi, A., Misteli, T., & Ozato, K. (2003). The double bromodomain protein Brd4 binds to acetylated chromatin during interphase and mitosis. *Proceedings of the National Academy of Sciences of the United States of America*, *100*(15), 8758–8763.

Di Cerbo, V., Mohn, F., Ryan, D. P., Montellier, E., Kacem, S., Tropberger, P., Kallis, E., Holzner, M., Hoerner, L., Feldmann, A., Richter, F. M., Bannister, A. J., Mittler, G., Michaelis, J., Khochbin, S., Feil, R., Schuebeler, D., Owen-Hughes, T., Daujat, S., & Schneider, R. (2014). Acetylation of histone H3 at lysine 64 regulates nucleosome dynamics and facilitates transcription. *eLife*, *3*, e01632.

Di Giorgio, E., Gagliostro, E., & Brancolini, C. (2015). Selective class IIa HDAC inhibitors: myth or reality. *Cellular and molecular life sciences: CMLS*, *72*(1), 73–86.

Dijkers, P. F., van Dijk, T. B., de Groot, R. P., Raaijmakers, J. A., Lammers, J. W., Koenderman, L., & Coffer, P. J. (1999). Regulation and function of protein kinase B and MAP kinase activation by the IL-5/GM-CSF/IL-3 receptor. *Oncogene*, *18*(22), 3334–3342.

Dovey, O. M., Foster, C. T., Conte, N., Edwards, S. A., Edwards, J. M., Singh, R., Vassiliou, G., Bradley, A., & Cowley, S. M. (2013). Histone deacetylase 1 and 2 are essential for normal T-cell development and genomic stability in mice. *Blood*, *121*(8), 1335–1344.

Duque-Afonso, J., Yalcin, A., Berg, T., Abdelkarim, M., Heidenreich, O., & Lübbert, M. (2011). The HDAC class I-specific inhibitor entinostat (MS-275) effectively relieves epigenetic silencing of the LAT2 gene mediated by AML1/ETO. *Oncogene*, *30*(27), 3062–3072.

Ehret, G. B., Reichenbach, P., Schindler, U., Horvath, C. M., Fritz, S., Nabholz, M., & Bucher, P. (2001). DNA binding specificity of different STAT proteins. Comparison of in vitro specificity with natural target sites. *The Journal of Biological Chemistry*, *276*(9), 6675–6688.

Ellis, D. J. P., Lawman, Z. K., & Bonham, K. (2008). Histone acetylation is not an accurate predictor of gene expression following treatment with histone deacetylase inhibitors. *Biochemical and Biophysical Research Communications*, *367*(3), 656–662.

Ellis, L., Hammers, H., & Pili, R. (2009). Targeting tumor angiogenesis with histone deacetylase inhibitors. *Cancer Letters*, *280*(2), 145–153.

Elumalai, N., Berg, A., Natarajan, K., Scharow, A., & Berg, T. (2015). Nanomolar Inhibitors of the Transcription Factor STAT5b with High Selectivity over STAT5a. *Angewandte Chemie (International Ed. in English)*.

Endo, T. A., Masuhara, M., Yokouchi, M., Suzuki, R., Sakamoto, H., Mitsui, K., Matsumoto, A., Tanimura, S., Ohtsubo, M., Misawa, H., Miyazaki, T., Leonor, N., Taniguchi, T., Fujita, T., Kanakura, Y., Komiya, S., & Yoshimura, A. (1997). A new protein containing an SH2 domain that inhibits JAK kinases. *Nature*, *387*(6636), 921–924.

Engblom, D., Kornfeld, J.-W., Schwake, L., Tronche, F., Reimann, A., Beug, H., Hennighausen, L., Moriggl, R., & Schütz, G. (2007). Direct glucocorticoid receptor-Stat5 interaction in hepatocytes controls body size and maturation-related gene expression. *Genes & Development*, *21*(10), 1157–1162.

Epling-Burnette, P. K., Garcia, R., Bai, F., Ismail, S., Loughran, T. P., Djeu, J. Y., Jove, R., & Wei, S. (2002). Carboxy-terminal truncated STAT5 is induced by interleukin-2 and GM-CSF in human neutrophils. *Cellular Immunology*, *217*(1-2), 1–11.

Estiu, G., West, N., Mazitschek, R., Greenberg, E., Bradner, J. E., & Wiest, O. (2010). On the inhibition of histone deacetylase 8. *Bioorganic & Medicinal Chemistry*, *18*(11), 4103–4110.

Fass, D. M., Shah, R., Ghosh, B., Hennig, K., Norton, S., Zhao, W.-N., Reis, S. A., Klein, P. S., Mazitschek, R., Maglathlin, R. L., Lewis, T. A., & Haggarty, S. J. (2010). Effect of Inhibiting Histone Deacetylase with Short-Chain Carboxylic Acids and Their Hydroxamic Acid Analogs on Vertebrate Development and Neuronal Chromatin. *ACS medicinal chemistry letters*, *2*(1), 39–42.

Felisbino, M. B., Gatti, M. S. V., & Mello, M. L. S. (2014). Changes in chromatin structure in NIH 3t3 cells induced by valproic acid and trichostatin A. *Journal of Cellular Biochemistry*, *115*(11), 1937–1947.

Ferbeyre, G., & Moriggl, R. (2011). The role of Stat5 transcription factors as tumor suppressors or oncogenes. *Biochimica Et Biophysica Acta*, *1815*(1), 104–114.

Filippakopoulos, P., Qi, J., Picaud, S., Shen, Y., Smith, W. B., Fedorov, O., Morse, E. M., Keates, T., Hickman, T. T., Felletar, I., Philpott, M., Munro, S., McKeown, M. R., Wang, Y., Christie, A. L., West, N., Cameron, M. J., Schwartz, B., Heightman, T. D., La Thangue, N., French, C. A., Wiest, O., Kung, A. L., Knapp, S., & Bradner, J. E. (2010). Selective inhibition of BET bromodomains. *Nature*, *468*(7327), 1067–1073.

Fischle, W., Dequiedt, F., Fillion, M., Hendzel, M. J., Voelter, W., & Verdin, E. (2001). Human HDAC7 histone deacetylase activity is associated with HDAC3 in vivo. *The Journal of Biological Chemistry*, *276*(38), 35826–35835.

Fischle, W., Dequiedt, F., Hendzel, M. J., Guenther, M. G., Lazar, M. A., Voelter, W., & Verdin, E. (2002). Enzymatic Activity Associated with Class II HDACs Is Dependent on a Multiprotein Complex Containing HDAC3 and SMRT/N-CoR. *Molecular Cell*, *9*(1), 45–57.

Foss, F., Horwitz, S., Pro, B., Prince, H. M., Sokol, L., Balser, B., Wolfson, J., & Coiffier, B. (2016). Romidepsin for the treatment of relapsed/refractory peripheral T cell lymphoma: prolonged stable disease provides clinical benefits for patients in the pivotal trial. *Journal of Hematology & Oncology*, *9*, 22.

Fournel, M., Bonfils, C., Hou, Y., Yan, P. T., Trachy-Bourget, M.-C., Kalita, A., Liu, J., Lu, A.-H., Zhou, N. Z., Robert, M.-F., Gillespie, J., Wang, J. J., Ste-Croix, H., Rahil, J., Lefebvre, S., Moradei, O., Delorme, D., Macleod, A. R., Besterman, J. M., & Li, Z. (2008). MGCD0103, a novel isotype-selective histone deacetylase inhibitor, has broad spectrum antitumor activity in vitro and in vivo. *Molecular Cancer Therapeutics*, *7*(4), 759–768.

Frank, C. L., Manandhar, D., Gordân, R., & Crawford, G. E. (2016). HDAC inhibitors cause site-specific chromatin remodeling at PU.1-bound enhancers in K562 cells. *Epigenetics & Chromatin*, *9*, 15.

Frasor, J., Park, K., Byers, M., Telleria, C., Kitamura, T., Yu-Lee, L. Y., Djiane, J., Park-Sarge, O. K., & Gibori, G. (2001). Differential roles for signal transducers and activators of transcription 5a and 5b in PRL stimulation of ERalpha and ERbeta transcription. *Molecular Endocrinology (Baltimore, Md.)*, *15*(12), 2172–2181.

Frye, R. A. (2000). Phylogenetic classification of prokaryotic and eukaryotic Sir2-like proteins. *Biochemical and Biophysical Research Communications*, *273*(2), 793–798.

Funakoshi-Tago, M., Tago, K., Abe, M., Sonoda, Y., & Kasahara, T. (2010). STAT5 activation is critical for the transformation mediated by myeloproliferative disorder-associated JAK2 V617f mutant. *The Journal of Biological Chemistry*, *285*(8), 5296–5307.

Galm, O., Yoshikawa, H., Esteller, M., Osieka, R., & Herman, J. G. (2003). SOCS-1, a negative regulator of cytokine signaling, is frequently silenced by methylation in multiple myeloma. *Blood*, *101*(7), 2784–2788.

Gaymes, T. J., Padua, R. A., Pla, M., Orr, S., Omidvar, N., Chomienne, C., Mufti, G. J., & Rassool, F. V. (2006). Histone deacetylase inhibitors (HDI) cause DNA damage in leukemia cells: a mechanism for leukemia-specific HDI-dependent apoptosis? *Molecular cancer research: MCR*, *4*(8), 563–573.

Gesbert, F., & Griffin, J. D. (2000). Bcr/Abl activates transcription of the Bcl-X gene through STAT5. *Blood*, *96*(6), 2269–2276.

Ghari, F., Quirke, A.-M., Munro, S., Kawalkowska, J., Picaud, S., McGouran, J., Subramanian, V., Muth, A., Williams, R., Kessler, B., Thompson, P. R., Fillipakopoulos, P., Knapp, S., Venables, P. J., & La Thangue, N. B. (2016). Citrullination-acetylation interplay guides E2f-1 activity during the inflammatory response. *Science Advances*, *2*(2), e1501257.

Ghislain, J. J., Wong, T., Nguyen, M., & Fish, E. N. (2001). The interferon-inducible Stat2:Stat1 heterodimer preferentially binds in vitro to a consensus element found

in the promoters of a subset of interferon-stimulated genes. *Journal of Interferon & Cytokine Research: The Official Journal of the International Society for Interferon and Cytokine Research*, *21*(6), 379–388.

Ginter, T., Bier, C., Knauer, S. K., Sughra, K., Hildebrand, D., Münz, T., Liebe, T., Heller, R., Henke, A., Stauber, R. H., Reichardt, W., Schmid, J. A., Kubatzky, K. F., Heinzel, T., & Krämer, O. H. (2012). Histone deacetylase inhibitors block IFNγ-induced STAT1 phosphorylation. *Cellular Signalling*, *24*(7), 1453–1460.

Glaser, K. B., Staver, M. J., Waring, J. F., Stender, J., Ulrich, R. G., & Davidsen, S. K. (2003). Gene expression profiling of multiple histone deacetylase (HDAC) inhibitors: defining a common gene set produced by HDAC inhibition in T24 and MDA carcinoma cell lines. *Molecular Cancer Therapeutics*, *2*(2), 151–163.

Gottlicher, M., Minucci, S., Zhu, P., Kramer, O. H., Schimpf, A., Giavara, S., Sleeman, J. P., Lo Coco, F., Nervi, C., Pelicci, P. G., & Heinzel, T. (2001). Valproic acid defines a novel class of HDAC inhibitors inducing differentiation of transformed cells. *The EMBO Journal*, *20*(24), 6969–6978.

Grant, S., Easley, C., & Kirkpatrick, P. (2007). Vorinostat. *Nature Reviews. Drug Discovery*, *6*(1), 21–22.

Greer, C. B., Tanaka, Y., Kim, Y. J., Xie, P., Zhang, M. Q., Park, I.-H., & Kim, T. H. (2015). Histone Deacetylases Positively Regulate Transcription through the Elongation Machinery. *Cell Reports*, *13*(7), 1444–1455.

Gregoretti, I. V., Lee, Y.-M., & Goodson, H. V. (2004). Molecular evolution of the histone deacetylase family: functional implications of phylogenetic analysis. *Journal of Molecular Biology*, *338*(1), 17–31.

Grewal, S. I. S., & Moazed, D. (2003). Heterochromatin and epigenetic control of gene expression. *Science (New York, N.Y.)*, *301*(5634), 798–802.

Grimley, P. M., Dong, F., & Rui, H. (1999). Stat5a and Stat5b: fraternal twins of signal transduction and transcriptional activation. *Cytokine & Growth Factor Reviews*, *10*(2), 131–157.

Groner, B., & Gouilleux, F. (1995). Prolactin-mediated gene activation in mammary epithelial cells. *Current Opinion in Genetics & Development*, *5*(5), 587–594.

Grönholm, J., Vanhatupa, S., Ungureanu, D., Väliaho, J., Laitinen, T., Valjakka, J., & Silvennoinen, O. (2012). Structure-function analysis indicates that sumoylation modulates DNA-binding activity of STAT1. *BMC biochemistry*, *13*, 20.

Guan, J.-S., Haggarty, S. J., Giacometti, E., Dannenberg, J.-H., Joseph, N., Gao, J., Nieland, T. J. F., Zhou, Y., Wang, X., Mazitschek, R., Bradner, J. E., DePinho, R. A., Jaenisch, R., & Tsai, L.-H. (2009). HDAC2 negatively regulates memory formation and synaptic plasticity. *Nature*, *459*(7243), 55–60.

Guccione, E., Martinato, F., Finocchiaro, G., Luzi, L., Tizzoni, L., Dall' Olio, V., Zardo, G., Nervi, C., Bernard, L., & Amati, B. (2006). Myc-binding-site recognition in the human genome is determined by chromatin context. *Nature Cell Biology*, *8*(7), 764–770.

Gupta, M., Han, J. J., Stenson, M., Wellik, L., & Witzig, T. E. (2012). Regulation of STAT3 by histone deacetylase-3 in diffuse large B-cell lymphoma: implications for therapy. *Leukemia*, *26*(6), 1356–1364.

Gurvich, N., Tsygankova, O. M., Meinkoth, J. L., & Klein, P. S. (2004). Histone Deacetylase Is a Target of Valproic Acid-Mediated Cellular Differentiation. *Cancer Research*, *64*(3), 1079 –1086.

Gyuris, A., Donovan, D. J., Seymour, K. A., Lovasco, L. A., Smilowitz, N. R., Halperin, A. L. P., Klysik, J. E., & Freiman, R. N. (2009). The chromatin-targeting protein Brd2 is required for neural tube closure and embryogenesis. *Biochimica Et Biophysica Acta*, *1789*(5), 413–421.

Haan, C., Kreis, S., Margue, C., & Behrmann, I. (2006). Jaks and cytokine receptors–an intimate relationship. *Biochemical Pharmacology*, *72*(11), 1538–1546.

Hakami, N. Y., Dusting, G. J., & Peshavariya, H. M. (2016). Trichostatin A, a histone deacetylase inhibitor suppresses NADPH Oxidase 4-Derived Redox Signalling and Angiogenesis. *Journal of Cellular and Molecular Medicine*.

Halsall, J. A., Turan, N., Wiersma, M., & Turner, B. M. (2015). Cells adapt to the epigenomic disruption caused by histone deacetylase inhibitors through a coordinated, chromatin-mediated transcriptional response. *Epigenetics & Chromatin*, *8*, 29.

Han, J. W., Ahn, S. H., Park, S. H., Wang, S. Y., Bae, G. U., Seo, D. W., Kwon, H. K., Hong, S., Lee, H. Y., Lee, Y. W., & Lee, H. W. (2000). Apicidin, a histone deacetylase inhibitor, inhibits proliferation of tumor cells via induction of p21waf1/Cip1 and gelsolin. *Cancer Research*, *60*(21), 6068–6074.

Han, M., & Grunstein, M. (1988). Nucleosome loss activates yeast downstream promoters in vivo. *Cell*, *55*(6), 1137–1145.

Han, R.-F., Li, K., Yang, Z.-S., Chen, Z.-G., & Yang, W.-C. (2014). Trichostatin A induces mesenchymal-like morphological change and gene expression but inhibits migration and colony formation in human cancer cells. *Molecular Medicine Reports*, *10*(6), 3211–3216.

Hebbes, T. R., Thorne, A. W., & Crane-Robinson, C. (1988). A direct link between core histone acetylation and transcriptionally active chromatin. *The EMBO journal*, *7*(5), 1395–1402.

Hess-Stumpp, H., Bracker, T. U., Henderson, D., & Politz, O. (2007). MS-275, a potent orally available inhibitor of histone deacetylases–the development of an anticancer agent. *The International Journal of Biochemistry & Cell Biology*, *39*(7-8), 1388–1405.

Hill, C. S., & Treisman, R. (1995). Differential activation of c-fos promoter elements by serum, lysophosphatidic acid, G proteins and polypeptide growth factors. *The EMBO journal*, *14*(20), 5037–5047.

Hirschhorn, J. N., Brown, S. A., Clark, C. D., & Winston, F. (1992). Evidence that SNF2/SWI2 and SNF5 activate transcription in yeast by altering chromatin structure. *Genes & Development*, *6*(12A), 2288–2298.

Hnilicová, J., Hozeifi, S., Stejskalová, E., Dušková, E., Poser, I., Humpolíčková, J., Hof, M., & Staněk, D. (2013). The C-terminal domain of Brd2 is important for chromatin interaction and regulation of transcription and alternative splicing. *Molecular Biology of the Cell*, *24*(22), 3557–3568.

Hodge, C., Liao, J., Stofega, M., Guan, K., Carter-Su, C., & Schwartz, J. (1998). Growth hormone stimulates phosphorylation and activation of elk-1 and expression of c-fos, egr-1, and junB through activation of extracellular signal-regulated kinases 1 and 2. *The Journal of Biological Chemistry*, *273*(47), 31327–31336.

Hoelbl, A., Schuster, C., Kovacic, B., Zhu, B., Wickre, M., Hoelzl, M. A., Fajmann, S., Grebien, F., Warsch, W., Stengl, G., Hennighausen, L., Poli, V., Beug, H., Moriggl, R., & Sexl, V. (2010). Stat5 is indispensable for the maintenance of bcr/abl-positive leukaemia. *EMBO molecular medicine*, *2*(3), 98–110.

Holmqvist, P.-H., & Mannervik, M. (2013). Genomic occupancy of the transcriptional co-activators p300 and CBP. *Transcription*, *4*(1), 18–23.

Hornbeck, P. V., Zhang, B., Murray, B., Kornhauser, J. M., Latham, V., & Skrzypek, E. (2015). PhosphoSitePlus, 2014: mutations, PTMs and recalibrations. *Nucleic Acids Research*, *43*(Database issue), D512–520.

Hou, J., Schindler, U., Henzel, W. J., Ho, T. C., Brasseur, M., & McKnight, S. L. (1994). An interleukin-4-induced transcription factor: IL-4 Stat. *Science (New York, N.Y.)*, *265*(5179), 1701–1706.

Hou, T., Ray, S., Lee, C., & Brasier, A. R. (2008). The STAT3 NH2-terminal domain stabilizes enhanceosome assembly by interacting with the p300 bromodomain. *The Journal of Biological Chemistry*, *283*(45), 30725–30734.

Hou, X. S., Melnick, M. B., & Perrimon, N. (1996). Marelle acts downstream of the Drosophila HOP/JAK kinase and encodes a protein similar to the mammalian STATs. *Cell*, *84*(3), 411–419.

Houzelstein, D., Bullock, S. L., Lynch, D. E., Grigorieva, E. F., Wilson, V. A., & Beddington, R. S. P. (2002). Growth and early postimplantation defects in mice deficient for the bromodomain-containing protein Brd4. *Molecular and Cellular Biology*, *22*(11), 3794–3802.

Howitz, K. T., Bitterman, K. J., Cohen, H. Y., Lamming, D. W., Lavu, S., Wood, J. G., Zipkin, R. E., Chung, P., Kisielewski, A., Zhang, L.-L., Scherer, B., & Sinclair, D. A. (2003). Small molecule activators of sirtuins extend Saccharomyces cerevisiae lifespan. *Nature*, *425*(6954), 191–196.

Hsu, W. W., Wu, B., & Liu, W. R. (2016). Sirtuins 1 and 2 Are Universal Histone Deacetylases. *ACS chemical biology*, *11*(3), 792–799.

Hu, E., Dul, E., Sung, C.-M., Chen, Z., Kirkpatrick, R., Zhang, G.-F., Johanson, K., Liu, R., Lago, A., Hofmann, G., Macarron, R., de los Frailes, M., Perez, P., Krawiec, J., Winkler, J., & Jaye, M. (2003). Identification of novel isoform-selective inhibitors within class I histone deacetylases. *The Journal of Pharmacology and Experimental Therapeutics*, *307*(2), 720–728.

Huang, B. H., Laban, M., Leung, C. H.-W., Lee, L., Lee, C. K., Salto-Tellez, M., Raju, G. C., & Hooi, S. C. (2005). Inhibition of histone deacetylase 2 increases apoptosis and p21cip1/WAF1 expression, independent of histone deacetylase 1. *Cell Death and Differentiation*, *12*(4), 395–404.

Hull, E. E., Montgomery, M. R., & Leyva, K. J. (2016). HDAC Inhibitors as Epigenetic Regulators of the Immune System: Impacts on Cancer Therapy and Inflammatory Diseases. *BioMed Research International*, *2016*, 8797206.

Irie-Sasaki, J., Sasaki, T., Matsumoto, W., Opavsky, A., Cheng, M., Welstead, G., Griffiths, E., Krawczyk, C., Richardson, C. D., Aitken, K., Iscove, N., Koretzky, G., Johnson, P., Liu, P., Rothstein, D. M., & Penninger, J. M. (2001). CD45 is a JAK phosphatase and negatively regulates cytokine receptor signalling. *Nature*, *409*(6818), 349–354.

Jacobs, S. A., & Khorasanizadeh, S. (2002). Structure of HP1 chromodomain bound to a lysine 9-methylated histone H3 tail. *Science (New York, N.Y.)*, *295*(5562), 2080–2083.

Jacobson, R. H., Ladurner, A. G., King, D. S., & Tjian, R. (2000). Structure and function of a human TAFII250 double bromodomain module. *Science (New York, N.Y.)*, *288*(5470), 1422–1425.

Jenuwein, T., & Allis, C. D. (2001). Translating the histone code. *Science (New York, N.Y.)*, *293*(5532), 1074–1080.

Jeon, H. W., & Lee, Y. M. (2010). Inhibition of histone deacetylase attenuates hypoxia-induced migration and invasion of cancer cells via the restoration of RECK expression. *Molecular Cancer Therapeutics*, *9*(5), 1361–1370.

Ji, Q., Hu, H., Yang, F., Yuan, J., Yang, Y., Jiang, L., Qian, Y., Jiang, B., Zou, Y., Wang, Y., Shao, C., & Gong, Y. (2014). CRL4b interacts with and coordinates the SIN3a-HDAC complex to repress CDKN1a and drive cell cycle progression. *Journal of Cell Science*, *127*(Pt 21), 4679–4691.

Jiang, Y. W., Veschambre, P., Erdjument-Bromage, H., Tempst, P., Conaway, J. W., Conaway, R. C., & Kornberg, R. D. (1998). Mammalian mediator of transcriptional regulation and its possible role as an end-point of signal transduction pathways. *Proceedings of the National Academy of Sciences of the United States of America*, *95*(15), 8538–8543.

Jobst, B., Weigl, J., Michl, C., Vivarelli, F., Pinz, S., Amslinger, S., & Rascle, A. (2016). Inhibition of interleukin-3- and interferon- α-induced JAK/STAT signaling by the synthetic α-X-2',3,4,4'-tetramethoxychalcones α-Br-TMC and α-CF3-TMC. *Biological Chemistry*, *397*(11), 1187–1204.

John, S., Vinkemeier, U., Soldaini, E., Darnell, J. E., & Leonard, W. J. (1999). The significance of tetramerization in promoter recruitment by Stat5. *Molecular and Cellular Biology*, *19*(3), 1910–1918.

Johnson, K. J., Peck, A. R., Liu, C., Tran, T. H., Utama, F. E., Sjolund, A. B., Schaber, J. D., Witkiewicz, A. K., & Rui, H. (2010). PTP1b suppresses prolactin activation of Stat5 in breast cancer cells. *The American Journal of Pathology*, *177*(6), 2971–2983.

Jurkin, J., Zupkovitz, G., Lagger, S., Grausenburger, R., Hagelkruys, A., Kenner, L., & Seiser, C. (2011). Distinct and redundant functions of histone deacetylases HDAC1 and HDAC2 in proliferation and tumorigenesis. *Cell Cycle (Georgetown, Tex.)*, *10*(3), 406–412.

Kaeberlein, M., McDonagh, T., Heltweg, B., Hixon, J., Westman, E. A., Caldwell, S. D., Napper, A., Curtis, R., DiStefano, P. S., Fields, S., Bedalov, A., & Kennedy, B. K. (2005). Substrate-specific activation of sirtuins by resveratrol. *The Journal of Biological Chemistry*, *280*(17), 17038–17045.

Kakidani, H., & Ptashne, M. (1988). GAL4 activates gene expression in mammalian cells. *Cell*, *52*(2), 161–167.

Kanai, T., Seki, S., Jenks, J. A., Kohli, A., Kawli, T., Martin, D. P., Snyder, M., Bacchetta, R., & Nadeau, K. C. (2014). Identification of STAT5a and STAT5b target genes in human T cells. *PloS One*, *9*(1), e86790.

Kang, X.-C., Chen, M.-L., Yang, F., Gao, B.-Q., Yang, Q.-H., Zheng, W.-W., & Hao, S. (2016). Promoter methylation and expression of SOCS-1 affect clinical outcome and epithelial-mesenchymal transition in colorectal cancer. *Biomedicine & Pharmacotherapy = Biomédecine & Pharmacothérapie*, *80*, 23–29.

Kanno, T., Kanno, Y., Siegel, R. M., Jang, M. K., Lenardo, M. J., & Ozato, K. (2004). Selective recognition of acetylated histones by bromodomain proteins visualized in living cells. *Molecular Cell*, *13*(1), 33–43.

Kaplan, N., Moore, I. K., Fondufe-Mittendorf, Y., Gossett, A. J., Tillo, D., Field, Y., LeProust, E. M., Hughes, T. R., Lieb, J. D., Widom, J., & Segal, E. (2009). The DNA-encoded nucleosome organization of a eukaryotic genome. *Nature*, *458*(7236), 362–366.

Kasten, M., Szerlong, H., Erdjument-Bromage, H., Tempst, P., Werner, M., & Cairns, B. R. (2004). Tandem bromodomains in the chromatin remodeler RSC recognize acetylated histone H3 Lys14. *The EMBO journal*, *23*(6), 1348–1359.

Kawata, T., Shevchenko, A., Fukuzawa, M., Jermyn, K. A., Totty, N. F., Zhukovskaya, N. V., Sterling, A. E., Mann, M., & Williams, J. G. (1997). SH2 signaling in a lower eukaryote: a STAT protein that regulates stalk cell differentiation in dictyostelium. *Cell*, *89*(6), 909–916.

Kazansky, A. V., Spencer, D. M., & Greenberg, N. M. (2003). Activation of signal transducer and activator of transcription 5 is required for progression of autochthonous prostate cancer: evidence from the transgenic adenocarcinoma of the mouse prostate system. *Cancer Research*, *63*(24), 8757–8762.

Kelly, R. D. W., & Cowley, S. M. (2013). The physiological roles of histone deacetylase (HDAC) 1 and 2: complex co-stars with multiple leading parts. *Biochemical Society Transactions*, *41*(3), 741–749.

Khan, N., Jeffers, M., Kumar, S., Hackett, C., Boldog, F., Khramtsov, N., Qian, X., Mills, E., Berghs, S. C., Carey, N., Finn, P. W., Collins, L. S., Tumber, A., Ritchie, J. W., Jensen, P. B., Lichenstein, H. S., & Sehested, M. (2008). Determination of the class and isoform selectivity of small-molecule histone deacetylase inhibitors. *The Biochemical Journal*, *409*(2), 581–589.

Kiernan, R., Brès, V., Ng, R. W. M., Coudart, M.-P., El Messaoudi, S., Sardet, C., Jin, D.-Y., Emiliani, S., & Benkirane, M. (2003). Post-activation turn-off of NF-kappa B-dependent transcription is regulated by acetylation of p65. *The Journal of Biological Chemistry*, *278*(4), 2758–2766.

Kim, M. S., Kwon, H. J., Lee, Y. M., Baek, J. H., Jang, J. E., Lee, S. W., Moon, E. J., Kim, H. S., Lee, S. K., Chung, H. Y., Kim, C. W., & Kim, K. W. (2001). Histone deacetylases induce angiogenesis by negative regulation of tumor suppressor genes. *Nature Medicine*, *7*(4), 437–443.

Kim, T. H., Kim, H. S., Kang, Y. J., Yoon, S., Lee, J., Choi, W. S., Jung, J. H., & Kim, H. S. (2015). Psammaplin A induces Sirtuin 1-dependent autophagic cell death in doxorubicin-resistant MCF-7/adr human breast cancer cells and xenografts. *Biochimica Et Biophysica Acta*, *1850*(2), 401–410.

Klampfer, L., Huang, J., Swaby, L.-A., & Augenlicht, L. (2004). Requirement of histone deacetylase activity for signaling by STAT1. *The Journal of Biological Chemistry*, *279*(29), 30358–30368.

Klingmüller, U., Lorenz, U., Cantley, L. C., Neel, B. G., & Lodish, H. F. (1995). Specific recruitment of SH-PTP1 to the erythropoietin receptor causes inactivation of JAK2 and termination of proliferative signals. *Cell*, *80*(5), 729–738.

Kontro, M., Kuusanmäki, H., Eldfors, S., Burmeister, T., Andersson, E. I., Bruserud, O., Brümmendorf, T. H., Edgren, H., Gjertsen, B. T., Itälä-Remes, M., Lagström, S., Lohi, O., Lundán, T., Martí, J. M. L., Majumder, M. M., Parsons, A., Pemovska, T., Rajala, H., Vettenranta, K., Kallioniemi, O., Mustjoki, S., Porkka, K., & Heckman, C. A. (2014). Novel activating STAT5b mutations as putative drivers of T-cell acute lymphoblastic leukemia. *Leukemia*, *28*(8), 1738–1742.

Koppikar, P., Lui, V. W. Y., Man, D., Xi, S., Chai, R. L., Nelson, E., Tobey, A. B. J., & Grandis, J. R. (2008). Constitutive activation of signal transducer and activator of transcription 5 contributes to tumor growth, epithelial-mesenchymal transition, and resistance to epidermal growth factor receptor targeting. *Clinical Cancer Research: An Official Journal of the American Association for Cancer Research*, *14*(23), 7682–7690.

Kosan, C., Ginter, T., Heinzel, T., & Krämer, O. H. (2013). STAT5 acetylation: Mechanisms and consequences for immunological control and leukemogenesis. *JAK-STAT*, *2*(4), e26102.

Krämer, O. H. (2009). HDAC2: a critical factor in health and disease. *Trends in Pharmacological Sciences*, *30*(12), 647–655.

Krämer, O. H., Baus, D., Knauer, S. K., Stein, S., Jäger, E., Stauber, R. H., Grez, M., Pfitzner, E., & Heinzel, T. (2006). Acetylation of Stat1 modulates NF-kappaB activity. *Genes & Development*, *20*(4), 473–485.

Krämer, O. H., & Heinzel, T. (2010). Phosphorylation-acetylation switch in the regulation of STAT1 signaling. *Molecular and Cellular Endocrinology*, *315*(1-2), 40–48.

Krämer, O. H., Knauer, S. K., Greiner, G., Jandt, E., Reichardt, S., Gührs, K.-H., Stauber, R. H., Böhmer, F. D., & Heinzel, T. (2009). A phosphorylation-acetylation switch regulates STAT1 signaling. *Genes & Development*, *23*(2), 223–235.

Kurdistani, S. K., Tavazoie, S., & Grunstein, M. (2004). Mapping global histone acetylation patterns to gene expression. *Cell*, *117*(6), 721–733.

Lagger, G., O'Carroll, D., Rembold, M., Khier, H., Tischler, J., Weitzer, G., Schuettengruber, B., Hauser, C., Brunmeir, R., Jenuwein, T., & Seiser, C. (2002). Essential function of histone deacetylase 1 in proliferation control and CDK inhibitor repression. *The EMBO journal*, *21*(11), 2672–2681.

Lahm, A., Paolini, C., Pallaoro, M., Nardi, M. C., Jones, P., Neddermann, P., Sambucini, S., Bottomley, M. J., Lo Surdo, P., Carfí, A., Koch, U., De Francesco, R., Steinkühler, C., & Gallinari, P. (2007). Unraveling the hidden catalytic activity of vertebrate class IIa histone deacetylases. *Proceedings of the National Academy of Sciences of the United States of America*, *104*(44), 17335–17340.

Längst, G., & Becker, P. B. (2004). Nucleosome remodeling: one mechanism, many phenomena? *Biochimica Et Biophysica Acta*, *1677*(1-3), 58–63.

Lara, E., Mai, A., Calvanese, V., Altucci, L., Lopez-Nieva, P., Martinez-Chantar, M. L., Varela-Rey, M., Rotili, D., Nebbioso, A., Ropero, S., Montoya, G., Oyarzabal, J., Velasco, S., Serrano, M., Witt, M., Villar-Garea, A., Imhof, A., Inhof, A., Mato, J. M., Esteller, M., & Fraga, M. F. (2009). Salermide, a Sirtuin inhibitor with a strong cancer-specific proapoptotic effect. *Oncogene*, *28*(6), 781–791.

Laubach, J. P., Moreau, P., San-Miguel, J. F., & Richardson, P. G. (2015). Panobinostat for the Treatment of Multiple Myeloma. *Clinical Cancer Research: An Official Journal of the American Association for Cancer Research*, *21*(21), 4767–4773.

Lee, H.-Z., Kwitkowski, V. E., Del Valle, P. L., Ricci, M. S., Saber, H., Habtemariam, B. A., Bullock, J., Bloomquist, E., Li Shen, Y., Chen, X.-H., Brown, J., Mehrotra, N., Dorff, S., Charlab, R., Kane, R. C., Kaminskas, E., Justice, R., Farrell, A. T., & Pazdur, R. (2015). FDA Approval: Belinostat for the Treatment of Patients with Relapsed or Refractory Peripheral T-cell Lymphoma. *Clinical Cancer Research: An Official Journal of the American Association for Cancer Research*, *21*(12), 2666–2670.

Leong, P. L., Xi, S., Drenning, S. D., Dyer, K. F., Wentzel, A. L., Lerner, E. C., Smithgall, T. E., & Grandis, J. R. (2002). Differential function of STAT5 isoforms in head and neck cancer growth control. *Oncogene*, *21*(18), 2846–2853.

LeRoy, G., Rickards, B., & Flint, S. J. (2008). The double bromodomain proteins Brd2 and Brd3 couple histone acetylation to transcription. *Molecular Cell*, *30*(1), 51–60.

Li, G., Wang, Z., Zhang, Y., Kang, Z., Haviernikova, E., Cui, Y., Hennighausen, L., Moriggl, R., Wang, D., Tse, W., & Bunting, K. D. (2007). STAT5 requires the N-domain to maintain hematopoietic stem cell repopulating function and appropriate lymphoid-myeloid lineage output. *Experimental Hematology*, *35*(11), 1684–1694.

Li, H., Ahonen, T. J., Alanen, K., Xie, J., LeBaron, M. J., Pretlow, T. G., Ealley, E. L., Zhang, Y., Nurmi, M., Singh, B., Martikainen, P. M., & Nevalainen, M. T. (2004). Activation of signal transducer and activator of transcription 5 in human prostate cancer is associated with high histological grade. *Cancer Research*, *64*(14), 4774–4782.

Li, M., Luo, J., Brooks, C. L., & Gu, W. (2002). Acetylation of p53 inhibits its ubiquitination by Mdm2. *The Journal of Biological Chemistry*, *277*(52), 50607–50611.

Liao, Z., Gu, L., Vergalli, J., Mariani, S. A., De Dominici, M., Lokareddy, R. K., Dagvadorj, A., Purushottamachar, P., McCue, P. A., Trabulsi, E., Lallas, C. D., Gupta, S., Ellsworth, E., Blackmon, S., Ertel, A., Fortina, P., Leiby, B., Xia, G., Rui, H., Hoang, D. T., Gomella, L. G., Cingolani, G., Njar, V., Pattabiraman, N., Calabretta, B., & Nevalainen, M. T. (2015). Structure-based screen identifies a potent small-molecule inhibitor of Stat5a/b with therapeutic potential for prostate cancer and chronic myeloid leukemia. *Molecular Cancer Therapeutics*.

Lim, C. P., & Cao, X. (2006). Structure, function, and regulation of STAT proteins. *Molecular bioSystems*, *2*(11), 536–550.

Lin, G., LaPensee, C. R., Qin, Z. S., & Schwartz, J. (2014). Reciprocal occupancy of BCL6 and STAT5 on Growth Hormone target genes: contrasting transcriptional outcomes and promoter-specific roles of p300 and HDAC3. *Molecular and Cellular Endocrinology*, *395*(1-2), 19–31.

Lin, J.-X., Li, P., Liu, D., Jin, H. T., He, J., Ata Ur Rasheed, M., Rochman, Y., Wang, L., Cui, K., Liu, C., Kelsall, B. L., Ahmed, R., & Leonard, W. J. (2012). Critical Role of STAT5 transcription factor tetramerization for cytokine responses and normal immune function. *Immunity*, *36*(4), 586–599.

Lin, J. X., Migone, T. S., Tsang, M., Friedmann, M., Weatherbee, J. A., Zhou, L., Yamauchi, A., Bloom, E. T., Mietz, J., & John, S. (1995). The role of shared receptor motifs and common Stat proteins in the generation of cytokine pleiotropy and redundancy by IL-2, IL-4, IL-7, IL-13, and IL-15. *Immunity*, *2*(4), 331–339.

Lin, Y. H., Huang, C. J., Chao, J. R., Chen, S. T., Lee, S. F., Yen, J. J., & Yang-Yen, H. F. (2000). Coupling of osteopontin and its cell surface receptor CD44 to the cell survival response elicited by interleukin-3 or granulocyte-macrophage colony-stimulating factor. *Molecular and Cellular Biology*, *20*(8), 2734–2742.

Litterst, C. M., Kliem, S., Marilley, D., & Pfitzner, E. (2003). NCoA-1/SRC-1 is an essential coactivator of STAT5 that binds to the FDL motif in the alpha-helical region of the STAT5 transactivation domain. *The Journal of Biological Chemistry*, *278*(46), 45340–45351.

Liu, N., Xiong, Y., Li, S., Ren, Y., He, Q., Gao, S., Zhou, J., & Shui, W. (2015). New HDAC6-mediated deacetylation sites of tubulin in the mouse brain identified by quantitative mass spectrometry. *Scientific Reports*, *5*, 16869.

Liu, S., Walker, S. R., Nelson, E. A., Cerulli, R., Xiang, M., Toniolo, P. A., Qi, J., Stone, R. M., Wadleigh, M., Bradner, J. E., & Frank, D. A. (2014). Targeting STAT5 in hematologic malignancies through inhibition of the bromodomain and extra-terminal (BET) bromodomain protein BRD2. *Molecular Cancer Therapeutics*, *13*(5), 1194–1205.

Liu, X., Robinson, G. W., Wagner, K. U., Garrett, L., Wynshaw-Boris, A., & Hennighausen, L. (1997). Stat5a is mandatory for adult mammary gland development and lactogenesis. *Genes & Development*, *11*(2), 179–186.

Lobera, M., Madauss, K. P., Pohlhaus, D. T., Wright, Q. G., Trocha, M., Schmidt, D. R., Baloglu, E., Trump, R. P., Head, M. S., Hofmann, G. A., Murray-Thompson, M., Schwartz, B., Chakravorty, S., Wu, Z., Mander, P. K., Kruidenier, L., Reid, R. A., Burkhart, W., Turunen, B. J., Rong, J. X., Wagner, C., Moyer, M. B., Wells, C., Hong, X., Moore, J. T., Williams, J. D., Soler, D., Ghosh, S., & Nolan, M. A. (2013). Selective class IIa histone deacetylase inhibition via a nonchelating zinc-binding group. *Nature Chemical Biology*, *9*(5), 319–325.

Lorch, Y., & Kornberg, R. D. (2015). Chromatin-remodeling and the initiation of transcription. *Quarterly Reviews of Biophysics*, *48*(4), 465–470.

Lorch, Y., LaPointe, J. W., & Kornberg, R. D. (1987). Nucleosomes inhibit the initiation of transcription but allow chain elongation with the displacement of histones. *Cell*, *49*(2), 203–210.

Luger, K., Mäder, A. W., Richmond, R. K., Sargent, D. F., & Richmond, T. J. (1997). Crystal structure of the nucleosome core particle at 2.8 A resolution. *Nature*, *389*(6648), 251–260.

Luo, H., & Dearolf, C. R. (2001). The JAK/STAT pathway and Drosophila development. *BioEssays: News and Reviews in Molecular, Cellular and Developmental Biology*, *23*(12), 1138–1147.

Ma, J., Przibilla, E., Hu, J., Bogorad, L., & Ptashne, M. (1988). Yeast activators stimulate plant gene expression. *Nature*, *334*(6183), 631–633.

Ma, J., & Ptashne, M. (1987). Deletion analysis of GAL4 defines two transcriptional activating segments. *Cell*, *48*(5), 847–853.

Ma, L., Gao, J.-s., Guan, Y., Shi, X., Zhang, H., Ayrapetov, M. K., Zhang, Z., Xu, L., Hyun, Y.-M., Kim, M., Zhuang, S., & Chin, Y. E. (2010). Acetylation modulates prolactin receptor dimerization. *Proceedings of the National Academy of Sciences of the United States of America*, *107*(45), 19314–19319.

Mackmull, M.-T., Iskar, M., Parca, L., Singer, S., Bork, P., Ori, A., & Beck, M. (2015). Histone Deacetylase Inhibitors (HDACi) Cause the Selective Depletion of Bromodomain Containing Proteins (BCPs). *Molecular & cellular proteomics: MCP*, *14*(5), 1350–1360.

Magné, S., Caron, S., Charon, M., Rouyez, M.-C., & Dusanter-Fourt, I. (2003). STAT5 and Oct-1 form a stable complex that modulates cyclin D1 expression. *Molecular and Cellular Biology*, *23*(24), 8934–8945.

Mai, A., Massa, S., Lavu, S., Pezzi, R., Simeoni, S., Ragno, R., Mariotti, F. R., Chiani, F., Camilloni, G., & Sinclair, D. A. (2005). Design, synthesis, and biological evaluation of sirtinol analogues as class III histone/protein deacetylase (Sirtuin) inhibitors. *Journal of Medicinal Chemistry*, *48*(24), 7789–7795.

Mandal, M., Powers, S. E., Maienschein-Cline, M., Bartom, E. T., Hamel, K. M., Kee, B. L., Dinner, A. R., & Clark, M. R. (2011). Epigenetic repression of the Igk locus by STAT5-mediated recruitment of the histone methyltransferase Ezh2. *Nature Immunology*.

Martínez-Balbás, M. A., Bauer, U. M., Nielsen, S. J., Brehm, A., & Kouzarides, T. (2000). Regulation of E2f1 activity by acetylation. *The EMBO journal*, *19*(4), 662–671.

Martinez-Moczygemba, M., & Huston, D. P. (2003). Biology of common beta receptor-signaling cytokines: IL-3, IL-5, and GM-CSF. *The Journal of allergy and clinical immunology*, *112*(4), 653–665; quiz 666.

Martinez-Moczygemba, M., Huston, D. P., & Lei, J. T. (2007). JAK kinases control IL-5 receptor ubiquitination, degradation, and internalization. *Journal of Leukocyte Biology*, *81*(4), 1137–1148.

Mathias, R. A., Guise, A. J., & Cristea, I. M. (2015). Post-translational modifications regulate class IIa histone deacetylase (HDAC) function in health and disease. *Molecular & cellular proteomics: MCP*, *14*(3), 456–470.

Matsumoto, A., Masuhara, M., Mitsui, K., Yokouchi, M., Ohtsubo, M., Misawa, H., Miyajima, A., & Yoshimura, A. (1997). CIS, a cytokine inducible SH2 protein, is a target of the JAK-STAT5 pathway and modulates STAT5 activation. *Blood*, *89*(9), 3148–3154.

Matsumura, I., Kitamura, T., Wakao, H., Tanaka, H., Hashimoto, K., Albanese, C., Downward, J., Pestell, R. G., & Kanakura, Y. (1999). Transcriptional regulation of the cyclin D1 promoter by STAT5: its involvement in cytokine-dependent growth of hematopoietic cells. *The EMBO journal*, *18*(5), 1367–1377.

Matsuoka, H., Fujimura, T., Hayashi, M., Matsuda, K., Ishii, Y., Aramori, I., & Mutoh, S. (2007). Disruption of HDAC4/N-CoR complex by histone deacetylase inhibitors leads to inhibition of IL-2 gene expression. *Biochemical Pharmacology*, *74*(3), 465–476.

Métivier, R., Penot, G., Hübner, M. R., Reid, G., Brand, H., Koš, M., & Gannon, F. (2003). Estrogen Receptor-α Directs Ordered, Cyclical, and Combinatorial Recruitment of Cofactors on a Natural Target Promoter. *Cell*, *115*(6), 751–763.

Metser, G., Shin, H. Y., Wang, C., Yoo, K. H., Oh, S., Villarino, A. V., O'Shea, J. J., Kang, K., & Hennighausen, L. (2015). An autoregulatory enhancer controls mammary-specific STAT5 functions. *Nucleic Acids Research*.

Meyer, J., Jucker, M., Ostertag, W., & Stocking, C. (1998). Carboxyl-truncated STAT5beta is generated by a nucleus-associated serine protease in early hematopoietic progenitors. *Blood*, *91*(6), 1901–1908.

Montgomery, R. L., Davis, C. A., Potthoff, M. J., Haberland, M., Fielitz, J., Qi, X., Hill, J. A., Richardson, J. A., & Olson, E. N. (2007). Histone deacetylases 1 and 2 redundantly regulate cardiac morphogenesis, growth, and contractility. *Genes & Development*, *21*(14), 1790–1802.

Moriggl, R., Gouilleux-Gruart, V., Jähne, R., Berchtold, S., Gartmann, C., Liu, X., Hennighausen, L., Sotiropoulos, A., Groner, B., & Gouilleux, F. (1996). Deletion of the carboxyl-terminal transactivation domain of MGF-Stat5 results in sustained DNA binding and a dominant negative phenotype. *Molecular and Cellular Biology*, *16*(10), 5691–5700.

Moriggl, R., Topham, D. J., Teglund, S., Sexl, V., McKay, C., Wang, D., Hoffmeyer, A., van Deursen, J., Sangster, M. Y., Bunting, K. D., Grosveld, G. C., & Ihle, J. N. (1999). Stat5 is required for IL-2-induced cell cycle progression of peripheral T cells. *Immunity*, *10*(2), 249–259.

Morinière, J., Rousseaux, S., Steuerwald, U., Soler-López, M., Curtet, S., Vitte, A.-L., Govin, J., Gaucher, J., Sadoul, K., Hart, D. J., Krijgsveld, J., Khochbin, S., Müller, C. W., & Petosa, C. (2009). Cooperative binding of two acetylation marks on a histone tail by a single bromodomain. *Nature*, *461*(7264), 664–668.

Mottus, R., Sobel, R. E., & Grigliatti, T. A. (2000). Mutational analysis of a histone deacetylase in Drosophila melanogaster: missense mutations suppress gene silencing associated with position effect variegation. *Genetics*, *154*(2), 657–668.

Mui, A. L., Wakao, H., Kinoshita, T., Kitamura, T., & Miyajima, A. (1996). Suppression of interleukin-3-induced gene expression by a C-terminal truncated Stat5: role of Stat5 in proliferation. *The EMBO journal*, *15*(10), 2425–2433.

Mui, A. L., Wakao, H., O'Farrell, A. M., Harada, N., & Miyajima, A. (1995). Interleukin-3, granulocyte-macrophage colony stimulating factor and interleukin-5 transduce signals through two STAT5 homologs. *The EMBO journal*, *14*(6), 1166–1175.

Mukhopadhyay, S. S., Wyszomierski, S. L., Gronostajski, R. M., & Rosen, J. M. (2001). Differential interactions of specific nuclear factor I isoforms with the glucocorticoid receptor and STAT5 in the cooperative regulation of WAP gene transcription. *Molecular and Cellular Biology*, *21*(20), 6859–6869.

Munshi, N., Agalioti, T., Lomvardas, S., Merika, M., Chen, G., & Thanos, D. (2001). Coordination of a transcriptional switch by HMGI(Y) acetylation. *Science (New York, N.Y.)*, *293*(5532), 1133–1136.

Munshi, N., Merika, M., Yie, J., Senger, K., Chen, G., & Thanos, D. (1998). Acetylation of HMG I(Y) by CBP turns off IFN beta expression by disrupting the enhanceosome. *Molecular Cell*, *2*(4), 457–467.

Myers, M. P., Andersen, J. N., Cheng, A., Tremblay, M. L., Horvath, C. M., Parisien, J. P., Salmeen, A., Barford, D., & Tonks, N. K. (2001). TYK2 and JAK2 are substrates of protein-tyrosine phosphatase 1b. *The Journal of Biological Chemistry*, *276*(51), 47771–47774.

Nadeau, K., Hwa, V., & Rosenfeld, R. G. (2011). STAT5b deficiency: an unsuspected cause of growth failure, immunodeficiency, and severe pulmonary disease. *The Journal of Pediatrics*, *158*(5), 701–708.

Nakajima, H., Brindle, P. K., Handa, M., & Ihle, J. N. (2001). Functional interaction of STAT5 and nuclear receptor co-repressor SMRT: implications in negative regulation of STAT5-dependent transcription. *The EMBO journal*, *20*(23), 6836–6844.

Nechay, M. R., Gallup, N. M., Morgenstern, A., Smith, Q. A., Eberhart, M. E., & Alexandrova, A. N. (2016). Histone Deacetylase 8: Characterization of Physiological Divalent Metal Catalysis. *The Journal of Physical Chemistry. B*.

Nelson, E. A., Walker, S. R., Alvarez, J. V., & Frank, D. A. (2004). Isolation of unique STAT5 targets by chromatin immunoprecipitation-based gene identification. *The Journal of Biological Chemistry*, *279*(52), 54724–54730.

Nie, Y., Erion, D. M., Yuan, Z., Dietrich, M., Shulman, G. I., Horvath, T. L., & Gao, Q. (2009). STAT3 inhibition of gluconeogenesis is downregulated by SirT1. *Nature cell biology*, *11*(4), 492–500.

Nocetti, N., & Whitehouse, I. (2016). Nucleosome repositioning underlies dynamic gene expression. *Genes & Development*, *30*(6), 660–672.

Nosaka, T., Kawashima, T., Misawa, K., Ikuta, K., Mui, A. L., & Kitamura, T. (1999). STAT5 as a molecular regulator of proliferation, differentiation and apoptosis in hematopoietic cells. *The EMBO journal*, *18*(17), 4754–4765.

Nural-Guvener, H. F., Zakharova, L., Nimlos, J., Popovic, S., Mastroeni, D., & Gaballa, M. A. (2014). HDAC class I inhibitor, Mocetinostat, reverses cardiac fibrosis in heart failure and diminishes CD90+ cardiac myofibroblast activation. *Fibrogenesis & Tissue Repair*, *7*, 10.

Nusinzon, I., & Horvath, C. M. (2003). Interferon-stimulated transcription and innate antiviral immunity require deacetylase activity and histone deacetylase 1. *Proceedings of the National Academy of Sciences of the United States of America*, *100*(25), 14742–14747.

Okada, M., & Fukagawa, T. (2006). Purification of a protein complex that associates with chromatin. *Protocol Exchange*.

Olins, A. L., & Olins, D. E. (1974). Spheroid chromatin units (v bodies). *Science (New York, N.Y.)*, *183*(4122), 330–332.

Onishi, M., Nosaka, T., Misawa, K., Mui, A. L., Gorman, D., McMahon, M., Miyajima, A., & Kitamura, T. (1998). Identification and characterization of a constitutively active STAT5 mutant that promotes cell proliferation. *Molecular and Cellular Biology*, *18*(7), 3871–3879.

O'Shea, J. J., Schwartz, D. M., Villarino, A. V., Gadina, M., McInnes, I. B., & Laurence, A. (2015). The JAK-STAT pathway: impact on human disease and therapeutic intervention. *Annual Review of Medicine*, *66*, 311–328.

Ott, C. J., Kopp, N., Bird, L., Paranal, R. M., Qi, J., Bowman, T., Rodig, S. J., Kung, A. L., Bradner, J. E., & Weinstock, D. M. (2012). BET bromodomain inhibition targets both c-Myc and IL7r in high-risk acute lymphoblastic leukemia. *Blood*, *120*(14), 2843–2852.

Paling, N. R. D., & Welham, M. J. (2002). Role of the protein tyrosine phosphatase SHP-1 (Src homology phosphatase-1) in the regulation of interleukin-3-induced survival, proliferation and signalling. *The Biochemical Journal*, *368*(Pt 3), 885–894.

Peart, M. J., Smyth, G. K., van Laar, R. K., Bowtell, D. D., Richon, V. M., Marks, P. A., Holloway, A. J., & Johnstone, R. W. (2005). Identification and functional significance of genes regulated by structurally different histone deacetylase inhibitors. *Proceedings of the National Academy of Sciences of the United States of America*, *102*(10), 3697–3702.

Peng, J., Dong, W., Chen, L., Zou, T., Qi, Y., & Liu, Y. (2007). Brd2 is a TBP-associated protein and recruits TBP into E2f-1 transcriptional complex in response to serum stimulation. *Molecular and Cellular Biochemistry*, *294*(1-2), 45–54.

Perrimon, N., & Mahowald, A. P. (1986). l(1)hopscotch, A larval-pupal zygotic lethal with a specific maternal effect on segmentation in Drosophila. *Developmental Biology*, *118*(1), 28–41.

Pfitzner, E., Jähne, R., Wissler, M., Stoecklin, E., & Groner, B. (1998). p300/CREB-binding protein enhances the prolactin-mediated transcriptional induction through direct interaction with the transactivation domain of Stat5, but does not participate in the Stat5-mediated suppression of the glucocorticoid response. *Molecular endocrinology (Baltimore, Md.)*, *12*(10), 1582–1593.

Phiel, C. J., Zhang, F., Huang, E. Y., Guenther, M. G., Lazar, M. A., & Klein, P. S. (2001). Histone deacetylase is a direct target of valproic acid, a potent anticonvulsant, mood stabilizer, and teratogen. *The Journal of Biological Chemistry*, *276*(39), 36734–36741.

Pinz, S., & Rascle, A. (2017). Assessing HDAC Function in the Regulation of Signal Transducer and Activator of Transcription 5 (STAT5) Activity Using Chromatin Immunoprecipitation (ChIP). *Methods in Molecular Biology (Clifton, N.J.)*, *1510*, 257–276.

Pinz, S., Unser, S., Brueggemann, S., Besl, E., Al-Rifai, N., Petkes, H., Amslinger, S., & Rascle, A. (2014a). The Synthetic α-Bromo-2',3,4,4'-Tetramethoxychalcone (α-Br-TMC) Inhibits the JAK/STAT Signaling Pathway. *PloS one*, *9*(3), e90275.

Pinz, S., Unser, S., Buob, D., Fischer, P., Jobst, B., & Rascle, A. (2015). Deacetylase inhibitors repress STAT5-mediated transcription by interfering with bromodomain and extra-terminal (BET) protein function. *Nucleic Acids Research*, *43*(7), 3524–3545.

Pinz, S., Unser, S., & Rascle, A. (2014b). The Natural Chemopreventive Agent Sulforaphane Inhibits STAT5 Activity. *PloS one*, *9*(6), e99391.

Pinz, S., Unser, S., & Rascle, A. (2016). Signal transducer and activator of transcription STAT5 is recruited to c-Myc super-enhancer. *BMC molecular biology*, *17*(1), 10.

Pivot-Pajot, C., Caron, C., Govin, J., Vion, A., Rousseaux, S., & Khochbin, S. (2003). Acetylation-dependent chromatin reorganization by BRDT, a testis-specific bromodomain-containing protein. *Molecular and Cellular Biology*, *23*(15), 5354–5365.

Purbey, P. K., Singh, S., Notani, D., Kumar, P. P., Limaye, A. S., & Galande, S. (2009). Acetylation-dependent interaction of SATB1 and CtBP1 mediates transcriptional repression by SATB1. *Molecular and Cellular Biology*, *29*(5), 1321–1337.

Rada-Iglesias, A., Enroth, S., Ameur, A., Koch, C. M., Clelland, G. K., Respuela-Alonso, P., Wilcox, S., Dovey, O. M., Ellis, P. D., Langford, C. F., Dunham, I., Komorowski, J., & Wadelius, C. (2007). Butyrate mediates decrease of histone acetylation centered on transcription start sites and down-regulation of associated genes. *Genome Research*, *17*(6), 708–719.

Rahman, S., Sowa, M. E., Ottinger, M., Smith, J. A., Shi, Y., Harper, J. W., & Howley, P. M. (2011). The Brd4 extraterminal domain confers transcription activation independent of pTEFb by recruiting multiple proteins, including NSD3. *Molecular and Cellular Biology*, *31*(13), 2641–2652.

Rajala, H. L. M., Eldfors, S., Kuusanmäki, H., van Adrichem, A. J., Olson, T., Lagström, S., Andersson, E. I., Jerez, A., Clemente, M. J., Yan, Y., Zhang, D., Awwad, A., Ellonen, P., Kallioniemi, O., Wennerberg, K., Porkka, K., Maciejewski, J. P., Loughran, T. P., Jr, Heckman, C., & Mustjoki, S. (2013). Discovery of somatic STAT5b mutations in large granular lymphocytic leukemia. *Blood*.

Ram, P. A., & Waxman, D. J. (1999). SOCS/CIS protein inhibition of growth hormone-stimulated STAT5 signaling by multiple mechanisms. *The Journal of Biological Chemistry*, *274*(50), 35553–35561.

Rascle, A., Johnston, J. A., & Amati, B. (2003). Deacetylase Activity Is Required for Recruitment of the Basal Transcription Machinery and Transactivation by STAT5. *Molecular and Cellular Biology*, *23*(12), 4162–4173.

Rascle, A., & Lees, E. (2003). Chromatin acetylation and remodeling at the Cis promoter during STAT5-induced transcription. *Nucleic Acids Research*, *31*(23), 6882–6890.

Ray, S., Boldogh, I., & Brasier, A. R. (2005). STAT3 NH2-terminal acetylation is activated by the hepatic acute-phase response and required for IL-6 induction of angiotensinogen. *Gastroenterology*, *129*(5), 1616–1632.

Reményi, A., Schöler, H. R., & Wilmanns, M. (2004). Combinatorial control of gene expression. *Nature Structural & Molecular Biology*, *11*(9), 812–815.

Ren, S., Cai, H. R., Li, M., & Furth, P. A. (2002). Loss of Stat5a delays mammary cancer progression in a mouse model. *Oncogene*, *21*(27), 4335–4339.

Richon, V. M., Sandhoff, T. W., Rifkind, R. A., & Marks, P. A. (2000). Histone deacetylase inhibitor selectively induces p21waf1 expression and gene-associated histone acetylation. *Proceedings of the National Academy of Sciences of the United States of America*, *97*(18), 10014–10019.

Robertson, E. D., Weir, L., Romanowska, M., Leigh, I. M., & Panteleyev, A. A. (2012). ARNT controls the expression of epidermal differentiation genes through HDAC- and EGFR-dependent pathways. *Journal of Cell Science*, *125*(Pt 14), 3320–3332.

Rodriguez, M. S., Desterro, J. M., Lain, S., Lane, D. P., & Hay, R. T. (2000). Multiple C-terminal lysine residues target p53 for ubiquitin-proteasome-mediated degradation. *Molecular and Cellular Biology*, *20*(22), 8458–8467.

Rodriguez-Tarduchy, G., Collins, M., & López-Rivas, A. (1990). Regulation of apoptosis in interleukin-3-dependent hemopoietic cells by interleukin-3 and calcium ionophores. *The EMBO journal*, *9*(9), 2997–3002.

Rogers, R. S., Horvath, C. M., & Matunis, M. J. (2003). SUMO modification of STAT1 and its role in PIAS-mediated inhibition of gene activation. *The Journal of Biological Chemistry*, *278*(32), 30091–30097.

Roh, T.-Y., Cuddapah, S., & Zhao, K. (2005). Active chromatin domains are defined by acetylation islands revealed by genome-wide mapping. *Genes & Development*, *19*(5), 542–552.

Romanov, V. S., Abramova, M. V., Svetlikova, S. B., Bykova, T. V., Zubova, S. G., Aksenov, N. D., Fornace, A. J., Pospelova, T. V., & Pospelov, V. A. (2010). p21(Waf1) is required for cellular senescence but not for cell cycle arrest induced by the HDAC inhibitor sodium butyrate. *Cell Cycle (Georgetown, Tex.)*, *9*(19), 3945–3955.

Ropero, S., & Esteller, M. (2007). The role of histone deacetylases (HDACs) in human cancer. *Molecular Oncology*, *1*(1), 19–25.

Ruefli, A. A., Ausserlechner, M. J., Bernhard, D., Sutton, V. R., Tainton, K. M., Kofler, R., Smyth, M. J., & Johnstone, R. W. (2001). The histone deacetylase inhibitor and chemotherapeutic agent suberoylanilide hydroxamic acid (SAHA) induces a cell-death pathway characterized by cleavage of Bid and production of reactive oxygen species. *Proceedings of the National Academy of Sciences of the United States of America*, *98*(19), 10833–10838.

Rycyzyn, M. A., & Clevenger, C. V. (2002). The intranuclear prolactin/cyclophilin B complex as a transcriptional inducer. *Proceedings of the National Academy of Sciences of the United States of America*, *99*(10), 6790–6795.

Sachweh, M. C. C., Drummond, C. J., Higgins, M., Campbell, J., & Laín, S. (2013). Incompatible effects of p53 and HDAC inhibition on p21 expression and cell cycle progression. *Cell death & disease*, *4*, e533.

Sadowski, I., Ma, J., Triezenberg, S., & Ptashne, M. (1988). GAL4-VP16 is an unusually potent transcriptional activator. *Nature*, *335*(6190), 563–564.

Saito, A., Yamashita, T., Mariko, Y., Nosaka, Y., Tsuchiya, K., Ando, T., Suzuki, T., Tsuruo, T., & Nakanishi, O. (1999). A synthetic inhibitor of histone deacetylase, MS-27-275, with marked in vivo antitumor activity against human tumors. *Proceedings of the National Academy of Sciences of the United States of America*, *96*(8), 4592–4597.

Sakamoto, S., Potla, R., & Larner, A. C. (2004). Histone deacetylase activity is required to recruit RNA polymerase II to the promoters of selected interferon-stimulated early response genes. *The Journal of Biological Chemistry*, *279*(39), 40362–40367.

Sasaki, A., Yasukawa, H., Suzuki, A., Kamizono, S., Syoda, T., Kinjyo, I., Sasaki, M., Johnston, J. A., & Yoshimura, A. (1999). Cytokine-inducible SH2 protein-3 (CIS3/SOCS3) inhibits Janus tyrosine kinase by binding through the N-terminal kinase inhibitory region as well as SH2 domain. *Genes to Cells: Devoted to Molecular & Cellular Mechanisms*, *4*(6), 339–351.

Savage, D. G., & Antman, K. H. (2002). Imatinib mesylate–a new oral targeted therapy. *The New England Journal of Medicine*, *346*(9), 683–693.

Schindler, C., & Plumlee, C. (2008). Inteferons pen the JAK-STAT pathway. *Seminars in Cell & Developmental Biology*, *19*(4), 311–318.

Schmitt-Ney, M., Happ, B., Ball, R. K., & Groner, B. (1992). Developmental and environmental regulation of a mammary gland-specific nuclear factor essential for transcription of the gene encoding beta-casein. *Proceedings of the National Academy of Sciences of the United States of America*, *89*(7), 3130–3134.

Schübeler, D., MacAlpine, D. M., Scalzo, D., Wirbelauer, C., Kooperberg, C., van Leeuwen, F., Gottschling, D. E., O'Neill, L. P., Turner, B. M., Delrow, J., Bell, S. P., & Groudine, M. (2004). The histone modification pattern of active genes revealed through genome-wide chromatin analysis of a higher eukaryote. *Genes & Development*, *18*(11), 1263–1271.

Sebastián, C., Serra, M., Yeramian, A., Serrat, N., Lloberas, J., & Celada, A. (2008). Deacetylase activity is required for STAT5-dependent GM-CSF functional activity in macrophages and differentiation to dendritic cells. *Journal of Immunology (Baltimore, Md.: 1950)*, *180*(9), 5898–5906.

Shah, R. D., Jagtap, J. C., Mruthyunjaya, S., Shelke, G. V., Pujari, R., Das, G., & Shastry, P. (2013). Sodium valproate potentiates staurosporine-induced apoptosis in neuroblastoma cells via Akt/survivin independently of HDAC inhibition. *Journal of cellular biochemistry*, *114*(4), 854–863.

Shang, E., Wang, X., Wen, D., Greenberg, D. A., & Wolgemuth, D. J. (2009). Double bromodomain-containing gene Brd2 is essential for embryonic development in mouse. *Developmental Dynamics: An Official Publication of the American Association of Anatomists*, *238*(4), 908–917.

Shelburne, C. P., McCoy, M. E., Piekorz, R., Sexl, V., Roh, K.-H., Jacobs-Helber, S. M., Gillespie, S. R., Bailey, D. P., Mirmonsef, P., Mann, M. N., Kashyap, M., Wright, H. V., Chong, H. J., Bouton, L. A., Barnstein, B., Ramirez, C. D., Bunting, K. D., Sawyer, S., Lantz, C. S., & Ryan, J. J. (2003). Stat5 expression is critical for mast cell development and survival. *Blood*, *102*(4), 1290–1297.

Shin, H. Y., & Reich, N. C. (2013). Dynamic trafficking of STAT5 depends on an unconventional nuclear localization signal. *Journal of Cell Science*, *126*(Pt 15), 3333–3343.

Shogren-Knaak, M., Ishii, H., Sun, J.-M., Pazin, M. J., Davie, J. R., & Peterson, C. L. (2006). Histone H4-K16 acetylation controls chromatin structure and protein interactions. *Science (New York, N.Y.)*, *311*(5762), 844–847.

Shuai, K., Stark, G. R., Kerr, I. M., & Darnell, J. E. (1993). A single phosphotyrosine residue of Stat91 required for gene activation by interferon-gamma. *Science (New York, N.Y.)*, *261*(5129), 1744–1746.

Simoncic, P. D., Lee-Loy, A., Barber, D. L., Tremblay, M. L., & McGlade, C. J. (2002). The T cell protein tyrosine phosphatase is a negative regulator of janus family kinases 1 and 3. *Current biology: CB*, *12*(6), 446–453.

Snow, J. W., Abraham, N., Ma, M. C., Herndier, B. G., Pastuszak, A. W., & Goldsmith, M. A. (2003). Loss of tolerance and autoimmunity affecting multiple organs in STAT5a/5b-deficient mice. *Journal of Immunology (Baltimore, Md.: 1950)*, *171*(10), 5042–5050.

Soldaini, E., John, S., Moro, S., Bollenbacher, J., Schindler, U., & Leonard, W. J. (2000). DNA binding site selection of dimeric and tetrameric Stat5 proteins reveals a large repertoire of divergent tetrameric Stat5a binding sites. *Molecular and Cellular Biology*, *20*(1), 389–401.

Spange, S., Wagner, T., Heinzel, T., & Krämer, O. H. (2009). Acetylation of non-histone proteins modulates cellular signalling at multiple levels. *The International Journal of Biochemistry & Cell Biology*, *41*(1), 185–198.

Sun, Y., Liu, P. Y., Scarlett, C. J., Malyukova, A., Liu, B., Marshall, G. M., MacKenzie, K. L., Biankin, A. V., & Liu, T. (2014). Histone deacetylase 5 blocks neuroblastoma cell differentiation by interacting with N-Myc. *Oncogene*, *33*(23), 2987–2994.

Suzuki, T., Ando, T., Tsuchiya, K., Fukazawa, N., Saito, A., Mariko, Y., Yamashita, T., & Nakanishi, O. (1999). Synthesis and histone deacetylase inhibitory activity of new benzamide derivatives. *Journal of Medicinal Chemistry*, *42*(15), 3001–3003.

Tam, S. P., Lau, P., Djiane, J., Hilton, D. J., & Waters, M. J. (2001). Tissue-specific induction of SOCS gene expression by PRL. *Endocrinology*, *142*(11), 5015–5026.

Tang, J.-Z., Zuo, Z.-H., Kong, X.-J., Steiner, M., Yin, Z., Perry, J. K., Zhu, T., Liu, D.-X., & Lobie, P. E. (2010). Signal transducer and activator of transcription (STAT)-5a and STAT5b differentially regulate human mammary carcinoma cell behavior. *Endocrinology*, *151*(1), 43–55.

Tang, X., Gao, J.-S., Guan, Y.-j., McLane, K. E., Yuan, Z.-L., Ramratnam, B., & Chin, Y. E. (2007). Acetylation-dependent signal transduction for type I interferon receptor. *Cell*, *131*(1), 93–105.

Tang, Z., Chen, W.-Y., Shimada, M., Nguyen, U. T. T., Kim, J., Sun, X.-J., Sengoku, T., McGinty, R. K., Fernandez, J. P., Muir, T. W., & Roeder, R. G. (2013). SET1 and p300 act synergistically, through coupled histone modifications, in transcriptional activation by p53. *Cell*, *154*(2), 297–310.

Tanner, K. G., Landry, J., Sternglanz, R., & Denu, J. M. (2000). Silent information regulator 2 family of NAD- dependent histone/protein deacetylases generates a unique product, 1-O-acetyl-ADP-ribose. *Proceedings of the National Academy of Sciences of the United States of America*, *97*(26), 14178–14182.

ten Hoeve, J., de Jesus Ibarra-Sanchez, M., Fu, Y., Zhu, W., Tremblay, M., David, M., & Shuai, K. (2002). Identification of a nuclear Stat1 protein tyrosine phosphatase. *Molecular and Cellular Biology*, *22*(16), 5662–5668.

Thorne, A. W., Kmiciek, D., Mitchelson, K., Sautiere, P., & Crane-Robinson, C. (1990). Patterns of histone acetylation. *European journal of biochemistry / FEBS*, *193*(3), 701–713.

Tokita, T., Maesawa, C., Kimura, T., Kotani, K., Takahashi, K., Akasaka, T., & Masuda, T. (2007). Methylation status of the SOCS3 gene in human malignant melanomas. *International Journal of Oncology*, *30*(3), 689–694.

Toniolo, P. A., Liu, S., Yeh, J. E., Moraes-Vieira, P. M., Walker, S. R., Vafaizadeh, V., Barbuto, J. A. M., & Frank, D. A. (2015). Inhibiting STAT5 by the BET Bromodomain Inhibitor JQ1 Disrupts Human Dendritic Cell Maturation. *Journal of Immunology (Baltimore, Md.: 1950)*.

Tse, C., Sera, T., Wolffe, A. P., & Hansen, J. C. (1998). Disruption of higher-order folding by core histone acetylation dramatically enhances transcription of nucleosomal arrays by RNA polymerase III. *Molecular and Cellular Biology*, *18*(8), 4629–4638.

Udy, G. B., Towers, R. P., Snell, R. G., Wilkins, R. J., Park, S. H., Ram, P. A., Waxman, D. J., & Davey, H. W. (1997). Requirement of STAT5b for sexual dimorphism of body growth rates and liver gene expression. *Proceedings of the National Academy of Sciences of the United States of America*, *94*(14), 7239–7244.

Ungerstedt, J. S., Sowa, Y., Xu, W.-S., Shao, Y., Dokmanovic, M., Perez, G., Ngo, L., Holmgren, A., Jiang, X., & Marks, P. A. (2005). Role of thioredoxin in the response of normal and transformed cells to histone deacetylase inhibitors. *Proceedings of the National Academy of Sciences of the United States of America*, *102*(3), 673–678.

Ungureanu, D., Vanhatupa, S., Grönholm, J., Palvimo, J. J., & Silvennoinen, O. (2005). SUMO-1 conjugation selectively modulates STAT1-mediated gene responses. *Blood*, *106*(1), 224–226.

Vaidya, A. S., Karumudi, B., Mendonca, E., Madriaga, A., Abdelkarim, H., van Breemen, R. B., & Petukhov, P. A. (2012). Design, synthesis, modeling, biological evaluation and photoaffinity labeling studies of novel series of photoreactive benzamide probes for histone deacetylase 2. *Bioorganic & Medicinal Chemistry Letters*, *22*(15), 5025–5030.

Van Nguyen, T., Angkasekwinai, P., Dou, H., Lin, F.-M., Lu, L.-S., Cheng, J., Chin, Y. E., Dong, C., & Yeh, E. T. H. (2012). SUMO-specific protease 1 is critical for early lymphoid development through regulation of STAT5 activation. *Molecular cell*, *45*(2), 210–221.

Vaquero, A., Scher, M., Lee, D., Erdjument-Bromage, H., Tempst, P., & Reinberg, D. (2004). Human SirT1 interacts with histone H1 and promotes formation of facultative heterochromatin. *Molecular Cell*, *16*(1), 93–105.

Vaquero, A., Sternglanz, R., & Reinberg, D. (2007). NAD+-dependent deacetylation of H4 lysine 16 by class III HDACs. *Oncogene*, *26*(37), 5505–5520.

Venne, A. S., Kollipara, L., & Zahedi, R. P. (2014). The next level of complexity: crosstalk of posttranslational modifications. *Proteomics*, *14*(4-5), 513–524.

Venters, B. J., & Pugh, B. F. (2009). How eukaryotic genes are transcribed. *Critical Reviews in Biochemistry and Molecular Biology*, *44*(2-3), 117–141.

Verdel, A., Curtet, S., Brocard, M. P., Rousseaux, S., Lemercier, C., Yoshida, M., & Khochbin, S. (2000). Active maintenance of mHDA2/mHDAC6 histone-deacetylase in the cytoplasm. *Current biology: CB*, *10*(12), 747–749.

Verdier, F., Rabionet, R., Gouilleux, F., Beisenherz-Huss, C., Varlet, P., Muller, O., Mayeux, P., Lacombe, C., Gisselbrecht, S., & Chretien, S. (1998). A sequence of the CIS gene promoter interacts preferentially with two associated STAT5a dimers: a distinct biochemical difference between STAT5a and STAT5b. *Molecular and Cellular Biology*, *18*(10), 5852–5860.

Vidal, O. M., Merino, R., Rico-Bautista, E., Fernandez-Perez, L., Chia, D. J., Woelfle, J., Ono, M., Lenhard, B., Norstedt, G., Rotwein, P., & Flores-Morales, A. (2007). In vivo transcript profiling and phylogenetic analysis identifies suppressor of cytokine signaling 2 as a direct signal transducer and activator of transcription 5b target in liver. *Molecular Endocrinology (Baltimore, Md.)*, *21*(1), 293–311.

Villarino, A., Laurence, A., Robinson, G. W., Bonelli, M., Dema, B., Afzali, B., Shih, H.-Y., Sun, H.-W., Brooks, S. R., Hennighausen, L., Kanno, Y., & O'Shea, J. J. (2016). Signal transducer and activator of transcription 5 (STAT5) paralog dose governs T cell effector and regulatory functions. *eLife*, *5*.

Villarino, A. V., Kanno, Y., Ferdinand, J. R., & O'Shea, J. J. (2015). Mechanisms of Jak/STAT signaling in immunity and disease. *Journal of Immunology (Baltimore, Md.: 1950)*, *194*(1), 21–27.

Vinkemeier, U., Moarefi, I., Darnell, J. E., & Kuriyan, J. (1998). Structure of the amino-terminal protein interaction domain of STAT-4. *Science (New York, N.Y.)*, *279*(5353), 1048–1052.

Vitali, C., Bassani, C., Chiodoni, C., Fellini, E., Guarnotta, C., Miotti, S., Sangaletti, S., Fuligni, F., De Cecco, L., Piccaluga, P. P., Colombo, M. P., & Tripodo, C. (2015). SOCS2 Controls Proliferation and Stemness of Hematopoietic Cells under Stress Conditions and Its Deregulation Marks Unfavorable Acute Leukemias. *Cancer Research*, *75*(11), 2387–2399.

Vo, N., Fjeld, C., & Goodman, R. H. (2001). Acetylation of Nuclear Hormone Receptor-Interacting Protein RIP140 Regulates Binding of the Transcriptional Corepressor CtBP. *Molecular and Cellular Biology*, *21*(18), 6181–6188.

Waltzer, L., & Bienz, M. (1998). Drosophila CBP represses the transcription factor TCF to antagonize Wingless signalling. *Nature*, *395*(6701), 521–525.

Walz, C., Ahmed, W., Lazarides, K., Betancur, M., Patel, N., Hennighausen, L., Zaleskas, V. M., & Van Etten, R. A. (2012). Essential role for Stat5a/b in myeloproliferative neoplasms induced by BCR-ABL1 and JAK2(V617f) in mice. *Blood*, *119*(15), 3550–3560.

Wang, R., Cherukuri, P., & Luo, J. (2005). Activation of Stat3 sequence-specific DNA binding and transcription by p300/CREB-binding protein-mediated acetylation. *The Journal of Biological Chemistry*, *280*(12), 11528–11534.

Wang, R., Li, Q., Helfer, C. M., Jiao, J., & You, J. (2012). Bromodomain protein Brd4 associated with acetylated chromatin is important for maintenance of higher-order chromatin structure. *The Journal of Biological Chemistry*, *287*(14), 10738–10752.

Wang, W., Dong, L., Saville, B., & Safe, S. (1999). Transcriptional activation of E2f1 gene expression by 17beta-estradiol in MCF-7 cells is regulated by NF-Y-Sp1/estrogen receptor interactions. *Molecular Endocrinology (Baltimore, Md.)*, *13*(8), 1373–1387.

Wang, X., & Hayes, J. J. (2008). Acetylation mimics within individual core histone tail domains indicate distinct roles in regulating the stability of higher-order chromatin structure. *Molecular and Cellular Biology*, *28*(1), 227–236.

Wang, Z., Zang, C., Cui, K., Schones, D. E., Barski, A., Peng, W., & Zhao, K. (2009). Genome-wide mapping of HATs and HDACs reveals distinct functions in active and inactive genes. *Cell*, *138*(5), 1019–1031.

Watanabe, S., Zeng, R., Aoki, Y., Itoh, T., & Arai, K. (2001). Initiation of polyoma virus origin-dependent DNA replication through STAT5 activation by human granulocyte-macrophage colony-stimulating factor. *Blood*, *97*(5), 1266–1273.

Weber, A., Borghouts, C., Brendel, C., Moriggl, R., Delis, N., Brill, B., Vafaizadeh, V., & Groner, B. (2013). The inhibition of stat5 by a Peptide aptamer ligand specific for the DNA binding domain prevents target gene transactivation and the growth of breast and prostate tumor cells. *Pharmaceuticals (Basel, Switzerland)*, *6*(8), 960–987.

Weber, A., Borghouts, C., Brendel, C., Moriggl, R., Delis, N., Brill, B., Vafaizadeh, V., & Groner, B. (2015). Stat5 Exerts Distinct, Vital Functions in the Cytoplasm and Nucleus of Bcr-Abl+ K562 and Jak2(V617f)+ HEL Leukemia Cells. *Cancers*, *7*(1), 503–537.

Whalen, S., Truty, R. M., & Pollard, K. S. (2016). Enhancer-promoter interactions are encoded by complex genomic signatures on looping chromatin. *Nature Genetics*, *48*(5), 488–496.

Wieczorek, M., Ginter, T., Brand, P., Heinzel, T., & Krämer, O. H. (2012). Acetylation modulates the STAT signaling code. *Cytokine & growth factor reviews*, *23*(6), 293–305.

Wirén, M., Silverstein, R. A., Sinha, I., Walfridsson, J., Lee, H.-M., Laurenson, P., Pillus, L., Robyr, D., Grunstein, M., & Ekwall, K. (2005). Genomewide analysis of nucleosome density histone acetylation and HDAC function in fission yeast. *The EMBO journal*, *24*(16), 2906–2918.

Witt, O., Deubzer, H. E., Milde, T., & Oehme, I. (2009). HDAC family: What are the cancer relevant targets? *Cancer Letters*, *277*(1), 8–21.

Wolfson, N. A., Pitcairn, C. A., & Fierke, C. A. (2013). HDAC8 substrates: Histones and beyond. *Biopolymers*, *99*(2), 112–126.

Wyrick, J. J., Holstege, F. C., Jennings, E. G., Causton, H. C., Shore, D., Grunstein, M., Lander, E. S., & Young, R. A. (1999). Chromosomal landscape of nucleosome-dependent gene expression and silencing in yeast. *Nature*, *402*(6760), 418–421.

Wyszomierski, S. L., & Rosen, J. M. (2001). Cooperative effects of STAT5 (signal transducer and activator of transcription 5) and C/EBPbeta (CCAAT/enhancer-binding protein-beta) on beta-casein gene transcription are mediated by the glucocorticoid receptor. *Molecular Endocrinology (Baltimore, Md.)*, *15*(2), 228–240.

Xiao, H., Hasegawa, T., & Isobe, K. (1999). Both Sp1 and Sp3 are responsible for p21waf1 promoter activity induced by histone deacetylase inhibitor in NIH3t3 cells. *Journal of Cellular Biochemistry*, *73*(3), 291–302.

Xu, R., Spencer, V. A., & Bissell, M. J. (2007). Extracellular matrix-regulated gene expression requires cooperation of SWI/SNF and transcription factors. *The Journal of Biological Chemistry*, *282*(20), 14992–14999.

Xu, W.-S., Perez, G., Ngo, L., Gui, C.-Y., & Marks, P. A. (2005). Induction of polyploidy by histone deacetylase inhibitor: a pathway for antitumor effects. *Cancer Research*, *65*(17), 7832–7839.

Xu, X., Sun, Y. L., & Hoey, T. (1996). Cooperative DNA binding and sequence-selective recognition conferred by the STAT amino-terminal domain. *Science (New York, N.Y.)*, *273*(5276), 794–797.

Xue, H.-H., Fink, D. W., Zhang, X., Qin, J., Turck, C. W., & Leonard, W. J. (2002). Serine phosphorylation of Stat5 proteins in lymphocytes stimulated with IL-2. *International Immunology*, *14*(11), 1263–1271.

Yamashita, H., Xu, J., Erwin, R. A., Farrar, W. L., Kirken, R. A., & Rui, H. (1998). Differential control of the phosphorylation state of proline-juxtaposed serine residues Ser725 of Stat5a and Ser730 of Stat5b in prolactin-sensitive cells. *The Journal of Biological Chemistry*, *273*(46), 30218–30224.

Yan, R., Small, S., Desplan, C., Dearolf, C. R., & Darnell, J. E. (1996). Identification of a Stat gene that functions in Drosophila development. *Cell*, *84*(3), 421–430.

Yar Saglam, A. S., Yilmaz, A., Onen, H. I., Alp, E., Kayhan, H., & Ekmekci, A. (2016). HDAC inhibitors, MS-275 and salermide, potentiates the anticancer effect of EF24 in human pancreatic cancer cells. *EXCLI journal*, *15*, 246–255.

Yi, T., Mui, A. L., Krystal, G., & Ihle, J. N. (1993). Hematopoietic cell phosphatase associates with the interleukin-3 (IL-3) receptor beta chain and down-regulates IL-3-induced tyrosine phosphorylation and mitogenesis. *Molecular and Cellular Biology*, *13*(12), 7577–7586.

Yoon, S., & Eom, G. H. (2016). HDAC and HDAC Inhibitor: From Cancer to Cardiovascular Diseases. *Chonnam Medical Journal*, *52*(1), 1–11.

Yoshida, M., Kijima, M., Akita, M., & Beppu, T. (1990). Potent and specific inhibition of mammalian histone deacetylase both in vivo and in vitro by trichostatin A. *The Journal of Biological Chemistry*, *265*(28), 17174–17179.

You, S.-H., Lim, H.-W., Sun, Z., Broache, M., Won, K.-J., & Lazar, M. A. (2013). Nuclear receptor co-repressors are required for the histone-deacetylase activity of HDAC3 in vivo. *Nature Structural & Molecular Biology*, *20*(2), 182–187.

Yuan, Z.-l. (2005). Stat3 Dimerization Regulated by Reversible Acetylation of a Single Lysine Residue. *Science*, *307*(5707), 269–273.

Zeng, L., Zhang, Q., Gerona-Navarro, G., Moshkina, N., & Zhou, M.-M. (2008). Structural basis of site-specific histone recognition by the bromodomains of human coactivators PCAF and CBP/p300. *Structure (London, England: 1993)*, *16*(4), 643–652.

Zhang, X., You, Q., Zhang, X., & Chen, X. (2015). SOCS3 Methylation Predicts a Poor Prognosis in HBV Infection-Related Hepatocellular Carcinoma. *International Journal of Molecular Sciences*, *16*(9), 22662–22675.

Zhu, P., Huber, E., Kiefer, F., & Göttlicher, M. (2004). Specific and redundant functions of histone deacetylases in regulation of cell cycle and apoptosis. *Cell Cycle (Georgetown, Tex.)*, *3*(10), 1240–1242.

Zimmermann, S., Kiefer, F., Prudenziati, M., Spiller, C., Hansen, J., Floss, T., Wurst, W., Minucci, S., & Göttlicher, M. (2007). Reduced body size and decreased intestinal tumor rates in HDAC2-mutant mice. *Cancer Research*, *67*(19), 9047–9054.

Zupkovitz, G., Tischler, J., Posch, M., Sadzak, I., Ramsauer, K., Egger, G., Grausenburger, R., Schweifer, N., Chiocca, S., Decker, T., & Seiser, C. (2006). Negative and positive regulation of gene expression by mouse histone deacetylase 1. *Molecular and Cellular Biology*, *26*(21), 7913–7928.